ENERGY FILTER PROPERTIES OF ECOSYSTEMS

By

DANIEL E. CAMPBELL

A DISSERTATION PRESENTED TO THE GRADUATE COUNCIL OF
THE UNIVERSITY OF FLORIDA
IN PARTIAL FULFILLMENT OF THE REQUIREMENTS FOR THE
DEGREE OF DOCTOR OF PHILOSOPHY

UNIVERSITY OF FLORIDA

1984

ACKNOWLEDGMENTS

I acknowledge and most gratefully thank all those who have contributed to my intellectual growth while a student at the University of Florida. I give special thanks to my major professor, Dr. Odum, for he gave me a new way of viewing the world. His inspiration and insight are largely responsible for that which is good in this dissertation. I thank my committee, Dr. Huber, Dr. Capehart, Dr. Nordlie, and Dr. Deevey, for their open-mindedness, patience in receiving this work as well as their intellectual contributions to its conception.

I have discussed this work with many students and faculty in addition to those already mentioned. I thank in chronological order Dr. Chet Kylstra, Dr. Bob Costanza, Dennis Swaney, Karin Limburg, John Richardson, and Dr. Clay Montague. I give special thanks to John Richardson for his generosity in sharing computer programs and his knowledge of computers as well as for discussion of problems in ecology and modeling.

I would like to thank Drs. Odum and Knox for choosing me to participate in the National Science Foundation U.S.-New Zealand exchange program. I thank all those at the University of Canturbury who made research work there so pleasurable.

Finally, I thank my wife, Kathy Trimmer, and son Elliott who provided much needed inspiration to finish this work. Special thanks go to Jean Breeze who typed thousands of my hand-written pages, to Steve Robuski who drafted the figures, and to Sofia Kohli who typed the final manuscript.

TABLE OF CONTENTS

Page

ACKNOWLEDGMENTS ii

LIST OF TABLES viii

LIST OF FIGURES xvii

LIST OF SYMBOLS xxiii

ABSTRACT xxv

INTRODUCTION 1

Frequency Characteristics 2
Hierarchical Organization 6
Relationships of Power, Frequency, and Magnitude 9
Wave Filter Concepts 13
Time Constants and Ecosystem Design 14
Filter Boundaries and the Window of Observation 20
Literature Review 21
Study Plan 27

METHODS 28

The Energy Circuit Language 29
Development of Models 34
Communications Engineering Techniques 35
    Classical Harmonic Analysis 35
    Frequency Response Analysis 37
    High Frequency Cutoff and Resonance 39
Concepts and Definitions Used in the Simulation Model 40
    Turnover and the Time Constant 40
    Mean, Variance, and Mean Square Calculations 41
    Definitions of Power Use Functions 42
    Unit Survival Time and Stability 46
    Resonance, Turnover, and Frequency Matching 46
    Superposition and Modulation 47
    Iteration Interval and Nested Models 47
    Analysis of Wave Filters 48
Simulation Methods 49
    Techniques Used in the Competition Minimodels 49
    Techniques Used in the Trophic Chain Minimodels 53
    Techniques Used in the Web Minimodels 55

Page

RESULTS 56

Filter Properties of Competition Models 56
    Frequency Filtering Properties of Linear Competition 56
    Comparison of Steady and Varying Power for Linear Competition 66
    Analog versus Digital Simulation of Autocatalytic Competition 66
    Filter Properties of the Iteration Interval and Aliasing 72
    Comparison of Linear and Autocatalytic Competition 78
    Dominance Controlled by Frequency and Turnover 83
    Behavior of the Autocatalytic Competition Model 85
    Filter Properties of Autocatalytic Competition 92
    Component Turnover Spacing 98
    The System High Frequency Cutoff and Maximum Power 103
    Superposition and Modulation in the Competition Model 103
    Modulation and Frequency Matching 110
    A Nested Competition Model 113
Filter Properties of Chain Models 116
    Filter Properties of a Linear Chain 119
    Filter Properties of an Autocatalytic Chain with No Secondary Positive Feedbacks 128
    Filter Properties of an Autocatalytic Chain with Three Secondary Positive Feedbacks 142
    Comparison of the Filter Properties of Three Unit Chain Models 142
    Filter Properties of Chain Models with Large Second Law Losses 159
    Filter Properties of Zero Positive Feedback Chain with One Variable and One Constant Energy Source 185
    Filter Properties of a Three Positive Feedback Chain with One Variable and One Constant Energy Source 200
    Filter Properties of a Zero Positive Feedback Autocatalytic Chain with Two Modulated Energy Sources 213
    Filter Properties of a Three Positive Feedback Autocatalytic Chain with Two Modulated Energy Sources 229
    A Nested Chain Model 245

Page

Some Filter Properties of Web Models 247
  Webs with the Same Turnover on Parallel Units 248
  Webs with Different Turnovers on Parallel Units 265
Filter Properties of an Evaluated Salt Marsh Competition Model 266
Filter Properties of an Evaluated Salt Marsh Minimodel 271
  Behavior of the Kaituna Salt Marsh Minimodel 271
  Power on Model Pathways 279
  Filter Properties of the Kaituna Salt Marsh Minimodel 284
Filter Properties of an Evaluated Salt Marsh Trophic Chain Model 290
  Behavior of the Salt Marsh Trophic Chain Model 290
  Filter Properties of the Salt Marsh Trophic Chain Model 297

DISCUSSION 316

Input Frequency Spectra and System Design 316
System Boundaries and the Frequency Domain 320
Transmission and Reception of Signal Frequencies 324
Competition, Turnover, and the Paradox of the Plankton 326
Trophic Chains: Hierarchy, Turnover, Power, and Stability 329
  Aquatic versus Terrestrial Food Chains 335
  The Interactions of a Second Energy Source and Maximum Power 339
Maximum Power in Competition 342
Stability 345
Discrete, Nonlinear Competition, and the Iteration Interval 348
Limitations on Frequency Response Analysis 361
Self-Organization of Ecosystem Design by Invading *Spartina* 352
  Competition between *Spartina* and the *Juncus-Leptocarpus* Marsh 354
  Salt Marsh Filter Relations 354
  Trophic Chain Characteristics and Self-Organization 357
  Ecosystem Adaptation and Variable Resources 361

SUMMARY 362

Page

APPENDIX A COMPUTER PROGRAMS 369

APPENDIX B DEVELOPMENT OF A SALT MARSH COMPETITION MODEL 388

APPENDIX C DEVELOPMENT OF A MINIMODEL FOR THE KAITUNA RIVER SALT MARSH 401

APPENDIX D DEVELOPMENT OF A SALT MARSH TROPHIC CHAIN MODEL 415

REFERENCES 444

BIOGRAPHICAL SKETCH 450

LIST OF TABLES

Table — Page

1. Some important characteristics of many natural phenomena — 3

2. A step by step procedure for constructing an energy circuit diagram — 33

3. The power (mean + variance) and variant power used by three competing linear units over a three decade frequency range for high and low energy inputs — 62

4. The power, mean power, and variant power produced and used by three competing linear storages as a function of amplitude for high and low energy inputs — 63

5. The effect of changes in signal mean, amplitude, and frequency on the power used by three competing linear storages — 67

6. The effect of iteration interval on the power produced and used by storage and the survival time of three competing autocatalytic units — 73

7. The power produced and used by storages and the survival time for units in autocatalytic competition when the inflow to Q_1 is increased by (A) 1% and by (B) 10% and the iteration interval, Dt, is variable — 77

8. The total and variant power produced and used by a single linear storage in Figure 12(b) and a single autocatalytic storage in Figure 14(b) — 79

9. The power produced and used by three linear units in competition for constant, periodic, and noise inputs — 81

10. The power produced and used by three autocatalytic units in competition for constant, periodic, and noise inputs — 82

Table Page

11 Comparison of competition between three autocatalytic units when all have equal turnover and when each one has a different turnover 84

12 The power (mean + variance) and variant power produced and used by three competing autocatalytic storages (Figure 14) over a three decade range of frequency for high and low energy inputs 93

13 The power (mean + variance) and variant power produced and used by three autocatalytic storages as a function of the amplitude for high and low energy inputs (see Figure 14) 96

14 The power (mean + variance) and variant power produced and used by three competing autocatalytic storages as a function of amplitude for high and low energy inputs 99

15 The effect of changes in signal mean, amplitude, and frequency of the power used by three competing autocatalytic storages (A) high energy input = 80, (B) low energy input = 30 101

16 The power produced and used and survival time of units (A) a system with closely spaced turnovers is exposed to inputs of varying frequency. (B) the effect of unit turnover separation on power produced and used for an input of 1 cycle per unit time. (C) competition between units with proportionally separated turnovers that match input frequency 102

17 Comparison of power produced and used and the survival of unit Q_1 in the same system with high and low high frequency cutoffs (A) linear competition, (B) autocatalytic competion, (C) autocatalytic competition with modulated inputs 104

18 The power produced and used and the survival time of unit Q_1 for (A) linear competition, (B) autocatalytic competition when input signals are superposed, and (C) the autocatalytic model with the input signals multiplied 108

19 The power produced and used by three competing autocatalytic components when the amplitude of two input frequencies changes from high to low 111

Table Page

20 The power produced and used by a system of three autocatalytic units in competition for modulated input signals of frequency 1 and 0.5 and amplitude 15 . . 112

21 The power, mean power, and variant power produced and used by a linear nested competition model 114

22 The power, mean power, and variant power produced and used by an autocatalytic nested competition model 116

23 The power, mean power, and variant power produced and used by an autocatalytic nested competition model with two modulated inputs 117

24 The power produced and used by storages in the linear chain in Figure 22 at high and low energy input as a function of frequency 125

25 The power produced and used by storages in a linear chain as a function of frequency for the four turnover arrangements given as A, B, C, and D 126

26 The power produced and used by storages in a linear chain model given in Figure 22 for four turnover arrangements given in A, B, C, D . 127

27 The power produced and used by storages in a linear chain model given in Figure 22 when input frequency is 1 cycle per unit time and the amplitude varies . 129

28 The effect of changes in the signal mean, amplitude, and frequency on the power produced and used by a three unit linear chain model . 130

29 The power produced and used by storages of an autocatalytic chain model with no secondary positive feedbacks [Figure 23(a)] at high and low levels of energy input 131

30 The power produced and used by storages of an autocatalytic chain with no secondary positive feedbacks as a function of frequency for four turnover arrangements given as A, B, C, and D 133

Table Page

31 The effect of changes in the signal mean, amplitude, and frequency on the power produced and used by the three unit chain model given in Figure 23(a) 137

32. The component of power due to the mean in model [Figure 23(a)] for four cases of different turnover and changing frequency 138

33 The part of the power due to variance in model [Figure 23(a)] for four cases of different turnover and changing frequency 140

34 The power, mean power, and variant power produced and used by storages of a three secondary positive feedback autocatalytic chain model [Figure 23(b)] 143

35, Power captured, produced, and used by storages of the chain models shown in Figure 23 with Case A turnover for variable input frequencies 146

36 The mean power captured, produced, and used by storages of the models in Figure 23 with Case A turnovers for variable input frequency 149

37 The variant power captured, produced, and used by storages of the models in Figure 23 with Case A turnovers for variable input frequency 152

38 Power produced and used in storages for chain models in Figure 23 with Case B turnovers 157

39 The mean power produced and used by storages of the chain models in Figure 23 with Case B storages 160

40 The variant power produced and used by storages of the chain models in Figure 23 with Case B turnovers 162

41 Power, mean power, and variant power produced and used by storages of the chain models in Figure 23 for Cases C and D turnovers 164

42 The power produced, used, and captured by storages of chain models in Figure 27 with Case A turnovers over a six decade range of input frequencies 170

43 The mean power produced, used, and captured by storages of chain models in Figure 27 over a six decade frequency range for Case A turnovers 172

Table Page

44 The variant power produced, used, and captured by storages of chain models in Figure 27 over a six decade range of frequency for Case A turnovers 174

45 The power produced, used, and captured by storages of the chain models in Figure 27 over a six decade range of frequency for Case B turnovers 177

46 The mean power produced, used, and captured by storages of the chain models in Figure 27 over a six decade frequency range of Case B turnovers 178

47 The variant power produced, used, and captured by storages of the chain models in Figure 27 over a six decade frequency range for Case B turnovers 179

48 The power produced, used, and captured by storages in the chain models in Figure 27 over a six decade frequency range for Case C and Case D turnovers 181

49. The mean power produced, used, and captured by storages of the chain models in Figure 27 over a six decade frequency range for Case C and D turnovers 183

50 The variant power produced, used, and captured by storages of the chain models in Figure 27 over a six decade frequency range for Case C and D turnovers 184

51. The total power produced and used by four time constant arrangements of the zero secondary positive feedback chain model in Figure 29 as a function of variations in the input frequency of the second energy source 190

52 The portion of the total power given in Table 51 attributable to the mean 192

53. The portion of the total power in Table 51 attributable to the variance 194

54 The mean square power produced and used by a zero secondary positive feedback autocatalytic chain model over a four decade frequency range for four turnover arrangements when the first input is constant and the second input enters at Q_1 with an amplitude of 214 5 201

Table		Page
55	The total power produced and used by four turnover arrangements of the three positive feedback model given in Figure 31 as a function of input frequency	205
56	The portion of the total power in Table 55 attributable to the mean	209
57	The portion of the total power in Table 55 attributable to the variance	211
58	The total power produced and used by a zero secondary positive feedback autocatalytic chain model (Figure 33) when four turnover arrangements are tested over a six decade frequency range	215
59	The portion of the total power in Table 58 due to the mean	222
60	The portion of the total power in Table 58 due to the variance	225
61	The total power produced and used by storages of the three positive feedback model in Figure 35 as a function of frequency	230
62	The contribution of the mean to the total power given in Table 61	235
63	The contribution of the variance to the total power given in Table 61	240
64.	The power produced and used by storages of the chain model in Figure 33 when turnover integrations are nested	246
65	The power produced, used, and captured by storages of the web models in Figure 37 over a six decade frequency range when parallel units have the same turnover	252
66	The mean power produced, used, and captured by storages of the web models in Figure 37 over a six decade frequency range when parallel units have the same turnover	254
67	The variant power produced, used, and captured by storages of the web models in Figure 37 over a six decade frequency range when parallel units have the same turnover	256

Table Page

68. The power produced, used, and captured by the web models in Figure 37 over a five decade frequency range when parallel units have widely separated turnovers . . . 259

69. The mean power produced, used, and captured by storages of the web models in Figure 37 over a five decade frequency range when parallel units have widely separated turnovers . . . 261

70 The variant power produced, used, and captured by storages of the web models in Figure 37 over a five decade frequency range when parallel units have widely separated turnovers . . . 263

71. The total power on several pathways or the summation of pathways in the Kaituna marsh minimodel (Figure 41) as a function of input frequencies . . . 280

72 Ratios of variant power output to variant power input defined for the salt marsh model in Figure 41 . . . 285

73. A variable's change in variant power as a percentage of the variable's total change in power for six solar input frequency increments calculated from Table C-3 in Appendix C . . . 291

74. Input frequency-tarnover matching related to maximum power capture and use by storage in several chain models . . . 318

75 Boundaries established in the frequency domain for a series of trophic chain models of different component turnover arrangement . . . 321

76. Four turnover arrangements examined in this study and thier power production and power use by storage as compared to their stability . . . 330

77. Four evaluated trophic chains are given with flows, biomass, and turnover representing aquatic and terrestrial systems . . . 336

78. The stability, connectance, interaction strength, and power for trophic chain models in Figure 23 . . . 346

Table		Page
B-1	Solar insolation data for Havelock estimated as the average of Nelson and Wellington	384
B-2.	Mean values with standard errors for live and dead biomass in vegetation of the Kaituna River marsh, Havelock, N.Z.	385
B-3	Gas metabolism data and concomitant conditions for *Spartina* and *Juncus* species of marshes at Crystal River, Florida	400
C-1	Mean tidal concentrations of suspended matter in three creeks of the Kaituna River marsh over a 15 hr sampling, March 16, 1982, neaptide	406
C-2	Estimate of net suspended matter, erosion, and sedimentation at Kaituna River marsh, March 16, 1982	408
C-3.	Total power, mean power, and variant power for all pathways in the salt marsh minimodel in Figure 41 when solar input frequency is variable	412
C-4	Total power, mean power, and variant power for all pathways in the salt marsh minimodel in Figure 41 when tidal input frequency is variable	413
C-5.	Total power, mean power, and variant power for all pathways in the salt marsh minimodel in Figure 41 when the river input frequency is variable	414
D-1.	Biomass of *Potamopyrgus* in *Spartina* marsh	420
D-2.	Fish collected from a blocked tidal creek in Havelock, N. Z.	423
D-3	Exploratory bird counts in Kaituna River marsh and mudflat, 11-12 a.m., February 19, 1982	424
D-4.	The total power on pathways and sums of pathways in the trophic chain models in Figure 50(a), (b), and (c)	426
D-5	Ratios of output to input variant power used to evaluate the chain models in Figure 50(a), (b), and (c)	428

Table Page

D-6 The mean square power, mean power, and variant power produced and used by the chain model in Figure 50(a) when the solar input frequency varies 432

D-7. The mean square power, mean power, and variant power produced and used by the trophic chain model in Figure 50(a) when the temperature input varies 434

D-8 The mean square power, mean power, and variant power produced and used by the chain model in Figure 50(a) when the frequency of river input varies 436

D-9 The mean square power, mean power, and variant power produced and used by the model in Figure 50(a) when the frequency of predator harvest varies [dotted portion of Figure 50(a)] 438

D-10 The mean square power, mean power, and variant power produced and used by the model in Figure 50(b) when frequency of a push-pull predator harvest varies 440

D-11 The mean square power, mean power, and variant power produced and used by the chain model in Figure 50(c) without secondary positive feedbacks when the frequency of temperature input varies 442

D-12 Ratios of output to input used to evaluate the power produced and used for the trophic chain models in Figure 50(a), (b), and (c) 444

LIST OF FIGURES

Figure		Page
1.	Important frequency characteristics of energy models	5
2	A set of diagrams representing several concepts of hierarchies and their properties	8
3.	Diagram of a one dimensional wave form modified from Halliday and Resnick (1974)	11
4.	A diagrammatic representation of three types of wave filters	15
5.	Bode plot for a linear first order system redrawn from Milsum (1966)	16
6.	Bode plot for an underdamped linear second order system redrawn from Milsum (1966)	18
7	System boundary frame outlining the window of observation on the hierarchy of natural phenomena selected for study	23
8	The major symbols of the energy circuit language used in this study	32
9	Systems as wave filters	36
10.	Diagrammatic definition of the power use function calculated in simulations	44
11.	Three possible arrangements of three autocatalytic units for a source-controlled flow	51
12.	A simulation model of linear competition between units (Q_1, Q_2, Q_3) of different turnover	58
13	Simulation of model in Figure 12 shows the power dissipated and storages maintained by three competing linear components with different turnovers Q_1, T = 10, Q_2, T = 1.0, Q_3, T = 0.1 exposed to superposed energy input with frequencies of 1, 10, and 50 cycles/sec and amplitude = 10	61

Figure Page

14 A simulation model of autocatalytic competition between components Q_1, Q_2, and Q_3, of different turnover, T 69

15. Analog simulation of three competing autocatalytic units in Figure 14 70

16 Output from a digital model of three competing autocatalytic units in Figure 14 71

17. Simulation of the model in Figure 14 with constant energy input and varying iteration interval that acts as a system filter 74

18. Simulation of model in Figure 14 with iteration intervals in a sensitive range for Q_1's behavior . . . 76

19. Simulation of model in Figure 14 with different frequencies of the forcing functions 87

20. Simulation of model in Figure 14 with varying source amplitude 90

21. A simulation model of autocatalytic competition between components Q_1, Q_2, and Q_3 of turnover 10, 1.0, 0.1, respectively 106

22. A linear chain model showing the flows that would result if there were a 10% power transfer between components of the chain, and the driving input is a variable time signal 118

23 The models given in (a) through (h) show eight possible combinations of secondary positive feedbacks within a chain of three autocatalytic units 121

24. A Bode-like plot of the frequency behavior of the three unit nonlinear chain model without secondary positive feedbacks in Figure 23(a) for four turnover arrangements 136

25. A comparison of Bode-like plots for the models shown in Figure 23(a), 23(b), and 23(d) 154

26. The relationship between the number of secondary positive feedbacks and power production, power use, and stability of the models in Figure 23 . . . 155

Figure		Page
27	Three unit chain models fettered as shown in Figure 23 with energy flows allowing large second law losses at each interaction	167
28.	Effects of increasing the number of secondary positive feedback loops in a three unit autocatalytic chain	186
29	An autocatalytic chain without secondary positive feedback driven by two energy sources, one constant and one variable	188
30.	A Bode-like plot of the variant power ratio as a function of frequency for the models in Figure 29 for four different turnover arrangements	197
31	An autocatalytic chain with three secondary positive feedbacks driven by two energy sources, one constant and one variable	204
32.	A Bode-like plot of the frequency response of the chain models with three secondary positive feedbacks shown in Figure 31 when one energy input is constant and a second variable energy input is entering the chain at Q_1	207
33.	An autocatalytic chain model without secondary positive feedbacks showing the interaction of two variable energy sources, one at the base of the chain, the second positioned at levels represented by components Q_1, Q_2, and Q_3	215
34	A Bode-like plot of the frequency response of a three unit chain model without secondary positive feedbacks (Figure 33) for four turnover arrangements when two variable energy sources interact	220
35.	An autocatalytic chain model with three secondary positive feedbacks showing the interaction of two energy sources, one at the base of the chain and the second positioned at different levels represented by components Q_1, Q_2, and Q_3	235
36.	A Bode-like plot of the frequency response of a three unit chain model with three secondary positive feedbacks for two turnover arrangements when two variable energy sources interact at the chain base	243

Figure Page

37. A three unit web of autocatalytic components 250

38. A model of competition between three marsh grasses at Havelock, New Zealand 268

39. A simulation of competition between invading Spartina townsendii and the natural Leptocarpus-Juncus complex at Havelock, N.Z 269

40. Simulation results of the competition minimodel given in Figure 38 when two input signals are modulated (dotted lines in Figure 38) 270

41. Minimodel of the Kaituna River salt marsh at Havelock, New Zealand 273

42. Comparison of simulation results of superposed and modulated signals in the marsh model given in Figure 41 274

43. Frequency response of the marsh minimodel components shown in Figure 41 to variation of the solar input frequency 275

44. Frequency response of the components of the marsh minimodel in Figure 41 to variation in the tide and river input frequencies 276

45. The phase of a hypothetical recycle aid (dotted pathway and source in Figure 41) changes the filter properties of the labile N component 277

46. The power on pathways or sums of pathways in the Kaituna River salt marsh model as a function of input frequency 282

47. A Bode-like plot of the frequency response of system functions in a salt marsh minimodel, Figure 41 287

48. A Bode-like plot of the frequency response of the three system components in the salt marsh minimodel, Figure 41 288

49. A Bode-like plot of the frequency response of variant power exported, variant power used, and their average as a function of input frequency 289

Figure Page

50. Evaluated trophic chain models for the Kaituna River salt marsh, Havelock, N Z . . . 293

51. The frequency response of the trophic chain model in Figure 50 to variations in solar input frequency . . . 296

52. The frequency response of the marsh trophic chain model given in Figure 50 to variation in the temperature input frequency . . . 298

53. Comparison of simulation runs of the trophic chain salt marsh model with predator harvest to those with push-pull predator harvest . . . 300

54. Filter characteristics of the trophic chain model given in Figure 50 when the total power and the ratio of circulating variant power to input variant power are evaluated for variations in the input frequencies . . . 303

55. Filter characteristics of the trophic chain marsh model when the ratios evaluated are variant power produced and variant power used to variant power input . . . 305

56. Filter characteristics of the trophic chain model in Figure 50 when the power remaining and the ratio of variant power remaining to variant power available are evaluated for variations in the input frequencies . . . 306

57. Filter characteristics of the trophic chain model with three secondary positive feedbacks in Figure 50(a) compared to those of the model in 50(c) with no secondary positive feedbacks when temperature input frequency varies . . . 309

58. Filter characteristics of the trophic chain model in Figure 50(a) with dotted predator harvest compared to the model given in Figure 50(b) where predators both stimulate and harvest *Potamopyrgus* . . . 311

59. Filter behavior of the model components (Figure 50) with respect to the ratios of variant power output to variant power input . . . 314

Figure Page

60. Typical systems of information processing 325

61. Connectance matrices for the models given in Figure 23 347

B-1. A map drawn from the aerial photograph of the Spartina and Juncus-Leptocarpus marsh at Havelock, N.Z., February 26, 1979 391

B-2. Light penetration graphs in salt marsh corrected for sun angle to the vertical, February 18, 1982 398

C-1. Diurnal record of the particulate matter and ashed content of the particulate matter on inflowing and outflowing tide, March 16, 1982 405

LIST OF SYMBOLS

Symbol	Definition
T	Turnover = $1/\tau$
τ	Time constant
f	Frequency, cycles/time
a	Amplitude
λ	Wave length
T^*	Period
t	Time
ω	Angular frequency = $2\pi f$
h	Planck's constant
ν	Frequency of electromagnetic radiation
y	Displacement
c	Celerity
F	Frequency cutoff
ζ	Damping coefficient
Q	Stored quantity
C	Capacitance
R	Resistance
V	Volume
A	Area
ℓ	Length

Symbol	Definition
F_b	High frequency boundary = $1/2t_b$
t_b	Sampling interval
F_B	Low frequency boundary = $1/t_B$
t_B	Period of observation
ϕ	Phase angle

Abstract of Dissertation Presented to the Graduate Council
of the University of Florida in Partial Fulfillment of the Requirements
for the Degree of Doctor of Philosophy

ENERGY FILTER PROPERTIES OF ECOSYSTEMS

By

Daniel E. Campbell

April 1984

Chairman: Howard T. Odum
Major Department: Environmental Engineering Sciences

The role of ecosystem structure and function in absorbing energy inputs was developed using wave filter concepts combining ecology and communications engineering. Analysis techniques used to trace signals and energy through linear systems were applied to nonlinear ecosystem models in 1,005 simulation runs.

The energy absorbed by different designs was simulated separating mean power and that due to variation about the mean, variant power. Where more energy absorption generates more potential for success, then these designs may be favored in survival. More power was used by linear competition at low energy input and autocatalytic competition at high energy input. In general, trophic chain models with increasing secondary positive feedbacks in multiplicative interactions transformed more power but were less stable. Simulation of four turnover arrangements in a three unit trophic chain model showed that hierarchically arranged turnovers ($Q_1 = 10$, $Q_2 = 1$, $Q_3 = 0.1$) were the most stable (82.7% of the time) and used the most power (37.6% of the time).

All models tested displayed increasing power use and transformation at lower input frequencies as would be expected for a low pass filter. Frequency matched and or noisy input signals transformed more power when modulated than when superposed.

The position of a second energy source entering a chain was the most important factor in determining the wave filter pattern observed. The position of the high frequency cutoff and resonant peaks was a function of turnover. Matching input frequencies to turnover properties usually determined power capture.

Filter design during self-organization was studied where the invading salt marsh in New Zealand was outcompeting the native marsh. The frequency response pattern of the Spartina marsh had a filter pattern with a minimum power capture at 10 cycles/year. Therefore, it was well adapted to capture solar input variations which occur at higher and lower frequency. Resonance was found in the organization of the new marsh trophic chain in response to interaction of annual and diurnal frequencies. Wave filter types, high frequency cutoff, resonance, and modulation were found in basic ecosystem designs and in evaluated ecosystem models.

In summary, by organizing filter properties ecosystems can adapt in the climate of input frequencies.

INTRODUCTION

Understanding structure and processes of environmental systems requires general concepts and models which simplify complexity and provide means for prediction. This dissertation examines the efficacy of an energy based wave filter approach to understanding ecosystem structure and function. The concept of an ecosystem as a nonlinear wave filter was used to explore aspects of the design of ecosystems which facilitate the production and use of power. The interactions of geophysical, biological, and cultural phenomena with an ecosystem may be expressed in terms of the transfer of signal frequencies from external forcing functions to the ecosystem components.

Self organization of designs capable of absorbing source energies in all their various frequencies may maximize available energy. In this dissertation frequency spectra of sources are related to filter characteristics and energy capture of ecosystem models. A study of the newly invading exotic salt marsh in New Zealand was used to study the role of filter design in self organization.

Study of the behavior of wave forms passing through a system is a technique traditionally used for systems analysis (Milsum, 1966). Since many of the natural and cultural phenomena influencing ecosystems are populations of waves of various frequency, analysis of response to inputs from external energy sources is appropriate for the study of ecosystems.

Ecosystems may have inherent tendencies to oscillate and pulsate, even when their inputs are steady Such systems may have their oscillatory tendencies accentuated by oscillating inputs, a property sometimes called resonance The study of the absorption of input wave forms is useful whether resonance exists or not The frequency characteristics of the external input waveforms, the wave forms within the ecosystem, and the relationship of these waves are all pertinent to understanding the designs of ecosystems and their causes

Frequency Characteristics

In this study frequency denotes the number of repetitions of a periodic process per unit time. Both the ecosystems and the system of phenomena influencing ecosystems may be thought of as hierarchially organized populations of nonlinear pulsators that generate wave forms Frequency, magnitude, and energy of these wave forms are important parameters A list of characteristics common to many natural phenomena and their implications is given in Table 1

The magnitude of energy flow and storage are general measures of the size of a phenomenon The energy magnitude of a wave form can be expressed as the energy of a mean level plus the energy in the amplitude of the wave form including that of the small waves regarded as noise in the system Frequency is another measure of size if the system inputs are matched by system response.

Frequency, magnitude and energy of oscillations are the products of thermodynamically irreversible processes which are directed in time Prigogine (1982) explaines how time is a kind of operator for phenomena

Table 1 Some important characteristics of many natural phenomena

Assumed Characteristic	Implication
(1) They are pulsators	Variability, frequency, and magnitude are important
(2) They are quasi-periodic to periodic	Simplification to the periodic case is a good first approximation of behavior Frequency domain may be useful in analysis
(3) They are ordered hierarchically	Time constant structure may produce distinct patterns in the frequency domain
(4) Sum of above	To understand and further to manage ecosystems we must understand how they are structured to handle variability

in which there are one or more intrinsic times that may be associated with an irreversible phenomenon based upon its dissipation of energy. These intrinsic times of a system component and their interactions will determine the wave fliter characteristics of the system. One simple example of an intrinsic time is the turnover of a stored quantity. The frequency of oscillating wave forms is almost always due to interactive processes. However, the ability to oscillate and the frequency of oscillation are determined by the turnover characteristics of the storages. Intrinsic times may be defined as the turnovers which are directly associated with the energy constraints to which an individual phenomenon is subject. Some examples of intrinsic times are the generation and turnover times for organisms and turnover times for water in ocean basins.

Most variations observed in nature have frequencies which are due to the interaction of individual phenomena with one another. Interactive frequencies may be further divided into those frequencies which are due to interactions of the elements within a system and those frequencies which are derived from elements or hierarchies outside the system of concern. The latter are usually called forcing frequencies, whereas the former comprise the natural frequencies of a system (see Figure 1). Some examples of exogenous interactive frequencies are the diurnal variation of solar energy due to the rotation of the earth, its yearly fluctuation due to the earth's revolution about the sun, and the variation of the ocean tides due to the variation of the field of gravitational attraction in the earth, moon, sun system. Examples of

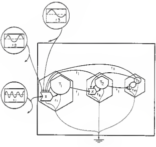

Figure 1 Important frequency characteristics of energy models Component turnovers T_1, T_2, T_3, forcing frequencies f_1, f_2, f_3 and natural frequencies f_i, f_k, and f_m generated by their interactions. Also shown are frequencies transmitted by storages f_j and f_l and frequency feedback through storages f_l and f_o

natural frequencies such are oscillations of alternating production and epidemic consumption in response to periods of rain and drought Interactive frequencies of larger earth systems become forcing frequencies on smaller ecosystems. The system of interactive frequency classification is relative to the placement of system boundaries Distinction between these categories of frequencies is not always clear cut in natural systems For example, many organisms of the intertidal ecosystems have distinct periods of activity corresponding to the tidal fluctuations, and these periods which one might believe to be forcing persist as if they were natural frequencies once the organism is isolated from its environment (Palmer, 1974) In some cases these periodicities tend to lengthen as the separation from the environment is extended This kind of observed behavior indicates that natural and forcing frequencies can and do become closely related in entities which evolve with the ability to be selectively adapted for survival

Hierarchical Organization

Hierarchical organizations are found in almost all animate and inanimate natural phenomena. In the literature dealing with complex systems the term hierarchy carries different connotations Figure 2 presents several combinations of hierarchical properties The original usage of the word refers to a multileveled system of vertical control used with reference to the structure of religions, governments, and other human systems [Figure 2(b)] A related meaning from systems theory implies a set of nested Chinese boxes which represent organizational levels, but instead of a single box within each box, a whole set of boxes is revealed when any box is opened (Simon, 1973)[Figure 2(a)]

Figure 2. A set of diagrams representing several concepts of hierarchies and their properties. (a) 'Chinese box' structural hierarchy showing sets of elements for each level of organization, (b) a divergent cascade hierarchy used to describe one aspect of turbulence, (c) a convergent hierarchy building higher organization also describing turbulence, (d) a hierarchy with power and control pathways, (e) spatial hierarchies showing the convergence of power and the divergence of control, (f) a typical ecosystem hierarchy where many small low quality units converge to a few large high quality units

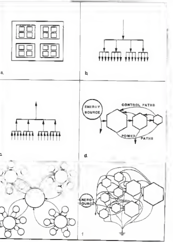
a.
b.
c.
ENERGY SOURCE
CONTROL PATHS
POWER PATHS
d.
e.
ENERGY SOURCE
f

Hierarchies may have transitions from many units to a few [Figure 2(c)] or from a few units to many [Figure 2(b)] or both. Sometimes the former process is designated as the power pathway of a system while the later process is termed the control pathway [see Figure 24(d), Odum, 1983]. Many ecosystems are sometimes conceived as hierarchies that have a transition from many, small, low energy quality components such as phytoplankton to a few, large, high energy quality components such as fish along a power pathway that is mediated by control actions (Odum, 1978) [see Figure 2(f)]

This kind of hierarchy has a characteristic spatial distribution in ecosystems where consumers are spatially concentrated by converging power from a larger region and in turn supplying control feedback action to this region from which their power is converged [see Figure 2(e)] Fiddler crabs operating on the surface of a *Spartina* marsh are an example of such a feedback control system as shown by Montague (1980). Many physical systems are hierarchies that transfer energy from a few to many units, and vice versa, e g., a common case is that of a turbulent flow 'feeding' on a mean velocity and building larger eddies from it [see Figure 2(b)]. In systems with one energy source energy flows along the power pathway away from the source of energy for the system and feeds back along the control pathways proceeding toward this source. The power pathway has a converging action, while the control pathway has diverging action (Odum, 1983)

Relationships of Power, Frequency, and Magnitude

Power in a wave form may be a function of frequency, magnitude or of both together depending on the physical system considered In the physics of waveforms the power of a progressive wave form is a function of both the square of the wave frequency and the square of the wave amplitude. Halliday and Resnick (1974) derive this result for one dimensional wave form as follows. The one dimensional wave of length λ, shown in Figure 3, passes point O in a time T^* equal to the wave's period. The power in the wave is simply the energy of the wave form over length λ divided by the period T^*. The wave is assumed to be composed of particles of equal mass and at point A the energy is all potential, at point B it is all kinetic, and at point C it is mixed. The kinetic energy at B for mass element dm is

$$dK = 1/2\ dm\ (\partial y/\partial t)^2_{max} \tag{1}$$

The total energy in every element is taken to be constant. Thus, the expression for kinetic energy may be summed over all elements of λ, where μ is the mass per unit length. The power is then

$$P = \frac{1}{2}\mu\lambda(\partial y/\partial t)^2_{max} \times \frac{1}{T^*} = \frac{1}{2}\ \mu c\ \left(\frac{\partial y}{\partial t}\right)^2_{max} \tag{2}$$

whose celerity = $c = \lambda/T^*$. The velocity at point B is the maximum. From the equation for displacement,

$$y = y_m \sin\ (kX - \omega t)$$

and $$\partial y/\partial t = -\omega y_m \cos\ (kX - \omega t)$$

and $$(\partial y/\partial t)_{max} = \omega y_m$$

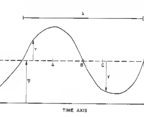

Figure 3. Diagram of a one dimensional wave form modified from Halliday and Resnick (1974) Definition of power transmitted past a point by a wave form is compared with the mean square power in the wave form

Therefore

$$P = 1/2\ \mu C \times \omega^2\ y_m^2 \qquad (3)$$

This derivation illustrates the fact that in all physical systems containing matter waves an analysis of energy flow through a point in space must consider both the frequency and magnitude characteristic of wave forms

In physical systems containing electromagnetic radiation energy is known to be a function of frequency only

$$E = h\nu \qquad (4)$$

where h is Planck's constant and ν is frequency. In these systems higher frequency gives an input with more power than one with a low frequency, since the speed of light is a constant.

Ecosystems generally are composed of components with interacting wave forms which are expressed in energy units or in units which are converted to energy through multiplication by a factor. Power in ecological systems is a function of the steady flow of energy carrying matter plus the energy of the variation. Here the area under a sinusoid of period T^*/n is a function of amplitude only, if the interval of integration is equal to or a multiple of the period (Cruz and Van Valkenburg, 1967)

For steady flows and wave forms of energy, information, or material input to an ecosystem, power is a function of the magnitude of mean and amplitude However, if the energy utilized by the ecosystem is affected by frequency, both frequency and magnitude must be considered in any analysis of power use by the ecosystem The energy in the variations around the mean is the variant power. The energy of the average flow is the mean power

The square of the displacement, y, of a wave form can be expressed as a variance (Figure 3). For some quantities such as velocity of water, variance is proportional to energy as the square of displacement For others such as flow of food the unsquared magnitude is proportional to energy. For most inputs to ecological systems where energy is proportional to magnitude, a mean square power function can be used to determine the proportion of total power used in a system that is contributed by the mean and variance (see Figure 3)

Wave Filter Concepts

One means of investigating the frequency characteristics of a system is to consider the system or its model as a wave filter The wave filter is a device for separating wave forms on the basis of a difference in frequency According to G A Campbell (1922), who was one of the developers of this concept, an electric wave filter transmits currents of all frequencies lying within one or more specified ranges and excludes currents of all other frequencies without absorbing the energy of these excluded frequencies Thus, an ecosystem or model may self design in order to match the frequency characteristics of its filter to those of the forcing energies entering the system in order to insure that its network power will be a maximum.

Brillouin (1962) observes that communications systems always use a finite frequency range and a similar conclusion may be considered when ecosystems are examined. Figure 4 shows filter action with three frequency ranges. An ecosystem wave filter may be of the low pass variety in which all frequencies are passed from 0 up to a cutoff frequency, F_{max}, the band pass type where frequencies in the range F_{min} to F_{max} are passed or the high pass type where frequencies from a lower limit, F_{min} to infinity are passed. No known natural system passes infinitely great frequencies and therefore the high pass case is discarded. Since all ecosystems contain storages which are low pass filters, this case may be the most common. Ecosystems may serve as band pass filters if inputs have a very wide frequency range. In ecosystems the upper frequency cutoff F_{max} of the low pass ecosystem filter may be set and adjusted in order to obtain a maximum network power in the system.

The concept of the high frequency cutoff of a low pass filter is illustrated in Figure 5, which shows a Bode plot for a first order linear system. A Bode plot has the ratio of output to input amplitude on log scale as a function of log of input frequency. The lower graph is a plot of the time lag as a function of frequency. The high frequency cutoff or break frequency is the point where frequency $\omega_b = T$, where T is the turnover of the storage. For this system, ω_b = represents the point where a constant low frequency asymptote intersects a high frequency asymptote of slope -1. Frequencies beyond ω_b are passed with increasing inefficiency.

Time Constants and Ecosystem Design

The frequencies which a low pass filter is able to capture and thereby pass into the system are determined by its high frequency cutoff,

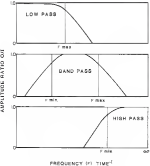

Figure 4. A diagrammatic representation of three types of wave filters The position of high and low frequency cutoffs are shown For similar flows smaller storages tend to pass higher frequencies.

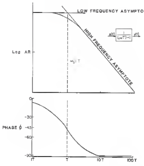

Figure 5. Bode plot for a linear first order system redrawn from Milsum (1966). AR is amplitude ratio, ω is the angular velocity of one input signal, phase ϕ is the lag in degrees of the sine functions.

which is a function of the component turnover Furthermore, certain systems may have their power augmented due to resonance phenomena when their natural frequencies closely match the frequencies of the system's forcing functions and damping is below a threshold Figure 8 shows the Bode plot of a second order underdamped linear system that exhibits resonance phenomena when the damping is below a threshold.

From these observations we might expect the turnovers of the system's components to be important factors in determining the magnitude and the frequencies of variable energy captured by an ecosystem. In addition, we might speculate that there are two kinds of turnover adjustments which affect power capture by a system

First, all components with similar turnover may be expected to compete in matching their high frequency cutoff characteristics with the frequencies of forcing energies and thereby outcompete their neighbors Second, the system filter as a whole may self design a set of components with natural frequencies that match the energy frequencies available to it through the forcing functions.

If we assume that the system time constants are parameters which may be adjusted to maximize power used, then we would like to know how these parameters might be adjusted. In terms of the phenomenological equations of irreversible thermodynamics (Onsager, 1931) and the relation between a storage quantity and driving variable N from Odum (1972),

$$J = LN \qquad (5)$$

where J is a flow, L is the conductivity, $L = 1/R$, and N is a

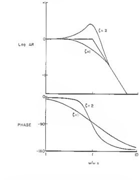

Figure 6 Bode plot for an underdamped linear second order system redrawn from Milsum (1966) A resonance phenomenon is seen when the forcing frequency ω approaches the system's natural oscillation frequency ω_n, where ζ is the damping coefficient

"population force", $N = Q/C$, where Q is a stored quantity, and C is the capacitance of the storage Then

$$J = \frac{1}{RC} Q \tag{6}$$

and RC is the time constant, τ, and $RC = Q/J = \tau$

The ratio of storage to flow may be altered by changing either R or C; R represents the pathway resistivity and is usually a function of physical constraints that are difficult if not impossible to alter. However, C, the capacity factor, is proportional to the volume to surface area ratio and thus to length for many ecosystem components (Odum, 1960, 1967).

$$C = kV/A \sim k\,\ell \tag{7}$$

where k is a constant dependent on the geometric shape, V is volume, A is area, and ℓ is length Therefore, a system component may adjust its time constant by altering its size. Smaller sizes give faster time constants and greater flows per unit storage, which allows the component to react fast enough to capture higher frequency energies of the forcing function. Thus, one might think of the observed size hierarchy of many natural phenomena as an adaptation for capturing energy of a wide range of forcing frequencies. The adjustment of a system component's capacity in order to optimize the use of incoming energy frequencies may be a critical factor in the maximization of network power. In addition, the pathway connections of a system may develop so that component interactions generate natural frequencies that are resonant with frequencies of the forcing functions, thereby further augmenting the power in a system network.

Filter Boundaries and the Window of Observation

The interactions of hierarchically organized natural phenomena compose the vast web that we observe as nature. One of the tasks of science is to discover the interaction points or the seams in this design which might logically be used to delineate the boundaries of systems. Simon (1973) points out that the interactions of most natural phenomena are strongest when the "particles" or pulses are closest together in space and time, therefore systems of natural phenomena are likely to act as localized subsystems over which there is a more or less equally strong field of interaction. This kind of interaction would tend toward the formation of hierarchical levels of increasing degrees of aggregation as different energy sources come into play, where these systems are composed of nonlinear oscillators, each individual level may have associated with it one or more frequencies. Simon (1973) states that if all frequencies of an arbitrarily determined system of n degrees of freedom are arranged in descending order from the highest to the lowest, then we might take advantage of the aforementioned property of the aggregation of natural phenomena called "near-decomposibility" in order to obtain an estimate of the important variable frequencies in the system. This task is accomplished by chosing a maximum time, t_a, over which the system is observed and a t_b to be the minimum time between observations of the system. These arbitrarily chosen limits determine an upper frequency boundary, 1/2 t_b, and a lower frequency boundary, 1/t_s, which describe the system of variables of concern (see Figure 7). This general rule in systems theory is derived from principles for data acquisition and record length used in the statistical theory of communications. This method of defining a system for study selects an arbitrary frequency window through which the natural phenomena of interest may be viewed. This frequency window is a kind of filter used to establish system boundaries in this study. A frequency window was defined on a spectrum of input signals and was used to delimit the boundaries of ecosystems and their models in the frequency domain.

Literature Review

Frequency response analysis is a well developed and useful technique in engineering systems analysis. A good review of this subject may be found in many texts including DiStefano et al. (1967), Grodins (1963), and Lee (1960). Milsum (1966) and Milhorn (1966) review this subject with biological systems applications. In general, frequency response analysis and other engineering systems analysis techniques have been most successful when applied to linear systems in order to solve design problems encountered in the construction of useful electrical or mechanical devices. Sandberg (1964) among others extended this approach to nonlinear systems by considering the system under investigation to be composed of a linear element and one or more nonlinear elements. A discussion of linearization methods for nonlinear

Figure 7 System boundary frame outlining the window of observation on the hierarchy of natural phenomena selected for study. Light boxes represent unit sizes and levels of organization. Inputs and outputs of the system represented as a heavy black box defined by the window boundaries $F_b = 1/2\ t_b$ and $F_B = 1/t_B$. Relationships to storage size and turnover, T, period of observation t_B, and hierarchical organization are shown, f_1 and f_2 are frequencies of the source energy f_i, f_j, and h_k are the frequencies transmitted by each level in the hierarchy.

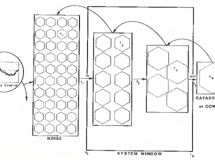
Energy Source
f_i f_j
NOISE
T_1
In
f_i
T_2
f_j
T_3
out
f_k
T_4
CATASTROPHE
or CONTROL
t_b
SYSTEM WINDOW
t_e

systems may be found in Brogan (1974). One extremely useful aspect of frequency response analysis is the ability to determine under what input conditions a system will be stable. Stability criteria for feedback systems were first elucidated by Nyquist (1932). A good historical collection of papers on frequency response and stability analysis in electrical engineering from Nyquist to the present may be found in MacFarlane (1979).

A general introduction to the analysis of signals and the filter concept in electrical engineering is found in Cruz and Van Valkenburg (1967). A more detailed consideration of analog and digital filters is given by Lam (1979). Otnes and Enochson (1978) discuss concepts and methods for time series and digital filter analysis.

Child and Shugart (1972) applied frequency response analysis to a linear model of magnesium cycling in a tropical forest ecosystem. They pointed out the potential usefulness of this technique in describing properties of the ecosystem as well as of its component parts. Child and Shugart (1972) used Bode plots to characterize the behavior of a linear trophic chain. By breaking a feedback loop they were able to use the Nichols diagram (see DiStefano et al., 1967) to describe the closed loop frequency response and stability from data taken for the open loop case. They also examined the natural frequency, damping and resonance in their system and found that the tropical moist forest was highly damped with a very low natural resonant frequency around 0.01 cycles per year.

Walde and Webster (1976) reviewed the application of several engineering techniques to ecosystem analysis. Among these techniques was frequency response analysis and its application to determining stability in the frequency domain. Waide and Webster (1976) gave a brief account of the frequency response technique and all applications considered by them are for linear feedback systems where energy was not considered as one of the input-output variables. In addition to Child and Shugart (1972), Waide and Webster list two similar frequency response studies of mineral cycling in forest ecosystems. Waide et al. (1974) examined calcium cycling in temperate forests and Shugart et al. (1976) examined calcium cycling in a Liriodendron forest.

In expressing ecosystems as analogous energy circuits Odum (1960, 1967, 1971) recognized the applicability of electrical engineering techniques in general to ecosystems analysis. Allen and Starr (1982) state that Koesler (1967) realized that hierarchical complexity in living systems may be described with the concept and properties of a filter. Allen and Starr (1982) point out that the idea of signal filters is basic for engineers and they give examples of its significance in aiding ecologists to understand the complexity of living systems. This study was based on insights from a systems ecology perspective rather than a population ecology perspective. It is interesting that many of the concepts useful in describing the behavior of ecosystems such as filters, signals, feedback or constraints and scale or the time constant and spatial size of units appear in both approaches.

The concept of power as a guiding principle for evolution was first proposed by Lotka (1922). Odum (1979) discussed principles of hierarchy and energy quality dictated by the laws of thermodynamics and the maximum power principle that act to determine ecosystem designs, spatiotemporal structures, and relationships. In the present study this work is expanded on by specifically considering the role of energy input frequencies in establishing system designs that give maximum power production.

The concept of hierarchy and the organization of systems was examined in a Ph.D. dissertation by Brown (1980). He gives a thorough review of many concepts and studies of hierarchical systems. In addition, he examined a series of five unit chain minimodels in order to determine their dynamic behavior when perturbed. Limburg (1981) simulated a set of three unit web models with an external energy source forcing each component in order to determine the effect of energy signature on system behavior.

Richardson and Odum (1981) examined the behavior of a pulsing minimodel at two ecological scales. These simulations show that the model went through a range of natural oscillation as a steady energy source was increased. For a given energy source and increasing total carbon in the model the most energy was captured in the range of oscillation. They note that this may not be a global maximum since total power captured also began to increase when the top consumer maintained a steady state of high power production. They reported a natural pulse period of 200-300 years when the model was calibrated with values similar to those for a forest ecosystem.

In biology there has been considerable study of the relationship between the frequencies of geophysical cycles and the rhythms manifested by living organisms. Palmer (1976) provides a good overall summary of knowledge in this field. Palmer (1974) considered specifically biological rhythms in marine organisms and Luce (1971) presents extensive information on rhythms in human and animal physiology. Biological rhythms are classified as circadian (24 hours), circalunadian (24.8 hours), circatidal (12.4 hours), etc. because these frequencies tend to persist in isolated organisms with frequencies that are approximately equal to the geophysical periodicities by which they are named.

The essence of the theoretical problem presented by these investigations is to determine the nature of the biological clock which correlates organism activities with input frequencies (Palmer, 1976). The major controversy exists between proponents of an escapement clock and those of a nonescapement clock. Escapement clocks are those with a working mechanism to generate a time signal like a pendulum, whereas nonescapement clocks take their time signal from an external source such as an electrical clock. Both the major types of theoretical explanation for biological clocks are compatible with a wave filter perspective on the problem, since an external driving signal must have a receiving unit and an internal pulse generator must still be influenced by an external signal in order to match its frequency. Biological clocks of living organisms are probably another aspect of frequency filters and therefore their mechanism may well be based on a biochemical or membrane activity turnover.

Study Plan

In this study filter properties of well known ecosystem designs were studied by means of computer simulations that generated graphs of frequency response, energy flow, and power utilization. Configurations studied included competition, trophic chains, and webs. These were diagrammed, calibrated with flows and storages consistent with energy laws, and represented with differential equations. Computer simulations were made to analyze the power, stability, and temporal patterns in response to input frequencies from one or two energy sources of various kinds. Filter characteristics of the various ecosystem designs were recorded in the frequency domain with Bode-like plots and their properties were described.

Several evaluated models of the ecosystem now organizing around invading Spartina townsendii sensu lato at Havelock, New Zealand, were employed to illustrate how these principles might operate in ecosystems. The significance of competition, trophic chain organization, and salt marsh ecosystem structure and function were examined by means of frequency response analysis of models representing these processes in the invading Spartina ecosystem.

METHODS

Methods used in this study were taken from two major sources, energy systems analysis and communications engineering. Simulation models were the major technique used to investigate the applicability of communications and systems engineering methods. Methods include definition of concepts and the energy language used to diagram energetic and mathematical relationships.

The Energy Circuit Language

A diagrammatic network language was used to design and represent systems, explain concepts, and define simulation experiments on filtering properties of systems. There are many such languages in use in various fields. Among them are Forrester's industrial dynamics, Paynter's bond diagrams, influence diagrams, and many others. The energy circuit language developed in the field of ecology by H. T. Odum (1960, 1971, 1972) will be employed in this study for the following reasons. (1) There is an exact correspondence between an energy circuit diagram and a set of differential equations which describe the time rate of change of the model components. (2) The energy circuit language includes the energetic as well as the kinetic relationships of dynamic systems and therefore concepts such as embodied energy and the energy transformation ratio are easily expressed and analyzed. (3) The set of symbols and conventions which compose the energy circuit language allow the consistent representation of hierarchy and energy quality in systems. Figure 8 presents a list of the major component and process symbols and Table 2 contains a list of the basic rules and conventions for the construction of an energy circuit diagram. Additional information on energy circuit language may be found in Odum and Odum (1976, 1981) and Odum (1983).

The energy circuit language was used to aid the process of system modelling and analysis in several ways. A large, detailed energy model can be employed to obtain an overview of an entire system. In the model the connectivity relationships of system components are visually presented to the mind as a whole instead of piecemeal in a set of equations and this presentation facilitates checking, group discussion, and understanding of the proposed model structure. Each energy circuit diagram translates into a unique set of differential or difference equations, which may be used to patch or write programs for simulation by analog or digital computers, respectively.

Certain model configurations occur again and again in the course of the analysis of many different kinds of systems using the energy circuit language. In this study minimodels were used to examine the wave filter properties of several of those commonly recurring forms. The minimodel is a convenient format for the analysis of complex nonlinear wave filters where simple linear models and linearization techniques are inadequate. In the minimodel, system connectivity relationships are reduced to a manageable size, but still retain some of the uniqueness found in the more complex phenomenon. The behavior of

Figure 8. The major symbols of the energy circuit language used in this study. For more details see Odum (1981, 1983). (a) An energy source of forcing function, (b) heat sink for the outflow of used energy, (c) an interaction where one type of energy A amplifies another type B of lesser quality—when X appears inside the symbol the flows in and out are in proportion to the product of A and B, (d) energy drawn from a flow limited energy source, (e) a storage with depreciation, (f) a general purpose box symbol for indicating boundaries and subsystems, (g) self-maintaining autocatalytic consumer unit, (h) a producing unit that contains autocatalytic and Michaelis-Menten kinetics. The mathematical relationship in (f), (g), and (h) are indicated by diagramming within the symbol as in Figures 10, 12, and 14

a

b

c

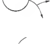

d.

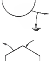

e

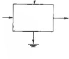

f

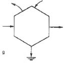

g

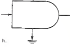

h.

Table 2 A step by step procedure for constructing an emergy circuit diagram

1. Identify a research problem
2. Write down all processes and components that are important in the problem
3. Establish the system boundaries.
4. Arrange all energy sources in order from lowest to highest, starting at the bottom left of the paper and moving to the top right
5. Arrange all important system components on the page, being mindful of their energy quality. Follow the convention that high quality (high transformation ratio) is placed up and to the right
6. Connect the components through processes to each other and to the forcing functions external to the system according to the information which you have.
7. Use group symbols to aggregate components and show hierarchy.

hypothetical minimodels was checked by the simulation of data from similar empirical systems.

Development of Models

Models were constructed in order to aid the human mind in conceptualizing and understanding the complexity of nature. A model is built by first identifying an appropriate problem for investigation. Second, all important phenomena bearing on the chosen problem are identified and some of these are incorporated into a system model. Relationships between the system components may be based upon theoretical considerations, but where possible each relationship should be validated with empirical evidence in order to insure that our understanding is correct as well as to obtain more accurate predictions in simulation. The amount of data available for the calculation of model parameters and the time available for model formulation and simulation may also affect the accuracy of the model's results.

The models developed in this study were used to examine the wave filter characteristics of ecosystem structures. Each of these models consists of a defined and where possible documented set of relationships between system components within the model and the external forcing functions which drive the system's dynamic behavior. All models evaluated were composed of a set of first order linear or nonlinear differential equations. In this study standard ecological generic unit models studied in population ecology are combined in models of increasing complexity so as to include webs, multiple energy sources, and models of observed ecosystems.

Communications Engineering Techniques

The field of classical and statistical communications and control engineering provides several techniques which are useful in the analysis of ecosystems and their simulation models. These techniques are usually employed for the identification and the discovery of the properties of the transfer functions of linear systems. The transfer function simply describes the relationship between the output and the input in lumped linear systems (Lee, 1960) (see Figure 9). Although the nonlinear problem is not as tractable, some of these techniques were employed to gain insights about the properties of nonlinear systems. Transfer functions and energy circuit models are both filters as shown in Figure 9. Some of the classical communications engineering techniques which may be useful in analysis of nonlinear systems are transient analysis, frequency analysis, classical harmonic analysis, and the concept of the transfer function or filter.

Classical Harmonic Analysis

Classical harmonic analysis is the basic method for the analysis of continuous waveforms in dynamic systems. Classical harmonic analysis represents signals and noise as transient or periodic phenomena composed of a sum of sinusoidal waveforms. The Fourier transform pair allows the composition of a signal from known frequencies and the decomposition of a known time signal into its frequency components. This technique assumes that the signal frequencies are additive and therefore the principle of the superposition of waveforms may be applied.

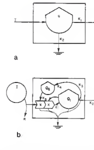

EQUATION

$\dot{Q} = I - k_1Q - k_2Q$

EQUATIONS

$R = I - k_0RQ_1Q_2$

$$\dot{Q}_1 = k_1RQ_1Q_2 - k_2Q_1 - k_3Q_1$$

$$\dot{Q}_2 = k_4Q_1 - k_5RQ_1Q_2$$

Figure 9 Systems as wave filters (a) Simple storage which can be easily transferred to the frequency domain and (b) a more complex energy circuit model which is nonlinear but can be expressed in the frequency domain through simulation

The minimodels and evaluated ecosystem models investigated in this study are deterministic phenomenological formulations of system structures. Therefore, the classical methods of harmonic analysis are appropriate for the study of these cases. Energy, material or information moving along a pathway into, out of, or within a system is defined to be a signal Signals are viewed as composed of a mean value which may have a trend, a periodic component and a noise component. If a signal increases or decreases monotonically over the period of observation it is said to have a trend. A periodic signal is one that repeats a pattern with a given frequency, for example $f(t) = \sin(2\pi ft)$ where t is time and f is frequency, repeats a sine wave with the frequency f Noise is defined to be a random fluctuation in a signal that would otherwise be constant or vary in a specified manner (Van Nostrand's Scientific Encyclopedia, 1976)

Frequency Response Analysis

Frequency response analysis is used to determine how a system output responds to changes in the frequency of system inputs Frequency response analysis observes that when a sinusoidal input signal, $x(t)$, of maximum amplitude a_1 and angular frequency ω rad/sec is input to a system the output $y(t)$ is also a sinusoidal wave of maximum amplitude a_2 and phase $\emptyset$ relative to the input (Milsum, 1966) The relationship between f, frequency, ω, angular frequency and T* period is

$$f = \omega/2\pi = 1/T^* \tag{1}$$

The phase angle ϕ is the angle by which instantaneous values of the sinusoidal waves differ and is usually taken as the phase of the output wave relative to the input. Thus, if a point of the output wave is behind the same point on the input wave it is said to lag the input wave, whereas an output point that precedes its equivalent input point leads the input wave. The amplitude of a sinusoidal wave is defined by the maximum displacement from a mean value. Systems to which frequency analysis is applied are said to have reached a steady state when the amplitude ratio and relative phase shift remain constant. The amplitude ratio is defined as the ratio of the output amplitude to the input amplitude.

Bode plots use logarithmic measures of the amplitude ratio and frequency and linear phase measurement to characterize the frequency response of linear systems (see Figure 5). These plots are often used in control engineering and they provide a linear simplification of system behavior similar to plotting exponential curves on semi-logarithmic paper (Milsum, 1966).

Frequency analysis on the minimodels in this study was performed by choosing a mean value for the input signal, an amplitude for its periodic component, and then allowing the frequency of the signal to vary. The power was then monitored for each component and for the system as a whole. The ratio of variant power used by storages (power out) to variant power input in the source is employed as the basis for evaluating filter properties of nonlinear systems. This ratio is the equivalent of the amplitude ratio used for linear systems. These plots have the $\log_{10}$ of the frequency on the abscissa and a quantity which is also the $\log_{10}$ of the amplitude ratio on the ordinant. When more than one input is driving the system, the frequency analysis is performed by establishing a base simulation run and then varying the frequency of each input signal in turn while the others are held constant.

High Frequency Cutoff and Resonance

Frequency response analysis is used in simulation models to investigate the frequency domain behavior of some nonlinear systems. A basic first order system can be used to illustrate the method and some important filter properties of linear systems that also might be expected to be important in nonlinear systems. Figure 5 shows a Bode frequency response plot for a basic first order system or storage (after Milsum, 1966). The graphs define a low frequency asymptote when ω is small, $\omega^{-\tau} << 1$ and a high frequency asymptote when ω is large, $\omega\tau >> 1$. The low frequency and high frequency asymptotes intersect at the break frequency $\omega_b = 1/\tau$, $\omega t = 1$ where τ is the time constant of the storage. The break frequency is a high frequency cutoff and the amplitude ratio of signals with frequencies greater than ω_b rapidly decreases beyond this point. The phase relationship of the first order system increases from 0 at zero frequency to 90° when ω approaches infinity and is found to be 45° at the break frequency. When more than one energy storage element exists the system may have natural frequencies of oscillation. Figure 6 shows Bode plots for underdamped and overdamped linear second order systems (after Milsum, 1966). The plot for an underdamped system shows resonance when input frequency equals the natural frequency. The high frequency cutoff and resonance frequency concepts are applied in the frequency response analysis of some nonlinear ecosystem filters through the simulation of models and the subsequent construction of frequency response graphs.

Concepts and Definitions Used in the Simulation Models

The following material defines measures and terms that are used in the simulation and evaluation of minimodels and ecosystem models in this study. These particular definitions were used to characterize simulation models in the energy circuit language and for applying concepts and techniques of communications engineering for ecosystem analysis.

Turnover and the Time Constant

The turnover, T, and the time constant, τ, of a system component are the reciprocals of one another. The time constant is commonly expressed as the ratio of storage to flow, whereas the turnover is the ratio of flow to storage. The time constant and the amount of time that it takes a system component to turnover or completely replace a stored quantity are the same. However, the turnover gives the number of times a component replaces itself in a given time unit. In this study turnover, abbreviated T, will be used to describe the turnovers per unit time, whereas the time constant, τ, is the time for a component to replace its storage. Frequency-turnover matching occurs when the turnover is almost equal to the input signal frequency. When turnover is said to be high the input frequency which matches it is also described as high. However, the low time constants match high input frequencies. The terms fast and slow are consistent in matching frequencies for both turnover and the time constant.

Mean, Variance, and Mean Square Calculations

The mean value of all signals evaluated in the minimodels is calculated by formula (2) for digital data from a time series (Otnes and Enochson, 1978).

$$\overline{X} = \frac{1}{N} \sum_{i=0}^{N-1} X(i) \tag{2}$$

The formula for calculating variance is given by (3)

$$S^2 = \frac{1}{N} \sum_{i=0}^{N-1} X(i)^2 - (\overline{X})^2 \tag{3}$$

Since the number of values averaged is always greater than 1,000, the error introduced by using N instead of N-1 in the formula for variance is always less than 0.001 of the actual value.

Equation (3) is the *mean square value* of a sampled signal.

$$m = (\overline{X})^2 + S^2 \tag{4}$$

Where flows were in units that are proportional to the square root of energy, the three terms in Equation (4) are in energy units. Where values used to calibrate the simulated minimodels already were proportional to energy, the mean square calculation had units of $(\text{energy}/\text{time})^2$ for all flows and $(\text{energy})^2$ for storages. The values given for mean square power of flows in the minimodels were then obtained by taking the square root of m giving units of (energy/time).

As indicated in Equation (4), the mean square power of a flow is the sum of the power in the mean (mean power) and that in varying components of the signal (variant power). Thus, the amount of power available to a system will always be the same for a given mean and amplitude of variation.

Definitions of Power Use Functions

In traditional study of system behavior in filtering input signals, some output leaving the system is defined that is compared with the input. In such work the main concern is with what is passed through the system.

In the present study, however, the emphasis is with what part of the input is used by the ecosystem. Instead of output going to another system, the flow of energy used and released from the system in degraded form is taken as the output in many of the analyses. In most cases and in results tables, the energy flow Z in Figure 10 is taken as the 'output' function (power out) for comparison with input. This flow is that which has passed through productive transformations, interactions and storage.

The functions used to evaluate energy flow in both competition and trophic chain minimodels are defined diagrammatically in Figure 10. The energy produced (Y) is the energy transformed at M and is proportional to the energy captured (W). The energy draining from storage (Z) is proportional to the storage (Q_1) and the energy used by the system

Figure 10. Diagrammatic definition of the power use function calculated in simulations. Symbols are defined as follows: energy captured (W), energy used by the system (X), energy produced (Y), energy depreciated by storage (Z), total energy captured (ΣW), sum of energy used by the system (ΣX), sum of energy produced (ΣY), and sum of depreciation (ΣZ). (a) Single autocatalytic consumer, (b) competition of three consumers for the same inflow E, (c) chain of three consumers in series. Equations for the flows that carry energy are:

Rate of change of storage: $Q_1 = k_1RQ_1 - k_2Q_1$

and available remainder of usable energy

$$R = E - k_0RQ_1 \text{ or } R = \frac{E}{(1 + k_0Q_1)}$$

Power used by the system: $X = k_3RQ_1 + k_2Q_1$

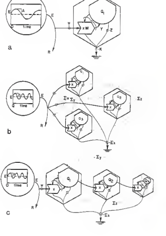
E
A
0
time
E
R
w
x M
Q
Y
-Z
-X
a
E
Q
time
E
R
Q
x
Σw
Σy
Q2
x
Σz
Q3
x
-Σx
b
- Σy
E
0
time
E
w
R
x
Q
x
Q2
x
Q3
Σz
Σx
c

(X) is composed of energy used in both M and Z. In this study the energy captured, the energy produced, and the energy depreciating from storage are employed as the output functions evaluating a minimodel's filter performance when compared to variable energy input in the source E.

An example of the distinction between these terms may be constructed by thinking of Figure 10 in the following manner. E is the energy of sunlight incident upon the biomass of plant matter Q_1 in a meter square surface, R is that portion of the incident light that remains unused, W is the energy of sunlight absorbed by the plant matter, Y represents the energy of sunlight fixed in chemical bonds for use by the plant, Z is the energy used in depreciation of the plant matter, X includes not only the energy of depreciation but also the additional energy used in the process of transforming energy through the interaction at M. In this simple system at steady state, production Y goes into storage Q_1 to replace depreciation loss Z.

Outputs in linear analysis are the flows emerging from a system "black box" beyond the interactions and storages. Output functions of interest in this study were not only leaving the "black box" of system boundaries, e.g., X, but also within a "white box" which reveals internal system structure, e.g., W, Y, and Z. The flow of used energy passing through and out of the system (Z in Figure 10) is made up of a mean power fraction and variant power fraction of the flow converging into the heat sink pathway (Figure 8).

Unit Survival Time and Stability

Another criterion employed in the evaluation of these minimodels is the time which a unit is able to remain a part of its system. The unit survival time is the time from the start to the time at which the unit has a zero value in the simulation. Autocatalytic units that reach zero cannot grow again without another initial seeding.

Stability of models examined in this study was determined by the conditions that no state variable increased without bound and that all components of the system did not go to zero within the time period simulated. If either of the two conditions were true, data for the simulation run was recorded as a dash (---) in the tabular form of the data.

Resonance, Turnover, and Frequency Matching

Resonance phenomena are described in this study by the terms external frequency matching and external-natural frequency matching. External frequency matching refers to the resonant interaction of two periodic input signals through modulation in an interaction (a work gate) (see Figure 8). External-natural frequency matching refers to the resonance possible when an input frequency is equal to a natural oscillation of the system brought about by the interaction of component turnover characteristics.

When the frequency of an input signal is equal to or less than the turnover of a system component, frequency-turnover matching occurs. Frequency-turnover matching should be a property of all systems with low pass components.

Superposition and Modulation

Superposition refers to the property that allows an output signal to be represented as a weighted sum of the input signals. This property is the basis for the simplicity and effectiveness of the transfer function method for analysis of linear systems (Lee, 1960).

Modulation refers to the interaction or multiplication of two periodic signals so that a characteristic such as amplitude, frequency, or phase is varied according to the same or another characteristic of a second wave (Van Nostrand's Scientific Encyclopedia, 1976). Amplitude modulation is the only type considered to be important for the models investigated in this study. When two signals interact the modulation of their amplitudes produces two additional frequency components, one for the sum and one for the difference of the original two frequencies.

Iteration Interval and Nested Models

For most simulation models in this study the iteration interval, dt, was taken to be 0.01 or ten times smaller than the smallest component time constant investigated. An alternate nested configuration employed the same ratio dt/τ for each of the model components. Thus, the solution of each model component could be represented to the same degree of accuracy (Forrester, 1961). This model structure represents the case which might be expected if the phenomena under study were discrete. This configuration was constructed by nesting small dt, fast time constant component DO loops within DO loops of larger iteration interval for the slower time constant components. The same ratio of dt to τ was maintained for each component. This method holds the slow time constant components constant while solving the equations containing faster time constants.

Analysis of Wave Filters

Each of the models examined through simulation in the Results is a linear or nonlinear wave filter. The frequency behavior of most of these models was monitored over all or part of the range of frequency defined by two critical points. The first point is the filter's high frequency cutoff which is approximated by the component turnover that is receiving a varying energy flow from outside the system boundaries. If more than one component receives energy from outside the system, the frequency filtering characteristics of the system will depend on the combination of component turnovers. The second point of interest is that frequency which is long enough to cause the elimination of a system or component. This frequency represents the lower limit of a band pass filter. When only the high frequency cutoff is important, the system behaves like a low pass filter, but when both a high frequency cutoff and a low frequency cutoff determined by catastrophe are relevant the system acts like a band pass filter (see Figure 4).

The characteristics of the minimodel wave filters were examined with respect to the configuration of system components, the component turnover arrangement and the manner in which these components interact. Thus, a system configuration of three components may go through one set of wave filter evaluations based on changing the component turnovers, and another set of evaluations based upon changes in the interaction of the components within the model. Figure 11 shows three possible configurations of three system components representing competition, a trophic chain building a hierarchy and a simple web with competition, cooperation, and hierarchy. Each of these three configurations represents the simplest arrangement of a type of system filter. Variations in component interaction lead to different filter properties for the models. Variations of the three turnover arrangements alter the high frequency cutoff, the low frequency cutoff and the possible resonance frequencies of the system.

Simulation Methods

Simulation of the time dependent behavior of models is the major method employed in this study for the investigation of properties of theoretical minimodels and salt marsh ecosystems. Digital analog and hybrid methods were used in these simulations which were performed on a DEC PDP-11 digital computer operating with an EAI 2000 hybrid-analog computer. Energy circuit diagrams were translated into a set of difference or differential equations for the digital or analog computer. The digital programs were written in Fortran and analog circuit diagrams were drawn and patched to obtain the analog programs.

Techniques Used for the Competition Minimodels

A three unit competition model was simulated with linear and autocatalytic components (production is proportional to a power of the component) for two energy levels. At each energy level the input frequency was varied and the response of power production and use was noted

Figure 11. Three possible arrangements of three autocatalytic units for a source-controlled flow. (a) Competition, (b) a hierarchical trophic chain with units in series, (c) a simple web hierarchy with parallel and series arrangement.

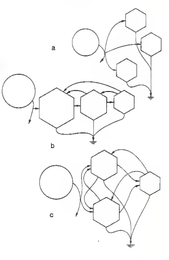
a
b
c

for each component and for the system as a whole. The power production and use was analyzed in terms of its two components, the mean and the variant power These simulations were performed using the same run time of 1,000 time units and using a signal of the same mean and amplitude, leaving frequency as the only variable.

The effect of amplitude variation on the competition models was tested by allowing the signal amplitude to vary while holding the total mean square energy in the input signal constant. Thus, if signal amplitude was increased the energy captured from the mean was decreased in order to compensate for the additional energy added by the increase in amplitude.

The turnover of each competing unit was set by altering the storage of the unit, thus all flows were initially equal for each unit. Flows were allowed to vary in order to test the effect of perturbations on the competition model.

The competition model was used to evaluate a single tank by disconnecting the two units which were not of interest in the simulation, while leaving all flows and storages unaltered The run time of the autocatalytic competition model was extended in order to observe the long run outcome of competition between units of different turnover when all other things were equal.

The differences between superposition and modulation in a system of three competing units were investigated for various combinations of two interacting frequencies The amplitude of the two signals was adjusted so that the model received the same total power that was given to the competition models above

Techniques Used for the Trophic Chain Minimodels

A three unit trophic chain model was simulated for linear and autocatalytic components at two different energy levels. Frequency and amplitude responses of the models were tested as described for the competition model. In addition, four separate turnover arrangements of each model were tested for their response to input frequency variation. The turnover arrangements were altered by changing the unit storages while all flows were left unchanged. The turnover arrangements tested were Case A, turnover of $Q_1 = 10$, $Q_2 = 1$, and $Q_3 = 0.1$, Case B, turnover of $Q_1 = 1$, $Q_2 = 1$, and $Q_3 = 1$, Case C, turnover of $Q_1 = 0.1$, $Q_2 = 1$, and $Q_3 = 10$, Case D, turnover of $Q_1 = 0.1$, $Q_2 = 10$, and $Q_3 = 1$.

The autocatalytic trophic chain model was simulated in eight different configurations representing all combinations of secondary positive feedback possible for a three unit chain structure. In addition, three of these configurations were chosen for further analysis. The units chosen for indepth analysis contained a primary feedback required by autocatalysis and either contained zero, three, or two additional (secondary) positive feedbacks. Model flows were calculated on the assumption that there would be a 10% transfer of energy to the next higher level in the chain and that a feedback must at least simulate as much production as it costs a higher unit in order to be selected.

The power available to the zero and three feedback models was originally set at the same level. But chain models with feedback required more energy to remain stable than did the zero feedback model. Therefore, all eight configurations fo the chain model were simulated with an excess power available which was equal to the power in the input signal variance. The frequency response of the trophic chain models was tested as described for the competition model. These models were simulated over a broad six decade frequency range for Case A turnovers and a narrower three decade frequency range for Cases B, C, and D.

Several models were simulated in another version that allowed large (90%) second law losses of energy at each interaction. The initial simulations did not consider the signal as energy and therefore no losses were subtracted across the interactions. These models were also simulated for the four time constant arrangements subsequently mentioned.

The trophic chain models with zero and three secondary positive feedbacks were simulated in order to examine the effect of the position of a second variable energy source entering the chain at level Q_1, Q_2, or Q_3 on power production and use. The interaction of this second variable energy source was considered for the case when the first energy source at the base of the chain was constant and for the case when it was allowed to vary.

The absolute value of the signal mean entering at each level and the amplitude of variation were adjusted so that the same amount of embodied energy would be present at each level. In addition, the first energy source was adjusted so that the total power entering the system was the same for all input configurations. The assumption that 10% of the energy at a given level is transferred to the next level causes the mean and amplitude of the input signal to fall by a factor of 10 between levels.

The zero secondary feedback model with two variable energy sources and the second source input at Q_1 was simulated sixteen times instead of six times in order to see what could be gained by increased resolution on the Bode-like plot of nonlinear frequency response. A nested version of the trophic chain model was simulated by the methods previously described. Both the linear and zero feedback trophic chains were simulated with excess energy equal to the power in the signal variation in order to compare with levels of power production and use by the models with secondary positive feedbacks.

Techniques Used in the Web Minimodels

The frequency response of four configurations of a three-unit web was tested. The general model has two competitive units in parallel and one hierarchical unit in series. The first configuration had competition between parallel units only, the second configuration had both competition and cooperation, the third configuration had competition and feedback from the next higher level, and the fourth configuration had competition and cooperation between parallel units and feedback from the next higher level. Cooperative flows were added into the power produced by the stimulated unit. However, hierarchical feedbacks were not added to the production of the parallel units. The webs were first simulated with equal turnovers on the parallel units and an order of magnitude slower turnover on the hierarchical unit. Next the competition and cooperation configurations were simulated for the case when parallel units had different turnover and the hierarchical unit had a turnover an order of magnitude slower than the largest parallel unit.

RESULTS

The results are presented as two major blocks of information. The first block considers the frequency filter properties of three commonly occurring ecosystem processes. Hypothetical models are used to examine competition, trophic chain energy transfers and web cooperation and competition, a second block examines three evaluated models of a salt marsh ecosystem at the Kaituna River mouth, Havelock, New Zealand. These models illustrate salt marsh competition, trophic chain organization and overall marsh function.

Filter Properties of Competition Models

Linear and autocatalytic competition between three units of different turnover was simulated in 162 runs. Subtopics examined for the competition model include the iteration interval as a system filter, component turnover spacing, superposition versus modulation, a nested hierarchical model structure and the relationship of the high frequency cutoff to maximum power generation.

Frequency Filtering Properties of Linear Competition

The wave filter properties of a configuration of three linear components in competition for a single flow limited energy were examined (see Figure 12). The three units were identical in all respects except their turnover. The units were unable to exclude one

Figure 12 A simulation model of linear competition between units (Q_1, Q_2, Q_3) of different turnover. The energy flows shown on pathways are for the initial steady state condition of the model. (a) Low energy input, (b) high energy input.

Abbreviations:

I: Inflow energy
R: Energy flow remaining unused
Q: Storage
T: Turnover

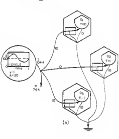

(a)

UNIT EQUATION

$R = I - k_0R$

$Q = k_1R - k_2Q$

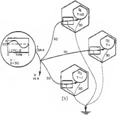

(b)

another, and all three units survived at the same level of storage and flow (see Figure 13). The energy captured by linear units was source controlled; therefore, it was always the same for a given energy input since it depended only on the R term in Figure 12 (see Table 3). Table 3 shows that for linear units the one with faster turnover is able to dissipate the most power over the three decade range of frequency and the two energy levels examined. As the input frequency becomes lower all units are able to exploit more of the incoming energy in variance and therefore they are able to dissipate a greater fraction of the energy available to them. This causes the total MSQ power used to increase as the input frequency becomes lower.

Figure 13 shows the manner in which the turnover of a linear system component sets the high frequency cutoff for variant power passed through the component, Q_1 has a turnover of 10 and is able to exploit most of the power from frequencies 1, 10, and 50 cycles per unit time, whereas component Q_3 with a turnover of 0.1 fails to absorb most of the power at 10 and 50 cycles per unit time.

The effect of a change in the energy available in variance upon the power used by storage was small compared to that of a similar change in the available mean power (see Table 4). Faster turnover units always use more of the variance captured than do slow turnover units even through they each capture the same amount. More variant power is captured and used by storages as the amplitude of the input signal increases.

Figure 13 Simulation of model in Figure 12 shows the power dissipated and storages maintained by three competing linear components with different turnovers Q_1, $T = 10$, Q_2, $T = 1.0$, Q_3, $T = 0.1$ exposed to superposed energy input with frequencies of 1, 10, and 50 cycles/sec and amplitude = 10. (a) Energy remaining, R, (b) storage, (c) power dissipated by storages

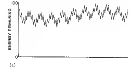
100
ENERGY REMAINING
0
(a)

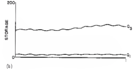
200
STORAGE
Q_3
Q_1
0
(b)

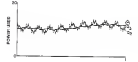
20
POWER USED
Q_1
Q_3
Q_2
0
(c)
TIME

Table 3 The power (mean + variance) and variant power used by three competing linear units over a three decade frequency range for high and low energy inputs * (A) The power used by storages (B) The variant power used by storages

	Input Frequency Cycles/Time Unit	Power Out			Total Power Out
		Q_1 T = 10	Q_2 T = 1.0	Q_3 T = 0.1	
(A)	10.0	9.581	9.577	9.581	28.74
Low energy	1.0	9.733	9.582	9.581	28.90
(30 units input)	0.1	9.788	9.731	9.590	29.11
	10.0	28.74	28.72	28.75	86.21
High energy	1.0	29.20	28.74	28.74	86.68
(90 units input)	0.1	29.36	29.19	28.77	87.32

		Variant Power Out			Total Variant Power Out
		Q_1	Q_2	Q_3	
(B)	10.0	0.008	0.001	0.012	0.021
Low energy	1.0	0.160	0.010	0.000	0.170
(30 units input)	0.1	0.216	0.157	0.010	0.383
	10.0	0.020	0.010	0.010	0.040
High energy	1.0	0.480	0.020	0.020	0.520
(90 units input)	0.1	0.640	0.470	0.050	1.160

*Signal amplitude = 30 units, Run time = 1,000, T = turnover, energy captured at low input = 9.788 for all frequencies, energy captured at high input = 29.37 for all frequencies

Table 4. The power, mean power, and variant power produced and used by three competing linear storages as a function of amplitude for high and low energy inputs. (A) Power produced and used by storages. (B) Mean power produced and used by storages. (C) Variant power produced and used by storages *

	Input Amplitude	Energy Remaining	Power Produced			Power Out			Total Power	
			Q_1 T = 10	Q_2 T = 1.0	Q_3 T = 0.1	Q_1 T = 10	Q_2 T = 1.0	Q_3 T = 0.1	Produced	Out
(A)	0	74.4	9.997	9.997	9.997	9.997	9.997	9.997	29.99	29.99
Low Energy	10	70.5	9.972	9.972	9.972	9.965	9.948	9.972	29.92	29.89
	30	74.4	9.788	9.788	9.788	9.733	9.582	9.581	29.36	28.90
	50	81.8	9.484	9.484	9.484	9.345	8.957	8.954	28.45	27.26
	0	14.4	30.01	30.01	30.01	30.01	30.01	30.01	90.03	90.03
High Energy	10	10.5	29.92	29.92	29.92	29.90	29.84	29.84	89.76	89.58
	30	14.4	29.37	29.37	29.37	29.20	28.74	28.74	88.11	86.68
	50	21.8	28.45	28.45	28.45	28.04	26.87	26.86	85.35	81.77

Table 4—Continued

	Input Amplitude	Energy Remaining	Mean Power Produced			Mean Power Out			Total Mean Power	
			Q_1 T = 10	Q_2 T = 1.0	Q_3 T = 0.1	Q_1 T = 10	Q_2 T = 1.0	Q_3 T = 0.1	Produced	Out
(8) Low energy	10	70.5	9.943	9.943	9.943	9.945	9.945	9.939	29.83	29.93
	30	74.4	9.572	9.573	9.572	9.573	9.572	9.581	28.72	28.73
	50	81.8	8.939	8.939	8.939	8.939	8.940	8.948	26.82	26.83
High energy	10	10.5	29.83	29.83	29.83	29.83	29.83	29.83	89.49	89.49
	30	14.4	28.72	28.72	28.72	28.72	28.72	28.72	86.16	86.16
	50	21.8	26.82	26.82	26.82	26.82	26.82	26.85	80.46	80.49

Table 4—Continued

	Input Amplitude	Energy Remaining	Variant Power Produced			Variant Power Out			Total Variant Power	
			Q_1 $T = 10$	Q_2 $T = 1.0$	Q_3 $T = 0.1$	Q_1 $T = 10$	Q_2 $T = 1.0$	Q_3 $T = 0.1$	Produced	Out
(C)	10	70.5	0.029	0.029	0.029	0.020	0.003	0.009	0.087	0.032
Low energy	30	74.4	0.216	0.216	0.216	0.160	0.009	0.000	0.648	0.169
	50	81.8	0.545	0.545	0.545	0.406	0.017	0.006	1.635	0.429
	10	10.5	0.090	0.090	0.090	0.070	0.010	0.010	0.270	0.090
High energy	30	14.4	0.650	0.650	0.650	0.630	0.130	0.010	1.950	0.770
	50	21.8	1.630	1.630	1.630	1.220	0.050	0.010	4.890	1.280

*Low energy - 30 units input, high energy = 90 units input, input frequency - 1 cycle per unit time. Run time = 1,000. MSQ power input to the system is constant at each amplitude

Comparison of Steady and Varying Power for Linear Competition

In general, there is more power available to a system in a steady signal than in a periodic or a noisy signal with the same mean square energy. Power in the mean energy available to the system is more easily exploited by components than the power in variance (Costanza, 1978). Table 4 demonstrates this result, since a constant signal contributes more power used by the system storage than one of equal power with varying amplitude. Also, Table 4 shows that the more power available to a linear system that is in the varying amplitude instead of the mean, the lower will be the power used by the system components.

Table 5 shows that there is approximately an order of magnitude difference between the change in power use effected by a change in the signal mean and that brought about by a similar change in the amplitude of the input signal. A decade change in signal frequency elicits a change in power use that is yet an order of magnitude smaller than that brought about by a change of 20 units of amplitude.

Analog versus Digital Simulation of Autocatalytic Competition

The minimodel shown in Figure 14 depicts autocatalytic competition among units for the same energy source. Initially the analog simulation of this minimodel seemed to give different results from its digital simulation. Figure 15 shows how one component outcompetes the other two when all are equal initially in the analog simulation. Figure 16 shows a digital simulation with the same values in which all three units survive. This seeming contradiction may be resolved if the

Table 5 The affect of changes in signal mean, amplitude, and frequency on the power used by three competing linear storages. The changes are calculated from data in Tables 3 and 4 for (A) the high energy input case and (B) the low energy input case

	Change in Mean	Change in Amplitude	Change in Frequency	Change in Total Power Out
(A)	+20	---	---	+20
	---	-20	---	+2.90
	---	+20	---	-4.41
	---	---	x10	-0.47
	---	---	x0.1	+0.64
(B)	+20	---	---	+20
	---	-20	---	+0.99
	---	+20	---	-1.64
	---	---	x10	-0.16
	---	---	x0.1	+0.21

Figure 14. A simulation model of autocatalytic competition between components Q_1, Q_2, and Q_3, of different turnover, T. The energy flows shown are for the initial steady state condition of the model. (a) Low energy captured; (b) high energy captured. For abbreviations see Figure 12.

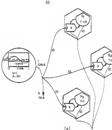

(a)

UNIT EQUATION

$R = I - k_0RQ$

$Q - k_1RQ - k_2Q$

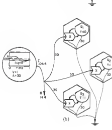

(b)

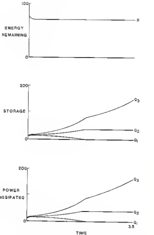

Figure 15 Analog simulation of three competing autocatalytic units in Figure 14. Turnover time of Q_1, Q_2, and Q_3 - 1.0

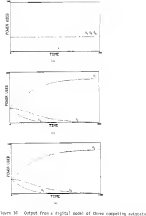

Figure 16 Output from a digital model of three competing autocatalytic units in Figure 14. Iteration interval, dt = 0.01. (a) When flows are set equal all units survive at a similar level, (b) when inflow to Q_1 is increased 10% and inflow to Q_2 is increased 5% Q_1 dominates, (c) when the outflow of Q_1 is increased 10% and the outflow of Q_2 is increased 5%, Q_3 dominates. All units have equal turnover

digital model's flows are slightly perturbed [see Figure 15(b) and (c)]. Under a small perturbation of either inflow or outflow a unit may be augmented or diminished enough to bring success or exclusion in the struggle for survival. Since the voltages on analog pots are hardly ever set precisely equal, one system component invariably is enough different from the others so that exclusion takes place.

Filter Properties of the Iteration Interval and Aliasing

The mean square power captured or used and the survival time of components in a three unit autocatalytic competition model is affected by the iteration interval chosen. Table 6 shows how the iteration interval acts as a system filter by causing components with time constants much smaller than dt to be unstable. This concept leads to spurious results when the input frequency is too high to be represented by dt. This is due in part to aliasing of high frequency input to lower frequencies. Aliasing is seen by examining the lines in Table 6 for input frequency, 10, with dt, 0.1, input frequency, 10, with dt, 1, and input frequency, 1, with dt, 1.0, where the values for energy captured and used approach those for a constant input. The instability of components with time constants very much less than dt occurs where input frequencies are faster than or equal to the iteration interval. Figure 17 shows that when dt is small units with fast time constants successfully compete with those of slower time constants, but as the system filter becomes coarser (dt increases) slower time constant

Table 6. The effect of the iteration interval on the power produced and used by storage and the survival time of three competing autocatalytic units.*

		Power Produced			Power Out				
Frequency	dt	Q_1 T = 10	Q_2 T = 1.0	Q_3 T = 0.1	Q_1 T = 10	Q_2 T = 1.0	Q_3 T = 0.1	Total Power Out	Survival Time Q_1, Q_2
10.0	0.01	9.647	50.10	32.50	9.458	48.99	31.76	90.21	400
1.0	0.01	10.780	49.58	32.41	10.620	48.51	31.70	90.83	400
0.1	0.01	29.820	31.42	30.19	29.800	31.35	30.12	91.27	>1,000
0.0	0.01	30.010	30.01	30.01	30.010	30.01	30.01	90.03	>1,000
10.0	0.10	28.250	29.03	29.88	28.250	29.03	29.89	87.17	>1,000
1.0	0.10	2.927	51.00	36.15	2.942	49.93	35.25	88.12	40
0.1	0.10	11.810	50.96	33.26	11.810	50.46	32.84	95.10	170
0.0	0.10	26.070	29.59	29.96	26.070	29.59	29.96	85.62	1,000
10.0	1.00	1.483	35.29	30.57	1.572	35.29	30.57	67.43	0
1.0	1.00	1.488	50.89	31.89	1.577	50.87	31.87	84.32	0
0.1	1.00	2.168	25.69	72.08	2.351	26.71	70.16	99.22	590
0.0	1.00	1,488	53.48	32.05	1.577	53.46	32.03	87.10	0

*Run time - 1,000, dt = iteration interval.

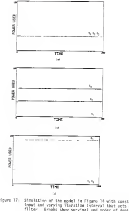

Figure 17. Simulation of the model in Figure 14 with constant energy input and varying iteration interval that acts as a system filter. Graphs show survival and order of dominance of units in competition when the units have different time constants. (a) Iteration interval = 0.01—all survive at the same level, (b) iteration interval = 1.0—T = 1 dominates, T = 10 excluded, (c) iteration interval = 5.0—T = 0.1 only survives.

components become dominant in turn as sensitive values of dt are crossed In this case the iteration interval acts as a high frequency cutoff determining survival of system components

When a sensitive range of dt is approached a small perturbation of the flows may lead to a large change in the system configuration For example, Figure 15 and Table 7 show the effect of perturbation upon the system structure, Dt = 0.6 is a sensitive point for the survival of Q_1. If the inflow to Q_1 is increased 10% at this dt, the Q_1 component flows and storage bifurcate into a noisy oscillation which eventually leads to the demise of Q_1 with a consequent increase of the other two components The system maintains a higher capture and use of available power at this point than it does at dt = 0.4 and 0.8 in Table 7. The model solutions were not noisy for a perturbation of 1% but they show bifurcated solutions at dt = 0.4, 0.6, and 0.8 When dt = 0.01 in Table 7, Q_1 dominates the other components for step increases of 1% and 10% of the inflow to Q_1

The minimodels used to investigate competition and trophic chains are simulated over a six decade range of frequency for a period of time that is at least as long as the largest period investigated. In order to have the results printed out on a reasonable length of paper and in a short period of time a large plotting interval must occasionally be used. The plotting interval acts as a system filter on the output just as the iteration interval does However, in the case of the plotting interval it is a matter of appearance only The large plotting interval aliases the absorbed high frequency inputs to lower

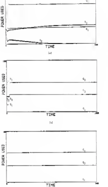

Figure 18 Simulation of model in Figure 14 with iteration intervals in a sensitive range for Q_1's behavior A perturbation of flow (inflow of Q_1 + 10% leads to bifurcation, then noise generation and the eventual transfer of dominance from Q_1 to Q_2 (a) Dt - 0.4, bifurcation gives two solutions, (b) Dt = 0.5, chaotic behavior or noise generation, (c) Dt - 0.8, Q_2 is dominant from the start

Table 7 The power produced and used by storage and the survival time for units in autocatalytic competition when the inflow to Q_1 is increased by (A) 1% and by (B) 10% and the iteration interval, Dt, is variable

Dt	Power Produced Q_1 T = 10	 Q_2 T = 1.0	 Q_3 T = 0.1	Power Out Q_1 T = 10	 Q_2 T = 1.0	 Q_3 T = 0.1	Total Power Produced	 Out	Survival Time Q_1, Q_2, Q_3
(A) Increase of 1%									
0.01	68.830	6.685	19.730	68.830	6.950	19.930	96.45	96.71	---, 290, ---
0.40	50.680	11.780	28.330	51.050	11.800	28.270	90.79	91.12	---, ---, ---
0.60	32.650	26.530	31.230	32.830	26.520	31.150	90.31	90.60	---, ---, ---
0.80	23.170	34.930	32.250	23.380	34.920	32.170	90.35	90.47	---, ---, ---
(B) Increase of 10%									
0.01	68.200	2.115	6.452	88.190	2.310	7.086	96.77	97.58	---, 40, 300
0.40	55.130	4.151	34.360	58.410	4.207	33.480	93.64	96.10	---, 430, ---
0.60	6.969	55.800	33.360	7.321	55.780	33.310	96.13	96.41	40, ---, ---
0.80	2.126	57.430	32.480	2.307	57.410	32.460	92.04	92.17	0, ---, ---

frequencies which are seen most clearly in the outputs of nested chain and competition configurations with high frequency inputs. This aliasing does not affect the dominance of components in the competition model, since several plotting intervals give the same result with respect to component survival and MSQ power values.

Comparison of Linear and Autocatalytic Competition

The high frequency cutoff is the critical factor in determining how successfully a low pass system component exploits incoming energy frequencies. This relation is true for both linear and autocatalytic units as can be seen by referring to Table 9. For a single storage not in competition with others, the unit with the fastest turnover uses the most power at all frequencies tested. In addition, the autocatalytic unit with the fastest turnover is able to capture the most power available to the units. These same relationships are seen in the variant power produced and used by storages of both types of units. In Table 9 the power captured by autocatalytic units exceeds that captured by linear units by almost 20 energy units. This indicates that where excess energy above a threshold is available, nonlinear system components are able to draw more power than are linear ones.

Table 9 gives the response of the linear competition model shown in Figure 12 to constant, periodic, and noisy input signals at low, medium, and high values of energy input to the model. Table 10 supplies the same information for the autocatalytic competition model given in Figure 14. In general, both linear and nonlinear competition

Table 8 The total power and variant power produced and used by a single linear storage in Figure 12(b) and a single autocatalytic storage in Figure 14(b) The frequency of an input signal of amplitude 30 varies

Storage Type	Frequency Input	Total Power Produced			Total Power Out		
		T = 30	T = 3.0	T = 0.3	T = 30	T = 3.0	T = 0.3
Linear	10.0	69.05	69.05	69.05	67.93	67.54	67.44
	1.0	69.05	69.05	69.05	69.00	67.82	67.45
	0.1	69.05	69.05	69.05	69.05	68.98	67.74
Autocatalytic	10.0	87.41	87.45	87.42	85.96	85.55	85.37
	1.0	88.12	87.55	87.42	88.04	85.93	85.38
	0.1	88.16	88.12	87.52	88.16	88.00	85.78

Table 8—Continued

Storage Type	Frequency Input	Variant Power Produced			Variant Power Used		
		T = 30	T = 3.0	T = 0.3	T - 30	T - 3.0	T - 0.3
Linear	10.0	1.53	1.53	1.53	0.41	0.04	0.07
	1.0	1.53	1.53	1.53	1.46	0.30	0.05
	0.1	1.53	1.53	1.53	1.53	1.47	0.31
Autocatalytic	10.0	1.98	1.92	1.93	0.53	0.03	0.11
	1.0	2.58	2.02	1.93	2.50	0.42	0.06
	0.1	2.62	2.58	2.02	2.62	2.48	0.43

*The inflow and outflow of two units in the three unit model is set to 0 to get the single unit case. Run time - 1,000

Table 9 Power produced and used by three linear units in competition for constant, periodic, and noise inputs

			Power Produced			Power Out			Total Power	
Frequency	Amplitude	Energy Input	Q_1 T = 10	Q_2 T = 1.0	Q_3 T = 0.1	Q_1 T = 10	Q_2 T = 1.0	Q_3 T = 0.1	Produced	Out
(A) Constant Input										
---	---	30	9.997	9.997	9.997	9.997	9.997	9.997	29.99	29.99
---	---	60	19.990	19.990	19.990	19.990	19.990	19.990	59.97	59.97
---	---	90	30.010	30.010	30.010	30.010	30.010	30.010	90.03	90.03
(B) Periodic Input										
1.0	30	30	9.788	9.788	9.788	9.788	9.733	9.531	29.36	29.10
1.0	30	60	19.580	19.580	19.580	19.550	19.190	19.160	58.74	57.90
1.0	30	90	29.370	29.370	29.370	29.350	28.850	28.730	88.11	86.93
(C) Noise Input										
All	30	30	9.592	9.592	9.592	9.444	9.437	9.442	28.78	28.32
All	30	60	19.180	19.180	19.180	18.890	18.870	18.880	57.54	56.47
All	30	90	28.780	28.780	28.780	28.330	28.310	28.320	86.34	84.96

*T - turnover, run time = 1,000

Table 10. The power produced and used by three autocatalytic units in competition for constant, periodic, and noise inputs

			Power Produced			Power Out			Total Power		Survival Time
Frequency	Amplitude	Energy Input	Q_1 T = 10	Q_2 T = 1.0	Q_3 T = 0.1	Q_1 T = 10	Q_2 T = 1.0	Q_3 T = 0.1	Produced	Out	Q_1
(A) Constant Input											
---	---	30	9.997	9.997	9.997	9.997	9.997	9.997	29.99	29.99	1,000
---	---	60	19.990	19.990	19.990	19.990	19.990	19.990	59.97	59.97	1,000
---	---	90	30.010	30.010	30.010	30.010	30.010	30.010	90.03	90.03	1,000
(B) Periodic Input											
1.0	30	30	2.165	14.470	10.680	2.129	14.150	10.440	27.32	26.72	140
1.0	30	60	3.690	33.650	22.350	3.653	32.940	21.860	59.69	58.45	60
1.0	30	90	10.780	49.580	32.410	10.620	48.510	31.700	92.77	90.83	50
(C) Noise Input											
All	30	30	1.757	13.090	10.500	1.734	12.870	10.320	25.35	24.92	280
All	30	60	7.101	30.710	21.260	7.009	30.250	20.930	59.07	58.19	530
All	30	90	11.800	47.410	31.380	11.650	46.690	31.480	91.17	89.82	590

*T = turnover, run time = 1,000

models are able to produce and use more of the energy available if presented with a constant signal. Both types of units are also better able to exploit periodic input signals than noisy input signals. Table 10 shows that autocatylic units at high energy input are able to capture and use more energy from a variable signal than they could from a constant signal. Comparing Table 9 to Table 10 reveals that linear competition captures and uses more power at low energy levels whereas autocatalytic units are more successful at higher energy inputs.

Dominance Controlled by Frequency and Turnover

When three units of different turnover are in either linear or autocatalytic competition for a constant input signal no one unit dominates its fellow competitors. If noise or periodicity is added to this constant energy input, an order of dominance is produced in the components of both models (see Tables 9 and 10). When three competing linear or autocatalytic units have the same turnover no single unit is able to dominate the others even though they are presented with variable energy inputs. However, when each unit is given a different turnover, an order of dominance is established (see Table 11). Autocatalytic dominance occurs faster and usually results in the exclusion of one or more components within a time frame of 1,000 units. Linear dominance consists of one unit using slightly more power than another and never results in the exclusion of a unit over the range of flows and times tested.

Table 11. Comparison of competition between three autocatalytic units when all have equal turnover and when each unit has a different turnover

	Power Produced			Power Out			Total Power		Survival Time
Frequency	Q_1 T = 1.0	Q_2 T = 1.0	Q_3 T = 1.0	Q_1 T = 1.0	Q_2 T = 1.0	Q_3 T = 1.0	Produced	Out	Q_1
10.0	29.160	29.16	29.16	28.630	28.53	28.53	87.48	86.59	1,000
1.0	29.160	29.16	29.16	28.540	28.54	28.54	87.48	85.62	1,000
0.1	29.310	29.31	29.31	29.100	29.10	29.10	87.93	87.30	1,000
	Power Produced			Power Out					
	Q_1 T = 10	Q_2 T = 1.0	Q_3 T = 0.1	Q_1 T = 10	Q_2 T = 1.0	Q_3 T = 0.1			
10.0	9.647	50.10	32.50	9.458	48.99	31.76	92.25	90.21	400
1.0	10.780	49.58	32.41	10.620	48.51	31.70	92.77	90.83	390
0.1	29.82	31.42	30.19	29.800	31.35	30.12	91.43	91.27	1,000

Behavior of the Autocatalytic Competition Model

If the system components of the autocatalytic competition model shown in Figure 14 are given different turnovers, an order of dominance in time is established when the system is supplied with a periodic or noisy input. Slow turnover units are dominant after longer times when they exclude faster turnover units that may be dominant in the short run [see Figures 19(i) and (k)]. The length of time that an autocatalytic unit may survive in competition is increased as the frequency of the input signal becomes slower or faster in relation to its turnover [observe Q_1 in Figure 19(a), (b), (c), and (d)]. The extent of time over which a unit dominates others may be decreased by matching the unit's time constant withthe incoming energy frequency. A unit reaches its maximum value and declines more quickly as the input signal frequency is closer to the units turnover (observe Q_2 in Figure 19).

Figure 20 shows the effect of variation in the amplitude of a given input frequency on the behavior of the autocatalytic competition model in Figure 14. As the amplitude of the input signal increases the matched unit, Q_2, reaches a maximum value more quickly as shown by Figure 20(a), (b), and (c). On the other hand, Q_1 with turnover time 10 does best for low input amplitude. A comparison of Figure 20(d) with Figure 19(h) demonstrates that Q_2 reaches a peak earlier and declines allowing the largest unit to dominate more quickly when input amplitude is greater and input frequency matches Q_2's turnover. A second comparison of Figure 20(e) with Figure 19(i) demonstrates the effect of an increase in signal amplitude on accelerating the dominance of a matched component even more dramatically.

Figure 19 Simulation of model in Figure 14 with different frequencies of the forcing functions. The energy input signal had a mean of 100 and an amplitude of 30 for all simulations.

(a) Input frequency = 50. Q_2 dominates Q_3, Q_1 excluded before 1,000 time units

(b) Input frequency = 10. Q_2 dominates Q_3, Q_1 excluded before 1,000 time units

(c) Input frequency = 1. Q_2 dominates Q_3, Q_1 excluded before 1,000 time units

(d) Input frequency = 0.1. Q_1, Q_2, and Q_3 exist at similar levels of energy use after time 1,000

(e) Input frequency = 0.01. Q_1, Q_2, and Q_3 exist at a similar level after time 1,000

(f) Input frequency = 0.001. Q_1, Q_2, and Q_3 exist at a similar mean level after time 1,000

(g) Input frequency = 10. Q_1 was excluded, Q_2 reached a maximum and declined, Q_3 continued to increase after time 10,000

(h) Input frequency = 1.0. Same as (g)

(i) Input frequency = 0.01. Q_1 excluded, Q_2 reaches maximum and declines, Q_3 continues to increase after time 10,000

(j) Input frequency = 0.01. Q_1, Q_2, and Q_3 all exist at a similar mean level after time 10,000

(k) Input frequency = 0.1. Q_3 is dominant, Q_1 and Q_2 are excluded after time 100,000

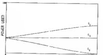
100
POWER USED
u_2
u_3
u_1
0
TIME
1000

(a)

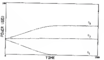
100
POWER USED
u_2
u_3
u_1
0
TIME
1000

(b)

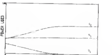
100
POWER USED
u_2
u_3
u_1
0
TIME
1000

(c)

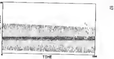
100
POWER USED
u_1
u_3
u_2
0
TIME
1000

(d)

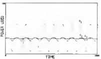
100
POWER USED
e_1
e_2
e_3
0
TIME
1000

(e)

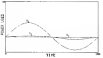
100
POWER USED
e_1
e_2
e_3
0
TIME
1000

(f)

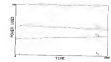
100
POWER USED
e_1
0
TIME
1000

(g)

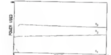
100
POWER USED
e_2
e_3
e_1
0
TIME
10000

(h)

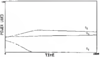
100
POWER USED
a_2
a_3
a_1
0
TIME
10000

(a)

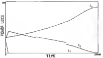
100
POWER USED
a_3
a_2
a_1
0
TIME
10000

(b)

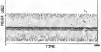
100
POWER USED
a_1
a_2
0
TIME
10000

(c)

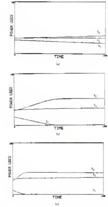

Figure 20. Simulation of model in Figure 14 with varying source amplitude. (a) Input frequency 1, amplitude 10, run time = 1,000; (b) input frequency 1, amplitude 30, run time - 1,000, (c) input frequency 1, amplitude 50, run time - 1,000, (d) input frequency 1, amplitude 50, run time = 10,000, (e) input frequency 0 1, amplitude 50, run time - 10,000

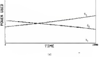
100
POWER USED
q_3
q_2
q_1
0
TIME
10000

(d)

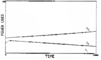
100
POWER USED
q_3
q_2
q_1
0
TIME
10000

(e)

Filter Properties of Autocatalytic Competition

The results of simulating autocatalytic competition over a range of frequencies at two energy levels are given in Table 12. The fast turnover unit is excluded by slower turnover units over the range of frequencies tested when a low proportion of the total energy available is utilized by the system. The total power captured and used by Q_1 increased with longer frequency inputs in both low and high energy cases. The survival time for the fast turnover unit is longest for low frequency high energy input and shortest for low frequency low energy input. Total energy captured and used may increase for two reasons. Either a unit exists as a part of the system for a longer period of time or it exists at a higher energy level for the same or a shorter time period. The increase in total power observed occurs for a different reason at low energy than at high energy. At low frequency and low energy input, Q_1, the unit with fastest turnover pulses and thus gives a higher power use in a shorter time period than it does for high frequencies. Whereas, in the low frequency, high energy case Q_1 exists for a longer period of time (see Table 12) than it does for high frequency input. Some additional information about these results is gained from examining the variant power in Table 12. Fast turnover units are almost always able to use a greater proportion of the variance they capture than are slower turnover units. When the input frequency is low all units capture variance equally well. The interesting thing with regard to autocatalytic units is the competition reflected by the amount of variant power each competing unit is able to produce and thereby prevent

Table 12. The power (mean + variance) and variant power produced and used by three competing autocatalytic storages (Figure 14) over a three decade range of frequency for high and low energy inputs

Frequency	Energy Input	Power Produced			Power Out			Total Power		Survival Time
		Q_1 T = 10	Q_2 T = 1.0	Q_3 T = 0.1	Q_1 T = 10	Q_2 T = 1.0	Q_3 T = 0.1	Produced	Out	Q_1
Low Energy										
10.0	30	2.012	14.480	10.690	1.974	14.160	10.450	26.86	26.58	110
1.0	30	2.165	14.470	10.690	2.129	14.160	10.440	27.32	26.72	140
0.1	30	5.876	14.160	10.510	5.862	13.910	10.310	30.55	30.08	10
High Energy										
50.0	90	13.700	45.200	31.970	13.480	44.20	31.250	90.94	88.93	810
10.0	90	9.647	50.100	32.500	9.458	48.990	31.760	92.25	90.21	400
1.0	90	10.780	49.580	32.410	10.620	48.510	31.700	92.77	90.83	390
0.1	90	29.820	31.420	30.190	29.800	31.350	30.120	91.43	91.27	1,000

Table 12—Continued

Frequency	Energy Input	Variant Power Produced Q_1 T = 10	 Q_2 T = 1.0	 Q_3 T = 0.1	Variant Power Used Q_1 T = 10	 Q_2 T = 1.0	 Q_3 T = 0.1	Total Variant Power Produced	 Out	Survival Time Q_1
Low Energy										
10.0	30	0.998	0.400	0.240	0.959	0.090	0.010	1.638	1.059	---
1.0	30	1.126	0.410	0.240	1.089	0.100	0.000	1.776	1.189	---
0.1	30	3.660	1.100	0.220	3.645	0.840	0.020	4.980	4.505	---
High Energy										
10.0	90	2.558	1.210	0.840	2.511	0.100	0.060	4.608	2.671	---
1.0	90	4.319	1.420	0.770	4.295	0.400	0.050	6.509	4.745	---
0.1	90	5.820	0.340	0.020	5.820	0.330	0.020	6.180	6.170	---

another unit from capturing for use in its production. Low time constant units are able to capture a portion of the variance available at high frequency but they are unable to use what they capture. As the input frequency becomes lower the high turnover unit captures more of the variant power and it is able to use what it captures.

Table 13 shows the behavior of the autocatalytic competition model given in Figure 14 when the input energy has a frequency of 1 cycle per unit time and amplitude is allowed to vary. For Table 13 the energy remaining is adjusted so that the same mean square power is available to the system regardless of the amplitude of the input signal. At low energy input the total power captured and used is greatest when constant energy input makes up the greatest proportion of the available input energy. However, in the case of high energy input the most energy is captured and used for amplitude 30 when the input frequency is 1 cycle per unit time. Component Q_2 has a turnover of one per unit time which matches the input signal frequency and this unit captures the most available energy at most amplitudes tested. Component Q_1 has a turnover of 10 and captures and uses more energy and survives longer when input amplitude is least. Component Q_3 with a turnover of 0.1 usually captures and uses more energy when input amplitude is greater. Examining the variant power portion of Table 13 reveals that the results of the competition for variance are almost the same at low and high energy input. In both cases units with fast turnover are more successful in the capture of variance at signal amplitude, 30. Units with slower turnover capture more variant power as the input amplitude is increased.

Table 13. The power (mean + variance) and variant power produced and used by three competing autocatalytic storages as a function of the amplitude for high and low energy inputs (see Figure 14)*

Amplitude	Energy Remaining	Power Produced			Power Out			Total Power		Survival Time Q_1
		Q_1 $T = 10$	Q_2 $T = 1.0$	Q_3 $T = 0.1$	Q_1 $T = 10$	Q_2 $T = 1.0$	Q_3 $T = 0.1$	Produced	Out	
Low Energy										
10	70.5	8.488	11.030	10.13	8.470	11.000	10.10	29.65	29.57	1,000
30	74.4	2.165	14.470	10.68	2.129	14.150	10.44	27.32	26.72	140
50	81.8	0.484	8.562	10.68	0.480	8.081	10.06	19.73	18.62	>10
High Energy										
10	10.5	26.900	32.650	30.33	26.850	32.580	30.26	89.88	89.69	1,000
30	14.4	10.780	49.680	32.41	10.620	48.510	31.70	92.77	90.83	400
50	21.8	4.900	47.610	34.07	4.631	44.910	32.10	86.48	81.63	100

Table 13—Continued

Amplitude	Energy Remaining	Variant Power Produced			Variant Power Used			Total Variant Power		Survival Time Q_1
		Q_1 $T = 10$	Q_2 $T = 1.0$	Q_3 $T = 0.1$	Q_1 $T = 10$	Q_2 $T = 1.0$	Q_3 $T = 0.1$	Produced	Out	
Low Energy										
10	70.5	0.101	0.050	0.03	0.083	0.020	0.00	0.181	0.013	---
30	74.4	1.126	0.410	0.24	1.088	0.100	0.00	1.776	1.128	---
50	81.8	0.444	0.501	0.62	0.438	0.017	0.00	1.565	0.455	---
High Energy										
10	10.5	3.330	1.050	0.07	3.310	0.880	0.01	4.450	4.300	---
30	14.4	4.318	1.420	0.77	4.295	0.400	0.05	6.508	4.745	---
50	21.8	2.310	3.040	2.72	2.280	0.880	0.35	8.070	3.520	---

*Input frequency = 1 cycle/unit time, run time = 1,000. The energy remaining is adjusted so that the MSQ energy input remains constant at each amplitude.

Table 14 gives the same results for amplitude variation at the given input frequency when the total energy remaining is kept constant, thereby creating additional mean square energy when amplitude is increased and decreasing the mean square energy when amplitude decreases. Power produced is greatest when input amplitude is largest but the power used is greatest at input amplitude 30. Unit Q_1 pulsed more quickly as input amplitude was increased, it produced and used more variant power but less mean power. This tradeoff produced a maximum power use at output amplitude 30.

Table 15 shows the magnitude of the effects of changes in input mean amplitude and frequency upon the autocatalytic competition model for both high and low energy levels. The changes in power use brought about by changes in amplitude and frequency can be greater in the autocatalytic model than in the linear model. Some changes in amplitude and frequency show that the mean is an order of magnitude greater effect than amplitude which in turn is an order of magnitude greater than frequency. Other changes show that an amplitude change can account for almost 50% of the variation produced by a similar change of the mean. Also a decade frequency change may be greater than some amplitude changes of 20 units and as much as 16% of a 20 unit change in the mean.

Component Turnover Spacing

When the turnovers of all system components in Figure 14 are close together (Q_1 = 2, Q_2 = 1, Q_3 = 0.5) as shown in Table 16(A), the total power produced and used by the system is greatest when the input

Table 14. The power (mean + variance) and variant power produced and used by three competing autocatalytic storages as a function of amplitude for high and low energy inputs*

Amplitude	Energy Remaining	Power Produced			Power Out			Total Power		Survival Time
		Q_1 T = 10	Q_2 T = 1.0	Q_3 T = 0.1	Q_1 T = 10	Q_2 T = 1.0	Q_3 T = 0.1	Produced	Out	Q_1
Low Energy										
10	74.4	5.159	10.49	10.08	5.148	10.47	10.05	25.73	25.67	1,000
30	74.4	2.165	14.47	10.68	2.129	14.15	10.44	27.32	26.72	1,000
50	74.4	1.460	15.41	11.33	1.466	14.53	10.67	28.20	26.61	30
High Energy										
10	14.4	23.360	32.32	30.30	23.320	32.24	30.23	85.98	85.79	1,000
30	14.4	10.780	49.58	32.41	10.620	48.51	31.70	92.77	90.83	400
50	14.4	7.011	54.31	34.50	6.765	51.24	32.51	95.82	90.52	130

Table 14—Continued

Amplitude	Energy Remaining	Variant Power Produced Q_1 T = 10	Variant Power Produced Q_2 T = 1.0	Variant Power Produced Q_3 T = 0.1	Variant Power Out Q_1 T = 10	Variant Power Out Q_2 T = 1.0	Variant Power Out Q_3 T = 0.1	Total Variant Power Produced	Total Variant Power Out	Survival Time Q_1
Low Energy										
10	74.4	1.091	0.940	0.660	1.036	0.060	0.010	2.691	1.106	---
30	74.4	1.126	0.410	0.240	1.089	0.100	0.000	1.776	1.189	---
50	74.4	0.002	0.009	0.011	0.003	0.009	0.012	0.022	0.021	---
High Energy										
10	14.4	0.240	0.120	0.070	0.200	0.050	0.000	0.430	0.250	---
30	14.4	4.319	1.420	0.770	4.295	0.400	0.050	6.509	4.745	---
50	14.4	4.917	3.400	1.960	4.669	0.340	0.020	10.300	5.029	---

*Input frequency = 1 cycle/unit, run time - 1,000; MSQ energy input increases with increasing amplitude.

Table 15 The effect of changes in signal mean, amplitude, and frequency on the power produced and used by three competing autocatylitic storages: (A) high energy input = 90, (B) low energy input = 30

Change in Mean	Change in Amplitude	Change in Frequency	Change in Power Produced	Change in Power Out
(A) High Energy				
±20	---	---	±20	±20
---	+20	---	-6.00	-9.19
---	-20	---	-2.89	-1.14
---	---	x10	-0.52	-0.62
---	---	x0.1	-1.34	-0.44
(B) Low Energy				
+20	---	---	±20	±20
---	+20	---	+2.33	+2.85
---	-20	---	-7.59	-8.10
---	---	x10	-0.46	-0.14
---	---	x0.1	+3.23	+3.36

Table 16 The power produced and used and survival time of units (A) a system with closely spaced turnovers is exposed to inputs of varying frequency, (B) the effect of unit turnover separation on power produced and used for an input of 1 cycle per unit time, (C) competition between units with proportionally separated turnovers that match input frequency*

Input Frequency	T_1	T_2	T_3	Power Produced Q_1	Power Produced Q_2	Power Produced Q_3	Power Out Q_1	Power Out Q_2	Power Out Q_3	Total Power Produced	Total Power Out	Survival Time Q_1, Q_2
(A)												
10.0	2.0	1.00	0.50	24.940	30.920	31.70	24.410	30.250	31.00	87.56	85.66	1,000
2.0	2.0	1.00	0.50	24.970	30.910	31.69	24.440	30.240	30.99	87.57	85.67	1,000
1.0	2.0	1.00	0.50	13.160	35.640	42.25	12.940	34.960	41.41	91.05	89.31	790
0.5	2.0	1.00	0.50	25.400	30.780	31.49	24.920	30.170	30.86	87.67	85.95	1,000
0.1	2.0	1.00	0.50	28.830	29.660	29.95	28.670	29.480	29.75	88.44	87.90	1,000
(B)												
1.0	1.2	1.00	0.80	28.210	29.240	30.04	27.610	28.620	29.40	87.49	85.63	1,000
1.0	2.0	1.00	0.50	13.160	35.640	42.25	12.940	34.960	41.41	91.05	89.31	790
1.0	10.0	1.00	0.10	10.780	49.580	32.41	10.620	48.510	31.70	92.77	90.83	60
(C)												
10.0	10.0	9.00	8.00	4.031	7.390	84.27	3.968	7.263	82.72	95.69	93.95	80,190
1.0	1.0	0.90	0.80	26.660	29.270	31.69	26.160	28.710	31.08	87.62	85.95	1,000
0.1	0.1	0.09	0.08	29.010	29.170	29.32	28.420	28.570	28.73	87.50	85.72	1,000

*Turnover are $Q_1 = T_1$, $Q_2 = T_2$, and $Q_3 = T_3$

frequency matches the turnover of Q_2. This effect is due to the disadvantage Q_1 suffers in competition as indicated by the lower values of power captured and used by Q_1 at input frequency 1 cycle per unit time. Table 16(B) demonstrates how an increase in the space between component turnovers decreases the survival time and the power produced and used by the high turnover component. Also the power used by the system as a whole increases. Table 16(C) shows how the intensity of competition is increased between units whose turnovers are clustered and matched with a high frequency input. In addition such a system is capable of capturing and using more power than a similar cluster of turnovers matched with lower frequency inputs.

The System High Frequency Cutoff and Maximum Power

Table 17 demonstrates that the high frequency cutoff of a system of three units in competition is a factor in determining the total power produced and used by the system. Given that there is energy available for exploitation at high frequency, the system that produces the most power has a high turnover receiving unit that is able to interact with the highest input frequency available. This result is seen to hold for linear and autocatalytic systems both with input frequencies superposed and input frequencies modulated.

Superposition and Modulation in the Competition Model

The model in Figure 21 was used to examine the effect of the modulation of input signal frequencies on the power produced and used by

Table 17 Comparison of power produced and used and the survival of unit Q_1 in the same system with high and low high frequency cutoffs. (A) linear competition, (B) autocatalytic competition, (C) autocatalytic competition with modulated inputs*

Input Frequency		Power Produced			Power Out			Total Power		Survival Time
f_0	f_1	Q_1	Q_2	Q_3	Q_1	Q_2	Q_2	Produced	Out	Q_1
(A) Linear High										
10	10.0	29.370	29.37	29.37	28.740	28.72	28.75	88.11	86.21	1,000
10	1.0	29.050	29.05	29.06	28.850	28.73	28.74	87.15	86.32	1,000
10	0.0	29.050	28.05	29.05	28.890	28.85	28.75	87.15	86.49	1,000
Linear Low										
10	10.0	29.370	29.37	29.37	28.720	28.75	28.85	88.11	86.32	1,000
10	1.0	29.050	29.05	29.05	28.730	28.74	28.85	87.15	86.32	1,000
10	0.0	29.050	29.05	29.05	28.850	28.76	28.86	87.16	86.46	1,000
(B) Autocatalytic High										
10	10.0	9.647	50.10	32.50	9.458	48.99	31.76	92.25	90.21	400
10	1.0	14.170	44.26	31.58	14.040	43.76	31.22	90.01	89.02	790
10	0.1	19.880	38.12	30.95	19.780	37.87	30.73	88.15	88.38	1,000
Autocatalytic Low										
10	10.0	26.320	30.51	30.65	25.760	29.84	29.94	87.48	85.59	1,000
10	1.0	26.200	30.04	30.30	25.920	29.71	29.98	86.54	85.61	1,000
10	0.1	26.530	29.97	30.26	26.280	29.67	29.96	86.76	85.91	1,000

Table 17—Continued

Input Frequency		Power Produced			Power Out			Total Power		Survival Time
f_0	f_1	Q_1	Q_2	Q_3	Q_1	Q_2	Q_3	Produced	Out	Q_1
(C) Modulated Input High Frequency										
10	10.0	8.656	51.64	32.82	8.439	50.19	31.96	93.12	90.58	310
10	1.0	9.628	48.94	32.72	7.446	47.57	31.78	89.29	86.80	280
10	0.1	9.478	48.18	32.44	9.292	47.00	31.63	90.10	87.92	290
Modulated Input Low Frequency										
10	10.0	25.690	30.81	30.85	25.960	30.00	30.00	86.35	85.91	1,000
10	1.0	23.590	30.45	30.82	23.040	29.97	29.97	85.91	82.61	1,000
10	0.1	23.990	30.37	30.78	23.370	29.95	29.95	85.14	82.87	1,000

*Turnovers for high frequency are $Q_1 - 10$, $Q_2 = 1.0$, $Q_3 = 0.1$. Turnovers for the low high frequency are $Q_1 = 1.0$, $Q_2 = 0.1$, $Q_3 - 0.01$

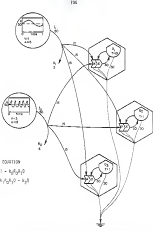

UNIT EQUATION

$$R = I - k_0R_0R_1Q$$

$$\dot{Q} = k_1R_0R_1Q - k_2Q$$

Figure 21. A simulation model of autocatalytic competition between components Q_1, Q_2, and Q_3 of turnover 10, 1.0, 0.1, respectively, when input signals to the model are multiplied. Energy flows given on the pathways are the initial steady state values for simulation. For abbreviations see Figure 12.

the autocatalytic competition model. The input signal mean and amplitude were divided so that the total mean square power available to the model is the same as that available for the single energy source model already tested.

The linear superposition of input signals shown in Table 18 shows results similar to those established earlier for linear systems. The fast turnover unit is able to use more power in competition and the total power used by the system increases as the input frequency becomes longer. The results of superposing input signals of equal amplitude but different frequency upon autocatalytic competition are shown in Table 18(B). The total power used increased as the input frequency became longer for both matched and unmatched input frequency components. The power produced and used by storage is greater when the two input frequencies are equal. The power produced is a maximum when the input frequencies 1 and 1 cycle per unit time are superposed but power out is a maximal for input frequencies 0.01 and 0.01.

The modulation of input frequencies is shown in Table 18(C). The pattern of power use and production is similar to that observed for superposition of inputs to the autocatalytic model. But in the modulated case signals that are of equal frequencies and in phase give the same or greater power capture and use as did the superposed inputs. Unmatched frequency inputs use more power when they are superposed rather than modulated. Matched frequency inputs that are modulated can resonate, accelerating pulsing and competition, and, therefore, they give greater power production and use than do similar inputs that are

Table 18. The power produced and used and the survival time of unit Q_1 for (A) linear competition, (B) autocatalytic competition when input signals are superposed, and (C) the autocatalytic model with the input signals multiplied

Input Frequency		Power Produced			Power Out			Total Power		Survival Time
f_0	f_1	Q_1 T = 10	Q_2 T = 1.0	Q_3 T = 0.1	Q_1 T = 10	Q_2 T = 1.0	Q_3 T = 0.1	Produced	Out	Q_1
(A) Linear Units										
10.00	10.00	29.370	29.37	29.37	28.740	28.72	28.75	88.11	86.21	1,000
10.00	1.00	29.050	29.05	29.05	28.850	28.73	28.74	87.15	86.32	1,000
10.00	0.10	29.050	29.05	29.05	28.890	28.85	28.75	87.15	86.49	1,000
(B) Autocatylitic Units Input Superposition										
10.00	10.00	9.647	50.10	32.50	9.458	48.99	31.76	92.25	90.21	400
10.00	1.00	14.170	44.26	31.58	14.040	43.76	31.22	90.01	89.02	790
10.00	0.10	19.880	38.12	30.95	19.780	37.87	30.73	88.95	88.38	1,000
1.00	1.00	10.780	49.58	32.41	10.620	48.51	31.70	92.77	90.83	400
1.00	0.10	21.000	37.03	30.83	20.920	36.81	30.64	88.86	88.37	1,000
0.10	0.10	29.820	31.42	30.19	29.800	31.35	30.12	91.43	91.27	1,000
0.10	0.01	28.950	29.75	29.97	28.940	29.74	29.96	88.67	88.64	1,000
0.01	0.01	32.570	28.89	29.85	32.570	28.89	29.85	91.31	91.31	1,000
All	All	16.550	40.18	31.15	16.440	39.86	30.90	87.88	87.20	1,000

Table 18—Continued

Input Frequency		Power Produced			Power Out			Total Power		Survival Time
f_0	f_1	Q_1 T = 10	Q_2 T = 1.0	Q_3 T = 0.1	Q_1 T = 10	Q_2 T = 1.0	Q_3 T = 0.1	Produced	Out	Q_1
(C) Autocatalytic Units Input Modulation										
10.00	10.00	8.656	51.64	32.82	8.439	50.19	31.95	93.12	90.58	310
10.00	1.00	7.628	48.94	32.72	7.446	47.57	31.78	89.29	86.80	280
10.00	0.10	9.478	46.18	32.44	9.292	47.00	31.63	90.10	87.92	290
1.00	1.00	10.230	50.42	32.62	10.060	49.17	31.80	93.27	91.03	340
1.00	0.10	14.090	40.00	31.21	13.960	39.55	30.87	85.30	84.38	650
0.10	0.10	29.760	31.53	30.20	29.740	31.46	30.13	91.49	91.33	1,000
0.10	0.01	25.040	29.16	29.92	25.040	29.15	29.90	84.12	84.09	1,000
0.01	0.01	32.570	28.89	29.85	32.570	28.89	29.85	91.31	91.31	1,000
All	All	10.940	47.58	32.05	10.790	46.80	31.52	90.57	89.11	540

superposed If both input signals are noisy a modulated system generates greater production and use of power than does a superposed system. The high turnover component in the modulated system has a shorter survival time than in a superposed system for almost all frequency inputs examined.

The effect of amplitude variations on the mean square power produced and used by storages of the autocatalytic competition models in Figures 14 and 21 is shown in Table 19 The results show that in general the more variance that is present at high frequency the greater the power produced and used by the system and the shorter the survival time of Q_1, the fast turnover component.

Modulation and Frequency Matching

Table 20(A) presents the results of simulating the model given in Figure 21 with system unit turnovers which match the input frequencies or their sum or difference. Table 20(A) showed that the total power produced and used by Run 4, with turnovers equal to the sum, T = 1.6, difference, T - 0.4, and the low frequency input, T - 0.6 exceeded the total power captured and used by all other runs

Table 20(B) gives the results of simulating the model shown in Figure 21 when only one of the component turnovers matches an input frequency or their sum or difference. The matched unit is able to capture and use the most power when its turnover is equal to the sum of the input frequencies As the matched component corresponds to lower frequencies, the power it is able to produce and use decreases The

Table 19. The power produced and used by three competing autocatalytic components when the amplitude of two input frequencies changes from high to low

Frequency		Amplitude		Power Produced			Power Out			Total Power		Survival Time
f_0	f_1	a_0	a_1	Q_1 $T = 10$	Q_2 $T = 1.0$	Q_3 $T = 0.1$	Q_1 $T = 10$	Q_2 $T = 1.0$	Q_3 $T = 0.1$	Produced	Out	Q_1
(A) Input Signals Superposed												
10	1.0	25	5	11.350	48.01	32.06	11.190	47.23	31.54	91.44	89.96	540
10	1.0	5	25	12.450	47.30	31.98	12.310	46.55	31.47	91.73	90.33	550
10	0.1	25	5	11.680	47.79	32.04	11.520	47.03	31.52	91.51	90.07	530
10	0.1	5	25	28.320	31.42	30.19	28.290	31.36	30.13	89.93	89.78	1,000
1	0.1	25	5	12.670	46.99	31.94	12.730	46.27	31.44	91.60	90.44	540
1	0.1	5	25	28.470	31.30	30.18	28.450	31.24	30.12	89.95	89.81	1,000
(B) Input Signals Modulated												
10	1.0	25	5	6.714	53.75	34.54	5.418	50.65	32.61	94.00	88.58	140
10	1.0	5	25	6.322	44.40	32.30	6.209	43.25	31.45	83.02	80.91	250
10	0.1	25	5	5.819	53.74	34.52	5.520	50.66	32.50	94.08	88.68	130
10	0.1	5	25	14.220	39.11	31.13	14.180	38.67	30.73	84.46	83.58	550
1	0.1	25	5	6.460	44.36	32.30	6.353	43.20	31.44	83.12	80.99	240
1	0.1	5	25	15.460	36.33	30.91	15.430	36.97	30.58	83.70	82.98	510

Table 20. The power produced and used by a system of three autocatalytic units in competition for modulated input signals of frequency 1.0 and 0.6 and amplitude 15. The turnovers present in the system vary as shown. (A) All turnovers match the input frequencies or their sum or difference. (B) Only one turnover matches.

	Power Produced						Power Out						Total Power	
Run	T=10	T=1.6	T=1.0	T=0.6	T=0.4	T=0.1	T=10	T=1.6	T=1.0	T=0.6	T=0.4	T=0.1	Produced	Out
(A) All turnovers—match the input frequencies or their sum or difference														
1		18.04	29.62	34.66				17.82	29.24	34.21			82.32	81.27
2			21.61	28.93	31.12				21.30	28.50	30.65		81.66	80.45
3		17.70	29.63		35.05			17.48	29.23		34.57		82.38	81.28
4		16.57		33.18	34.04			15.35		32.69	33.54		82.79	81.58
(B) One turnover—matches the input frequencies or their sum or difference														
1	5.542	46.60				33.80	5.528	46.03				33.36	85.94	84.92
2	5.777		45.69			33.57	5.760		45.90			33.07	85.94	84.75
3	6.337			46.10		33.72	6.316			45.38		33.18	86.16	84.87
4	6.973				45.18	34.26	6.984				44.45	33.71	86.41	84.81

total power produced becomes greater as the matched unit corresponds to lower frequencies in the input. However, the total power used in the system is greatest when the frequency matched is highest, and has a minimum at turnover 1.0.

A Nested Competition Model

The linear and autocatalytic competition model programs were rewritten in order to incorporate a nested time constant structure. These programs are given in Appendix A. The nested program runs each storage at a dt such that the ratio dt/τ equals a constant. Therefore, fast or small time constants run at small dt's and conversely large time constants run with large dt's.

The results of simulating the nested linear competition model over a three decade range of frequency are given in Table 21. The results are very similar to those shown for the linear model without nesting (see Table 3). Unit Q_3 in the nested model uses more power at input frequency 1 than it does in the unnested model.

The autocatalytic nested model simulation results are given in Table 22. Unit Q_1 with a turnover of 10 is dominant when the input signal is 10 cycles per unit time. However, if the input signal frequency decreases to 1 cycle per unit time, Q_3 excludes the other two units. For a lower input frequency of 0.1 all three units survive past time 1,000. These results are similar to the unnested case for frequency 0.1 but very different from the unnested case at input frequencies 10 and 1 (see Tables 12 and 22). Unit Q_2 is the dominant unit over 1,000

Table 21 The power, mean power, and variant power produced and used by a linear nested competition model Units with turnover 10, 1.0, and 0.1 compete for input signals at 10, 1.0, and 0.1 cycles per unit time

Input Frequency	Q_1 $T = 10$	Q_2 $T = 1.0$	Q_3 $T = 0.1$	Q_1 $T = 10$	Q_2 $T = 1.0$	Q_3 $T = 0.1$	Total Power Produced	Total Power Out
(A)	Power Produced			Power Out				
10.0	29.38	29.38	29.38	28.75	28.53	28.33	88.14	85.61
1.0	29.38	29.38	29.38	29.21	28.75	31.01	88.14	88.97
0.1	29.38	29.38	29.38	29.37	29.21	28.75	88.14	87.33
(B)	Mean Power Produced			Mean Power Out				
10.0	28.74	28.74	28.74	28.73	27.89	27.82	86.22	84.35
1.0	28.74	28.74	28.74	28.74	28.73	30.71	86.22	88.18
0.1	28.74	28.74	28.74	28.74	28.74	28.73	88.22	86.21
(C)	Variant Power Produced			Variant Power Out				
10.0	0.64	0.64	0.64	0.02	0.64	0.57	1.92	1.23
1.0	0.64	0.64	0.64	0.47	0.02	0.30	1.92	0.79
0.1	0.64	0.64	0.64	0.63	0.47	0.02	1.92	1.12

Table 22. The power, mean power, and variant power produced and used by an autocatalytic nested competition model. Units with turnovers 10, 1.0, and 0.1 compete for input signals at 10, 1.0, and 0.1 cycles per unit time

Input Frequency	Q_1 T = 10	Q_2 T = 1.0	Q_3 T = 0.1	Q_1 T = 10	Q_2 T = 1.0	Q_3 T = 0.1	Total Power Produced	Total Power Out	Survival Time Q_1, Q_2, Q_3
(A)	Power Produced			Power Out					
10.0	84.400	1.422	4.637	82.630	1.639	5.446	90.460	89.770	---, 40, ---
1.0	8.453	19.150	82.910	8.321	18.800	82.680	110.500	109.800	360, 430, ---
0.1	31.570	29.700	29.940	31.560	29.650	29.890	91.210	91.100	---, ---, ---
(B)	Mean Power Produced			Mean Power Out					
10.0	82.360	0.157	2.704	82.350	0.1870	2.926	85.220	85.520	
1.0	4.328	12.130	77.640	4.331	12.160	77.290	94.110	93.730	
0.1	26.14	29.520	29.880	26.140	29.520	29.880	85.540	85.540	
(C)	Variant Power Produced			Variant Power Out					
10.0	2.040	1.265	1.933	0.280	1.502	2.460	5.238	4.242	
1.0	4.125	7.020	5.270	3.390	6.640	5.390	16.420	16.020	
0.1	5.430	0.180	0.050	5.420	0.130	0.010	5.670	5.560	

time units in the unnested version but in the nested version Q_2 pulses and is quickly excluded at frequencies 10 and 1 The results of simulating a nested autocatalytic competition model with two modulated inputs are shown in Table 23. The behavior of the model in this simulation is similar to that described for the autocatalytic model without modulation. Once again the dominant units of the nested model were different from those dominant in the unnested model for input frequencies 10 and 1 but close to the same at input frequency 0.1

Filter Properties of Chain Models

Linear and autocatalytic three unit chain models were examined in 734 simulation runs to determine their wave filter properties. The linear model is given in Figure 22 A group of autocatalytic chain models with a variable number of feedbacks is given in Figure 23 The linear model and the autocatalytic models with zero and three secondary positive feedbacks were simulated over a three decade range of frequency at high and low energy levels. In addition, the significance of the order of component turnovers in the chain was explored by simulating four arrangements of component turnover over a six decade frequency range for the models in Figure 23(a), (b), and (d). The five additional autocatalytic models in Figure 23 were simulated over a three decade range of frequency using the same four turnover arrangements but with an excess of available energy equal to the mean square energy of the input signal

The effect of the position of a second varying energy source upon the power generated by a three component autocatalytic chain with

Table 23 The power, mean power, and variant power produced and used by an autocatalytic nested competition model with two modulated inputs. Units with turnovers 10, 1.0, and 0.1 compete for input signals at 10, 10, 1.0, 1.0, and 0.1, 0.1 cycles per unit time

Input Frequency		Q_1 $T = 10$	Q_2 $T = 1.0$	Q_3 $T = 0.1$	Q_1 $T = 10$	Q_2 $T = 1.0$	Q_3 $T = 0.1$	Total Power	
f_0	f_1							Produced	Out
(A)		Power Produced			Power Out				
10.0	10.0	85.740	1.352	4.324	83.440	1.629	5.181	91.420	90.250
1.0	1.0	7.545	19.360	83.420	7.413	18.850	83.190	110.300	109.600
0.1	0.1	31.460	29.870	29.940	31.440	29.810	29.890	91.270	91.140
(B)		Mean Power Produced			Mean Power Out				
10.0	10.0	83.160	0.144	2.234	83.150	0.174	2.621	85.540	85.850
1.0	1.0	3.643	12.110	78.390	3.646	12.140	78.030	94.140	93.820
0.1	0.1	26.99	29.680	29.680	25.590	29.670	29.880	85.560	85.54
(C)		Variant Power Produced			Variant Power Out				
10.0	10.0	2.580	1.208	2.090	0.290	1.455	2.660	5.878	4.405
1.0	1.0	3.902	7.250	5.030	3.767	6.810	5.160	16.180	15.740
0.1	0.1	5.470	0.190	0.126	5.460	0.140	0.010	5.920	5.600

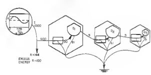

$$R = I - k_0R$$

$$Q_1 = k_1R - k_2Q_1 - k_3Q_1$$

$$Q_2 = k_3Q_1 - k_4Q_2 - k_5Q_2$$

$$Q_3 = k_5Q_2 - k_6Q_3$$

Figure 22 A linear chain model showing the flows that would result if there were a 10% power transfer between components of the chain, and the driving input is a variable time signal

zero and three secondary positive feedbacks were also investigated. These systems were first simulated with a constant energy at the chain base and a variable second energy interaction at unit one, unit two, or unit three. Simulations were run over a six decade range of frequency for each of the four time constant arrangements defined above. Next the systems were simulated with variable energies at the chain base and interacting at each of the three system component levels. These simulations were also run over a six decade range of frequency for the four time constant arrangements.

Filter Properties of a Linear Chain

The results of simulating the linear chain model given in Figure 23 are given in Tables 24, 25, and 26. In Table 24 the results of simulating the linear model for high and low energy inputs are shown. The power produced at Q_1 is always the same since it depends only on the value of the energy remaining. In both the high energy and low energy cases the power produced and used increases as the frequency input becomes slower. Table 25 gives the results of simulation runs in which models with four arrangements of the three component turnovers were exposed to various input frequencies. In all cases the power produced and used increased (or remained the same for less elastic frequency, turnover matches) as input frequency became slower. The model with turnover arrangement $Q_1 = 10$, $Q_2 = 1$, $Q_3 = 0.1$ produced and used more power than the other configurations over the three decade range of frequency tested. This was due to the greater efficiency of power transfer up the chain and not to more efficient energy capture

Figure 23 The models given in (a) through (h) show eight possible combinations of secondary positive feedbacks within a chain of three autocatalytic units. The flows shown are calculated on the assumption that 10% of the energy produced by a unit is transferred to the next level whether up or down the chain

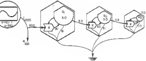

(a) EQUATIONS

$R = I - k_0Q_1$

$Q_1 = k_1Q_1R - k_2Q_1Q_2 - k_3Q_1$

$\dot{Q}_2 = k_2Q_1Q_2 - k_4Q_2Q_3 - k_5Q_2$

$Q_3 = k_4Q_2Q_3 - k_6Q_3$

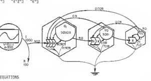

(b) EQUATIONS

$R = I - k_0Q_1Q_2Q_3R$

$Q_1 = k_1Q_1Q_2Q_3R - k_2Q_1Q_2Q_3 - k_3Q_1$

$Q_2 = k_4Q_1Q_2Q_3 - k_5Q_2Q_3 - k_6Q_2Q_1Q_3R - k_7Q_2$

$Q_3 = k_5Q_2Q_3 - k_8Q_1Q_2Q_3R - k_9Q_1Q_2Q_3 - k_{10}Q_3$

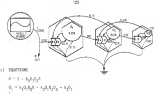

(c) EQUATIONS

$$R = I - k_0Q_1Q_2R$$

$$Q_1 = k_1Q_1Q_2R - k_2Q_1Q_2Q_3 - k_3Q_1$$

$$\dot{Q}_2 = k_4Q_1Q_2Q_3 - k_5Q_2Q_3 - k_6Q_2$$

$$Q_3 = k_5Q_2Q_3 - k_7Q_1Q_2Q_3 - k_8Q_3$$

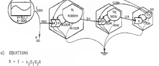

(d) EQUATIONS

$$R = I - k_0Q_1Q_3R$$

$$Q_1 = k_1Q_1Q_3R - k_2Q_1Q_2Q_3 - k_3Q_1$$

$$Q_2 = k_4Q_1Q_2Q_3 - k_5Q_2Q_3R - k_6Q_2$$

$$Q_3 = k_5Q_2Q_3 - k_7Q_1Q_3R - k_8Q_1Q_2Q_3 - k_9Q_3$$

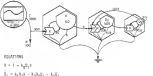

(e) EQUATIONS

$R = 1 - k_0Q_1R$

$Q_1 = k_1Q_1R - k_2Q_2Q_3 - k_3Q_1$

$Q_2 = k_4Q_1Q_2Q_3 - k_5Q_2Q_3 - k_6Q_2$

$Q_3 = k_5Q_2Q_3 - k_7Q_1Q_2Q_3 - k_8Q_3$

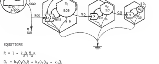

(f) EQUATIONS

$R = 1 - k_0Q_1Q_2R$

$Q_1 = k_1Q_1Q_2R - k_2Q_1Q_2 - k_3Q_1$

$\dot{Q}_2 = k_2Q_1Q_2 - k_4Q_2Q_3 - k_5Q_1Q_2R - k_6Q_2$

$Q_3 - k_4Q_2Q_3 - k_7Q_3$

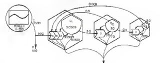

(g) EQUATIONS

$$\dot{R} = I - k_0Q_1Q_2Q_3R$$
$$\dot{Q}_1 = k_1Q_1Q_2Q_3R - k_2Q_1Q_2 - k_3Q_1$$
$$\dot{Q}_2 = k_2Q_1Q_2 - k_4Q_2Q_3 - k_5Q_1Q_2Q_3R - k_6Q_2$$
$$\dot{Q}_3 = k_4Q_2Q_3 - k_7Q_1Q_2Q_3R - k_8Q_3$$

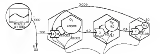

(h) EQUATIONS

$$\dot{R} = I - k_0Q_1Q_3R$$
$$\dot{Q}_1 = k_1Q_1Q_3R - k_2Q_1Q_2 - k_3Q_1$$
$$\dot{Q}_2 = k_2Q_1Q_2 - k_4Q_2Q_3 - k_5Q_2$$
$$\dot{Q}_3 = k_4Q_2Q_3 - k_6Q_1Q_3R - k_7Q_3$$

Table 24. The power produced and used by storages in the linear chain in Figure 22 at high and low energy input as a function of frequency

Input Frequency	Power Produced Q_1 T = 10	Power Produced Q_2 T = 1.0	Power Produced Q_3 T = 0.1	Power Out Q_1 T = 10	Power Out Q_2 T = 1.0	Power Out Q_3 T = 0.1	Total Power Produced	Total Power Out
(A) Low Energy								
10.00	29.37	2.874	0.2870	25.87	2.585	0.287	32.53	28.74
1.00	29.37	2.920	0.2870	26.28	2.587	0.287	32.58	29.15
0.10	29.37	2.936	0.2919	26.43	2.627	0.288	32.60	29.35
(B) High Energy								
10.00	88.10	8.623	0.8620	77.61	7.756	0.862	97.59	86.23
1.00	88.10	8.760	0.8620	78.84	7.760	0.862	97.72	87.46
0.10	88.10	8.809	0.8760	79.28	7.882	0.863	97.79	88.03
0.01	88.10	8.810	0.8810	79.29	7.928	0.877	97.79	88.10

Table 26. The power produced and used by storages in a linear chain as a function of frequency for the four turnover arrangements given as A, B, C, and D*

Input Frequency	Power Produced			Power Out			Total Power	
	Q_1	Q_2	Q_3	Q_1	Q_2	Q_3	Produced	Out
(A) T = 10, 1.0, 0.1								
10.0	88.10	8.623	0.862	77.61	7.756	0.862	97.59	86.23
1.0	88.10	8.760	0.862	78.84	7.760	0.862	97.72	86.46
0.1	88.10	8.809	0.876	79.28	7.862	0.863	97.79	88.03
(B) T = 1.0, 1.0, 1.0								
10.0	88.10	8.618	0.862	77.57	7.755	0.862	97.58	86.19
1.0	88.10	8.624	0.862	77.61	7.757	0.862	97.59	86.23
0.1	88.10	8.758	0.872	78.82	7.849	0.870	97.73	87.54
(C) T = 0.1, 1.0, 10.0								
10.0	88.10	8.624	0.862	77.58	7.758	0.862	97.59	86.20
1.0	88.10	8.622	0.862	77.60	7.759	0.862	97.58	86.22
0.1	88.10	8.631	0.863	77.68	7.767	0.863	97.59	86.31
(D) T = 0.1, 10.0, 1.0								
10.0	88.10	8.624	0.862	77.58	7.767	0.862	97.59	86.20
1.0	88.10	8.622	0.862	77.60	7.759	0.862	97.58	86.22
0.1	88.10	8.631	0.863	77.68	7.768	0.863	97.59	86.31

*Signal amplitude = 300, run time = 1,000, energy remaining = 144

Table 26 The power produced and used by storages in a linear chain model given in Figure 22 for four turnover arrangements given in A, B, C, and D*

Input Frequency	Power Produced			Power Out			Total Power	
	Q_1	Q_2	Q_3	Q_1	Q_2	Q_3	Produced	Out
(A) T = 10, 1.0, 0.1								
10.0	91.97	9.003	0.900	81.02	8.103	0.900	101.9	90.02
1.0	91.97	9.145	0.900	82.31	8.101	0.900	102.0	91.31
0.0	91.97	9.197	0.914	82.77	8.228	0.901	102.1	91.90
(B) T = 1.0, 1.0, 1.0								
10.0	91.97	8.997	0.900	80.98	8.108	0.900	101.9	89.99
1.0	91.97	9.002	0.900	81.02	8.098	0.900	101.9	90.02
0.1	91.97	9.143	0.910	82.29	8.194	0.908	102.0	91.38
(C) T = 0.1, 1.0, 10								
10.0	91.97	8.997	0.900	80.97	8.108	0.900	101.9	89.98
1.0	91.97	8.998	0.900	80.98	8.108	0.900	101.9	89.98
0.1	91.97	9.006	0.901	81.05	8.106	0.901	101.9	90.06
(D) T = 0.1, 10, 1.0								
10.0	91.97	8.997	0.900	80.97	8.108	0.900	101.9	89.98
1.0	91.97	8.998	0.900	80.98	8.097	0.900	101.9	89.98
0.1	91.97	9.006	0.901	81.05	8.106	0.901	101.9	90.06

*Signal amplitude = 300, run time = 1,000, energy remaining = 100

Table 26 gives the values for MSQ power produced and used by the linear chain when there is excess mean square energy of 4.4 units available for exploitation.

Table 27 shows the mean square power produced and used by the linear chain as a function of amplitude. The greater the proportion of the total power available that is in variant power the less total power is produced and used by the model. Table 28 gives the effect of changes in the signal mean, amplitude, and frequency on the power produced and used by a linear chain model. The results show that the mean effect is about an order of magnitude greater than the amplitude effect which in turn is an order of magnitude greater than the effect of changes in frequency.

Filter Properties of an Autocatalytic Chain with No Secondary Positive Feedbacks

Table 29 contains the results of simulating the zero secondary positive feedback autocatalytic chain model given in Figure 23(a). The power produced and used in the model increased as the input frequency became slower. The power produced and used at a given frequency was larger for more constant signals as shown by (8) of Table 28. Table 30 shows the simulations of this autocatalytic chain for four different arrangements of the component turnovers given as A, B, C, and D. Input frequency 10 is exploited approximately the same by all configurations because its variation is too rapid to be captured by any of the turnovers tested. Input frequency 1 is exploited most successfully by turnovers in the order 10, 1, 0.1 because of the position of this model's

Table 27 The power produced and used by storages in a linear chain model given in Figure 22 when input frequency is 1 cycle per unit time and the amplitude varies. Energy remaining is adjusted so that the total MSQ energy available is constant

Amplitude	Remaining Energy	Power Produced Q_1 $T = 10$	 Q_2 $T = 1.0$	 Q_3 $T = 0.1$	Power Out Q_1 $T = 10$	 Q_2 $T = 1.0$	 Q_3 $T = 0.1$	Total Power Produced	 Out
(A) Low Energy									
---	700	30.01	2.989	0.300	26.99	2.700	0.300	33.31	29.99
100	705	29.92	2.980	0.298	26.91	2.686	0.298	33.21	29.90
300	744	29.37	2.920	0.287	26.28	2.587	0.287	32.58	29.15
500	816	28.45	2.804	0.269	25.23	2.417	0.269	31.52	27.92
(B) High Energy									
---	100	90.01	8.997	0.900	81.00	8.108	0.900	99.91	90.01
100	105	89.75	8.969	0.895	80.72	8.057	0.895	99.61	89.67
300	144	88.10	8.760	0.862	78.84	7.760	0.862	97.72	87.46
500	218	85.36	8.411	0.806	75.70	7.253	0.806	94.58	83.76

Table 28 The effect of changes in the signal mean, amplitude, and frequency on the power produced and used by a three unit linear chain model

Change in Mean	Change in Amplitude	Change in Frequency	Change in Power	
			Produced	Out
(A) High Energy Input				
±20	---	---	±22.20	±20.00
---	+20	---	-3.14	-3.70
---	-20	---	+1.89	+2.21
---	---	x10	-0.20	-1.23
---	---	x0.1	+0.07	+0.57
(B) Low Energy Input				
±20	---	---	±22.20	±20.00
---	+20	---	-1.06	-1.23
---	-20	---	+0.63	+0.75
---	---	x10	-0.05	-0.41
---	---	x0.1	+0.02	+0.20

Table 29 The power produced and used by storages of an autocatalytic chain model with no secondary positive feedbacks [Figure 23(a)] at high and low levels of energy input* (A) a function of frequency and (B) a function of amplitude when the MSQ energy available is constant

Frequency	Input Amplitude	Power Produced Q_1 T = 10	Power Produced Q_2 T = 1.0	Power Produced Q_3 T = 0.1	Power Out Q_1 T = 10	Power Out Q_2 T = 1.0	Power Out Q_3 T = 0.1	Total Power Produced	Total Power Out
(A) Low Energy Frequency Varies									
All	300	26.82	1.886	0.030	24.50	1.884	0.060	28.75	26.44
10.00	300	27.22	2.264	0.029	24.41	2.256	0.040	29.51	26.71
1.00	300	28.36	2.373	0.031	25.55	2.260	0.041	30.76	27.85
0.10	300	33.79	2.472	0.075	31.18	3.051	0.062	37.34	34.29
---	---	29.99	2.990	0.300	26.99	2.700	0.300	33.28	29.99
High Energy Frequency Varies									
All	300	85.49	8.366	0.320	75.84	8.043	0.328	96.41	84.21
10.00	300	87.44	8.511	0.460	77.09	8.045	0.466	96.41	86.60
1.00	300	87.93	8.685	0.462	78.66	8.051	0.467	97.08	87.18
0.10	300	86.16	9.308	0.503	79.41	8.581	0.477	97.97	86.47
0.01	300	87.90	14.630	1.160	78.75	13.990	0.944	103.70	93.68
---	---	90.01	8.997	0.900	81.00	8.108	0.900	99.91	90.00

Table 29—Continued

Frequency	Input Amplitude	Power Produced Q_1 $T = 10$	Power Produced Q_2 $T = 1.0$	Power Produced Q_3 $T = 0.1$	Power Out Q_1 $T = 10$	Power Out Q_2 $T = 1.0$	Power Out Q_3 $T = 0.1$	Total Power Produced	Total Power Out
(B) Low Energy Amplitude Varies									
1.0	100	29.71	2.960	0.250	29.69	2.694	0.250	32.92	29.63
1.0	300	28.36	2.373	0.031	25.55	2.260	0.041	30.76	27.85
1.0	500	28.42	0.471	0.016	26.87	0.429	0.029	28.91	27.32
High Energy Amplitude Varies									
1.0	100	89.73	8.962	0.850	80.70	8.033	0.851	99.54	89.64
1.0	300	87.93	8.685	0.452	78.66	8.051	0.457	97.08	87.18
1.0	500	85.19	6.052	0.065	77.48	5.714	0.102	91.32	83.30

*High energy input - 900, low energy input = 300

Table 30 The power produced and used by storages of an autocatalytic chain with no secondary positive feedbacks as a function of frequency for four turnover arrangements given as A, B, C, and D*

Frequency	Power Produced			Power Out			Total Power	
	Q_3	Q_2	Q_3	Q_1	Q_2	Q_3	Produced	Out
(A) T = 10, 1.0, 0.1								
10.0000	87.44	8.511	0.460	77.09	8.046	0.466	96.41	85.60
1.0000	87.93	8.685	0.462	78.66	8.051	0.467	97.08	87.18
0.1000	88.16	9.308	0.503	79.41	8.581	0.477	97.97	88.47
0.0100	87.90	14.630	1.150	78.75	13.990	0.944	103.70	93.68
0.0010	88.65	7.666	1.804	82.15	5.884	1.804	98.02	89.84
0.0001	88.57	7.603	1.799	82.15	5.940	1.799	98.07	89.89
(B) T = 1.0, 1.0, 1.0								
10.0000	87.47	8.553	0.461	77.03	8.102	0.462	96.48	85.59
1.0000	87.48	8.558	0.462	77.07	8.092	0.462	96.50	85.62
0.1000	88.00	9.309	0.569	78.85	8.635	0.560	97.90	88.04
0.0100	87.26	17.570	0.582	74.99	17.460	0.581	105.40	93.33
0.0010	88.63	7.640	1.800	82.01	5.989	1.800	98.07	89.80
0.0001	88.66	7.622	1.798	82.13	5.965	1.798	98.08	89.89

Table 30—Continued

Frequency	Power Produced			Power Out			Total Power	
	Q_1	Q_2	Q_3	Q_1	Q_2	Q_3	Produced	Out
(C) T = 0.1, 1.0, 10								
10.0000	87.48	8.562	0.469	77.07	8.097	0.459	96.51	85.64
1.0000	87.48	8.663	0.473	77.07	8.097	0.473	96.52	85.65
0.1000	86.89	11.720	0.537	73.57	11.660	0.529	99.14	85.76
0.0100	87.31	24.250	0.523	75.02	23.300	0.523	112.10	99.44
0.0010	88.34	10.620	3.047	60.39	9.681	2.905	102.0	92.88
0.0001	100.50	32.320	0.001	74.54	32.320	0.007	132.80	106.90
(D) T = 0.1, 10, 1.0								
10.0000	87.48	8.557	0.467	77.08	8.093	0.467	96.50	85.64
1.0000	87.48	8.559	0.467	77.07	8.093	0.468	96.61	85.63
0.1000	87.50	15.990	1.643	77.12	15.230	0.963	105.13	93.31
0.0100	89.24	2.502	0.520	87.93	2.016	0.520	92.26	90.47
0.0010	88.63	15.640	5.273	82.03	12.720	2.457	109.60	97.21
0.0001	89.49	6.707	0.459	88.99	6.601	6.237	96.66	95.83

*Signal amplitude = 300, run time = 1,000, energy remaining = 144

high frequency cutoff (see Figure 24). Input frequency 0.1 is most successfully utilized by the configuration in D with turnover 0.1, 10, and 1 because of resonance set up at the second chain component [see Table 30(D) and Figure 24]. The power produced and the power used by each configuration have distinct resonance peaks as shown in Figure 24. Cases A and B have a single peak at input frequency 0.01, whereas cases C and D have double peaks at frequencies 0.1 and 0.001 and 0.01 and 0.0001, respectively.

Table 31 gives the effect of changes in mean, amplitude, and frequency of the input signal upon the change in power produced and used by the autocatalytic chain model in Figure 23(a). The mean effect is largest but amplitude and frequency effects can be a fourth and a third as large as the mean effect, respectively. Sometimes the amplitude effect can be larger than the frequency effect. In general, the frequency effects for the autocatalytic chain are much larger than those for the linear chain models.

Tables 32 and 33 take the power produced and used by storages in Table 30 and split it into fractions due to the mean and variance. This breakdown shows that case A does best at input frequency 1 because its variant power produced and used is greater than the alternative cases while the mean power is about the same for all cases. The variant power produced by case D due to resonance at unit Q_2 is responsible for the dominance of this configuration at input frequency 0.1. On the other hand, case C does not handle variant power as well as case A and B at frequency 0.1 yet because it is able to generate more

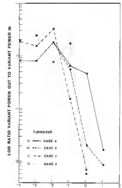

Figure 24 A Bode-like plot of the frequency behavior of the three unit nonlinear chain model without secondary positive feedbacks in Figure 23(a) for four turnover arrangements

Table 31. The effect of changes in the signal mean, amplitude, and frequency on the power produced and used by the three unit chain model given in Figure 23(a). The changes are calculated from data in Table 29

Change in Mean	Change in Amplitude	Change in Frequency	Change in Power Produced	Change in Power Out
(A) High Energy Input				
±20	---	---	±22.20	±20.00
	+20	---	-5.76	-3.88
	-20	---	2.46	2.46
	---	+10	-0.89	-1.29
	---	-10	5.73	5.21
(B) Low Energy Input				
±20	---	---	±22.20	±20.00
	+20	---	-1.85	-0.53
	-20	---	2.16	1.78
	---	+10	-1.25	-1.14
	---	-10	7.00	6.44

Table 32 The component of power due to the mean in model [Figure 23(a)] for four cases of different turnover and changing frequency input

Input Frequency	Mean Power Produced Q_1	Q_2	Q_3	Mean Power Out Q_1	Q_2	Q_3	Total Mean Power Produced	Out
(A) T = 10, 1.0, 0.1								
10.0000	85.52	8.4780	0.4571	77.02	8.046	0.4635	94.46	85.53
1.0000	85.54	8.5000	0.4599	77.04	8.039	0.4642	94.64	85.54
0.1000	85.55	8.5010	0.4652	77.05	8.040	0.4697	94.52	85.56
0.0100	85.60	8.3360	0.5410	77.26	7.804	0.5500	94.48	85.61
0.0010	85.20	5.6280	1.2020	80.57	4.435	1.2110	93.03	86.23
0.0001	86.25	5.6480	1.1920	80.60	4.457	1.1930	93.99	87.15
(B) T = 1.0, 1.0, 1.0								
10.0000	85.54	8.5490	0.4603	77.00	8.095	0.4608	94.55	85.56
1.0000	85.54	8.5500	0.4606	77.00	8.090	0.4613	94.55	85.55
0.1000	85.55	8.5560	0.4635	77.01	8.097	0.4639	94.57	85.57
0.0100	84.98	11.3800	0.1230	73.59	11.270	0.1240	96.48	84.98
0.0010	86.17	5.7520	1.1940	80.41	4.567	1.1950	93.12	86.17
0.0001	86.24	5.6670	1.1900	80.57	4.477	1.1900	93.10	86.24

Table 32--Continued

Input Frequency	Mean Power Produced Q_1	Mean Power Produced Q_2	Mean Power Produced Q_3	Mean Power Out Q_1	Mean Power Out Q_2	Mean Power Out Q_3	Total Mean Power Produced	Total Mean Power Out
(C) T - 0.1, 1.0, 10								
10.0000	85.55	8.5590	0.4648	77.01	8.094	0.4648	94.57	85.57
1.0000	85.55	8.5590	0.4650	77.05	8.094	0.4661	94.57	85.61
0.1000	84.95	11.6100	0.0652	73.47	11.540	0.0653	96.63	85.08
0.0100	84.96	11.5700	0.1200	73.50	11.460	0.1210	96.65	85.08
0.0010	85.89	7.1010	1.0260	78.76	6.083	1.0260	98.49	85.87
0.0001	98.28	23.9500	0.0000	74.32	23.950	0.0000	122.20	98.27
(D) T - 0.1, 10, 1.0								
10.0000	85.55	8.5550	0.4662	77.01	8.090	0.4667	94.57	85.57
1.0000	85.55	8.5550	0.4665	77.05	8.089	0.4600	94.57	85.61
0.1000	85.54	8.6500	0.4550	77.00	8.195	0.4550	94.65	85.65
0.0100	86.91	0.6363	0.1200	86.37	0.518	0.1200	87.67	87.01
0.0010	86.17	5.6890	1.1810	80.45	4.510	1.1820	93.04	86.14
0.0001	86.95	0.5290	0.0210	86.41	0.508	0.0210	87.50	86.94

Table 33 The part of the power due to variance in model [Figure 23(a)] for four cases of different turn
over and changing frequency input

Input Frequency	Variant Power Produced			Variant Power Out			Total Variant Power	
	Q_1	Q_2	Q_3	Q_1	Q_2	Q_3	Produced	Out
(A) T = 10, 1.0, 0.1								
10.0000	1.92	0.013	0.001	0.07	0.000	0.003	2.000	0.073
1.0000	2.39	0.185	0.002	1.62	0.012	0.003	2.577	1.635
0.1000	2.61	0.807	0.038	2.36	0.541	0.007	3.455	2.908
0.0100	2.30	6.294	0.609	1.49	6.186	0.394	9.203	8.070
0.0010	2.45	1.938	0.602	1.58	1.449	0.593	4.990	3.622
0.0001	2.42	1.955	0.607	1.55	1.480	0.606	4.982	3.636
(B) T = 1.0, 1.0, 1.0								
10.0000	1.93	0.004	0.001	0.03	0.007	0.001	1.935	0.030
1.0000	1.94	0.008	0.001	0.07	0.020	0.001	1.949	0.091
0.1000	2.45	0.753	0.126	1.84	0.538	0.096	3.329	2.474
0.0100	2.28	6.190	0.459	1.40	6.390	0.457	8.929	8.047
0.0010	2.46	1.888	0.606	1.60	1.422	0.605	4.954	3.627
0.0001	2.42	1.955	0.608	1.56	1.488	0.608	4.983	3.655

Table 33—Continued

Input Frequency	Variant Power Produced			Variant Power Out			Total Variant Power	
	Q_1	Q_2	Q_3	Q_1	Q_2	Q_3	Produced	Out
(C) T - 0.1, 1.0, 10								
10.0000	1.93	0.003	0.004	0.06	0.003	0.004	1.964	0.067
1.0000	1.93	0.004	0.008	0.02	0.002	0.008	1.942	0.031
0.1000	1.94	0.110	0.472	0.10	0.120	0.464	2.522	0.684
0.0100	2.35	12.680	0.403	1.52	12.440	0.402	15.430	14.360
0.0010	2.45	3.519	2.021	1.63	3.489	1.879	7.990	6.998
0.0001	2.22	8.370	0.001	0.22	8.370	0.068	10.590	8.658
(D) T - 0.1, 10, 1.0								
10.0000	1.93	0.002	0.002	0.07	0.003	0.001	1.934	0.074
1.0000	1.93	0.004	0.002	0.02	0.004	0.002	1.935	0.026
0.1000	1.96	7.340	1.188	0.12	7.035	0.508	10.490	7.663
0.0100	2.33	1.866	0.400	1.56	1.500	0.400	4.556	3.460
0.0010	2.46	9.951	4.090	1.58	8.210	1.275	16.500	11.065
0.0001	2.54	6.178	0.438	2.58	6.093	0.216	9.156	8.889

mean power than any other configuration it has the second highest value for power produced at this frequency However, case C uses less of this mean power than the other configurations and it does not use its varying power as well as the others so it has the lowest value of power used at frequency 0.1

Filter Properties of an Autocatalytic Chain with Three Secondary Positive Feedbacks

The autocatalytic chain [Figure 23(b) with three secondary positive feedbacks was simulated at the same values of high and low energy that were used to evaluate the linear and zero positive feedback cases. The four turnover arrangements previously discussed were simulated over a four decade range of frequency The results of these simulations are given in Table 34 All low energy cases with variable input became zero very quickly Only models with high energy input from turnover cases A and B were not zero at time 1,000 Case A was stable for input frequencies of 0.1 and 0.01 while case B was stable for frequency inputs 1 and 0.1. Also, case A was stable for input frequency 1 at amplitude 10.0. The stable runs of the three positive feedback models were able to produce and use much more power than any of the models with zero feedback. Turnover case A was able to produce slightly more variant power but less mean power than case B (see Table 34)

Comparison of the Filter Properties of Three Unit Chain Models

The eight chain models shown in Figure 23 were simulated with four component turnover arrangements over at least a three decade range

Table 34 The power, mean power, and variant power produced and used by storages of a three secondary positive feedback autocatalytic chain model [Figure 23(b)] Input energy is 300 and 900. Run time is 1,000 All runs given in Tables 29 and 30 were made. (A) power, (B) mean power, (C) variant power

Frequency	Amplitude	Energy Input	Q_1	Q_2	Q_3	Q_1	Q_2	Q_3	Produced	Out
			Power Produced			Power Out			Total Power	
(A) Case A T = 10, 1.0, 0.1										
---	---	300	30.31	3.027	0.300	27.280	2.424	0.270	33.64	29.97
---	---	900	90.98	9.080	0.900	81.920	7.278	0.810	101.00	90.01
1.00	100	900	99.89	90.850	83.040	15.610	7.500	81.380	273.80	104.50
0.10	300	900	101.60	93.420	85.470	11.490	7.665	81.750	280.50	100.90
0.01	300	900	101.50	92.930	85.190	13.990	7.754	82.930	279.60	104.70
Case B T = 1.0, 1.0, 1.0										
1.00	300	900	101.50	96.250	87.610	12.200	7.078	82.360	285.40	101.60
0.10	300	900	101.60	93.800	86.440	10.670	6.845	84.500	281.80	102.00
			Mean Power Produced			Mean Power Out			Total Mean Power	
(A) Case A T = 10, 1.0, 0.1										
0.10			99.30	90.64	82.69	9.483	6.963	81.01	272.60	97.46
0.01			99.18	89.66	81.93	10.130	6.959	80.36	271.00	97.45
Case B T = 1.0, 1.0, 1.0										
1.00			99.16	90.34	82.71	9.705	6.660	81.80	272.20	98.17
0.10			99.31	90.95	83.32	9.246	6.653	82.43	273.60	98.33

Table 34—Continued

Frequency	Amplitude	Energy Input	Q_1	Q_2	Q_3	Q_1	Q_2	Q_3	Produced	Out
			Variant Power Produced			Variant Power Out			Total Variant Power	
(C) Case A T = 10, 1.0, 0.1										
0.10			2.30	2.780	4.780	2.010	0.692	0.740	9.86	3.44
0.01			2.32	3.070	3.270	3.860	0.795	2.570	8.66	7.23
Case B T - 1.0, 1.0, 1.0										
1.00			2.34	5.910	4.900	2.500	0.418	0.560	13.15	3.48
0.10			2.29	2.850	3.120	1.420	0.192	2.070	8.26	3.68

of frequency. The previous results in Table 34 showed that the survival of most configurations with positive feedback depended on having excess energy available. For this reason these chain models were simulated with energy remaining equal to 100 giving 944 units of energy input available to the system. Table 35 gives the results of simulating these chain models with turnovers of $Q_1 = 10$, $Q_2 = 1$, $Q_3 = 0.1$. Highly stable models (a), (b), and (d) in Figure 23 were simulated over a six decade range of frequency. The other configurations were simulated over a three decade frequency range. Both the power produced and used by model (a) increased to a peak at frequency 0.01 and declined. The power produced by models (b) and (d) showed an increase with decreasing input frequency. However, the power used by these models declined to a minimum for input frequency 0.1 and reached a maximum for input frequency 0.001. Tables 36 and 37 show the breakdown of power due to the signal mean and that due to the signal variance, respectively. The variant power used by the positive feedback models is greatest for input frequency 0.001 and has a local minimum at input frequency 0.1 and a global minimum at input 0.0001. The mean values for power produced and used generally increase slightly with frequency models (b) and (d) but at frequency 0.0001 they increase precipitously. Figure 25 shows a Bode plot comparing variant power use by models (a), (b), and (d). The mean value of power produced and used between models shows large differences. The more positive feedbacks a model has the more mean power it is able to transform and the smaller the number of stable runs obtained (see Figure 26). The results for mean power used

Table 35 Power captured, produced, and used by storages of the chain models shown in Figure 23 with Case A turnovers for variable input frequencies*

Chain Model	Power Produced Q_1 T = 10	 Q_2 T = 1.0	 Q_3 T = 0.1	Power Out Q_1 T = 10	 Q_2 T = 1.0	 Q_3 T = 0.1	Total Power Produced	 Out	 Captured
(A) Input Frequency = 10									
a	91.94	9.000	0.893	81.000	8.103	0.897	101.84	90.00	941.4
b	102.00	93.280	83.140	14.700	7.489	81.500	278.40	103.80	1,027.4
c	52.85	40.900	32.990	15.380	7.364	32.250	126.70	54.99	
d	100.90	92.060	82.120	16.020	8.329	80.580	275.10	104.90	1,023.8
e	54.84	42.420	34.170	16.900	8.084	33.480	131.40	58.46	
f	---	---	---	---	---	---	---	---	
g	---	---	---	---	---	---	---	---	
h	---	---	-	---	---	---	---	---	
(B) Input Frequency = 1									
a	92.28	9.172	0.900	82.540	8.101	0.899	102.40	91.54	943.2
b	102.10	93.700	85.210	12.930	7.609	81.940	281.00	102.50	1,030.1
c	55.43	44.910	33.880	14.490	7.669	31.530	134.20	53.69	
d	101.00	92.580	84.280	13.710	8.460	81.090	277.90	103.30	1,027.0
e	55.78	45.160	35.640	14.870	8.274	33.960	136.50	57.12	
f	---	---	---	---	---	---	---	---	
g	---	---	---	---	---	---	---	---	
h	92.99	9.243	0.968	83.170	8.103	0.958	103.20	92.230	

Table 35—Continued

Chain Model	Power Produced			Power Out			Total Power		
	Q_1 T = 10	Q_2 T = 1.0	Q_3 T = 0.1	Q_1 T = 10	Q_2 T = 1.0	Q_3 T = 0.1	Produced	Out	Captured
(C) Input Frequency = 0.1									
a	92.43	9.830	0.957	83.190	8.546	0.905	103.20	92.740	944.0
b	102.10	93.940	85.980	11.360	7.628	82.260	262.00	101.300	1,032.0
c	---	---	---	---	---	---	---	---	
d	101.10	92.940	85.130	11.440	8.561	81.520	279.20	101.500	1,023.7
e	53.81	43.350	36.030	12.310	8.357	34.200	133.80	54.870	
f	---	---	---	---	---	---	-	---	
g	---	---	---	---	---	---	---	---	
h	---	---	---	---	---	---	--	---	
(D) Input Frequency = 0.1									
a	92.22	16.130	2.140	82.420	14.910	1.631	110.50	98.960	943.2
b	102.10	93.790	86.030	12.240	7.697	83.770	281.90	103.700	1,030.9
d	101.10	92.810	85.220	12.350	8.556	83.000	279.10	103.900	1,028.6
(E) Input Frequency = 0.001									
a	92.76	7.361	2.099	85.850	5.009	2.099	102.80	93.960	948.2
b	102.10	93.570	85.970	13.610	7.511	84.490	281.50	105.600	1,029.0
d	101.00	92.540	85.150	14.060	8.365	83.650	278.70	106.100	1,026.5

Table 35—Continued

Chain Model	Power Produced			Power Out			Total Power		
	T = 10	T = 1.0	T = 0.1	T = 10	T = 1.0	T = 0.1	Produced	Out	Captured
(F) Input Frequency = 0.0001									
a	92.780	8.021	2.094	85.850	6.070	2.094	102.90	94.010	
b	102.700	94.670	87.260	9.779	6.770	86.330	284.60	102.900	1,032.3
d	101.800	93.820	66.600	9.786	7.645	85.640	282.20	103.100	1,032.5
(G) Input Frequency = 100									
b	9.256	0.772	0.079	8.563	0.651	0.058	10.11	9.312	30.0
d	14.190	0.874	0.088	13.570	0.829	0.105	15.15	14.500	39.0

*Amplitude = 300, energy remaining = 100, average input energy = 900, run time = 1,000

Table 36 The mean power captured, produced, and used by storages of the models in Figure 23 with Case A turnovers for variable input frequency

Chain Model	Mean Power Produced Q_1 $T = 10$	Q_2 $T = 1.0$	Q_3 $T = 0.1$	Mean Power Out Q_1 $T = 10$	Q_2 $T = 1.0$	Q_3 $T = 0.1$	Total Mean Power Produced	Out	Captured
(A) Input Frequency = 10									
a	89.920	8.992	0.898	80.930	8.099	0.898	99.80	89.93	898.0
b	99.680	90.080	82.110	10.410	6.975	80.460	271.90	97.85	987.5
c	51.060	40.050	32.610	11.420	6.930	31.830	123.70	50.18	
d	98.640	88.610	80.770	10.830	7.842	79.140	268.00	97.81	987.0
e	52.960	41.430	33.630	11.950	7.798	32.860	128.00	52.61	
f	---	---	---	---	---	---	---	---	
g	---	---	---	---	---	---	---	--	
h	---	---	---	---	---	---	---	---	
(B) Input Frequency = 1									
a	89.930	8.892	0.898	80.940	8.094	0.898	99.92	89.93	900.0
b	99.760	90.710	82.760	9.861	6.970	81.010	273.23	97.84	988.3
c	49.970	39.390	31.980	10.970	6.925	31.240	121.34	49.13	
d	98.750	89.520	81.680	10.040	7.834	79.950	269.95	97.83	988.1
e	52.800	42.100	34.310	11.120	7.789	33.510	129.21	52.42	
f	---	---	---	---	---	---	---	---	
g	---	---	---	---	---	---	---	---	
h	90.640	9.064	0.968	81.580	8.096	0.958	100.70	90.63	

Table 36—Continued

Chain Model	Mean Power Produced Q_1 T = 10	 Q_2 T = 1.0	 Q_3 T = 0.1	Mean Power Out Q_1 T = 10	 Q_2 T = 1.0	 Q_3 T = 0.1	Total Mean Power Produced	 Out	 Captured
(C) Input Frequency = 0.1									
a	89.940	8.992	0.9024	80.940	8.094	0.903	99.83	89.94	900.1
b	99.810	91.200	83.2500	9.428	6.963	81.560	274.30	97.95	988.8
c	---	---	---	---	---	---	---	---	
d	98.830	90.230	82.4100	9.409	7.824	80.720	271.50	97.95	988.9
e	52.440	42.430	34.6500	10.430	7.778	33.880	129.52	52.09	
(D) Input Frequency = 0.01									
a	89.980	8.769	0.9630	81.200	7.809	0.978	99.72	89.99	900.5
b	99.780	90.930	82.9800	9.873	6.955	81.470	273.70	98.04	988.5
d	98.800	89.970	82.1600	9.644	7.815	80.600	270.90	98.06	988.6
(E) Input Frequency = 0.001									
a	90.370	6.061	1.4380	84.310	4.632	1.447	97.87	90.39	904.4
b	99.730	90.430	82.4700	10.130	6.972	80.760	272.80	97.86	988.0
d	98.730	89.310	81.4800	10.230	7.834	79.790	269.50	97.85	987.8
(F) Input Frequency = 0.0001									
a	90.43	6.080	1.4280	84.350	4.653	1.429	97.94	90.43	
b	100.10	92.830	85.0400	9.181	6.665	84.130	279.00	99.98	988.7
d	100.30	92.180	84.3700	9.122	7.629	83.410	276.90	100.20	989.5

Table 36—Continued

Chain Model	Mean Power Produced Q_1 T = 10	Mean Power Produced Q_2 T = 1.0	Mean Power Produced Q_3 T = 0.1	Mean Power Out Q_1 T = 10	Mean Power Out Q_2 T = 1.0	Mean Power Out Q_3 T = 0.1	Total Mean Power Produced	Total Mean Power Out	Total Mean Power Captured
(G) Input Frequency = 100									
b	1.037	0.080	0.008	0.967	0.071	0.016	1.125	1.054	12.1
d	2.609	0.109	0.011	2.510	0.107	0.018	2.729	2.635	27.1

Table 37. The variant power captured, produced, and used by storages of the models in Figure 23 with Case A turnovers for variable input frequency

Chain Model	Variant Power Produced			Variant Power Out			Total Variant Power		
	Q_1 T = 10	Q_2 T = 1.0	Q_3 T = 0.1	Q_1 T = 10	Q_2 T = 1.0	Q_3 T = 0.1	Produced	Out	Captured
(A) Input Frequency = 10									
a	2.020	0.008	0.000	0.070	0.004	0.001	2.028	0.075	43.40
b	2.320	3.200	1.030	4.290	0.514	1.140	6.550	5.944	39.90
c	1.790	0.850	0.380	3.960	0.434	0.420	3.020	4.814	
d	2.260	3.450	1.350	5.190	0.487	1.440	7.060	7.117	36.83
e	1.890	0.990	0.540	4.950	0.286	0.620	3.420	5.860	
(B) Input Frequency = 1.0									
a	2.350	0.180	0.001	1.600	0.007	0.001	2.531	1.608	43.20
b	2.340	2.990	2.450	3.070	0.639	0.930	7.780	4.639	41.80
c	5.460	5.520	1.900	3.720	0.744	0.290	12.880	4.754	
d	2.250	3.060	2.600	3.670	0.626	1.140	7.910	5.436	38.94
e	2.980	3.050	1.330	3.750	0.485	0.470	7.360	4.705	
h	2.350	0.179	0.001	1.590	0.007	0.001	2.530	1.598	
(C) Input Frequency 0.1									
a	2.490	0.838	0.064	2.250	0.552	0.003	3.392	2.805	43.90
b	2.280	2.740	2.730	1.930	0.665	0.700	7.750	3.297	43.20
c	2.200	--	---	---	---	---	---	---	
d	2.270	2.710	2.720	2.030	0.727	0.800	7.700	3.557	40.90
e	1.370	1.520	1.380	1.880	0.579	0.320	4.270	2.779	

Table 37—Continued

Chain Model	Variant Power Produced			Variant Power Out			Total Variant Power		
	Q_1 $T = 10$	Q_2 $T = 1.0$	Q_3 $T = 0.1$	Q_1 $T = 10$	Q_2 $T = 1.0$	Q_3 $T = 0.1$	Produced	Out	Captured
(D) Input Frequency = 0.01									
a	2.240	7.361	1.171	1.220	7.101	0.653	10.770	8.974	42.80
b	2.320	2.860	3.050	2.570	0.742	2.360	9.230	5.672	42.40
d	2.300	2.380	3.060	2.706	0.741	2.400	7.740	5.847	40.00
(E) Input Frequency = 0.001									
a	2.390	1.920	0.661	1.540	1.377	0.652	4.971	3.569	43.80
b	2.370	3.140	3.560	3.480	0.539	3.730	9.070	7.749	41.00
d	2.270	3.230	3.670	3.850	0.521	3.900	9.170	8.271	38.70
(F) Input Frequency = 0.0001									
a	2.350	1.841	0.666	1.500	1.417	0.665	4.957	3.582	
b	1.600	1.840	2.220	0.595	0.105	2.200	5.660	2.900	43.60
d	1.500	1.640	2.230	0.664	0.016	2.230	5.370	2.910	43.00
(G) Input Frequency - 100									
b	8.219	0.691	0.070	7.596	0.581	0.081	8.980	8.258	17.90
d	11.580	0.766	0.077	11.060	0.722	0.087	12.420	11.870	11.10

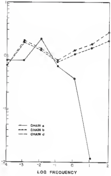

Figure 25. A comparison of Bode-like plots for the models shown in Figure 23(a), 23(b), and 23(d). Turnovers are $Q_1 = 10$, $Q_2 = 1.0$, $Q_3 = 0.1$

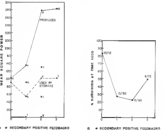

Figure 25. The relationship between the number of secondary positive feedbacks and power production, power use, and stability of the models in Figure 23. (a) Power production and use, (b) stability.

are more complex because the one feedback model used less power than the zero feedback case. One feedback model [Figure 23(f)] and two feedback model [Figure 23(g)] were not able to exist under any of the variable inputs tested. One feedback model (h) was only viable at input frequency 1, and one feedback model (c) did not exist at input frequency less than 0.1. Model (d) with two feedbacks was able to use more total power than model (b) with three feedbacks, but model (b) was able to produce more power than model (d). The superiority of model (d) is seen to be due to its ability to use variant power, whereas the superiority of model (b) comes from its generation of more mean productive power. Tables 35, 36, and 37 also show the values for power, mean power, and variant power captured by models (a), (b), and (d). Model (b) captures more total power because it is able to capture more variant power than model (d) except at input frequency 0.0001, when model (d) wins because it takes more mean power and about the same variant power.

Table 38 gives the mean square power produced and used by eight chain models given in Figure 23 with all turnover times equal one over a three decade range of frequency. Two feedback models (g) and (c) and one feedback model (f) were zero before the run time was over, and one feedback model (h) existed only at input frequency 10. The power produced and used by chain (a), the zero positive feedback model, increased as the frequency became slower. However, models (b), (d), and (e) chains which have three, two, and one positive feedback, respectively, had the maximum power produced at input frequency 1. The

Table 38 Power produced and used in storages for chain models in Figure 23 with Case B turnovers*

Chain Model	Power Produced			Power Out			Total Power	
	Q_1 T = 1.0	Q_2 T = 1.0	Q_3 T = 1.0	Q_1 T = 1.0	Q_2 T = 1.0	Q_3 T = 1.0	Produced	Out
(A) Input Frequency = 10								
a	91.97	8.980	0.900	80.97	8.108	0.900	101.9	89.98
b	102.00	91.680	84.070	11.23	6.738	83.130	278.1	101.10
c	---	---	---	---	---	---	---	---
d	101.10	90.870	83.400	11.14	7.563	82.420	275.4	101.10
e	53.43	42.640	35.160	11.96	7.575	34.580	131.2	54.12
h	93.03	9.092	1.003	81.91	8.032	0.994	103.1	91.00
(B) Input Frequency = 1.0								
a	91.98	9.003	0.900	81.02	8.097	0.900	101.9	90.02
b	102.10	96.870	88.340	10.75	7.075	83.110	287.4	101.20
c	---	---	---	---	---	---	---	---
d	101.20	95.970	87.520	10.59	7.923	82.550	284.7	101.10
e	54.35	44.710	35.930	11.63	7.749	34.540	135.0	53.92
f	---	---	---	---	---	---	---	---
g	---	---	---	---	---	---	---	---
h	91.97	9.034	1.237	80.98	8.131	1.230	102.2	90.34

Table 38—Continued

Chain Model	Power Produced Q_1 T = 1.0	 Q_2 T = 1.0	 Q_3 T = 1.0	Power Out Q_1 T = 1.0	 Q_2 T = 1.0	 Q_3 T = 1.0	Total Power Produced	 Out
(C) Input Frequency - 0.1								
a	92.34	10.42	1.745	82.79	9.189	1.560	102.2	93.54
b	102.10	94.32	86.960	10.58	6.851	84.990	283.4	102.40
c	---	---	---	--	---	---	---	---
d	101.20	93.47	86.280	10.38	7.686	84.360	281.0	102.40
e	53.22	44.12	36.060	11.42	7.749	36.620	134.2	54.83
f	---	---	---	---	---	---	---	---
g	---	---	---	---	---	---	---	---
h	---	---	---	---	---	---	---	---

*Amplitude - 300, initial energy remaining = 100, run time - 1,000 power used by all models increased as the input frequency became slower. The total power produced is greater the more positive feedbacks a chain has for this turnover arrangement. However, the total power used by one feedback model (e) is less than the power use of the zero feedback model (a). The portion of the mean square power due to the mean is given in Table 39 and that part of the total due to the variance is shown in Table 40. For a given model the mean values of power produced and used did not change very much with input frequency. Comparison of the mean values between models showed that power production increased with increasing positive feedbacks. The maximum in power production at input frequency 1 is seen from Table 40 to be due to the large amount of variant power produced by models (b) and (d) at this frequency. The variant power use increases as the frequency becomes slower. The survival times for those models that were zero before time 1,000 are given in Table 38.

Table 41 shows the power, mean power, and variant power produced and used by storages of the chain models in Figure 23 when the turnovers are arranged $Q_1 = 0.1$, $Q_2 = 1$, $Q_3 = 10$, and $Q_1 = 0.1$, $Q_2 = 10$, $Q_3 = 1$. The zero feedback model (a) exists at the end of 1,000 time units for both of these turnover arrangements. The one feedback model (h) was also stable for case D turnovers $Q_1 = 0.1$, $Q_2 = 10$, $Q_3 = 1$. Both the mean and variant power increase slightly as frequency decreases.

Filter Properties of Chain Models with Large Second Law Losses

Three chain models with zero, two, and three secondary positive feedbacks are shown in Figure 27. These models are similar in

Table 33 The mean power produced and used by storages of the chain models in Figure 23 with Case 8 turnovers

Chain Model	Mean Power Produced Q_1 $T = 1.0$	 Q_2 $T = 1.0$	 Q_3 $T = 1.0$	Mean Power Out Q_1 $T = 1.0$	 Q_2 $T = 1.0$	 Q_3 $T = 1.0$	Total Mean Power Produced	 Out
(A) Input Frequency = 10.0								
a	89.04	8.994	0.8985	80.940	8.101	0.899	99.83	89.94
b	99.79	91.310	83.6600	9.379	6.656	82.790	274.80	98.82
c	---	---	---	---	---	---	---	---
d	98.88	90.490	83.0300	9.278	7.477	82.180	272.40	98.94
e	52.14	42.370	34.8900	10.270	7.493	34.450	129.40	52.21
h	90.97	9.089	1.0030	81.880	8.078	0.993	101.10	90.95
(B) Input Frequency = 1.0								
a	89.94	8.994	0.9000	80.950	8.096	0.899	99.83	89.95
b	99.76	91.340	83.7000	9.307	6.656	82.790	274.80	98.75
c	---	---	---	---	---	---		
d	98.91	90.610	83.1400	9.182	7.479	82.240	272.70	98.90
e	---	---	--	---	---	---	---	---
h	91.02	9.095	1.0007	81.930	8.087	0.998	101.1	91.02

Table 39--Continued

Chain Model	Mean Power Produced Q_1 T = 1.0	Mean Power Produced Q_2 T = 1.0	Mean Power Produced Q_3 T = 1.0	Mean Power Out Q_1 T = 1.0	Mean Power Out Q_2 T = 1.0	Mean Power Out Q_3 T = 1.0	Total Mean Power Produced	Total Mean Power Out
(C) Input Frequency = 0.1								
a	89.94	8.930	0.8986	80.970	8.094	0.899	99.83	89.96
b	99.81	91.490	83.8500	9.217	6.653	82.950	275.20	98.82
c	---	---	---	---	---	--	---	---
d	98.91	90.710	83.2300	9.035	7.475	82.340	272.90	98.89
e	52.15	42.420	34.9200	10.230	7.494	34.470	129.50	52.19

Table 40 The variant power produced and used by storages of the chain models in Figure 23 with Case II turnovers

Chain Model	Variant Power Produced Q_1 $T = 1.0$	 Q_2 $T = 1.0$	 Q_3 $T = 1.0$	Variant Power Out Q_1 $T = 1.0$	 Q_2 $T = 1.0$	 Q_3 $T = 1.0$	Total Variant Power Produced	 Out
(A) Input Frequency = 10								
a	2.03	0.003	0.001	0.030	0.007	0.001	2.034	0.038
b	2.21	0.370	0.410	1.851	0.083	0.340	2.990	2.274
c	---	---	---	---	---	---	---	---
d	2.22	0.380	0.370	1.862	0.086	0.240	2.370	2.108
e	1.29	0.270	0.270	1.690	0.082	0.130	1.293	1.903
h	2.06	0.003	0.000	0.030	0.014	0.001	2.063	0.044
(B) Input Frequency = 1.0								
a	2.04	0.009	0.000	0.070	0.001	0.000	2.049	0.071
b	2.34	5.630	4.640	1.443	0.419	0.320	12.610	2.420
c	---	---	---	---	---	---	---	---
d	2.29	5.360	4.3800	1.408	0.444	0.310	12.030	2.162
e	---	---	---	---	---	---	---	---
h	2.06	0.008	0.000	0.070	0.004	0.000	2.068	0.074

Table 40--Continued

Chain Model	Variant Power Produced			Variant Power Out			Total Variant Power	
	Q_1 T = 1.0	Q_2 T = 1.0	Q_3 T = 1.0	Q_1 T = 1.0	Q_2 T = 1.0	Q_3 T = 1.0	Produced	Out
(C) Input Frequency = 0.1								
a	2.40	1.430	0.846	1.820	1.095	0.661	4.676	3.576
b	2.29	2.830	3.110	1.363	0.198	2.040	8.230	3.601
c	---	---	---	---	---	---	---	---
d	2.29	2.760	3.050	1.285	0.213	2.020	8.100	3.518
e	1.07	1.700	1.940	3.926	0.255	1.150	4.710	5.331
h	---	---	---	---	---	---	---	---

Table 41. Power, mean power, and variant power produced and used by storages of the chain models in Figure 23 for Case C and D turnovers

Chain Model	Input Frequency	Q_1	Q_2	Q_3	Q_1	Q_2	Q_3	Produced	Out
		Power Produced			Power Out			Total Power	
(A) Case C	T = 0.1, 1.0, 10								
a	1.0	91.97	9.034	1.237	80.98	8.131	1.230	102.200	90.34
a	0.1	91.39	13.870	0.959	76.33	13.630	0.849	106.200	90.91
(B) Case D	T = 0.1, 10, 1.0								
a	1.0	91.97	9.026	0.906	80.88	8.123	0.903	100.300	90.01
b	1.0	92.98	9.068	0.966	81.85	8.091	0.987	103.000	90.93
a	0.1	91.98	0.658	1.114	81.05	8.668	1.027	102.800	90.75
		Mean Power Produced			Mean Power Out			Total Mean Power	
(A) Case C;	T = 0.1, 1.0, 10								
a	1.0	89.94	8.992	0.901	80.95	8.092	0.901	99.830	89.94
a	0.1	89.36	13.34	0.359	76.15	12.970	0.360	103.060	89.48
(B) Case D	T = 0.1, 10, 1.0								
a	1.0	89.94	8.996	0.900	80.95	8.096	0.880	99.840	89.46
b	1.0	90.93	9.084	0.985	81.82	8.088	0.987	101.000	90.90
a	0.1	89.94	8.999	0.903	80.98	8.096	0.903	99.840	89.98

Table 41—Continued

Chain Model	Input Frequency	Q_1	Q_2	Q_3	Q_1	Q_2	Q_3	Produced	Out
		Variant Power Produced			Variant Power Used			Total Variant Power	
(A) Case C, T = 0.1, 1.0, 10									
a	1.0	2.03	0.042	0.336	0.03	0.039	0.329	2.410	0.358
a	0.1	2.03	0.530	0.600	0.18	0.660	0.590	3.160	1.430
(B) Case D T = 0.1, 10, 1.0									
a	1.0	2.03	0.030	0.006	0.03	0.027	0.003	2.066	0.060
h	1.0	2.05	0.004	0.001	0.03	0.003	0.000	2.055	0.033
a	0.1	2.04	0.659	0.209	0.07	0.572	0.124	2.908	0.766

*Configurations b-g were unstable for these turnovers, run time = 1,000, energy remaining = 100, inputs of amplitude = 300.

Figure 27 Three unit chain models lettered as shown in Figure 23 with energy flows allowing large second law losses at each interaction

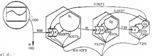

Model d

EQUATIONS

$R = I - k_0 Q_1 Q_2 R_4$

$\dot{Q}_1 = k_1 Q_1 Q_3 R - k_2 Q_2 - k_3 Q_1 Q_2 Q_3$

$\dot{Q}_2 = k_4 Q_1 Q_2 Q_3 - k_5 Q_2 - k_6 Q_2 Q_3$

$\dot{Q}_3 = k_7 Q_2 Q_3 - k_8 Q_3 - k_9 Q_1 Q_3 R - k_{10} Q_1 Q_2 Q_3$

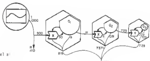

Model a

EQUATIONS

$R - I - k_0 R Q_1$

$\dot{Q}_1 = k_1 R Q_1 + k_2 Q_1 - k_3 Q_1 Q_2$

$\dot{Q}_2 = k_4 Q_1 Q_2 - k_5 Q_2 - k_6 Q_2 Q_3$

$\dot{Q}_3 = k_7 Q_2 Q_3 - k_8 Q_3$

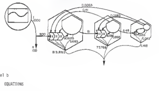

Model b

EQUATIONS

$R = I - k_0 Q_1 Q_2 Q_3 R$

$\dot{Q}_1 = k_1 Q_1 Q_2 Q_3 R - k_2 Q_1 - k_3 Q_1 Q_2 Q_3$

$\dot{Q}_2 = k_4 Q_1 Q_2 Q_3 - k_5 Q_2 - k_6 Q_2 Q_3 - k_7 Q_1 Q_2 Q_3 R$

$\dot{Q}_3 = k_8 Q_2 Q_3 - k_9 Q_3 - k_{10} Q_1 Q_2 Q_3 R - k_{11} Q_1 Q_2 Q_3$

configurations to their counterparts in Figure 23. However, energy flows in Figure 27 are adjusted so that 90% of the available energy is lost at each interaction. Table 42 gives the power produced, used, and captured by these chain models as a function of the input frequency when component turnovers are $Q_1 = 10$, $Q_2 = 1$, $Q_3 = 0.1$. Section A of Table 42 contains the results of simulation for the model configuration without secondary positive feedbacks. The total power produced, used, and captured show a similar pattern as a function of frequency. There is a peak of produced, used, and captured power when the input frequency is 1. These increases are due to increases in the variant power produced, used, and captured as may be seen from Tables 43 and 44. As the input frequency increases from 0.1 to 0.001 power produced, used, and captured first fall and then rise steadily due to changes in the variant power. At input frequency 0.001 all values continue to rise but for a different reason. At this frequency the variation is not as successfully exploited as it was at higher frequencies, but enough additional power is produced, used, and captured from the mean to allow the power to continue to increase.

Section B of Table 42 shows the power produced, used, and captured by model (d) in Figure 27. The pattern of power production, use, and capture as a function of the input frequency is quite similar to that produced by model a.

Table 42 (C) gives the values of power production, use, and capture for model (b) in Figure 27. Power use, production, and capture by model (b) have a variation with frequency that is similar to model (d)

Table 42 The power produced, used, and captured by storages of chain models in Figure 27 with Case A turnovers over a six decade range of input frequencies

Input Frequency	Power Produced Q_1 T = 10	Power Produced Q_2 T = 1.0	Power Produced Q_3 T = 0.1	Power Out Q_1 T = 10	Power Out Q_2 T = 1.0	Power Out Q_3 T = 0.1	Total Power Produced	Total Power Out	Total Power Captured
(A) Chain Model a									
1.0000	91.94	8.100	0.729	9.000	0.810	0.729	100.8	10.54	919.4
1.0000	92.33	8.279	0.729	9.198	0.810	0.729	101.3	10.74	923.2
0.1000	92.07	8.332	0.747	9.067	0.829	0.730	101.1	10.52	920.7
0.0100	92.29	8.318	0.753	9.175	0.816	0.748	101.4	10.74	922.9
0.0010	92.44	8.320	0.753	9.245	0.810	0.754	101.5	10.61	924.4
0.0001	92.85	8.355	0.757	9.308	0.827	0.757	102.0	10.69	928.8
(B) Chain Model d									
10.0000	91.32	8.089	0.721	9.096	0.877	0.648	100.7	10.62	919.2
1.0000	92.31	8.266	0.721	9.293	0.877	0.648	100.7	10.82	923.0
0.1000	92.06	8.318	0.739	9.226	0.897	0.649	101.2	10.65	920.5
0.0100	92.20	8.335	0.748	9.185	0.887	0.667	101.3	10.74	922.0
0.0010	92.40	8.357	0.752	9.212	0.878	0.676	101.5	10.77	923.7
0.0001	92.84	8.391	0.764	9.344	0.889	0.679	102.0	10.91	927.6

Table 42—Continued

Input Frequency	Power Produced			Power Out			Total Power		
	Q_1 T = 10	Q_2 T = 1.0	Q_3 T = 0.1	Q_1 T = 10	Q_2 T = 1.0	Q_3 T = 0.1	Produced	Out	Captured
(C) Chain Model b									
10.0000	92.77	8.185	0.648	9.520	0.867	0.583	101.6	11.27	919.4
1.0000	93.08	8.325	0.648	10.040	0.868	0.583	102.1	11.49	922.4
0.1000	93.25	8.425	0.664	10.040	0.892	0.582	102.3	11.51	924.1
0.0100	93.24	8.430	0.676	9.979	0.862	0.602	102.3	11.46	924.0
0.0010	93.25	8.430	0.677	9.997	0.869	0.610	102.4	11.48	924.1
0.0001	93.68	8.466	0.680	10.200	0.895	0.612	102.8	11.71	927.8

Table 43 The mean power produced, used, and captured by storages of chain models in Figure 27 over a six decade frequency range for Case A turnovers

Input Frequency	Mean Power Produced			Mean Power Out			Total Mean Power		
	Q_1 T = 10	Q_2 T = 1.0	Q_3 T = 0.1	Q_1 T = 10	Q_2 T = 1.0	Q_3 T = 0.1	Produced	Out	Captured
(A) Chain Model a									
10.0000	89.92	8.092	0.728	8.992	0.810	0.729	98.74	10.53	899.2
1.0000	89.93	8.093	0.729	8.995	0.810	0.728	98.75	10.53	899.3
0.1000	89.95	8.094	0.729	8.998	0.809	0.729	98.77	10.54	899.5
0.0100	89.96	8.095	0.729	9.012	0.808	0.730	98.78	10.55	899.6
0.0010	89.95	8.095	0.729	8.997	0.809	0.729	98.77	10.54	899.5
0.0001	91.45	8.194	0.736	9.106	0.824	0.736	100.40	10.67	909.1
(B) Chain Model d									
10.0000	89.90	8.082	0.721	9.086	0.876	0.648	98.70	10.61	899.0
1.0000	89.92	8.083	0.721	9.089	0.876	0.648	98.72	10.61	899.1
0.1000	89.93	8.080	0.720	9.127	0.876	0.648	98.73	10.65	899.2
0.0100	89.89	8.071	0.720	9.174	0.875	0.649	98.68	10.70	898.8
0.0010	89.80	8.050	0.718	9.202	0.877	0.646	98.58	10.73	898.0
0.0001	90.81	8.154	0.727	9.313	0.887	0.653	99.69	10.85	907.5

Table 43—Continued

Input Frequency	Mean Power Produced			Mean Power Out			Total Mean Power		
	Q_1 T = 10	Q_2 T = 1.0	Q_3 T = 0.1	Q_1 T = 10	Q_2 T = 1.0	Q_3 T = 0.1	Produced	Out	Captured
(C) Chain Model b									
10.0000	90.73	8.150	0.648	9.810	0.866	0.583	99.53	11.26	899.2
1.0000	90.71	8.147	0.647	9.818	0.867	0.582	99.50	11.26	898.8
0.1000	90.66	8.136	0.646	9.880	0.867	0.582	99.44	11.33	898.4
0.0100	90.63	8.124	0.645	9.960	0.866	0.582	99.40	11.41	898.1
0.0010	90.62	8.122	0.644	9.980	0.869	0.580	99.39	11.43	898.1
0.0001	91.79	8.218	0.653	10.140	0.864	0.586	100.70	11.61	907.6

Table 44 The variant power produced, used, and captured by stages of chain models in Figure 27 over a six decade frequency range for Case A turnovers

Input Frequency	Variant Power Produced			Variant Power Out			Total Variant Power		
	Q_1 T = 10	Q_2 T = 1.0	Q_3 T = 0.1	Q_1 T = 10	Q_2 T = 1.0	Q_3 T = 0.1	Produced	Cut	Captured
(A) Chain Model a									
10.0000	2.02	0.008	0.001	0.008	0.000	0.000	2.029	0.008	20.2
1.0000	2.40	0.184	0.000	0.203	0.000	0.001	2.586	0.203	23.3
0.1000	2.12	0.238	0.018	0.059	0.019	0.001	2.376	0.079	21.2
0.0100	2.45	0.223	0.024	0.163	0.008	0.018	2.697	0.189	23.3
0.0010	2.60	0.225	0.024	0.248	0.001	0.025	2.849	0.274	24.9
0.0001	1.40	0.161	0.021	0.202	0.003	0.021	1.582	0.266	20.7
(B) Chain Model b									
10.000	2.02	0.007	0.000	0.009	0.001	0.000	2.027	0.010	20.2
1.0000	2.36	0.181	0.001	0.200	0.000	0.000	2.542	0.200	23.6
0.1000	2.56	0.286	0.021	0.119	0.023	0.000	2.867	0.142	25.9
0.0100	2.57	0.293	0.033	0.012	0.013	0.020	2.896	0.045	25.8
0.0010	2.58	0.294	0.033	0.009	0.001	0.030	2.907	0.040	25.9
0.0001	2.03	0.237	0.027	0.031	0.002	0.026	2.294	0.059	20.1

Table 44--Continued

Input Frequency	Variant Power Produced Q_1 $T = 10$	Q_2 $T = 1.0$	Q_3 $T = 0.1$	Variant Power Out Q_1 $T = 10$	Q_2 $T = 1.0$	Q_3 $T = 0.1$	Total Variant Power Produced	Out	Captured
(C) Chain Model b									
10.0000	2.04	0.008	0.000	0.010	0.001	0.000	2.120	0.011	20.2
1.0000	2.37	0.178	0.001	0.222	0.001	0.001	2.549	0.224	23.6
0.1000	2.56	0.289	0.018	0.160	0.025	0.000	2.897	0.185	25.7
0.0100	2.61	0.306	0.031	0.019	0.016	0.020	2.947	0.055	25.9
0.0010	2.63	0.308	0.033	0.017	0.000	0.030	2.971	0.047	26.0
0.0001	1.88	0.248	0.027	0.080	0.011	0.026	2.165	0.097	20.2

except there is no local peak at input 1.0 cycles/time and the values in model (b) are greater than those for model (d) and model (a). Tables 43 and 44 show that generally model (a) captures more mean power whereas models (d) and (b) capture more variant power except at very high and very low frequencies when model (a) does best. Model (a) captures the most power at input frequencies 1.0, 0.001, and 0.0001, whereas model (b) does best at frequencies 0.1 and 0.01.

Table 45 presents the power produced, used, and captured for models in Figure 27 with all turnovers equal one per unit time. Section A of Table 45 supplies this information for model (a) in Figure 27 which is without secondary positive feedbacks. The frequency variation of power production use and capture by model (a) with all turnovers equal is similar to that with turnovers decreasing an order of magnitude at each level in the chain. However, there is no peak in power use or capture at input frequency 1.0. Variant power produced, used, and captured increase to a maximum at input frequency 0.001 and then fall off (see Table 47). The total power produced, used, and captured continues to increase at input frequency 0.0001 because the mean values of these three increase precipitously for this input frequency.

Table 45 (B) gives similar results for model (d) in Figure 27. Tables 46 and 47 show that only three of six frequency inputs gave stable runs for this model. Those runs which were stable did not do as well as other pathway and turnover configurations already examined. More variant power appears in the unstable runs because of the increased variance caused by zero values which lower the mean as well as the fact that excluded units tend to pulse before going to zero.

Table 46 The power produced, used, and captured by storages of chain models in Figure 27 over a six decade frequency range for Case 8 turnovers*

Input Frequency	Power Produced			Power Out			Total Power		
	Q_1 T = 1.0	Q_2 T = 1.0	Q_3 T = 1.0	Q_1 T = 1.0	Q_2 T = 1.0	Q_3 T = 1.0	Produced	Out	Captured
(A) Model a									
10.0000	91.97	8.096	0.729	8.997	0.810	0.729	100.80	10.540	919.7
1.0000	91.98	8.102	0.729	9.003	0.810	0.729	100.80	10.540	919.8
0.1000	92.07	8.228	0.754	9.060	0.819	0.746	101.00	10.630	920.7
0.0100	92.43	8.317	0.753	9.240	0.810	0.753	101.50	10.800	924.3
0.0010	92.44	8.320	0.753	9.244	0.810	0.753	101.50	10.810	924.4
0.0001	92.85	8.355	0.757	9.308	0.828	0.757	102.00	10.890	929.8
(B) Model d									
10.0000	91.95	8.087	0.721	9.089	0.877	0.648	100.80	10.610	919.5
1.0000	91.96	8.092	0.721	9.100	0.877	0.648	100.80	10.630	919.6
0.1000	13.45	1.283	0.143	3.672	0.153	0.110	14.88	3.935	134.5*
0.0100	92.39	8.356	0.762	9.223	0.878	0.676	101.50	10.780	923.8
0.0010	85.22	7.757	0.703	8.180	0.757	0.633	93.68	9.570	852.1*
0.0001	82.52	7.551	0.687	7.145	0.693	0.613	90.76	8.457	824.9*

*Unstable by time = 1,000

Table 46. The mean power produced, used, and captured by storages of the chain models in Figure 27 over a six decade frequency range for Case 8 turnovers

Input Frequency	Mean Power Produced			Mean Power Out			Total Mean Power		
	Q_1 T = 1.0	Q_2 T = 1.0	Q_3 T = 1.0	Q_1 T = 1.0	Q_2 T = 1.0	Q_3 T = 1.0	Produced	Out	Captured
(A) Model a									
10.0000	89.940	8.093	0.729	8.994	0.809	0.729	98.78	10.530	899.40
1.0000	89.940	8.095	0.729	8.994	0.809	0.729	98.76	10.530	899.40
0.1000	89.940	8.095	0.729	8.998	0.809	0.729	98.76	10.540	899.40
0.0100	89.940	8.095	0.729	8.995	0.809	0.729	98.76	10.530	899.40
0.0010	89.950	8.095	0.729	8.995	0.810	0.729	98.77	10.530	899.40
0.0001	91.450	8.194	0.736	9.107	0.824	0.736	100.40	10.670	909.10
(B) Model d									
10.0000	89.920	8.083	0.721	9.086	0.877	0.648	98.72	10.610	899.20
1.0000	89.930	8.084	0.721	9.090	0.876	0.648	98.74	10.610	899.20*
0.1000	2.045	0.142	0.013	0.715	0.020	0.012	2.20	0.747	20.45*
0.0100	89.790	8.058	0.718	9.211	0.879	0.645	98.57	10.740	897.80*
0.0010	72.060	6.502	0.586	7.118	0.658	0.527	79.14	8.303	720.40*
0.0001	64.570	5.892	0.536	5.639	0.548	0.482	71.00	6.723	645.60*

*Unstable by time = 1,000.

Figure 47 The variant power produced, used, and captured by storages of the chain models in Figure 27 over a six decade frequency range for Case B turnovers

Input Frequency	Variant Power Produced			Variant Power Out			Total Varinat Power		
	Q_1 T = 1.0	Q_2 T = 1.0	Q_3 T = 1.0	Q_1 T = 1.0	Q_2 T = 1.0	Q_3 T = 1.0	Produced	Out	Captured
(A) Model a									
10.0000	2.03	0.003	0.000	0.003	0.001	0.000	2.033	0.004	20.3
1.0000	2.04	0.007	0.000	0.010	0.001	0.000	2.047	0.011	20.4
0.1000	2.13	0.113	0.025	0.062	0.010	0.017	2.288	0.089	21.3
0.0100	2.49	0.222	0.024	0.245	0.001	0.024	2.736	0.270	24.9
0.0010	2.49	0.226	0.024	0.249	0.001	0.024	2.739	0.273	25.0
0.0001	1.40	0.161	0.021	0.201	0.004	0.021	1.582	0.226	20.7
(B) Model d									
10.0000	2.03	0.004	0.000	0.003	0.000	0.000	2.034	0.003	20.3
1.0000	2.03	0.008	0.000	0.010	0.001	0.000	2.038	0.011	20.4
0.1000	11.41	1.141	0.130	2.957	0.133	0.098	12.680	3.188	114.1*
0.0100	2.60	0.298	0.034	0.012	0.000	0.031	2.932	0.043	26.0
0.0010	13.17	1.255	0.118	1.062	0.099	0.106	14.540	1.267	131.7*
0.0001	17.95	1.659	0.152	1.506	0.145	0.137	19.760	1.788	179.3*

*Unstable by time - 1,000

Model (b) was unstable at all frequencies tested when each of the component turnovers was equal to one per unit time. Only nine of eighteen simulation runs were stable when unit turnovers all equaled 1 whereas all of the eighteen simulation runs were stable when turnovers decrease by a factor of 10 with each succeeding level. Only model (a) was stable for turnover cases $Q_1 = 0.1$, $Q_2 = 10$, $Q_3 = 1$ and $Q_1 = 0.1$, $Q_2 = 1$, $Q_3 = 10$.

Table 48 gives the power produced, used, and captured by model (a) in Figure 27 as a function of frequency when unit turnovers are $Q_1 = 0.1$, $Q_2 = 10$, $Q_3 = 1$. For this case the system first oscillates producing and using a lot of variant power. As the run continues units Q_2 and Q_3 go to zero leaving only unit Q_1 which grows to 10 times its initial size. This very large storage at Q_1 is able to produce, use, and capture more power than any other configuration tested at this efficiency of energy transfer. The power used and captured have a peak at input frequency 1.0 from which there is a steady decline to a low at input frequency 0.001. At frequency 0.0001 both power used and captured are highest. The observed pattern is due primarily to the behavior of the mean power. The variant power used peaks at input frequency 0.01. The power produced increases to a high at input frequency 0.001 and then falls off. This drop is due to the fall in variant power captured and produced at this low frequency.

Table 48 (B) presents the MSQ power produced, used, and captured by model (a) of Figure 27 when frequency varies over a six decade range and turnovers are $Q_1 = 0.1$, $Q_2 = 1$, $Q_3 = 10$. This turnover

Table 48 The power produced, used, and captured by storages in the chain models in Figure 27 over a six frequency range for Case C and Case D turnovers

Input Frequency	Power Produced			Power Out			Total Power		
	Q_1	Q_2	Q_3	Q_1	Q_2	Q_3	Produced	Out	Captured
(A) Model a, Case D T = 0.1, 10, 1.0									
10.0000	99.18	5.619	0.606	80.470	0.574	0.348	105.40	81.390	991.8
1.0000	99.81	5.007	0.545	84.660	0.511	0.286	105.40	85.460	998.2
0.1000	99.48	5.305	0.571	82.500	0.543	0.320	105.40	83.360	994.8
0.0100	99.03	5.763	0.627	79.550	0.618	0.372	105.40	80.640	930.3
0.0010	98.74	6.405	0.665	76.580	0.512	0.427	106.80	77.530	987.3
0.0001	101.50	1.995	0.207	99.400	0.194	0.138	103.70	99.730	1,014.0
(B) Model a, Case C T = 0.1, 1.0, 10									
10.0000	60.80	6.019	0.580	4.332	4.183	0.512	67.40	9.027	608.0
1.0000	57.71	5.772	0.518	3.738	4.330	0.459	64.00	8.527	577.1
0.1000	59.50	5.945	0.586	4.025	4.269	0.507	65.96	8.801	595.0
0.0100	62.68	6.553	0.685	4.661	4.244	0.576	69.92	9.481	626.8
0.0010	66.52	6.928	0.741	5.376	4.040	0.631	74.19	10.050	665.2
0.0001	50.54	4.979	0.202	1.849	4.707	0.181	55.72	6.736	506.1

Table 48—Continued

Input Frequency	Average Turnovers	
	Q_1	Q_2
(C) Model a, Case C: $\tau = 0.1, 1.0, 10$		
10.0000	0.21	0.140
1.0000	0.24	0.130
0.1000	0.23	0.140
0.0100	0.20	0.150
0.0010	0.18	0.160
0.0001	0.42	0.105

Table 48. The mean power produced, used, and captured by storages of the chain models in Figure 27 over a six decade frequency range for Case C and Case D turnovers

Input Frequency	Mean Power Produced			Mean Power Out			Total Mean Power		
	Q_1	Q_2	Q_3	Q_1	Q_2	Q_3	Produced	Out	Captured
(A) Model a, Case D $T = 0.1, 10, 1.0$									
10.0000	96.92	1.591	0.143	72.030	0.159	0.144	98.65	72.330	969.2
1.0000	97.56	1.015	0.091	78.440	0.102	0.092	98.67	78.639	975.7
0.1000	97.23	1.320	0.119	75.080	0.132	0.120	98.34	76.330	972.3
0.0100	96.75	1.760	0.159	70.620	0.175	0.159	98.67	70.950	967.5
0.0010	96.75	2.073	0.190	68.380	0.176	0.191	99.01	68.750	967.5
0.0001	100.00	0.256	0.023	96.620	0.025	0.023	100.30	96.670	998.3
(B) Model a, Case C $T = 0.1, 1.0, 10$									
10.0000	56.61	5.471	0.160	2.711	3.830	0.161	62.24	6.702	566.1
1.0000	54.06	5.264	0.117	2.223	4.060	0.117	59.44	6.400	540.6
0.1000	55.19	5.358	0.136	2.440	3.960	0.136	60.68	6.536	551.9
0.0100	57.49	5.540	0.176	2.883	3.749	0.178	63.21	6.844	574.9
0.0010	59.53	5.715	0.212	3.284	3.558	0.212	65.56	7.054	596.3
0.0001	49.20	4.814	0.023	1.156	4.579	0.023	54.04	5.758	491.8

Table 50. The variant power produced, used, and captured by storages of the chain models in Figure 27 over a six decade frequency range for Case C and Case D turnovers

Input Frequency	Variant Power Produced			Variant Power Out			Total Variant Power		
	Q_1	Q_2	Q_3	Q_1	Q_2	Q_3	Produced	Out	Captured
(A) Model a, Case D	T = 0.1, 10, 1.0								
10.0000	2.26	4.029	0.463	8.440	0.415	0.204	6.751	9.059	22.6
1.0000	2.25	3.992	0.454	6.220	0.409	0.194	6.696	6.823	22.5
0.1000	2.25	3.985	0.452	7.420	0.411	0.200	6.687	8.031	22.5
0.0100	2.28	4.003	0.468	8.930	0.443	0.213	6.751	9.856	22.8
0.0010	1.99	4.332	0.475	8.200	0.345	0.236	6.797	8.781	19.8
0.0001	1.50	1.740	0.184	2.780	0.169	0.115	3.424	3.064	15.7
(B) Model a, Case C	T = 0.1, 1.0, 10								
10.0000	4.19	0.548	0.420	1.621	0.353	0.351	5.158	2.325	41.9
1.0000	3.65	0.508	0.401	1.515	0.270	0.342	4.559	2.127	36.5
0.1000	4.31	0.587	0.450	1.585	0.309	0.371	5.347	2.265	43.1
0.0100	6.19	1.013	0.509	1.776	0.495	0.400	6.712	2.671	51.9
0.0010	6.89	1.213	0.529	2.092	0.482	0.419	8.632	2.993	68.9
0.0001	1.34	0.165	0.179	0.692	0.128	0.158	1.684	0.978	14.3

arrangement produced the least power at all frequencies. Unit Q_1 is unable to maintain its initial storage while Q_2 grows to a value greater than its initial value Unit Q_3 oscillates and then goes to zero This results in the creation of a chain that has a pattern of decreasing turnover for each successively higher unit in the chain. This is just the opposite pattern from that which was given initially All other cases approximately maintained their initial turnovers averaged over 1,000 time units Power produced, used, and captured increase gradually with decreasing input frequency to a peak at input frequency 0 001 and then fall off

Figure 28 shows that there is an exponential decline in the stability of chain models with large second law losses with increasing numbers of secondary positive feedbacks These models are able to generate very little additional power by establishing secondary positive feedbacks [see Figure 28(b)]. When power captured is viewed as a function of the number of secondary feedbacks the less power lost in a feedback interaction the more power the system is able to capture as feedbacks are increased.

Filter Properties of Zero Positive Feedback Chain with One Variable and and One Constant Energy Source

An autocatalytic chain model without secondary positive feedback between units was simulated over a six decade frequency range for four different arrangements of the unit turnovers (see Figure 29) One energy source was constant and entered at the base of the chain and a

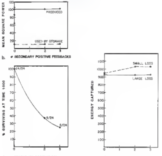

Figure 28 Effects of increasing the number of secondary positive feedback loops in a three unit autocatalytic chain (a) The relationship between the number of secondary positive feedbacks and the stability in chain models with large second law losses given in Figure 27, (b) the relationship between the number of secondary positive feedbacks and the power produced (—) and used (---) by the chain model in Figure 27, (c) a comparison between the power captured by chain models with large second law losses (—) and those with small second law losses (---) at interactions

Figure 29. An autocatalytic chain without secondary positive feedback driven by two energy sources, one constant and one variable Initial values for Q_1, Q_2, and Q_3 are variable depending on the turnover arrangement.

Equations:

(a) Second input at Q_1

$$R_0 = I_0 - k_0Q_1R_1R_0$$
$$R_1 = I_1 = k_{01}Q_1R_0R_1$$
$$\dot{Q}_1 = k_1Q_1R_1R_0 - k_2Q_1 - k_3Q_1Q_2$$
$$\dot{Q}_2 = k_3Q_1Q_2 - k_4Q_2 - k_5Q_2Q_3$$
$$\dot{Q}_3 = k_5Q_2Q_3 - k_6Q_3$$

(b) Second Input at Q_2

$$R_0 = I_0 - k_0Q_1R_0$$
$$R_1 = I_1 - k_{10}Q_1Q_2R_1$$
$$\dot{Q}_1 = k_1Q_1R_0 - k_2Q_1 - k_3Q_1Q_2R_1$$
$$\dot{Q}_2 = k_4Q_1Q_2R_1 - k_5Q_2 - k_6Q_2Q_3$$
$$\dot{Q}_3 = k_6Q_2Q_3 - k_7Q_3$$

(c) Second Input at Q_3

$$R_0 = I_0 - k_0Q_1R_0$$
$$R_1 = I_1 - k_{01}Q_2Q_3R_1$$
$$\dot{Q}_1 = k_1Q_1R_0 - k_2Q_1 - k_3Q_1Q_2$$
$$\dot{Q}_2 = k_3Q_1Q_2 - k_4Q_2 - k_5Q_2Q_3R_1$$
$$\dot{Q}_3 = k_6Q_2Q_3R_1 - k_7Q_3$$

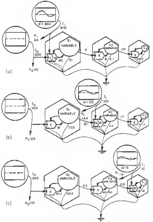
A' = 300
I_1
500
R_1
84
I_0
500
R_0 50
(a)
Q_1
VARIABLE
X
X
90
81
8
Q_2
VARIABLE
X
8
8.1
08
Q_3
X
0.8/.8
AI = 30
I_1
100
I_0
500
R_0 129
(b)
Q_1
VARIABLE
X
81
72.9
R_1
14.4
8.1
Q_2
VARIABLE
X
X
17
14.4
1.7
Q_3
X
1.7
1.7
AI = 3
I_1
10
R_1
14
I_0
890
R_0 132
(c)
Q_1
VARIABLE
X
89.1
80.2
8.9
Q_2
VARIABLE
X
8.9
8.0
0.9
Q_3
X
X
1.8
1.8

second variable energy source entered at either unit one, two, or three. A summary of these results is given in Table 51 and Figure 30. The complete simulation results are given in the data supplement to this dissertation.

Table 51 demonstrates that the power generated by this chain model for a given source position and frequency input is remarkably similar regardless of the turnover configuration. The position of the second variable energy source seems to be the most important factor in determining the power produced and used by this model. The pattern of frequency response that emerges at the Q_1 and Q_2 level is determined largely by the model's high frequency cutoff. However, at level Q_3 turnover Case D produces and uses more energy than any of the other cases due to resonance set up at frequencies 10 to 0.1. Tables 52 and 53 give the portion of the power due to the mean and variance, respectively. The data supplement gives the complete breakdown of power generated by the mean and variance for each of the four time constant arrangements tested.

The frequency response of the model to a variable energy input entering at Q_1 is given in section A of Tables 51, 52, and 53 and by the Bode-like plot in Figure 30(a). Both the high frequency and noisy inputs produce and use more power than low frequency inputs tested here. Table 52 and 53 show that this result is due to the increased mean power produced and used by the turnover arrangements at these frequencies. Figure 30(a) shows that the frequency response of power used is primarily that of a low pass filter at high frequencies with resonant power

Table 51 The total power produced and used by four time constant arrangements of the zero secondary positive feedback chain model in Figure 29 as a function of variations in the input frequency of the second energy source

Input Frequency	Total Power							
	Case A T - 10, 1.0, 0.1		Case B T = 1.0, 1.0, 1.0		Case C T = 0.1, 1.0, 10		Case D T = 0.1, 10, 1.0	
	Produced	Out	Produced	Out	Produced	Out	Produced	Out
(A) Second Input at Q_1, a_1 = 300								
All	96.59	86.56	97.09	86.56	102.70	86.06	102.10	87.51
10.0000	103.10	86.65	103.63	86.83	103.70	85.89	103.70	86.86
1.0000	82.50	78.30	82.56	78.25	82.80	76.37	82.70	76.32
0.1000	82.50	79.35	82.24	78.21	82.01	75.18	82.46	76.70
0.0100	85.07	81.73	85.07	81.73	85.51	81.66	81.60	79.81
0.0010	86.85	79.85	86.85	79.85	86.97	79.84	86.97	79.92
0.0001	86.85	79.93	86.87	79.93	93.96	81.31	86.56	85.61
(B) Second Input at Q_2, a_2 = 30								
All	98.54	89.67	98.64	89.65	98.64	89.71	98.56	89.70
10.0000	98.87	89.66	86.80	89.74	98.78	89.71	98.78	89.73
1.0000	98.82	89.68	98.81	89.74	98.78	89.74	98.87	90.04
0.1000	98.93	89.97	86.95	90.04	100.03	91.20	99.04	90.18
0.0100	99.16	90.23	99.82	90.92	98.96	90.90	99.79	90.84
0.0010	100.70	90.68	100.70	90.67	100.70	90.68	100.70	90.66
0.0001	100.70	90.73	100.70	90.72	100.70	90.73	107.00	90.72

Table 51--Continued

Input Frequency	Total Power							
	Case A T = 10, 1.0, 0.1		Case B T = 1.0, 1.0, 1.0		Case C T = 0.1, 1.0, 10		Case D T = 0.1, 10, 1.0	
	Produced	Out	Produced	Out	Produced	Out	Produced	Out
(C) Second Input at Q_3, a_3 = 3								
All	100.78	89.87	100.79	89.87	100.82	89.87	115.28	102.27
10.0000	100.81	89.77	100.82	89.87	100.82	89.87	115.31	102.29
1.0000	100.81	89.87	100.82	89.86	100.84	89.90	115.33	102.31
0.1000	100.78	89.88	100.79	89.91	100.85	89.94	115.02	101.98
0.0100	97.33	91.51	98.73	91.18	100.51	92.81	115.50	102.61
0.0010	42.48	42.18	42.46	41.65	42.57	42.79	41.60	41.83
0.0001	41.56	41.55	41.55	41.30	41.57	41.61	41.42	41.27

Table 52. The portion of the total power given in Table 51 attributable to the mean

Input Frequency	Total Mean Power							
	T = 10, 1.0, 0.1		T = 1.0, 1.0, 1.0		T = 0.1, 1.0, 10		T = 0.1, 10, 1.0	
	Produced	Out	Produced	Out	Produced	Out	Produced	Out
(A) Second Input at Q_1								
All	95.72	86.52	95.72	86.52	96.76	87.38	95.75	87.39
10.0000	95.57	86.43	96.04	86.80	96.20	86.81	96.05	86.80
1.0000	79.00	76.00	79.34	76.09	79.62	76.23	79.45	76.22
0.1000	78.82	75.86	78.73	76.09	78.86	75.92	78.78	75.92
0.0100	78.94	75.85	78.94	75.85	79.18	76.28	76.55	76.11
0.0010	81.65	75.79	81.65	75.79	81.72	75.74	81.59	75.74
0.0001	81.61	75.84	81.62	75.84	86.48	75.52	76.63	76.03
(B) Second Input at Q_2								
All	98.38	89.63	98.31	89.63	98.31	86.67	98.31	89.66
10.0000	98.40	89.62	98.35	89.71	98.33	89.69	98.32	89.68
1.0000	98.45	89.63	98.35	89.61	98.34	89.69	98.34	89.70
0.1000	98.43	89.62	98.40	89.62	98.32	89.62	98.35	89.61
0.0100	98.50	89.61	98.47	89.73	97.71	89.66	98.48	89.59
0.0010	99.26	89.51	99.28	89.52	99.26	89.50	99.27	89.48
0.0001	99.34	89.58	99.34	89.58	99.34	89.58	99.34	89.58

Table 52—Continued

Input Frequency	Total Mean Power T = 10, 1.0, 0.1 Produced	 T = 10, 1.0, 0.1 Out	 T = 1.0, 1.0, 1.0 Produced	 T = 1.0, 1.0, 1.0 Out	 T = 0.0, 1.0, 10 Produced	 T = 0.0, 1.0, 10 Out	 T = 0.1, 10, 1.0 Produced	 T = 0.1, 10, 1.0 Out
(C) Second Input at Q_3								
All	100.70	89.85	100.70	89.86	100.70	89.85	101.60	88.68
10.0000	100.70	89.85	100.70	89.85	100.70	89.86	101.60	88.68
1.0000	100.70	89.84	100.70	89.84	100.70	89.86	101.60	88.70
0.1000	100.70	89.84	100.70	89.84	100.70	89.86	101.70	88.82
0.0100	96.15	90.36	97.83	90.17	97.85	89.98	101.60	88.77
0.0010	41.05	41.05	41.05	41.09	41.11	41.54	41.09	41.52
0.0001	41.06	41.08	41.08	41.08	41.06	41.11	41.06	41.11

Table 53. The portion of the total power in Table 51 attributable to the variance

Input Frequency	Total Variant Power							
	T = 10, 1.0, 0.1		T = 1.0, 1.0, 1.0		T = 0.1, 1.0, 10		T = 0.1, 10, 1.0	
	Produced	Out	Produced	Out	Produced	Out	Produced	Out
(A) Second Input at Q_1								
All	1.371	0.039	1.371	0.039	5.937	0.679	5.376	0.123
10.0000	7.629	0.226	7.594	0.027	7.602	0.082	7.595	0.075
1.0000	3.449	2.300	3.223	0.108	3.280	0.136	3.201	0.047
0.1000	3.880	3.466	3.511	2.399	3.154	0.262	3.680	0.778
0.0100	6.133	5.880	6.133	5.880	6.332	5.383	5.044	3.701
0.0010	5.205	4.064	5.205	4.064	5.262	4.098	5.371	4.177
0.0001	5.290	4.086	5.242	4.093	7.476	5.786	9.931	9.582
(B) Second Input at Q_2								
All	0.158	0.033	0.333	0.024	0.334	0.044	0.334	0.043
10.0000	0.468	0.040	0.451	0.052	0.550	0.021	0.450	0.041
1.0000	0.379	0.050	0.462	0.042	0.543	0.052	0.542	0.342
0.1000	0.511	0.352	0.547	0.417	1.714	1.679	0.684	0.557
0.0100	0.660	0.618	1.351	1.313	1.243	1.243	1.310	1.254
0.0010	1.438	1.169	1.431	1.150	1.439	1.179	1.432	1.150
0.0001	1.432	1.152	1.419	1.138	1.402	1.152	1.399	1.138

Table 53—Continued

Input Frequency	Total Variant Power							
	T = 10, 1.0, 0.1		T = 1.0, 1.0, 1.0		T = 0.1, 1.0, 10		T = 0.1, 10, 1.0	
	Produced	Out	Produced	Out	Produced	Out	Produced	Out
(C) Second Input at Q_3								
All	0.117	0.014	0.160	0.014	0.096	0.021	13.710	13.590
10.0000	0.129	0.015	0.119	0.013	0.119	0.122	13.730	13.610
1.0000	0.119	0.017	0.129	0.017	0.127	0.044	13.740	13.610
0.1000	0.116	0.042	0.126	0.047	0.152	0.085	13.330	13.160
0.0100	1.184	1.133	0.897	1.011	2.659	2.031	13.920	13.840
0.0010	1.430	1.129	1.347	0.557	1.460	1.253	0.505	0.303
0.0001	0.493	0.491	0.492	0.213	0.504	0.501	0.358	0.158

Figure 30. A Bode-like plot of the variant power ratio as a function of frequency for the models in Figure 29 for four different turnover arrangements

Case A turnovers are $Q_1 = 10$, $Q_2 = 1.0$, $Q_3 = 0.1$ ————

Case B turnovers are $Q_1 = 1.0$, $Q_2 = 1.0$, $Q_3 = 1.0$ – – – –

Case C turnovers are $Q_1 = 0.1$, $Q_2 = 1.0$, $Q_3 = 10$ —·—·—

Case D turnovers are $Q_1 = 0.1$, $Q_2 = 10$, $Q_3 = k,9$ -·····

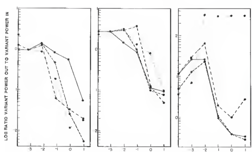

a) Second energy source enters at Q_1 b) Second energy source enters at Q_2 c) Second energy source enters at Q_3

becoming more important at low frequency inputs. Turnover Case A handles variant power best over a band from 10 to 0.001 cycles per unit time for this input case.

The frequency filter aspect of the turnover arrangement also is seen by examining Table 53. The 10 cycle/unit time frequency and noisy inputs are too fast to be exploited by the turnovers used here as can be seen by examining the power used columns in Table 53. Turnover Case A produces more variant power at frequencies 1 and 0.1 cycle per time unit than do the other three cases. For input frequency 0.01, Case B does as well as Case A but Case C produces the most power. At lower frequency inputs case D produces and uses the most variant power. Noisy and 10 cycle per time unit inputs produce a considerable amount of variant power regardless of the model's turnover structure. This variant power is not transmitted up the chain or used by unit Q_1.

Table 51 (B) and Figure 30(b) show the simulation results when the variable energy enters at unit Q_2. The second input energy and its signal amplitude are less at this level reflecting the increased quality of this input energy. There are only small differences between the four arrangements with the second input at Q_2. Cases A, B, and D all show a slight increase in the total power produced and used as the input frequency becomes larger. Case C has maximum power use at input frequency 0.1 cycles per time unit. These results are seen to be largely the result of the differences in production and use of variant power (see Table 53). The maximum shown by Case C reflects a resonance of unit three's fast turnover with the input frequency to produce and use the extra variable power as shown by its resonant peak on Figure 30(b). The turnover arrangement case D has the fastest turnover for Q_2 and uses power best at frequency one cycle per time and higher.

Table 51 (C) and Figure 30(c) give the results of simulations when the second energy source is input at Q_3. Turnover Case D exhibits resonant response over a frequency band from 10 to 0.01 cycles per unit time but is unstable for lower frequency input signals [see Figure 30(c)]. Cases A and B show a distinct drop in the power produced at input frequency 0.01 cycles per time unit and they are unstable at lower frequencies. Cases B and C show a gradual increase in the power used to peak at 0.01 cycles per unit time and then they become unstable. Table 52 (C) shows that the drop in power produced at frequency 0.01 for Cases A, B, and C is due to a drop in the mean power produced. The data supplement Tables 2, 5, and 7 show this effect to be due to the loss of mean power produced by unit Q_2 in the chain. Table 53 (C) shows that the increased power produced and used by Case D is due to a large increase in the variant power component. The data supplement Table 12 shows this increase to be attributable almost entirely to the increased use and production of variant power by unit Q_2 in the chain with a fast turnover of 10.

Of the three positions that a second variable energy source may enter a three unit autocatalytic chain with zero positive feedbacks an interaction at Q_3 or the highest compound level generates more power and uses more power over a large band of frequencies from 10 to 0.01 cycles per time unit for four turnover arrangements tested. An exception occurs for the power produced by Cases A through C when the multiplication of a high frequency signal, 10, by a constant generates additional variant power that is not used by the model components. For frequencies lower than 0.01, input at unit Q_2 gives the most power used and produced. Table 54 gives the frequency analysis simulation results for the four turnover cases when the input at Q_1 has an amplitude of 214.5 which has total power equivalent to the single input amplitude of 300. If the totals in Table 54 are substituted for those in Table 52 (A) one finds that a second input at unit Q_3 always gives the most power produced and used over its band of stable input frequencies.

Filter Properties of a Three Positive Feedback Chain with One Variable and One Constant Energy Source

The results of simulating an autocatalytic chain model with three secondary positive feedbacks over a six decade frequency range for four turnover arrangements is given in Table 55. These simulations were performed with an excess energy available for use in the model which amounted to the energy contained in the variable signal. Only 25 of 48 simulation runs were stable. Turnover arrangements represented by Cases A and B had 8 of 12 stable runs, Case C had 5 of 12 stable and Case D had only 4 of 12 stable. Table 56 shows that of the three possible positions for a second energy to interact with this model the Q_1 position yields a far greater amount of power produced than do positions Q_2 and Q_3. Forty-one percent of the 24 runs were stable when the second energy entered at Q_1. When the second energy entered at Q_2 33% of the runs were stable and about 36% of the runs were stable when the second energy source interacts at Q_3. Figure 32 shows that

Table 54 The mean square power produced and used by a zero secondary positive feedback autocatalytic chain model over a four decade frequency range for four turnover arrangements when the first input is constant and the second input enters at unit Q_1 with an amplitude of 210.5*

Input Frequency	MSQ Power Produced			MSQ Power Out			Total Power	
	Q_1	Q_2	Q_3	Q_1	Q_2	Q_3	Produced	Out
(A) T = 10, 1.0, 0.1								
All	89.49	8.670	0.584	78.21	8.080	0.586	98.74	86.88
10.00	90.39	8.627	0.555	78.00	8.060	0.559	99.57	86.62
1.00	81.71	7.166	0.069	74.14	7.056	0.105	88.94	81.30
0.10	81.55	7.332	0.094	74.49	7.197	0.120	88.98	81.81
0.01	81.52	10.250	0.314	74.37	10.160	0.313	92.08	84.84
(B) T = 1.0, 1.0, 1.0								
All	89.55	8.689	0.595	78.17	8.101	0.595	98.83	86.87
10.00	90.60	8.667	0.573	78.03	8.104	0.573	99.84	86.71
1.00	81.66	7.268	0.053	72.95	7.262	0.050	88.98	80.27
0.10	81.46	7.349	0.100	73.99	7.244	0.102	88.91	81.34
0.01	81.50	10.46	0.297	74.24	10.380	0.298	92.23	84.92
(C) T = 0.1, 1.0, 10								
All	89.56	8.744	0.973	78.19	8.150	0.967	99.28	87.31
10.00	90.63	8.675	0.584	78.05	8.098	0.584	99.89	86.74
1.00	81.69	7.354	0.065	72.94	7.344	0.066	89.11	80.35
0.10	81.36	7.138	0.108	73.01	7.123	0.108	88.61	80.24
0.01	81.45	13.000	0.287	74.23	12.880	0.287	94.74	87.40

Table 64—Continued

Input Frequency	MSQ Power Produced			MSQ Power Out			Total Power	
	Q_1	Q_2	Q_3	Q_1	Q_2	Q_3	Produced	Out
(D) T = 0.1, 10, 1.0								
All	89.56	8.733	0.599	78.20	8.139	0.596	98.89	86.93
10.00	90.63	8.671	0.578	78.06	8.094	0.574	99.88	86.73
1.00	81.69	7.332	0.063	72.97	7.321	0.069	89.09	80.36
0.10	81.36	8.072	0.126	73.05	8.050	0.115	89.56	81.21
0.01	81.85	2.256	0.285	80.86	1.980	0.286	84.39	83.13

*R_6 = 500, R_1 = 940. These give the same total MSQ power as the one source case

Figure 31. An autocatalytic chain with three secondary positive feedbacks driven by two energy sources, one constant and one variable. Initial values for Q_1, Q_2, and Q_3 are variable depending on the turnover arrangement.

Equations: (a) Second input at Q_1

$$R_0 = I_0 - k_0Q_1Q_2Q_3R_1R_0$$
$$R_1 - I_1 - k_{01}Q_1Q_2Q_3R_0R_1$$
$$\dot{Q}_1 = k_1Q_1Q_2Q_3R_0R_1 - k_2Q_1 - k_3Q_1Q_2Q_3$$
$$Q_2 = k_4Q_1Q_2Q_3 - k_5Q_2 - k_6Q_1Q_2Q_3R_0R_1 - k_7Q_2Q_3$$
$$Q_3 - k_7Q_2Q_3 - k_8Q_1Q_2Q_3 - k_9Q_1Q_2Q_3R_0R_1 - k_{10}Q_3$$

(b) Second input at Q_2

$$R_0 = I_0 - k_0Q_1Q_2Q_3R_0$$
$$R_1 = I_1 - k_{01}Q_1Q_2Q_3R_1$$
$$Q_1 = k_1Q_1Q_2Q_3R_0 - k_2Q_1 - k_3Q_1Q_2Q_3R_1$$
$$Q_2 = k_4Q_1Q_2Q_3R_1 - k_5Q_2 - k_6Q_1Q_2Q_3R_0 - k_7Q_2Q_3$$
$$Q_3 = k_7Q_2Q_3 - k_8Q_1Q_2Q_3R_1 - k_9Q_1Q_2Q_3R_0 - k_{10}Q_3$$

(c) Second input at Q_3

$$R_0 = I_0 - k_0Q_1Q_2Q_3R_0$$
$$R_1 = I_1 - k_{01}Q_2Q_3R_1$$
$$Q_1 = k_1Q_1Q_2Q_3R_0 - k_2Q_1 - k_3Q_1Q_2Q_3$$
$$Q_2 = k_4Q_1Q_2Q_3 - k_5Q_2 - k_6Q_1Q_2Q_3R_0 - k_7Q_2Q_3R_1$$
$$Q_3 = k_8Q_2Q_3R_1 - k_9Q_1Q_2Q_3 - k_{10}Q_1Q_2Q_3R_0 - k_{11}Q_3$$

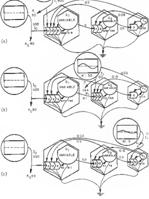
(a)
A 215
T_1 500
R_1 50
500
I_0
R_0 90
0.01
0.9
Q_1
VARIABLE
X
505/519
9
0.08
Q_2
VARIABLE
505/738
0.9
Q_3
10/18
(b)
I_0
900
R_0 80
A 30
T_1
00
7
144
R_1
8.1
0.15
0.02
Q_1
VARIABLE
827/746
Q_2
VARIABLE
172/138
Q_3
7/15
(c)
I_0
990
R_0 99
0.02
0.9
A 3
0
I_1
R_1
Q_1
VARIABLE
90/811
8.9
0.6
Q_2
VARIABLE
81/73
0.9
Q_3
18/18

Table 55 The total power produced and used by four turnover arrangements of the three positive feedback chain model given in Figure 31 as a function of input frequency

Input Frequency	Total Power							
	T = 10, 1.0, 0.1		T = 1.0, 1.0, 1.0		T = 0.1, 1.0, 10		T = 0.1, 10, 1.0	
	Produced	Out	Produced	Out	Produced	Out	Produced	Out
(A) Second Input at Q_1, e = 214.5								
10.0000	280.0	101.90	277.4	99.90	---	--	--	--
1.0000	---	---	--	---	---	---	---	---
0.1000	239.1	89.46	240.9	88.68	---	---	---	---
0.0100	239.2	90.09	240.5	89.52	---	---	---	---
0.0010	248.7	91.63	240.3	90.04	---	---	---	---
0.0001	242.1	88.82	242.3	88.47	---	---	---	---
(B) Second Input at Q_2, a = 30.0								
10.0000	108.5	94.45	108.2	94.29	108.50	94.42	108.00	94.16
1.0000	108.2	94.34	108.7	94.35	108.20	94.32	108.00	94.29
0.1000	---	---	---	---	---	---	---	---
0.0100	--	---	---	---	--	---	---	---

Table 55—Continued

Input Frequency	Total Power							
	T = 10, 1.0, 0.1		T = 1.0, 1.0, 1.0		T = 0.1, 1.0, 10		T = 0.1, 10, 1.0	
	Produced	Out	Produced	Out	Produced	Out	Produced	Out
(C) Second Input at Q_3, a = 3.0								
10.0000	116.2	95.03	116.2	95.09	116.2	95.14	116.6	95.25
1.0000	115.8	94.81	116.4	95.07	116.4	94.95	116.5	95.16
0.1000	114.2	94.65	114.6	94.75	114.6	94.72	---	---
0.0100	---	---	---	---	---	---	---	---

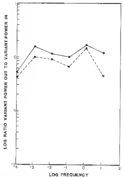

Figure 32. A Bode-like plot of the frequency response of the chain models with three secondary positive feedbacks shown in Figure 31 when one energy input is constant and a second variable energy input is entering the chain at Q_1.

Case A turnovers are $Q_1 = 10$, $Q_2 = 1.0$, $Q_3 - 0.1$ ——

Case B turnovers are $Q_1 = 1.0$, $Q_2 - 1.0$, $Q_3 = 1.0$ – – –

only Cases A and B are stable over a broad frequency band from 1 to 0.0001 cycles. The Q_3 interaction position uses more power than do the Q_1 or Q_2 positions for input frequencies 1 and 0.1, but Q_1 is unstable at input frequency 1.0. Tables 56(a) and 57(b) show the portion of the power due to the mean and variance, respectively. When turnover Case A uses more power than Case B at input position Q_1, it does so because it uses variant power more efficiently. Case B develops more productive power at frequencies 0.1 and 0.01 and 0.0001 because it produces slightly more mean power and almost as much variant power as Case A. However, Case A produces the most power at frequencies 10 and 0.001 because of greater variant power production that exceeds the advantage Case B obtains in mean power production.

Table 56 (B) gives the results of simulation when the second energy source interacts at unit Q_2 of a three deedback autocatalytic chain. Only the higher frequencies 10 and 1 cycle per unit time are stable and at these frequencies the turnovers tested treat the input as if it were a constant (see Table 57). There is not a great deal of difference between the power produced and used by the four turnover arrangements when the second input energy entered at Q_2. Table 56 (C) shows the results of simulating the four turnover cases of a three positive feedback chain when the second input energy entered at Q_3. Case D produces and uses slightly more power at input frequencies 10 and 1 due to the greater mean power it generates. Data supplement Tables 13 and 15 demonstrate that the large increase in power produced by the three feedback chain is due to the increased efficiency of the

Table 56. The portion of the total power in Table 55 attributable to the mean

Input Frequency	Mean Power T = 10, 1.0, 0.1 Produced	 Out	 T = 1.0, 1.0, 1.0 Produced	 Out	 T = 0.1, 1.0, 10 Produced	 Out	 T = 0.1, 10, 1.0 Produced	 Out
(A) Second Input at Q_1								
10.0000	269.2	96.61	272.1	97.87	---	---	---	---
1.0000	---	---	---	---	---	---	---	---
0.1000	233.0	84.95	235.0	85.72	---	---	---	---
0.0100	233.2	84.96	234.6	85.65	---	---	---	---
0.0010	232.1	84.73	234.2	85.62	---	---	---	---
0.0001	237.6	86.49	237.9	85.59	---	---	--	---
(B) Second Input at Q_2								
10.0000	108.0	94.39	107.7	94.25	108.0	94.42	107.6	94.12
1.0000	107.8	94.28	107.8	94.27	107.8	94.27	107.5	93.90
0.1000	---	---	---	---	---	---	---	---
0.0100	---	---	---	---	---	---	---	---

Table 56—Continued

Input Frequency	Mean Power T = 10, 1.0, 0.1 Produced	Out	T = 1.0, 1.0, 1.0 Produced	Out	T = 0.1, 1.0, 10 Produced	Out	T = 0.1, 10, 1.0 Produced	Out
(C) Second Input at Q_3								
10.0000	116.0	94.89	116.0	95.09	116.1	95.00	116.4	95.17
1.0000	115.4	94.67	116.2	95.00	115.9	94.85	116.3	95.07
0.1000	113.2	93.94	113.7	94.08	113.4	93.91	---	---
0.0100	---	---	---	---	---	---	---	---

Table 57. The portion of the total power in Table 55 attributable to the variance

Input Frequency	Variant Power							
	T = 10, 1.0, 0.1		T = 1.0, 1.0, 1.0		T = 0.1, 1.0, 10		T = 0.1, 10, 1.0	
	Produced	Out	Produced	Out	Produced	Out	Produced	Out
(A) Second Input at Q_1								
10.0000	10.920	5.309	5.290	2.032	---	---	---	---
1.0000	---	---	---	---	---	---	---	---
0.1000	6.120	4.509	5.970	2.960	---	---	---	---
0.0100	5.970	5.130	5.960	3.591	---	---	---	---
0.0010	6.520	6.945	6.060	4.421	---	---	---	---
0.0001	4.470	2.335	4.380	1.688	---	---	---	---
(B) Second Input at Q_2								
10.0000	0.422	0.062	0.435	0.038	0.423	0.001	0.471	0.040
1.0000	0.436	0.066	0.439	0.078	0.446	0.057	0.556	0.390
0.1000	---	---	---	---	---	---	---	---
0.0100	---	---	---	---	---	---	---	---

Table 57—Continued

Input Frequency	Variant Power							
	T = 10, 1.0, 0.1		T = 1.0, 1.0, 1.0		T = 0.1, 1.0, 10		T = 0.1, 10, 1.0	
	Produced	Out	Produced	Out	Produced	Out	Produced	Out
(C) Second Input at Q_3								
10.0000	0.192	0.132	0.193	0.120	0.173	0.142	0.153	0.070
1.0000	0.416	0.141	0.133	0.071	0.495	0.091	0.112	0.072
0.1000	0.969	0.711	0.924	0.673	1.227	0.811	---	---
0.0100	---	---	---	---	---	---	---	---

transfer of power between levels in the chain. The structure of the power used by units in the chain is also altered so that the highest unit in the chain is responsible for the most power use. These conditions are only true for the simulations when the two energy sources interact at Q_1. When the energies interact at Q_2 or Q_3 the three feedback chain produces and uses more power than its zero feedback counterpart but the efficiency of transfer and the structure of energy use is not radically altered. The ability of the zero feedback model with Case A turnovers to handle increased energy is shown in Table 20. It is clear that although there is a slight increase in the power produced and used by the zero feedback model with increased energy available, the magnitude of the increase does not approach the increase found with the three feedback chain.

Filter Properties of a Zero Positive Feedback Autocatalytic Chain with Two Modulated Energy Sources

The mean square power produced and used by storages of the zero secondary positive feedback autocatalytic chain model given in Figure 33 is summarized in Table 58 and shown in full in the data supplement Tables 20 to 32. One variable energy source enters at the base of the chain and a second variable energy source interacts at units Q_1, Q_2, or Q_3. The results are given over a six decade frequency range for each of four turnover arrangements. Table 58 (A) and Figure 34 give the results of simulation runs in which the second energy source interacts at unit Q_1. The broad pattern of the frequency response for all turnover arrangements is similar to that of a low pass filter. In

Figure 33 An autocatalytic chain model without secondary positive feedbacks showing the interaction of two variable energy sources, one at the base of the chain, the second positioned at levels represented by components Q_1, Q_2, and Q_3. Initial values for Q_1, Q_2, and Q_3 are variable depending on the turnover arrangement.

Equations (a) Second input at Q_1

$$\dot{R}_0 = I_0 - k_0 Q_1 R_1 R_0$$
$$\dot{R}_1 = I_1 - k_{01} Q_1 R_0 R_1$$
$$\dot{Q}_1 = k_1 Q_1 R_0 R_1 - k_2 Q_2 - k_3 Q_1 Q_2$$
$$\dot{Q}_2 = k_3 Q_1 Q_2 - k_4 Q_2 - k_6 Q_2 Q_3$$
$$\dot{Q}_3 = k_5 Q_2 Q_3 - k_6 Q_3$$

(b) Second input at Q_2

$$\dot{R}_0 = I_0 - k_0 Q_1 R_0$$
$$\dot{R}_1 = I_1 - k_{01} Q_1 Q_2 R_1$$
$$\dot{Q}_1 = k_1 Q_1 R_0 - k_2 Q_2 - k_3 Q_1 Q_2 R_1$$
$$\dot{Q}_2 = k_4 Q_1 Q_2 R_1 - k_5 Q_2 - k_6 Q_2 Q_3$$
$$\dot{Q}_3 = k_6 Q_2 Q_3 - k_7 Q_3$$

(c) Second input at Q_3

$$\dot{R}_0 = I_0 - k_0 Q_1 R_0$$
$$\dot{R}_1 = I_1 - k_{01} Q_2 Q_3 R_1$$
$$\dot{Q}_1 = k_1 Q_1 R_0 - k_2 Q_1 - k_3 Q_1 Q_2$$
$$\dot{Q}_2 = k_3 Q_1 Q_2 - k_4 Q_2 - k_5 Q_2 Q_3 R_1$$
$$\dot{Q}_3 = k_6 Q_2 Q_3 R_1 - k_7 Q_3$$

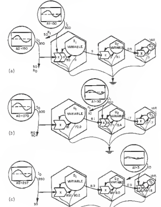
AI=150
I_1 500
50 R_1
AD=150
I_0 500
50 R_0
(a)
Q_1 VARIABLE
X
X
90
9
Q_2 VARIABLE
X
9
8.1
0.9
VAR
Q_3
X
.9
AD=270
I_0 900
R_0 90
(b)
Q_1 VARIABLE
X
81
72.9
AI=30
I_1 100
R_1 10
8.1
Q_2 VARIABLE
X
X
17.1
15.4
1.7
VAR
Q_3
X
1.7
AD=297
I_0 990
99
(c)
Q_1 VARIABLE
X
89.1
80.2
8.9
Q_2 VARIABLE
X
8.9
8.0
0.9
AI=3
10
VAR
Q_3
X
X
1.8
1.8

Table 58 The total power produced and used by a zero secondary positive feedback autocatalytic chain model (Figure 33) when four turnover arrangements are tested over a six-decade frequency range

Input Frequencies		Total Power							
		T = 10, 1.0, 0.1		T = 1.0, 1.0, 1.0		T = 0.1, 1.0, 10		T = 0.1, 10, 1.0	
f_0	f_1	Produced	Out	Produced	Out	Produced	Out	Produced	Out
(A) Second Input at Q_1									
All	All	95.00	84.88	95.08	84.85	95.15	84.95	95.14	84.94
10.0000	10.0000	97.34	85.94	97.43	85.92	97.46	86.02	97.44	86.01
10.0000	1.0000	89.56	81.44	89.71	80.96	89.61	81.03	89.98	81.04
10.0000	0.1000	89.57	81.64	89.66	82.00	89.59	80.99	90.17	81.60
10.0000	0.0100	91.29	83.71	91.98	83.80	93.66	85.52	102.60	94.34
1.0000	1.0000	97.16	87.24	96.92	85.72	96.95	85.74	96.95	85.72
1.0000	0.1000	88.85	81.63	90.49	80.71	88.64	80.24	89.06	80.67
0.1000	0.1000	97.77	88.46	98.03	88.14	100.20	85.95	107.30	94.79
0.0100	0.0100	104.20	94.13	106.60	93.82	113.00	100.00	91.76	85.92
0.0010	0.0010	97.78	89.60	97.86	89.57	102.30	93.03	109.40	97.00
0.0001	0.0001	89.16	89.97	98.20	89.98	110.10	93.73	96.58	92.60

Table 58—Continued

Input Frequencies		Total Power							
		T = 10, 1.0, 0.1		T = 1.0, 1.0, 1.0		T = 0.1, 1.0, 10		T = 0.1, 10, 1.0	
f_0	f_1	Produced	Out	Produced	Out	Produced	Out	Produced	Out
(A) Second Input at Q_1									
All	All	96.66	85.63	95.51	85.58	96.53	85.63	95.52	85.63
10.0000	10.0000	96.25	85.59	96.22	85.58	96.24	85.68	96.23	85.63
10.0000	1.0000	96.23	85.61	96.23	85.59	95.24	85.71	96.34	86.00
10.0000	0.1000	96.32	85.91	96.38	85.96	97.29	86.99	96.46	86.16
10.0000	0.0100	96.55	86.16	97.21	86.79	96.51	86.86	97.19	86.79
1.0000	1.0000	96.72	86.88	96.24	85.61	96.24	85.63	96.34	85.92
1.0000	0.1000	96.55	87.39	96.31	86.00	97.29	86.99	96.47	86.16
0.1000	0.1000	97.05	88.00	96.72	87.25	97.29	87.05	96.49	86.23
0.0100	0.0100	97.27	88.34	97.90	89.00	97.06	88.42	97.69	88.32
0.0010	0.0010	99.26	88.71	99.34	88.81	99.34	88.89	99.34	88.87
0.0001	0.0001							99.75	89.22

Table 5B—Continued

Input Frequencies		Total Power							
		T = 10, 1.0, 0.1		T = 1.0, 1.0, 1.0		T = 0.1, 1.0, 10		T = 0.1, 10, 1.0	
f_0	f_1	Produced	Out	Produced	Out	Produced	Out	Produced	Out
(C) Second Input at Q_3									
All		90.94	87.36	90.88	87.24	90.94	87.23	106.20	94.90
10.0000	10.0000	91.63	87.31	91.49	87.22	91.56	87.25	106.80	95.83
10.0000	1.0000	91.53	87.31	91.49	87.22	91.57	87.26	107.00	95.06
10.0000	0.1000	91.50	87.30	91.46	87.25	91.70	87.38	106.20	94.36
10.0000	0.0100	93.98	88.46	92.92	87.54	94.62	87.97	106.80	95.11
1.0000	1.0000	91.98	88.87	91.51	87.28	91.60	87.27	107.50	94.82
1.0000	0.1000	91.97	88.87	91.50	87.31	91.73	87.36	106.80	95.74
0.1000	0.1000	92.61	89.99	92.42	89.05	92.00	87.62	104.00	96.07
0.0100	0.0100	103.80	93.84	106.80	98.82	113.40	99.21	110.60	99.87
0.0010	0.0010	44.69	43.80	44.84	44.04	44.97	44.19	44.00	44.23
0.0001	0.0001	44.04	43.75					43.80	43.75

Figure 34. A Bode-like plot of the frequency response of a three unit chain model without secondary positive feedbacks (Figure 33) for four turnover arrangements when two variable energy sources interact

Case A turnover $Q_1 = 10$, $Q_2 = 1.0$, $Q_3 = 0.1$ ————

Case B turnover $Q_1 = 1.0$, $Q_2 = 1.0$, $Q_3 = 1.0$ - - - -

Case C turnover $Q_1 = 0.1$, $Q_2 = 1.0$, $Q_3 = 10$ -·-·-

Case D turnover $Q_1 = 0.1$, $Q_2 = 10$, $Q_3 = 1.0$ --------

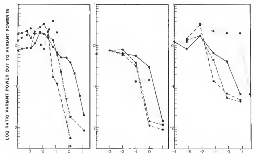

a) Second input at Q_1

b) Second input at Q_2

c) Second input at Q_3

addition, Cases A and B show a single resonance peak while Cases C and D have double resonance peaks over the six decade range of frequency tested. In general the power produced and used by the model is greater when the modulated input frequencies are matched than when they are not. This external frequency resonance is further enhanced when the interacting system components have natural frequencies which match the input frequencies. For example, turnover Case A produces and uses the most power when the input frequencies are 0.005 and 0.005 cycles per unit time, which corresponds to a resonant peak on Figure 34. Case A produces and uses the most variant power at input frequencies 0.2 and greater because its turnover is fast enough to capture the power in these high frequencies. When the input frequencies are lowered to 0.1 and 0.1 cycles per unit time Case D is able to produce and use the most power. Tables 59 and 60 and Figure 34(a) show that Case D's dominance is due to a superior production and use of variant power. In this case, the additional variant power must be generated by a natural oscillation of the model at these frequencies since it is not passed up the chain. This can be verified by examining Table 32 in the data supplement. A similar situation occurs when the input frequencies are 0.01 and 0.01 cycles per unit time but this time the oscillation is set up in turnover Case C. Turnover Case D again produces and uses the most power at another resonance peak when stimulated by frequency 0.001 at the Q_1 level [see entry 5, Table 58 (A)] and Figure 34(a).

Table 58 (B) and Figure 34(b) show the simulation results when the second input frequency interacts at component Q_2. The behavior of all four turnover cases shows a low pass filter pattern in these

Table 59. The portion of the total power in Table 58 due to the mean

Input Frequencies		Mean Power							
		T = 10, 1.0, 0.1		T = 1.0, 1.0, 1.0		T = 0.1, 1.0, 10		T = 0.1, 10, 1.0	
f_0	f_1	Produced	Out	Produced	Out	Produced	Out	Produced	Out
(A) Second Input at Q_1									
All	All	93.58	84.79	93.66	84.81	93.69	84.86	93.68	84.85
10.0000	10.0000	94.87	85.84	94.94	85.88	94.97	85.98	93.97	85.97
10.0000	1.0000	88.49	80.83	88.79	80.85	88.87	80.94	88.84	80.94
10.0000	0.1000	88.39	80.77	88.55	80.74	80.87	80.87	88.53	80.87
10.0000	0.0100	87.00	80.09	88.46	80.77	88.52	80.81	88.47	80.83
1.0000	1.0000	94.50	85.54	94.20	85.64	94.70	85.72	94.69	85.72
1.0000	0.1000	87.06	80.07	87.09	80.00	87.17	80.12	87.15	80.11
0.1000	0.1000	94.52	85.56	94.58	85.58	97.52	85.43	94.68	85.68
0.0100	0.0100	94.49	85.62	97.10	85.29	97.28	80.39	87.03	86.38
0.0010	0.0010	92.70	85.91	92.80	85.88	94.00	85.70	92.73	85.84
0.0001	0.0001	93.68	86.80	93.70	86.79	100.70	85.75	88.31	87.13

Table 59—Continued

Input Frequencies		Mean Power							
		T = 10, 1.0, 0.1		T = 1.0, 1.0, 1.0		T = 0.1, 1.0, 10		T = 0.1, 10, 1.0	
f_0	f_1	Produced	Out	Produced	Out	Produced	Out	Produced	Out
(B) Second Input at Q_2									
All	All	94.13	85.51	94.10	85.54	94.10	85.59	94.09	85.59
10.0000	10.0000	94.14	85.52	94.12	85.52	94.13	85.64	94.12	85.63
10.0000	1.000	94.13	85.51	94.12	85.55	94.13	85.61	94.13	85.64
10.0000	0.1000	94.13	85.50	94.12	85.55	94.10	85.57	94.13	85.57
10.0000	0.0100	94.21	85.50	94.20	86.62	93.54	85.61	94.21	85.69
1.0000	1.0000	94.16	85.53	94.13	85.55	94.13	85.62	94.13	85.58
1.0000	0.1000	94.18	85.42	94.12	85.55	94.10	85.60	94.13	85.59
0.1000	0.1000	94.04	85.51	93.99	85.54	94.10	85.63	94.14	85.62
0.0100	0.0100	94.02	85.50	94.02	85.50	93.53	85.77	94.18	85.73
0.0010	0.0010	95.29	85.43	95.26	85.40	95.26	85.50	95.28	85.50
0.0001	0.0001							96.46	86.48

Table 59—Continued

Input Frequencies		Mean Power							
		T = 10, 1.0, 0.1		T=1.0, 1.0, 1.0		T = 0.1, 1.0, 10		T = 0.1, 10, 1.0	
f_0	f_1	Produced	Out	Produced	Out	Produced	Out	Produced	Out
(C) Second Input at Q_3									
All	All	89.37	87.03	89.38	87.03	89.39	86.98	96.64	85.75
10.0000	10.0000	89.35	87.02	89.37	87.02	89.39	87.04	95.66	85.76
10.0000	1.0000	89.35	87.02	89.37	87.02	89.38	87.03	95.78	85.67
10.0000	0.1000	89.33	87.02	89.32	87.04	89.43	87.04	95.58	85.85
10.0000	0.0100	90.39	86.81	90.40	86.96	91.50	86.89	95.52	85.82
1.0000	1.0000	89.39	87.05	89.38	87.03	89.39	86.96	95.70	85.77
1.0000	0.1000	89.37	87.05	89.33	87.04	89.44	86.97	95.56	85.81
0.1000	0.1000	89.50	87.03	89.66	87.03	89.50	87.00	94.70	85.88
0.0100	0.0100	95.09	86.10	97.83	84.99	97.96	85.08	88.19	86.93
0.0010	0.0010	38.08	38.10	38.09	38.11	38.19	38.68	38.17	38.66
0.0001	0.0001	38.34	38.34					38.35	38.39

Table 60. The portion of the total power in Table 58 due to the variance

Input Frequencies		Variant Power							
		T = 10, 1.0, 0.1		T = 1.0, 1.0, 1.0		T = 0.1, 1.0, 10		T = 0.1, 10, 1.0	
f_0	f_1	Produced	Out	Produced	Out	Produced	Out	Produced	Out
(A) Second Input at Q_1									
All	All	1.421	0.089	1.415	0.043	1.462	0.092	1.462	0.087
10.0000	10.0000	2.475	0.094	2.494	0.038	2.489	0.038	1.484	0.051
10.0000	1.0000	1.058	0.600	0.927	0.093	0.942	0.090	0.929	0.101
10.0000	0.1000	1.187	0.871	1.116	0.659	0.922	0.123	1.531	0.732
10.0000	0.0100	4.297	3.626	3.516	3.027	5.146	4.709	14.120	13.51
1.0000	1.0000	2.564	1.699	2.250	0.083	2.253	0.023	2.768	0.016
1.0000	0.1000	1.886	1.465	1.691	0.706	1.469	0.117	1.908	0.562
0.1000	0.1000	3.459	2.910	3.445	2.565	2.661	0.516	12.610	9.11
0.0100	0.0100	9.697	8.509	9.530	8.527	15.780	14.640	4.730	3.537
0.0010	0.0010	5.063	3.692	5.042	3.695	8.320	7.336	16.650	11.160
0.0001	0.0001	4.500	3.170	4.503	3.185	9.422	7.983	7.271	5.676

Table 60—Continued

Input Frequencies		Variant Power							
		T = 10, 1.0, 0.1		T = 1.0, 1.0, 1.0		T = 0.1, 1.0, 10		T = 0.1, 10, 1.0	
f_0	f_1	Produced	Out	Produced	Out	Produced	Out	Produced	Out
(B) Second Input at Q_2									
All	All	1.422	0.124	1.414	0.044	1.434	0.044	1.424	0.044
10.0000	10.0000	2.100	0.066	2.103	0.053	2.110	0.040	2.103	0.063
10.0000	1.0000	2.100	0.105	2.103	0.033	2.116	0.063	2.211	0.364
10.0000	0.1000	2.093	0.408	2.260	0.413	3.181	1.419	2.337	0.592
10.0000	0.0100	2.340	0.663	3.009	1.811	2.966	1.246	2.984	1.237
1.0000	1.0000	2.563	1.365	2.123	0.063	2.113	0.053	2.337	0.654
1.0000	0.1000	2.627	1.973	2.260	0.453	3.181	1.390	2.347	0.572
0.1000	0.1000	3.004	2.493	2.731	1.712	3.194	1.423	2.348	0.593
0.0100	0.0100	3.261	2.867	3.876	3.498	3.534	2.654	3.516	2.589
0.0010	0.0010	3.969	3.282	4.085	3.373	4.079	3.389	4.062	3.370
0.0001	0.0001							3.020	2.738

Table 60—Continued

Input Frequencies		Variant Power							
		T = 10, 1.0, 0.1		T = 1.0, 1.0, 1.0		T = 0.1, 1.0, 10		T = 0.1, 10, 1.0	
f_0	f_1	Produced	Out	Produced	Out	Produced	Out	Produced	Out
(C) Second Input at Q_3									
All	All	1.570	0.323	1.495	0.215	1.554	0.247	10.640	9.149
10.0000	10.0000	2.170	0.269	2.120	0.199	2.173	0.212	11.150	9.059
10.0000	1.0000	2.178	0.287	2.120	0.199	2.193	0.227	11.270	9.169
10.0000	0.1000	2.163	0.279	2.144	0.211	2.272	0.339	10.570	8.608
10.0000	0.0100	3.585	1.639	2.521	0.584	3.034	1.083	11.300	9.287
1.0000	1.0000	2.590	1.832	2.135	0.245	2.212	0.305	11.120	9.051
1.0000	0.1000	2.598	1.825	2.172	0.267	2.287	0.383	11.920	9.930
0.1000	0.1000	3.110	2.961	2.759	2.018	2.498	0.618	12.140	9.988
0.0100	0.0100	8.676	7.743	8.949	7.830	15.400	14.130	15.850	14.940
0.0010	0.0010	6.610	6.703	6.746	5.907	6.780	6.515	5.824	5.563
0.0001	0.0001	5.694	5.407					5.448	5.357

simulation runs. However, the resonance patterns described for Section A are not readily discernable when energy enters at the Q_2 level. Figure 34(b) shows that Case A exploits variant power most successfully at high frequencies. This fact is due to the best matching of turnover with input frequency at both energy input points in the chain. Case B has a path similar to Case A only its maximum variant power use occurs at a lower frequency. Cases C and D are not able to use the most variant power because their large storage at Q_1 is unable to pass power up the chain (see data supplement Tables 29 and 32). These tables show that additional resonant variance is not generated by turnover Cases C and D when the second input frequency enters at Q_2. Case C produced the most variant power at input frequencies 0.1 and 0.1 but Case A uses the most power at this input. When the input frequencies are 0.01 and 0.01 Case B produces and uses more power primarily due to the larger generation and more efficient use of variant power. It should be noted that as mentioned noisy and high frequency inputs are treated as if they were constants by slow turnover time units.

Table 58 (C) and Figure 34(c) present the simulation results when the second input frequency enters at unit Q_3. Here we see a distinct difference between Case D and the other three turnover arrangements. Case D produces and uses more power than the other three cases. In all cases the power produced and used increases to a peak at frequency 0.01. But Case D shows a steep high frequency cutoff and a broad band of increased resonant power production and use while Cases A, B, and C have a much flatter slope of energy use in the frequency domain. Tables 59 and 60 show that the greater power production by Case D is due to an increase in the mean as well as the variant power production over Cases A through C. The high values for power produced by Cases A, B, and C for input frequencies 0.01 and 0.01 are also brought about by increased contributions from both the mean and variant power. The overall pattern of power use is determined by the variant power use for all four turnover arrangements. Data supplement Tables 21 to 32 show that all turnover cases are unstable at frequencies less than 0.01 for energy inputs at the Q_3 level. The high power values exhibited by Case D are mostly the result of a large generation of variant power by the model which is produced and used by the second component unit. In addition the mean power Case D produces is increased over Cases A through C except for frequency inputs 0.01 and 0.01 when the mean value of Cases A through C increases while the value of Case D decreases from its level at higher frequency inputs.

The Q_3 input position on the model with Case D turnovers produced and used the most power over the range of frequencies from 10 to 0.01 cycles. For low frequency inputs energy entering Case C or D at Q_1 gives the most power produced and used. The maximum power production and use within a model configuration depends on the frequency input as well as the turnover structure and the position at which the second input enters the chain.

Filter Properties of a Three Positive Feedback Autocatalytic Chain with Two Modulated Energy Sources

The power produced and used by a three unit autocatalytic chain model with three secondary positive feedbacks is given in Table 61

Table 61. The total power produced and used by storages of the three positive feedback model in Figure 35, as a function of frequency. Four different sets of turnovers were used for simulation runs One input enters the base of the chain, a second input interacts at Q_1, Q_2, or Q_3

Input Frequencies		Total Power							
		T = 10, 1.0, 0.1		T = 1.0, 1.0, 1.0		T = 0.1, 1.0, 10		T = 0.1, 10, 1.0	
f_0	f_1	Produced	Out	Produced	Out	Produced	Out	Produced	Out
(A) Second Input at Q_1									
10.0000	10.0000	271.9	101.20	271.4	98.80	---	---	---	---
10.0000	1.0000	---	---	---	---	---	---	---	---
10.0000	0.1000	---	---	246.3	90.75	---	---	---	---
10.0000	0.0100	244.5	93.28	---	---	---	---	---	---
1.0000	1.0000	274.2	100.40	280.8	98.68	---	---	---	---
1.0000	0.1000	---	---	246.0	89.99	---	---	---	---
0.1000	0.1000	275.4	99.06	276.8	100.30	---	---	---	---
0.0100	0.0100	275.3	101.60	276.6	101.30	---	---	---	---
0.0010	0.0010	275.0	103.60	276.4	101.80	---	---	---	---
0.0001	0.0001	278.0	100.70	278.1	100.30	---	---	---	---

Table 61—Continued

Input Frequencies		Total Power							
		T = 10, 1.0, 0.1		T = 1.0, 1.0, 1.0		T = 0.1, 1.0, 10		T = 0.1, 10, 1.0	
f_0	f_1	Produced	Out	Produced	Out	Produced	Out	Produced	Out
(B) Second Input at Q_2									
10.0000	10.0000	---	---	110.0	94.23	110.4	94.45	109.9	94.16
10.0000	1.000	---	---	110.2	94.35	110.2	94.32	109.9	94.29
10.0000	0.1000	108.1	93.20	---	---	---	---	---	---
10.0000	0.0100	---	---	---	---	---	---	---	---
1.0000	1.0000	---	---	110.2	94.38	110.1	99.51	109.5	94.47
1.0000	0.1000	---	---	---	---	---	---	---	---
0.1000	0.1000	---	---	---	---	---	---	---	---
0.0100	0.0100	---	---	---	---	---	---	---	---

Table 61—Continued

Input Frequencies		Total Power							
		T = 10, 1.0, 0.1		T = 1.0, 1.0, 1.0		T = 0.1, 1.0, 10		T = 0.1, 10, 1.0	
f_0	f_1	Produced	Out	Produced	Out	Produced	Out	Produced	Out
(C) Second Input at Q_3									
10.0000	10.0000	118.30	95.05	118.3	95.01	118.3	95.10	118.7	95.20
10.0000	1.0000	118.44	95.07	118.5	95.03	118.5	94.96	118.6	95.14
10.0000	0.1000	118.50	95.10	116.7	94.75	116.7	94.72	---	---
10.0000	0.0100	---	---	---	---	---	---	---	---
1.0000	1.0000	119.00	96.49	118.6	95.10	119.5	95.12	118.4	95.07
1.0000	0.1000	119.00	96.49	116.7	94.81	---	---	---	---
0.1000	0.1000	117.40	97.00	---	---	117.6	95.14	---	---
0.0100	0.0100	---	---	---	---	---	---	---	---

One variable energy source supplies the base of the chain and a second variable energy interacts at component units Q_1, Q_2, or Q_3 as shown in Figure 35. The results are shown for four different turnover arrangements over a six decade frequency range. Excess energy above that required for a steady state balance is available to this model and is equal to the energy carried by the variable portion of the signal. Data supplement Table 33 shows the zero positive feedback chain with Case A turnovers simulated with the same excess energy given to the three positive feedback model. A comparison between this table and Case A in Table 61 shows that the three positive feedback model produced and used much more power than did the zero positive feedback model. However, the three positive feedback model is less stable than is the zero feedback model (compare Tables 58 and 61). The increased production of power by the three feedback model is due primarily to the increased efficiency of energy capture and transfer (see data supplement Tables 34 to 43).

Only a third of the stimulation runs were stable when the second energy source entered at unit Q_1. All runs for turnover Cases C and D were unstable. Six runs of eight for Case B were stable and five runs of eight for Case A were stable. Case B produced slightly more power than Case A in all runs except input frequencies 10 and 10. Case A used more power than Case B except for input frequencies 0.1 and 0.1. Both Case A and Case B had greater power production and use when the interacting input frequencies were matched than when they were not. This difference is due to the smaller mean power produced and used by

Figure 35 An autocatalytic chain model with three secondary positive feedbacks showing the interaction of two energy sources, one at the base of the chain and the second positioned at different levels represented by components Q_1, Q_2, and Q_3. Initial values for storages Q_1, Q_2, and Q_3 are variable depending on the turnover arrangement.

Equations (a) Second input at Q_1

$$R_0 = I_0 - k_0Q_1Q_2Q_3R_0R_1$$

$$R_1 = I_1 - k_{01}Q_1Q_2Q_3R_0R_1$$

$$\dot{Q}_1 = k_1Q_1Q_2Q_3R_0R_1 - k_2Q_1 - k_3Q_1Q_2Q_3$$

$$\dot{Q}_2 = k_4Q_1Q_2Q_3 - k_5Q_2 - k_6Q_1Q_2Q_3R_1R_0 - k_7Q_2Q_3$$

$$\dot{Q}_3 = k_7Q_2Q_3 - k_8Q_1Q_2Q_3 - k_9Q_1Q_2Q_3R_0R_1 - k_{10}Q_3$$

(b) Second input at Q_2

$$R_0 = I_0 - k_0Q_1Q_2Q_3R_0$$

$$R_1 = I_1 - k_{01}Q_1Q_2Q_3R_1$$

$$\dot{Q}_1 = k_1Q_1Q_2Q_3R_1 - k_2Q_2 - k_3Q_1Q_2Q_3R_1$$

$$\dot{Q}_2 = k_4Q_1Q_2Q_3R_1 - k_5Q_2 - k_6Q_1Q_2Q_3R_0 - k_7Q_2Q_3$$

$$\dot{Q}_3 = k_7Q_2Q_3 - k_8Q_1Q_2Q_3R_1 - k_9Q_1Q_2Q_3R_0 - k_{10}Q_3$$

(c) Second input at Q_3

$$R_0 = I_0 - k_0Q_1Q_2Q_3R_0$$

$$R_1 = I_1 - k_{01}Q_2Q_3R_1$$

$$\dot{Q}_1 = k_1Q_1Q_2Q_3R_0 - k_2Q_1 - k_3Q_1Q_2Q_3$$

$$\dot{Q}_2 = k_4Q_1Q_2Q_3 - k_5Q_2 - k_6Q_1Q_2Q_3R_0 - k_7Q_2Q_3R_1$$

$$\dot{Q}_3 = k_8Q_2Q_3R_1 - k_9Q_1Q_2Q_3R_0 - k_{10}Q_1Q_2Q_3 - k_{11}Q_3$$

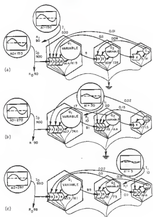
AI=150
AO=150
I_1
500
R_1
50
I_0
900
R_0 90
Q_1
VARIABLE
Q_2
VARIABLE
Q_3
0.01
0.9
0.09
9
X
(a)
AI=30
AO=270
I_1
00
17
0.02
0.15
R_1
10
I_0
900
R 90
81
(b)
AI=3
AO=297
I_0
990
R_0 98
I_1
10
0.02
0.9
0.9
0.9
99
81
73
811
(c)

unmatched energy inputs, as can be seen from Tables 62 and 63 where the power is partitioned into components due to the mean and variance, respectively. The low pass filter pattern of increasing power production and use with decreasing frequency does not stand out upon examining Figure 36. There is a notch in the power use of Case A at frequencies 0.1 and 0.1 and a resonant peak at frequencies 0.001 and 0.001 for both Case B and Case A. Data supplement Tables 35 and 36 demonstrate that these patterns are largely due to the differential manner in which variant power is handled by the two turnover cases given different input frequencies. When the second energy enters at Q_1 most of the energy use takes place at unit Q_3 due to the large transfer of power through the chain (data supplement Tables 34, 37).

When the second energy is input at component Q_2 about one-third of the simulation runs were stable. Only one run with turnover Case A was stable at frequencies 10, 0.1 and three runs of frequencies 10, 10, 10, 1, and 1, 1 were stable for turnover Cases B, C, and D. All runs for Cases B and C were at frequencies too high to be utilized effectively by the component turnovers. The increased energy used and produced by the three feedback model in Table 61 (B) is primarily due to the increased efficiency of mean power capture and transfer over its zero feedback counterpart.

Almost 60% of the simulation runs for the three positive feedback chain were stable when the second input entered at component Q_3. Turnover Case A had six stable runs, Cases B and C each had five stable runs, and Case D had three stable runs. Case A usually produced and

Table 62. The contribution of the mean to the total power given in Table 61

Input Frequencies		Total Mean Power							
		T = 10, 1.0, 0.1		T = 1.0, 1.0, 1.0		T = 0.1, 1.0, 10		T = 0.1, 10, 1.0	
f_0	f_1	Produced	Out	Produced	Out	Produced	Out	Produced	Out
(A) Second Input at Q_1									
10.0000	10.0000	265.5	95.57	268.4	95.75	---	---	---	---
10.0000	1.0000	---	---	---	---	---	---	---	---
10.0000	0.1000	---	---	243.4	88.47	---	---	---	---
10.0000	0.0100	240.9	87.66	---	---	---	---	---	---
1.0000	1.0000	266.3	95.68	267.8	96.47	---	---	---	---
1.0000	0.1000	---	---	240.5	87.62	---	---	---	---
0.1000	0.1000	267.5	95.75	268.4	96.61	---	---	---	---
0.0100	0.0100	266.9	95.85	268.1	96.60	---	---	---	---
0.0010	0.0010	265.8	95.68	267.8	96.57	---	---	---	---
0.0001	0.0001	271.7	97.71	271.9	97.80	---	---	---	---

Table 52—Continued

Input Frequencies		Total Mean Power							
		T = 10, 1.0, 0.1		T = 1.0, 1.0, 1.0		T = 1.0, 1.0, 1.0		T = 0.1, 10, 1.0	
f_0	f_1	Produced	Out	Produced	Out	Produced	Out	Produced	Out
(B) Second Input at Q_2									
10.0000	10.0000	---	---	107.7	94.16	108.0	94.28	107.5	94.13
10.0000	1.0000	---	---	107.8	94.29	107.7	94.28	107.5	93.91
10.0000	0.1000	105.7	92.78	---	---	107.8	94.24	107.7	94.17
10.0000	0.0100	---	---	---	---	---	---	---	---
1.0000	1.0000	---	---	107.8	94.28	---	---	---	---
1.0000	0.1000	---	---	---	---	---	---	---	---
0.1000	0.1000	---	---	---	---	---	---	---	---
0.0100	0.0100	---	---	---	---	---	---	---	---

Table 62—Continued

Input Frequencies		Total Mean Power							
		T = 10, 1.0, 0.1		T = 1.0, 1.0, 1.0		T = 0.1, 1.0, 10		T = 0.1, 10, 1.0	
f_0	f_1	Produced	Out	Produced	Out	Produced	Out	Produced	Out
(C) Second Input at Q_3									
10.0000	10.0000	116.1	94.87	116.1	94.90	116.1	94.98	116.5	95.15
10.0000	1.0000	116.2	94.92	116.2	94.94	115.9	94.85	116.3	95.07
10.0000	0.1000	116.2	94.95	113.6	94.06	113.4	93.91	---	---
10.0000	0.0100	---	---	---	---	---	---	---	---
1.0000	1.0000	116.2	94.95	116.4	94.98	116.3	95.00	116.2	94.98
1.0000	0.1000	116.2	94.94	113.6	94.07	---	---	---	---
0.1000	0.0000	113.9	94.16	---	---	114.1	94.28	---	---
0.0100	0.0100	---	---	---	---	---	---	---	---

Table 63. The contribution of the variance to the total power given in Table 61

Input Frequencies		Total Variant Power							
		T = 10, 1.0, 0.1		T = 1.0, 10, 1.0		T = 0.1, 1.0, 10		T = 1.0, 10, 0.1	
f_0	f_1	Produced	Out	Produced	Out	Produced	Out	Produced	Out
(A) Second Input at Q_1									
10.0000	10.0000	6.410	5.644	3.070	2.043	---	---	---	---
10.0000	1.0000	---	---	---	---	---	---	---	---
10.0000	0.1000	---	---	2.850	2.281	---	---	---	---
10.0000	0.0100	3.590	3.590	---	---	---	---	---	---
1.0000	1.0000	7.910	4.743	12.96	2.212	---	---	---	---
1.0000	0.1000	---	---	7.510	2.465	---	---	---	---
0.1000	0.1000	7.960	3.309	8.440	3.651	---	---	---	---
0.0100	0.0100	8.400	5.708	8.440	4.725	---	---	---	---
0.0010	0.0010	9.180	7.900	8.580	5.274	---	---	---	---
0.0001	0.0001	6.310	2.962	5.190	2.459	---	---	---	---

Table 63—Continued

Input Frequencies		Total Variant Power							
		T = 10, 1.0, 0.1		T = 0.1, 0.1, 0.1		T = 0.1, 1.0, 10		T = 1.0, 10, 0.1	
f_0	f_1	Produced	Out	Produced	Out	Produced	Out	Produced	Out
(6) Second Input at Q_2									
10.0000	10.0000	---	---	2.385	0.067	2.363	0.021	2.381	0.030
10.0000	1.0000	---	---	2.379	0.056	2.376	0.047	2.486	0.360
10.0000	0.1000	2.477	0.426	---	---	2.315	0.035	---	---
10.0000	0.0100	---	---	---	---	---	---	---	---
1.0000	1.0000	---	---	2.369	0.098	---	---	2.614	0.300
1.0000	0.1000	---	---	---	---	---	---	---	---
0.1000	0.1000	---	---	---	---	---	---	---	---
0.0100	0.0100	---	---	---	---	---	---	---	---

Table 63—Continued

Input Frequencies		Total Variant Power							
		T = 10, 1.0, 0.1		T = 1.0, 1.0, 1.0		T = 0.1, 1.0, 10		T = 1.0, 10, 0.1	
f_0	f_1	Produced	Out	Produced	Out	Produced	Out	Produced	Out
(C) Second Input at Q_3									
10.0000	10.0000	2.272	0.200	2.253	0.110	2.273	0.122	2.223	0.050
10.0000	1.0000	2.263	0.150	2.230	0.091	2.605	0.101	2.252	0.072
10.0000	0.1000	2.232	0.141	3.024	0.693	3.313	0.811	---	---
10.0000	0.0100	---	---	---	---	---	---	---	---
1.0000	1.0000	2.772	1.541	2.273	0.122	3.170	0.130	2.202	0.092
1.0000	0.1000	2.762	1.542	3.034	0.743	---	---	---	---
0.1000	0.1000	3.532	2.831	---	---	3.547	0.862	---	---
0.0100	0.0100	---	---	---	---	---	---	---	---

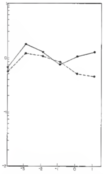

Figure 36. A Bode-like plot of the frequency response of a three unit chain model with three secondary positive feedbacks for two turnover arrangements when two variable energy sources interact at the chain base

Case A turnover $Q_1 = 10$, $Q_2 = 1.0$, $Q_3 = 0.1$ ——

Case B turnover $Q_1 = 1.0$, $Q_2 = 1.0$, $Q_3 = 1.0$ – – –

used more power than the other turnover arrangements However, Case C produced the most power for input frequencies 1, 1 and Case D both produced and used the most power for input frequencies 10, 10 and 10, 0.1 which carried variation that was essentially undetectable by the turnovers tested The values for power produced and used in Table 61 (C) are about the same for all turnover cases.

The small advantage in power use attained by Case A is seen from Tables 62 (A) and 63 (A) to be due to its more efficient use of variant power. The use of variant power by all turnover cases has a low pass filter pattern when the second energy enters at Q_3 The greater power generated by the model runs in Table 61 (C) over Table 58 (C) is due to the greater efficiency of mean power transfer and capture in the three feedback model

If we compare total power production and use by the three feedback model when the second energy interacts at each of the three component levels we find that the Q_1 level produces and uses the most power in almost all cases. The exceptions occur for unmatched frequency inputs at the Q_1 level. In these instances the system used more power if the second energy entered at the Q_3 component for the frequencies tested here However, in one of these situations when input frequencies were 10 and 0.01, the model was not stable with an input at the Q_3 component Input frequencies 0 01 and 0 01 and greater caused the model with input at Q_3 to be unstable for all turnover cases tested (see Table 61) Therefore, low frequency inputs at the Q_1 level are best for this system

A Nested Chain Model

The chain model shown in Figure 33 with turnovers $Q_1 = 10$, $Q_2 = 1$, $Q_3 = 0.1$ was rewritten to incorporate a nested structure in the model program given in Appendix A. The results of simulating this nested chain model over a range of frequencies for three different positions of the second energy input are given in Table 64. The results of the nested configuration were very close to the results shown in data supplement Table 21 for the unnested version of the same model.

Some Filter Properties of Web Models

Four possible configurations of a three unit web model are given in Figure 37. The model in Figure 37(a) shows a web with competition between parallel units and hierarchy. Figure 37(b) represents a case where there is both competition and cooperation between parallel units in the web. The structure given in Figure 37(c) has competition between parallel units and secondary positive feedbacks between levels in the hierarchy. Figure 37(d) includes all the aspects of the other three cases so that competition, cooperation, and hierarchical positive feedbacks are combined in a single highly connected web.

Webs with the Same Turnover for Parallel Units

Table 65 gives the results of simulating the web configurations in Figure 37 over a five decade range of frequency when the two parallel units have the same turnover. The third unit in each case has a turnover ten times lower than the parallel units.

The power produced and used by these webs with parallel unit turnovers equal has a low pass filter pattern as a function of the

Table 64. The power produced and used by storages of the chain model given in Figure 33 when turnover integrations are nested. Input frequency f_0 enters at the base, input frequency f_1 enters at Q_1, Q_2, or Q_3

Input Frequencies		Power Produced			Power Out			Total Power	
f_0	f_1	Q_1 T = 10	Q_2 T = 1.0	Q_3 T = 0.1	Q_1 T = 10	Q_2 T = 1.0	Q_3 T = 0.1	Produced	Out
(A) Input at Q_1									
All	All	85.72	8.499	0.441	76.89	8.057	0.446	94.66	85.83
10.00	10.00	88.31	8.778	0.580	77.56	8.433	0.562	97.67	86.55
10.00	1.00	81.75	7.757	0.067	73.65	7.697	0.102	89.57	81.45
10.00	0.10	81.67	7.833	0.791	73.80	7.761	0.110	90.29	81.67
10.00	0.01	81.60	9.651	0.228	74.45	9.457	0.227	91.48	84.13
1.00	1.00	88.01	8.792	0.439	78.62	8.155	0.439	97.24	87.21
1.00	0.10	81.62	7.172	0.075	74.37	7.039	0.106	88.87	81.52
0.10	0.10	88.16	9.360	0.472	79.35	8.638	0.446	97.99	88.43
0.01	0.01	87.99	15.710	0.997	78.02	15.190	0.312	104.70	94.02

Table E4—Continued

Input Frequencies		Power Produced			Power Out			Total Power	
f_0	f_1	Q_1 $T = 10$	Q_2 $T = 1.0$	Q_3 $T = 0.1$	Q_1 $T = 10$	Q_2 $T = 1.0$	Q_3 $T = 0.1$	Produced	Out
(B) Input at Q_2									
All	All	77.37	21.33	1.094	69.43	15.73	1.070	99.79	86.23
10.00	10.00	78.70	16.49	0.558	69.40	15.80	0.560	95.75	85.76
10.00	1.00	78.67	15.63	0.730	69.33	15.58	0.732	96.03	85.64
10.00	0.10	78.67	15.67	0.947	69.36	15.60	0.938	96.29	85.90
10.00	0.01	78.67	16.70	1.125	69.37	15.68	1.108	96.50	86.12
1.00	1.00	79.09	16.72	0.723	70.60	15.61	0.724	96.53	86.93
1.00	0.10	79.08	16.58	0.858	70.94	16.61	0.850	96.52	87.40
0.10	0.10	79.35	16.76	0.855	71.41	15.73	0.872	97.00	88.01
0.01	0.01	79.36	16.77	1.081	71.42	15.85	1.057	97.21	88.33

Table 64—Continued

Input Frequencies		Power Produced			Power Out			Total Power	
f_0	f_1	Q_1 $T = 10$	Q_2 $T = 1.0$	Q_3 $T = 0.1$	Q_1 $T = 10$	Q_2 $T = 1.0$	Q_3 $T = 0.1$	Produced	Out
(C) Input at Q_3									
All	All	88.03	2.302	0.679	84.71	1.987	0.671	91.01	87.37
10.00	10.00	88.24	6.031	0.938	81.90	0.938	0.906	95.21	88.49
10.00	1.00	88.30	5.480	1.141	82.25	1.141	1.095	94.92	88.42
10.00	0.10	88.35	5.145	1.105	82.60	1.105	1.044	94.60	88.40
10.00	0.01	88.39	5.276	1.148	82.96	1.148	1.066	94.81	88.98
1.00	1.00	89.04	2.389	0.673	86.19	0.673	0.529	92.10	88.84
1.00	0.10	89.06	2.241	0.658	86.30	0.658	0.648	91.96	88.34
0.10	0.10	89.25	2.636	0.670	87.03	0.670	0.655	92.56	89.35
0.01	0.01	87.39	14.590	1.254	78.78	1.254	1.138	103.80	93.87

Figure 37 A three unit web of autocatalytic components (a) Competition between Q_1 and Q_2, (b) competition and cooperation between Q_1 and Q_2; (c) competition between Q_1 and Q_2 with feedbacks from Q_3, (d) competition and cooperation between Q_1 and Q_2 with feedbacks from Q_3.

(a)

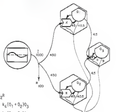

EQUATIONS

$R = I - k_0Q_1R - k_1Q_2R$

$Q_1 = k_2Q_1R - k_3Q_1 - k_4(Q_1 + Q_2)Q_3$

$Q_2 = k_5Q_2R - k_6Q_2 - k_7(Q_2 + Q_1)Q_3$

$Q_3 = k_8(Q_1 + Q_2)Q_3 - k_9Q_3$

(b)

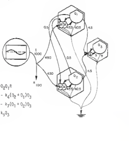

EQUATIONS

$R = I - k_0Q_1Q_2R - k_1Q_2Q_1R$

$\dot{Q}_1 = k_2Q_1Q_2R - k_3Q_1 - k_4(Q_2 + Q_1)Q_3$

$Q_2 = k_5Q_1Q_2R - k_6Q_2 - k_7(Q_1 + Q_2)Q_3$

$Q_3 = k_8(Q_1 + Q_2)Q_3 - k_9Q_3$

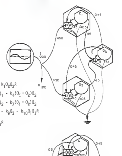

(c)

EQUATIONS

$$R = I - k_0Q_1Q_3R - k_1Q_2Q_3R$$

$$\dot{Q}_1 = k_2Q_1Q_3R - k_3Q_1 - k_4(Q_1 + Q_2)Q_3$$

$$\dot{Q}_2 = k_5Q_2Q_3R - k_6Q_2 - k_7(Q_1 + Q_2)Q_3$$

$$\dot{Q}_3 = k_8(Q_1 + Q_2)Q_3 - k_9Q_3 - k_{10}Q_1Q_3R - k_{11}Q_2Q_3R$$

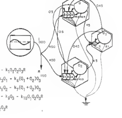

(d)

EQUATIONS

$$R = I - k_0Q_1Q_2Q_3R - k_1Q_1Q_2Q_3R$$

$$\dot{Q}_1 = k_2Q_1Q_2Q_3R - k_3Q_1 - k_4(Q_1 + Q_2)Q_3$$

$$\dot{Q}_2 = k_5Q_1Q_2Q_3R - k_6Q_2 - k_7(Q_1 + Q_2)Q_3$$

$$\dot{Q}_3 = k_8(Q_1 + Q_2)Q_3 - k_9Q_3 - k_{10}Q_1Q_2Q_3R - k_{11}Q_1Q_2Q_3R$$

Table 65. The power produced, used, and captured by storages of the web models in Figure 37 over a six decade frequency range when parallel units have the same turnover

Input Frequency	Power Produced Q_1 T = 1.0	 Q_2 T = 1.0	 Q_3 T = 0.1	Power Out Q_1 T = 1.0	 Q_2 T = 1.0	 Q_3 T = 0.1	Total Power Produced	 Out	 Captured
(A) Competition									
10.0000	45.98	45.98	8.995	40.49	40.49	8.997	101.00	89.98	94.18
1.0000	45.99	45.99	9.004	40.51	40.51	9.000	101.00	90.02	94.18
0.1000	46.14	46.14	9.211	41.23	41.23	9.004	101.60	91.50	94.32
0.0100	46.19	46.19	10.330	41.33	41.33	10.120	102.70	92.78	94.36
0.0010	45.80	45.80	19.160	38.06	38.06	19.170	110.80	95.29	93.76
0.0001	46.01	46.01	19.490	38.47	38.47	19.490	111.20	96.43	93.75
(B) Competition and Cooperation									
10.0000	46.49	46.49	8.993	40.49	40.49	7.997	102.00	89.98	94.17
1.0000	46.50	46.50	8.993	40.51	40.51	8.995	102.00	90.02	94.16
0.1000	46.64	46.64	8.834	41.35	41.35	8.649	102.10	91.35	93.61
0.0100	46.67	46.67	9.853	41.62	41.62	9.608	103.20	92.86	93.09
0.0010	45.98	45.98	19.220	37.68	37.68	19.220	111.20	94.58	92.83
0.0001	46.29	46.29	19.490	38.04	38.04	19.490	112.10	95.57	92.87

Table 65—Continued

Input Frequency	Power Produced Q_1 T = 1.0	 Q_2 T = 1.0	 Q_3 T = 0.1	Power Out Q_1 T = 1.0	 Q_2 T = 1.0	 Q_3 T = 0.1	Total Power Produced	 Out	 Captured
(C) Competition and Positive Feedback									
10.0000	46.37	46.37	10.090	40.37	40.37	9.124	102.80	89.86	94.89
1.0000	47.08	47.09	12.780	39.89	39.89	11.780	107.00	91.56	96.19
0.1000	47.74	47.74	14.990	40.13	40.13	13.730	110.50	93.99	97.41
0.0100	47.73	47.73	15.740	40.20	40.20	14.490	111.20	94.89	97.20
0.0010	---	---	---	---	---	---	---	---	---
(D) Competition, Cooperation, and Positive Feedback									
10.0000	45.46	45.46	8.520	39.76	39.76	7.680	99.44	87.20	92.40
1.0000	46.90	46.90	12.111	39.49	39.49	11.120	105.90	90.10	95.85
0.1000	---	---	---	---	---	---	---	---	---
0.0100	---	---	---	---	---	---	---	---	---

Table 66. The mean power produced, used, and captured by storages of the web models in Figure 37 over a six decade frequency range when parallel units have the same turnover

Input Frequency	Mean Power Produced Q_1 T = 1.0	 Q_2 T = 1.0	 Q_3 T = 0.1	Mean Power Out Q_1 T = 1.0	 Q_2 T = 1.0	 Q_3 T = 0.1	Total Mean Power Produced	 Out	 Captured
(A) Competition									
10.0000	44.97	44.97	8.993	40.47	40.47	8.994	98.93	89.93	90.00
1.0000	44.97	44.97	8.996	40.47	40.47	8.998	98.97	89.94	90.00
0.1000	44.97	44.97	9.033	40.46	40.46	9.036	98.97	89.96	90.00
0.0100	44.94	44.94	9.426	40.23	40.23	9.467	99.31	89.93	89.95
0.0010	44.70	44.70	13.800	37.79	37.79	13.860	103.20	89.47	89.47
0.0001	45.37	45.37	13.500	38.42	38.42	13.510	104.20	90.35	89.37
(B) Competition and Cooperation									
10.0000	45.47	45.47	8.990	40.47	40.47	8.990	99.93	89.93	90.00
1.0000	45.46	45.46	8.985	40.47	40.47	8.991	99.91	89.93	89.99
0.1000	45.24	45.24	8.633	40.44	40.44	8.641	99.11	89.52	89.56
0.0100	45.02	45.02	8.749	40.15	40.15	8.798	98.79	89.10	89.12
0.0010	44.72	44.72	13.760	37.34	37.34	13.85	103.20	88.63	88.51
0.0001	46.26	45.26	13.490	37.99	37.99	13.50	104.00	89.48	88.49

Table 56—Continued

Input Frequency	Mean Power Produced Q_1 T = 1.0	Q_2 T = 1.0	Q_3 T = 0.1	Mean Power Out Q_1 T = 1.0	Q_2 T = 1.0	Q_3 T = 0.1	Total Mean Power Produced	Out	Captured
(C) Competition and Positive Feedback									
10.0000	45.35	45.35	9.979	40.36	40.36	9.014	100.70	89.73	90.76
1.0000	46.04	46.04	12.390	39.85	39.85	11.380	104.30	91.08	92.15
0.1000	46.58	46.58	14.420	39.38	39.38	13.400	107.60	92.16	93.23
0.0100	46.51	46.51	14.720	39.16	39.16	13.780	107.70	92.10	93.09
0.0010	---	---	---	---	---	---	---	---	---
(D) Competition, Cooperation, and Positive Feedback									
10.0000	44.41	44.41	8.425	39.73	39.73	7.605	97.25	87.07	88.89
1.0000	45.86	45.86	11.800	39.45	39.45	10.800	103.50	89.70	91.78
0.1000	---	---	---	---	---	---	---	---	---
0.0100	---	---	---	---	---	---	---	---	---

Table 67. The variant power produced, used, and captured by storages of the web models in Figure 37 over a six decade frequency range when parallel units have the same turnover

Input Frequency	Variant Power Produced			Variant Power Used			Total Variant Power		
	Q_1 T = 1.0	Q_2 T = 1.0	Q_3 T = 0.1	Q_1 T = 1.0	Q_2 T = 1.0	Q_3 T = 0.1	Produced	Out	Captured
(A) Web Competition									
10.0000	1.01	1.01	0.002	0.020	0.020	0.003	2.022	0.043	4.18
1.0000	1.02	1.02	0.008	0.040	0.040	0.002	2.048	0.082	4.18
0.1000	1.39	1.39	0.178	0.770	0.770	0.008	2.958	1.548	4.32
0.0100	1.25	1.25	0.904	1.100	1.100	0.653	3.404	2.853	4.40
0.0010	1.10	1.10	5.360	0.270	0.270	5.280	7.560	5.320	4.29
0.0001	0.64	0.64	5.990	0.050	0.050	5.980	7.270	6.080	4.28
(B) Web Competition, Cooperation									
10.0000	1.02	1.02	0.003	0.020	0.020	0.007	2.043	0.047	4.17
1.0000	1.04	1.04	0.008	0.040	0.040	0.004	2.088	0.084	4.17
0.1000	1.40	1.40	0.201	0.910	1.910	0.008	3.001	1.828	4.05
0.0100	1.62	1.62	1.104	1.470	0.470	0.081	4.344	3.021	3.96
0.0010	1.26	1.26	5.460	0.340	0.340	5.370	7.980	6.050	4.32
0.0001	1.03	1.03	6.000	0.050	0.050	5.990	8.060	6.090	4.38

Table 57—Continued

Input Frequency	Variant Power Produced Q_1 T = 1.0	Variant Power Produced Q_2 T = 1.0	Variant Power Produced Q_3 T = 0.1	Variant Power Used Q_1 T = 1.0	Variant Power Used Q_2 T = 1.0	Variant Power Used Q_3 T = 0.1	Total Variant Power Produced	Total Variant Power Out	Total Variant Power Captured
(C) Web Competition and Positive Feedback									
10.0000	1.02	1.02	0.111	0.01	0.01	0.110	2.150	0.130	4.13
1.0000	1.05	1.05	0.390	0.04	0.04	0.400	2.490	0.480	4.08
0.1000	1.16	1.16	0.570	0.75	0.75	0.330	2.890	1.830	4.18
0.0100	1.22	1.22	1.020	1.04	1.04	0.710	3.460	2.790	4.11
0.0001	---	---	---	---	---	---	---	---	---
(D) Web Competition, Cooperation, and Positive Feedback									
10.0000	1.05	1.05	0.095	0.03	0.03	0.075	2.195	0.135	3.51
1.0000	1.04	1.04	0.310	0.04	0.04	0.320	2.390	0.400	4.07
0.1000	---	---	---	---	---	---	---	---	---
0.0100	---	---	---	---	---	---	---	---	---

input frequency. This pattern is produced by the increasing efficiency of variant power production at lower frequencies. The web model with cooperative and competitive pathways produces more power than the model with competitive pathways only. However, this model does not capture as much power at any frequency as the model with competition only and it dissipates more power through its storages only at input frequency 0.1. More variant power is produced and used by the web with cooperative pathways for all input frequencies, but less of the available variant power is captured at frequencies 0.01 and higher. The cooperative web produces more mean power at the higher input frequencies and uses less mean power at lower input frequencies than did the web with competition only. The mean power captured by the cooperative web was less than or equal to that captured by a web with competition only for all cases examined.

When secondary positive feedbacks are added to the three unit web as shown in Figure 37(c), the power produced, used, and captured is greater than for the models with competition and or cooperation. Tables 67 and 67 show that this result is brought about by secondary positive veedback stimulating greater mean flows of power production, use, and capture. The web with feedback does not handle variant power production and use as well as the cooperative or the competitive webs. The web with secondary positive feedbacks goes to zero at input frequencies 0.001 or below.

The web given in Figure 37(d) has competition cooperation and positive feedback but it went to zero within 1,000 time units at all frequencies tested except 10 and 1.0 cycles per unit time. At input

Table 68. The power produced, used, and captured by the web models in Figure 37 over a five decade frequency range when parallel units have widely separated turnovers

Input Frequencies		Power Produced			Power Out			Total Power		
f_0	f_1	Q_1 T = 10	Q_2 T = 0.1	Q_3 T=0.01	Q_1 T = 10	Q_2 T = 0.1	Q_3 T=0.01	Produced	Out	Captured
(A) Competition										
10.000		13.460	83.38	66.630	11.700	51.08	60.760	163.60	123.50	88.78
1.000		9.209	84.68	69.100	8.098	51.14	63.440	163.20	122.70	88.41
0.100		4.914	85.91	70.850	4.577	61.26	65.200	161.70	121.00	88.18
0.010		16.790	83.92	68.460	16.760	62.46	61.220	169.20	129.40	89.04
0.001		79.960	16.79	2.954	79.280	15.98	3.866	99.70	99.13	95.29
10.000	1.00	12.630	82.78	67.150	11.130	51.09	61.330	164.80	123.60	88.88
10.000	0.10	8.800	84.15	69.430	7.908	51.18	63.760	162.40	122.80	88.55
1.000	0.10	7.708	84.42	69.860	6.961	51.19	64.230	162.00	122.40	88.48
1.000	0.01	76.450	19.35	3.176	75.600	18.31	4.074	98.98	97.98	95.22
0.100	0.01	15.110	82.80	67.370	14.010	51.54	61.290	165.30	126.80	88.98

Table 6B—Continued

Input Frequencies		Power Produced			Power Out			Total Power		
f_0	f_1	Q_1 T = 10	Q_2 T = 0.1	Q_3 T=0.01	Q_1 T = 10	Q_2 T = 0.1	Q_3 T=0.01	Produced	Out	Captured
(B) Competition and Cooperation										
10.000		46.48	46.48	8.993	40.51	40.48	9.003	102.0	89.99	94.14
1.000		46.63	46.63	8.973	41.36	40.47	8.978	102.2	90.81	94.24
0.100		46.72	46.72	8.992	41.84	40.49	8.991	102.4	91.32	94.28
0.010		46.67	46.67	9.267	41.60	41.21	9.100	102.6	91.91	93.45
0.001		46.20	46.20	13.480	39.33	39.31	13.360	105.9	92.02	92.16
10.000	1.00	46.02	46.02	8.990	40.71	40.48	8.997	101.0	90.19	94.30
10.000	0.10	46.04	46.04	9.001	40.83	40.49	9.004	101.1	90.32	94.30
1.000	0.10	46.08	46.08	8.959	41.04	40.49	9.001	101.6	90.53	94.33
1.000	0.01	46.07	48.07	9.136	40.94	40.64	9.101	101.3	90.68	94.13
0.100	0.01	46.09	48.09	9.148	41.06	40.65	9.111	101.3	90.62	94.14

Table 69 The mean power produced, used, and captured by storages of the web models in Figure 37 over a five decade range of frequency when parallel units have widely separated turnovers

Input Frequencies		Mean Power Produced			Mean Power Out			Total Mean Power		
f_0	f_1	Q_1 T = 10	Q_2 T = 0.1	Q_3 T=0.01	Q_1 T = 10	Q_2 T = 0.1	Q_3 T=0.01	Produced	Out	Captured
(A) Competition										
10.000		4.164	80.77	61.820	3.684	49.85	54.590	146.80	108.10	85.00
1.000		1.896	82.63	65.610	1.669	49.98	58.250	150.00	109.80	84.60
0.100		0.390	83.87	68.010	0.362	49.90	60.740	152.00	111.00	84.33
0.010		4.372	80.52	61.880	4.078	49.53	55.060	146.30	108.80	84.96
0.001		77.540	13.30	1.465	75.810	12.93	2.364	92.31	92.10	90.09
10.000	1.00	3.695	81.13	62.590	3.268	49.86	55.350	147.40	108.6	84.92
10.000	0.10	1.637	82.85	65.960	1.463	49.88	58.700	150.40	110.70	84.55
1.000	0.10	1.230	83.18	66.620	1.102	49.89	59.360	151.00	110.40	84.48
10.000	0.01	74.470	16.32	1.747	73.690	15.79	2.645	92.54	92.03	90.83
0.100	0.01	4.036	80.84	62.260	3.722	49.74	55.230	147.10	108.70	84.94

Table 69—Continued

Input Frequencies		Mean Power Produced			Mean Power Out			Total Mean Power		
f_0	f_1	Q_1 T = 10	Q_2 T = 0.1	Q_3 T = 0.01	Q_1 T = 10	Q_2 T = 0.1	Q_3 T = 0.01	Produced	Out	Captured
(B) Competition and Cooperation										
10.000		45.46	45.46	8.989	40.47	40.47	8.994	99.91	89.93	89.98
1.000		45.44	43.44	8.968	40.46	40.45	8.971	99.85	89.89	89.94
0.100		45.42	46.42	8.983	40.43	40.43	8.986	99.82	89.86	89.90
0.010		43.13	45.13	9.032	40.12	40.21	9.089	99.29	89.42	89.34
0.001		44.54	44.34	12.000	38.06	38.04	12.410	101.10	88.51	88.17
10.000	1.00	45.46	45.46	8.984	40.47	40.47	8.994	99.90	89.93	89.98
10.000	0.10	45.46	45.43	8.997	40.46	40.47	8.997	99.90	89.93	89.98
1.000	0.10	45.45	45.45	8.996	40.46	40.46	9.000	99.90	89.91	89.97
1.000	0.01	45.38	45.38	9.076	40.34	40.38	9.096	99.84	89.82	89.82
0.100	0.01	43.37	45.37	9.086	40.33	40.38	9.106	99.84	89.82	89.81

Table 70. The variant power produced, used, and captured by storages of the web models given in Figure 37 over a five decade frequency range when parallel units have widely separated turnovers

Input Frequencies		Variant Power Produced			Variant Power Out			Total Variant Power		
f_0	f_1	Q_1 T = 10	Q_2 T = 0.1	Q_3 T=0.01	Q_1 T = 10	Q_2 T = 0.1	Q_3 T=0.01	Produced	Out	Produced
(A) Competition										
10.000		9.296	2.61	4.811	8.016	1.23	6.170	16.720	15.420	3.78
1.000		7.313	2.25	3.580	6.419	1.26	5.190	13.150	12.870	4.00
0.100		4.524	2.04	2.840	4.215	1.35	4.460	9.404	10.030	3.85
0.010		12.420	3.40	5.580	11.680	2.83	6.160	22.400	20.670	4.08
0.001		2.420	3.49	1.469	2.470	3.05	1.502	7.399	7.022	5.20
10.000	1.00	8.935	1.63	4.560	7.862	1.23	5.980	15.130	15.070	3.96
10.000	0.10	7.163	1.30	3.470	6.445	1.30	5.060	11.930	12.810	4.00
1.000	0.10	6.478	1.24	3.240	6.859	1.30	4.870	10.940	12.030	4.00
1.000	0.01	1.980	1.03	1.429	2.010	2.52	1.429	6.439	5.959	4.37
0.100	0.01	11.070	1.96	5.110	10.290	1.80	6.060	18.140	18.150	4.04

Table 70—Continued

Input Frequencies		Variant Power Produced			Variant Power Used			Total Variant Power		
f_0	f_1	Q_1 T = 10	Q_2 T = 0.1	Q_3 T=0.01	Q_1 T = 10	Q_2 T = 0.1	Q_3 T=0.01	Produced	Out	Captured
(B) Competition and Cooperation										
10.000		1.02	1.02	0.004	0.04	0.01	0.009	2.044	0.059	4.16
1.000		1.19	1.19	0.005	0.90	0.02	0.007	2.385	0.927	4.30
0.100		1.30	1.30	0.009	1.41	0.06	0.005	2.609	1.475	4.38
0.010		1.54	1.54	0.235	1.48	1.00	0.011	3.316	2.491	4.11
0.001		1.66	1.66	1.480	1.27	1.27	0.950	4.800	3.490	3.99
10.000	1.00	0.56	0.56	0.006	0.24	0.01	0.003	1.126	0.253	4.32
10.000	0.10	0.59	0.59	0.004	0.38	0.02	0.005	1.184	0.405	4.32
1.000	0.10	0.63	0.63	0.003	0.59	0.03	0.001	1.263	0.621	4.36
1.000	0.01	0.69	0.69	0.060	0.60	0.26	0.005	1.440	0.865	4.31
0.000	0.01	0.72	0.72	0.062	0.73	0.27	0.005	1.502	1.005	4.33

frequency 1.0 cycles per unit tiem values for power production use and capture were greater than those shown by webs in Figure 37(a) and (b) but not as great as those given by the web with positive feedback only.

Webs with Different Turnovers on Parallel Units

Table 58 presents the results for simulation runs given that the two parallel units shown in Figure 37 have turnovers of 10 and 0.1 and the third unit in series has a turnover of 0.01. Table 58 (A) shows that competition between two such widely separated turnovers usually leads to the demise of one unit and the success of the other. The unit with the slower turnover is generally able to outcompete the unit with the fast turnover. Only at input frequencies 0.001 and the superposition of input frequencies 1 and 0.01 is Q_1 with turnover 10 able to maintain a higher power than Q_2 with turnover 0.1. Unit Q_3 uses more power than it produces at these frequencies, eventually resulting in the loss of hierarchy. The values of power used by Q_1 and Q_2 approach closely those of power produced. Power captured is a maximum for these input frequencies. The other input frequencies give an unstable model which passes through a transient phase of high power use and production culminating in the loss of unit Q_1 and the establishment of a two unit chain. Large and variable values of variant power with frequency changes may indicate resonance in the model.

The addition of cooperative pathways stabilizes the three unit web model so that the two parallel units with different turnovers are unable to eliminate one another. The values of power produced only exceed those in the competition web where hierarchy is lost. The competition web uses more power at all input frequencies. Power captured is usually greater for a web with cooperation. Competition only captures more power when its fast turnover is dominant. Variant power produced and used shows a low pass filter pattern for the cooperative web but not for the competition web.

A comparison between the cooperation webs with widely separated and closely spaced turnovers shows that in general cooperation between closely spaced units is able to produce and use more power, but they capture less power than more widely separated units at high input frequencies.

Filter Properties of an Evaluated Salt Marsh Competition Model

An evaluated model of possible competition between invading Spartina townsendii and the indigenous Juncus-Leptocarpus association of the Kaituna River salt marsh, Havelock, N.Z., is given in Figure 38. Further details of the model's development are given in Appendix B. Figure 39 shows that Spartina wins this competition quickly for periodic, noisy, and constant solar inputs. Leptocarpus has a turnover of 3.1 per year and is excluded within two years. Juncus with a turnover of 4.4 per year survives in competition with Spartina of turnover 6.0 per year for five years.

Figure 40 shows a similar competition when two input signals are modulated as shown by the dotted lines in Figure 38. Simulation results are similar to those given for a single input frequency but both Juncus and Leptocarpus survive for a shorter period of time when

Figure 38 A model of competition between three marsh grasses at Havelock, New Zealand The stocks and flow given with the model are based on data from January and February 1982 and estimates from gas metabolism measurement of *Spartina* and *Juncus* at Crystal River, Florida All pathway flows are in the units of the appropriate source or storage, turnover (T) for each storage is given

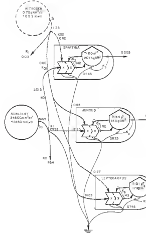
NITROGEN
0.75 gNm² d⁻¹
*0.5 5 n(wt)
I1
125
K00
062
R1
003
SPARTINA
T=6.0 yr⁻¹
2075 gCm²
K2
342
0.005
060
K01
0.985
K3
2013
K0
055
SUNLIGHT
34500 cal m² d⁻¹
42250 Bm(wt)
5769
JD
K1
2622
2193
JUNCUS
T=4.4 yr⁻¹
150 gCm²
K4
192
0.25
K5
0825
R5
R54
027
LEPTOCARPUS
T=3.1 yr⁻¹
178 gCm²
K6
143
0.745
1629
K7
0745

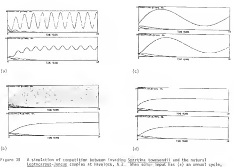

Figure 39 A simulation of competition between invading Spartina townsendii and the natural Leptocarpus-Juncus complex at Havelock, N.Z. When solar input has (a) an annual cycle, (b) a random value for each day, (c) a 10 year cycle, (d) a constant value

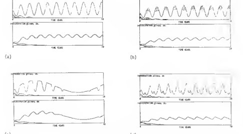

(a) (b) (c) (d)

Figure 40 Simulation results of the competition minimodel given in Figure 38 when two input signals are modulated (dotted lines in Figure 38). (a) Both input signals have frequency 1 cycle per year and are in phase, (b) one signal has an annual cycle, the second signal has a random value for each day, (c) one signal has an annual cycle, the second has a 10 year cycle, (d) both inputs have an annual cycle but they are 120° out of phase

the input frequencies are modulated. Figure 40(b) shows that random differences can be amplified and diminished when modulated so that the observed signal seems constant some time and random at other times. Figure 40(d) demonstrates the importance of the phase of modulated signals in producing the observed pattern of variation.

Filter Properties of an Evaluated Salt Marsh Minimodel

A macroscopic minimodel of the Kaituna River salt marsh at Havelock, N.Z., is given in Figure 41. A full description of the development of this model is given in Appendix C. The model consists of a component representing Spartina as well as components for labile or fast turnover nitrogen and for refractory or slow turnover nitrogen. These components are driven by three forcing functions, sun, tide, and river flow.

Behavior of the Kaituna Salt Marsh Minimodel

This model provides a framework for observing the differences between superposed and modulated inputs to a simple ecosystem minimodel. Variable signals from the river and tide are seen to be superposed in the labile N signal whereas solar and tidal inputs are modulated in the labile N signal. Figure 42(a) shows no variation of the frequency component due to tidal amplitude with variation in the amplitude of the river. Figure 42(b), on the other hand, shows the amplitude modulation of the tidal input frequency with solar input frequency.

The frequency response of the Kaituna marsh minimodel viewed as a wave filter is given in Figures 43-45. Figure 43 gives the

Figure 41 Minimodel of the Kaituna River salt marsh at Havelock, New Zealand. All flows are in the storage units per day except solar energy which is in units of the source. The k_i symbols are used to refer to the various model pathways.

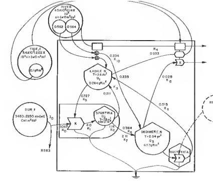
RIVER
45X10⁶±2.14X 10⁶ sin(wt) m³ da⁻¹
0.562
0.584
TIDE, E
5.4X10⁶±2.02X 10⁶ sin(wt) m³ da⁻¹
0.1gRm⁻³
SUN, I
3460±2250 sin(wt) Cal m⁻² da⁻¹
J_0
R583
5067
K_0
K
4.0
K_1
SPARTINA
Q_2
T=2.8 yr⁻¹
328gRm⁻²
116
K_2
LABILE N
T=3.6 da⁻¹
Q_1
0.284gRm⁻²
0.234
K_{10}
0.235
K_3
0.211
0.727
K_5
R_4
0.233
X
0.028
K_8
0.515
K_9
0.384
K_6
2.11
K_7
SEDIMENT N
T=0.34 yr⁻¹
Q_3
657gRm⁻²
BACTERIA
X
RECYCLE
AID
S

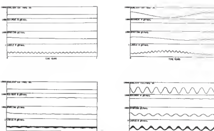

Figure 42 Comparison of simulation results of superposed and modulated signals in the marsh model given in Figure 41 (a) Superposed solar input is constant, river varies 1 cycle per year, tide varies 26 cycles per year, (b) modulation solar input varies once per year, tide varies 26 times per year, and river is constant

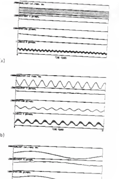

Figure 43. Frequency response of the marsh minimodel components shown in Figure 41 to variation of the solar input frequency (a) Solar input 365 cycles per year, tide 26 cycles per year, river 1 cycle per year, (b) solar input 1 cycle per year, tide 26 cycles per year, river 1 cycle per year, (c) solar input 0.1 cycle per year, tide 26 cycles per year, river 1 cycle per year.

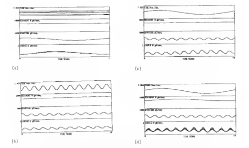

Figure 44. Frequency response of the components of the marsh minimodel in Figure 41 to variation in the tide and river input frequencies (a) The solar input is 1 cycle per year, the tide is 730 cycles per year, and the river is 1 cycle per year. (b) all inputs have a frequency of 1 cycle per year. (c) the solar and river inputs have annual cycles, the tide has a frequency of 0 1 cycle per year. (d) the solar input is 1 cycle per year, tide is 26 cycles per year, and the river is 0 1 cycles per year.

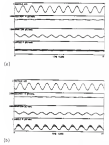

Figure 45 The phase of a hypothetical recycle aid (dotted pathway and source in Figure 41) changes the filter properties of the labile N component (a) Solar input 1 cycle per year, tide 26 cycles per year, river 1 cycle per year, recycle aid 1 cycle per year and in phase with the solar input, (b) solar input 1 cycle per year, tide 26 cycles per year, river 1 cycle per year, recycle aid 1 cycle per year, 90° lag behind solar input

response of each one of the system components to variations in the solar input frequency when tidal and river input frequencies are held at 26 and 1 cycles per year, respectively. Each component of this system acts like a low pass filter. This result may be seen by comparing Figure 43(a), (b), and (c) and noting that the labile nitrogen component transmits all three solar signal frequencies tested. *Spartina* transmits only the two lower frequency solar signals whereas sediment nitrogen absorbs and thereby passes on only the lowest solar input frequency. In addition Figure 43(c) shows that the manner in which the forcing functions and components interact helps to determine the frequency transmission. Note that *Spartina* shows no annual cycle due to river input because it is insulated from direct effects of this forcing function, but sediment nitrogen which has a slower turnover absorbs some energy at river input frequency 1 cycle per year since this input interacts directly with its storage (see Figure 41).

The frequency response of this marsh minimodel to variations in the tidal input frequency is given in Figure 44(a), (b), and (c). When the tide is semidiurnal very little of its variation is absorbed by the labile N component. However, for frequencies of 1 and 0.1 cycles per year this component absorbs some of the tidal variability. This fact is seen in Figure 44(b) where the annual peaks of labile nitrogen are skewed and in Figure 44(c) as amplitude modulation of the solar and tidal inputs in the labile N component. Tidal input frequency has little effect upon the signals passed by the *Spartina* and sediment N components. Figure 44(d) shows that labile N and sediment nitrogen absorb a low frequency river input signal but *Spartina* does not.

Figure 45 demonstrates the importance of a signal's phase to the absorption and transmission of variability. The model in Figure 41 is modified so that the dotted recycle aid is functioning. Figure 45(a) and (b) contrast the signal transmission characteristics of the system when the frequency of recycle aid is in phase with input and when it is 90° out of phase with the solar input.

Power on Model Pathways

Table 71 gives the power on some of the pathways or pathway summations in Figure 41 Figure 46 shows this information in graphic form Figure 46(a) and (b) show that the pattern of power captured and produced as a function of variability in the input signals is quite similar Power captured and produced have a minimum at intermediate frequencies of solar input and increase sharply as the input frequency is increased or decreased. The power captured and produced have a maximum at tidal input frequency 1 cycle per year River input frequency variation causes small variation in power capture and production, tidal frequency variation brings about slightly larger variation, and solar input frequency changes cause the greatest variability in these parameters. The total power ciruclating in the model as a function of frequency is given in Figure 46(c). Changes in solar input frequency caused the greatest variation in the power circulating Figure 46(d) gives the power exported as a function of variation in the input frequencies. The pattern of power exported as a function of solar input frequency has dual maxima at 0.1 cycles per year and 10 cycles per year and falls off sharply at high and low frequency Variation in the

Table 71. The total power on several pathways or the summation of pathways in the Kaituna Marsh minimodel (Figure 41) as a function of input frequencies. The input and output parameters are defined in Appendix C.

Input Frequencies Sun, Tide, River	Total Power of Pathways					
	J_{circ}	$J_{captured}$	J_{prod}	J_{out}	J_{in}	J_{ex}
10,000, 26, 1	15.84	3,498	2.762	0.903	6.47	5.84
1,000, 26, 1	15.70	3,487	2.752	0.899	6.43	5.83
100, 26, 1	15.50	3,424	2.703	0.888	6.43	6.08
10, 26, 1	15.41	3,395	2.680	0.883	6.43	6.18
1, 26, 1	15.43	3,402	2.685	0.888	6.43	6.12
0.1, 26, 1	16.03	3,440	2.716	0.973	6.43	6.23
0.01, 26, 1	16.10	3,476	2.743	0.974	6.44	2.92
1, 1,000, 1	15.43	3,400	2.684	0.888	6.43	6.19
1, 100, 1	15.43	3,401	2.685	0.888	6.43	6.14
1, 10, 1	15.43	3,402	2.686	0.888	6.43	6.11
1, 1, 1	15.49	3,421	2.700	0.892	6.43	6.12
1, 0.1, 1	15.42	3,402	2,685	0.888	6.43	6.10
1, 0.01, 1	15.52	3,408	2.690	0.883	6.44	6.19
1, 26, 1,000	15.45	3,403	2.686	0.889	6.43	6.15
1, 26, 100	15.45	3,398	2.683	0.886	6.43	6.17
1, 26, 10	15.43	3,397	2.681	0.887	6.43	6.17
1, 26, 1	15.43	3,402	2.686	0.888	6.43	6.12
1, 26, 0.1	15.58	3,399	2.683	0.888	6.43	6.35
1, 26, 0.01	15.49	3,380	2.668	0.877	6.43	6.45

Figure 46 The power on pathways or sums of pathways in the Kaituna River salt marsh model as a function of input frequency (a) The power captured as a function of frequency variation in solar, tidal, and river input, (b) the power produced as a function of frequency variation in solar, tidal, and river input, (c) the power circulating in the model as a function of frequency variation in solar tidal and river input, (d) the power exported as a function of frequency variation in solar, tidal, and river inputs

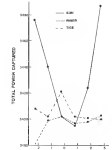
SUN
RIVER
TIDE
TOTAL POWER CAPTURED
3480
3460
3440
3420
3400
3380
2
1
0
1
2
3
LOG FREQUENCY

(a)

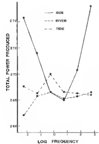
SUN
RIVER
TIDE
TOTAL POWER PRODUCED
2.74
2.72
2.70
2.68
2.66
2
1
0
1
2
3
LOG FREQUENCY

(b)

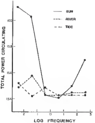
TOTAL POWER CIRCULATING
16.0
15.8
15.6
15.4
LOG FREQUENCY
2
1
0
1
2
3
SUN
RIVER
TIDE

(c)

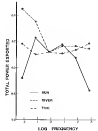
TOTAL POWER EXPORTED
6.4
6.2
6.0
5.8
5.6
LOG FREQUENCY
2
1
0
1
2
3
SUN
RIVER
TIDE

(d)

tidal input frequency gives little change in the power exported, however, as the river input frequency decreases below 1 cycle per year the power exported rises sharply.

Filter Properties of the Kaituna Salt Marsh Minimodel

Table 72 displays ratios of variable power for several system and component parameters of the salt marsh minimodel shown in Figure 41. The ratios were calculated from Tables C-3, C-4, and C-5 in Appendix C according to the formulas provided there. Figures 47-49 present the frequency response of the salt marsh minimodel for the various input-output parameters given in Table 72.

Figure 47 shows the filter characteristics of the salt marsh minimodel at the system level. The total variable power circulating through pathways in the model is between one and two times the variant power input and has a minimum at 10 cycles per year, increasing to a maximum at 0.01 cycle per year, the slowest frequency investigated. The variant power exported has a maximum 1.75 times greater than the imported variant power at input frequency 10 cycles per year. The variant power used to maintain *Spartina* storage in this model has a low pass filter pattern [see Figure 47(c)]. Figure 48 gives the filter patterns for components in the salt marsh minimodel. Both *Spartina* and sediment N are low pass filters, but labile N acts like a notch filter wtih a minimum at 10 cycles per year. Figure 47(e) shows a similar notch pattern and minimum for the ratio of variant power captured to variant power available. Figuare 49 shows that variation in solar input

Table 72 Ratios of variant power output to variant power input defined for the salt marsh model in Figure 41

Input Frequencies Sun, Tide, River	Variant Power Ratios							
	$\frac{J_{circ}}{J_{in}}$	$\frac{J_{out}}{J_{in}}$	$\frac{J_{exp}}{J_{imp}}$	$\frac{J_{used}}{J_{prod}}$	$\frac{J_{captured}}{J_{available}}$	$\frac{Q_{2in}}{Q_{2out}}$	$\frac{Q_{1in}}{Q_{1out}}$	$\frac{Q_{3in}}{Q_{3out}}$
(A) Sun Varies								
10,000, 26, 1	1.317	0.020	0.268	0.011	0.910	0.060	1.934	0.196
1,000, 26, 1	1.222	0.213	0.371	0.004	0.926	0.012	1.643	0.011
100, 26, 1	1.170	0.641	1.089	0.005	0.857	0.013	0.823	0.006
10, 26, 1	1.147	0.810	1.650	0.005	0.828	0.014	0.676	0.011
1, 26, 1	1.369	0.745	1.220	0.048	0.834	0.129	0.739	0.006
0.1, 26, 1	1.605	0.645	0.863	0.334	0.865	0.945	0.973	0.143
0.01, 26, 1	1.855	0.383	0.407	0.335	0.965	1.000	1.607	0.677
(B) Tide Varies								
1, 1,000, 1	1.199	0.740	1.210	0.046	0.837	0.129	0.736	0.011
1, 100, 1	1.199	0.779	1.279	0.046	0.834	0.133	0.709	0.011
1, 26, 1	1.369	0.745	1.220	0.048	0.834	0.129	0.739	0.006
1, 10, 1	1.198	0.741	1.217	0.046	0.834	0.128	0.737	0.011
1, 1, 1	1.215	0.771	1.276	0.047	0.853	0.132	0.737	0.004
1, 0.1, 1	1.199	0.741	1.216	0.046	0.836	0.156	0.736	0.011
1, 0.01, 1	1.208	0.733	1.209	0.042	0.833	0.121	0.747	0.023

Table 72—Continued

Input Frequencies Sun, Tide, River	$\frac{J_{circ}}{J_{in}}$	$\frac{J_{out}}{J_{in}}$	$\frac{J_{exp}}{J_{imp}}$	$\frac{J_{used}}{J_{prod}}$	$\frac{J_{captured}}{J_{available}}$	$\frac{Q_{2in}}{Q_{2out}}$	$\frac{Q_{1in}}{Q_{1out}}$	$\frac{Q_{3in}}{Q_{3out}}$
	Variant Power Ratios							
(C) River Varies								
1, 26, 1,000	1.363	0.774	1.300	0.046	0.834	0.129	0.701	0.006
1, 26, 100	1.193	0.801	1.310	0.046	0.831	0.128	0.693	0.006
1, 26, 10	1.194	0.808	1.320	0.046	0.831	0.129	0.650	0.006
1, 26, 1	1.369	0.744	1.220	0.048	0.834	0.129	0.739	0.006
1, 26, 0.1	1.220	0.890	1.464	0.046	0.831	0.133	0.645	0.087
1, 26, 0.01	2.300	1.200	1.976	0.043	0.819	0.118	0.511	0.393

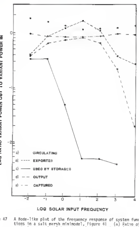

Figure 47 A Bode-like plot of the frequency response of system functions in a salt marsh minimodel, Figure 41 (a) Ratio of variant power circulating to variant power input (- - -), (b) ratio of variant power exported to variant power imported (-----), (c) ratio of variant power used by storages to variant power produced (——), (d) ratio of variant power leaving the system to variant power input (— — —), (e) ratio of variant power captured to variant power available (- — - —)

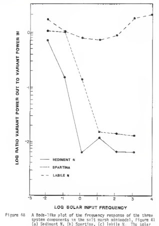

Figure 48 A Bode-like plot of the frequency response of the three system components in the salt marsh minimodel, Figure 41 (a) Sediment N, (b) Spartina, (c) labile N. The solar input frequency is variable while river and tide are held constant.

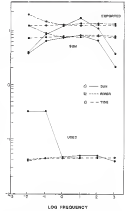

Figure 49 A Bode-like plot of the frequency response of variant power exported, variant power used, and their average as a function of input frequency. (a) Solar, (b) river, and (c) tidal input.

causes greater changes in variant power used and exported than do changes in either river or tidal input Table 73 demonstrates that while the variant power accounts for less than 10% of the total power it is responsible for a much larger fraction of the change in power brought about by a change in the solar input frequency.

Filter Properties of an Evaluated Salt Marsh Trophic Chain Model

A salt marsh trophic chain model and several variations are given in Figure 50(a), (b), and (c) The chain consists of Spartina, a very slow turnover component, bacteria, a very fast turnover component, and Petanogyrgus, a slow turnover component In addition the model contains a fast storage and medium turnover storage that buffer interactions between the autocatalytic components This model is developed in detail in Appendix D The model is driven by four forcing functions, sunlight, temperature, river DOC, and predator harvest

Behavior of the Salt Marsh Trophic Chain Model

The salt marsh trophic chain model's behavior is dependent on the input frequency that is variable These differences are brought about in part by the manner in which the inputs interact to drive the model Figure 51 shows one type of response to solar input frequency variation The solar input frequency must be 1 cycle per year or slower in order for the model to absorb its variant energy. Figure 51(d) shows the modulation of fast frequencies of 1 cycle per year for the temperature and river with a slow solar frequency of 0.1 cycle per year

Table 73 A variable's change in variant power as a percentage of the variable's total change in power for six solar input frequency increments, calculated from Table C-3 in Appendix C

Variable	% Total Power Change Due to Variant Power Frequency Increments					Range in % Variant Power/ MSQ Power
	1,000-100	100-10	10-1	1-0.1	0.1-0.01	
R	+43.0	+41.6	-47.9	-33.9	-47.2	8-16
I	---	100.0	---	---	---	~9
J_{10}	-38.0	-37.9	+28.6	+40.7	+38.9	~8
J_{11}	---	---	---	---	---	~5
J_{12}	---	---	---	---	---	~5
J_1	-36.7	-39.1	+33.0	+30.0	+37.0	8.4-9.3
J_2	---	---	+71.4	+81.2	+53.3	0.01-9.0
J_3	---	-10.0	+65.5	+80.0	+58.0	0.007-9.2
J_4	+45.0	+92.0	-83.3	-35.0	-53.0	2.3-7.9
J_5	-44	-50.0	+50.0	+20.0	+40.0	8.5-9.4
J_6	---	---	---	+10.0	+41.0	2-3.8
J_7	---	---	+68.0	+82.5	+55.6	0.1-9.1
J_8	---	--	+78.3	+82.1	+40.0	0.03-9.0
J_9	---	---	---	+10.7	+47.6	0.02-2.3

Figure 50 Evaluated trophic chain models for the Kaituna River salt marsh, Havelock, N Z (a) Trophic chain model with three secondary positive feedbacks, (b) trophic chain model with push-pull predator harvest and positive feedback, (c) trophic chain model without secondary positive feedbacks

Equations for (a)

(1) $SP = k_1*SP*P*B*R - k_2*SP - k_3*SP - k_{14}*SP$

(2) $SC = k_3*SP - k_4*SC - k_5*SC*P + k_6*SC*P - k_{17}*SC$

(3) $DOC = k_{14}*SP + k_{15}*K + k_4*SC - k_9*DOC*B*P*E + k_{10}*DOC*B*P*E$

(4) $B = k_{11}*DOC*B*P*E - k_7*B - k_{12}*B*P$

(5) $P = k_{13}*B*P - k_8*P - k_{16}*S*P$

(6) $R = I/(1 + k_D*SP*B*P)$

Note: See Appendix D for equations for (b) and (c)

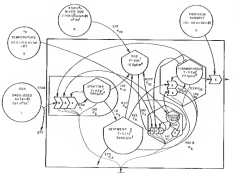
45X10⁶+
RIVER DOC
214X10⁶sin(wt+ϕ)
m³ dd⁻¹
K
°C
TEMPERATURE
20.0+(8.0 sin(wt+ϕ)
E
SUN
3450-2250
sin(wt+ϕ)
Cal m⁻²d⁻¹
I
5769
577
SPARTINA
T=4.2yr⁻¹
589gCm⁻²
6.8d
K1
185
K2
14
X3
519
K10
DOC
T=4dd⁻¹
10.5gCm⁻²
1.58
K14
6.57
K4
523
X5
30.77
K10
661
K9
SEDIMENT C
T=0.1ds⁻¹
5230gCm⁻²
273
K17
PREDATOR
HARVEST
10+ 0.5 sin(wt+ϕ)
G
POTAMOPYRGUS
T=5.5yr⁻¹
7.77gCm⁻²
0.24 K18
K15
200
178
K8
BACTERIA
1.533
K11
537
K7
652.9
K6
X

(a)

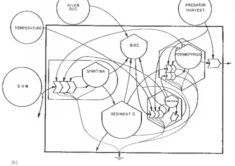
RIVER DOC
PREDATOR HARVEST
TEMPERATURE
DOC
POTAMOPYRGUS
SUN
SPARTINA
BACTERIA
SEDIMENT C

(b)

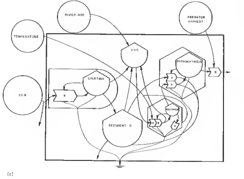
RIVER DOC
PREDATOR HARVEST
TEMPERATURE
DOC
POTAMOPYRGUS
SPARTINA
SUN
x
x
x
BACTERIA
x
x
x
SEDIMENT C
x

(c)

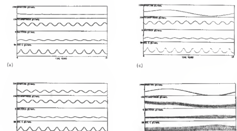

(a)

(b)

(c)

(d)

Figure 51 The frequency response of the trophic chain model in Figure 50 to variations in solar input frequency (a) Solar input - 1,000 cycles/year, (b) solar input = 1 cycle/year, (c) solar input = 0 1 cycle/year, (d) solar input = 0 01 cycle/year In all cases the temperature and river vary with periods of 1 cycle per year and external predation is constant.

An entirely different mode of behavior is seen in Figure 52 when the frequency of the temperature driving function is varied. Temperature variation at high frequencies (1,000 cycles per year) gives a typical low pass response and thus energy absorption occurs only by very fast turnover bacteria (12 times per day). When the temperature input frequency is lowered to 365 cycles per year a strong resonance pattern is set up in the bacteria and DOC (turnover four times per day) storages. A temperature frequency variation of 100 cycles per year is still within the resonance zone, however, when the input decreases to 10 cycles per year, Figure 52(d) shows that resonance no longer occurs. Amplitude modulation again shows up clearly in the pattern of variation seen in Figure 52(f) where a temperature cycle of 0.07 per year interacts with solar and river cycles of 1 per year.

Figure 50(a) showed that the temperature interaction is of a push-pull type and Figure 52 demonstrated the resonant behavior brought about by variation in temperature input frequency. Figure 53 further demonstrates the significance of push-pull kinetics to resonance behavior in this model. Figure 53(a) shows that predator harvest alone does not generate resonance in the trophic chain model. However, when predator harvest has positive as well as negative feedback dynamics a strong resonance is set up at sensitive frequencies as shown by Figure 53(b).

Filter Properties of the Salt Marsh Trophic Chain Model

The trophic chain model may be viewed as a filter by using different output-input ratios, which provide several perspectives on

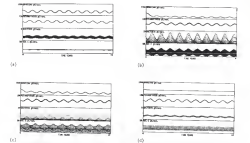

(a)

(b)

(c)

(d)

Figure 52 The frequency response of the marsh trophic chain model given in Figure 50 to variation in the temperature input frequency (a) Temperature input = 1,000 cycles per year, (b) temperature input is 365 cycles per year, (c) temperature input is 100 cycles per year, (d) temperature input is 10 cycles per year, (e) temperature input is 0 1 cycle per year, (f) temperature input is 0 01 cycle per year Solar and river input frequencies are 1 cycle per year for all cases and external predation is constant

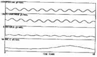

(e)

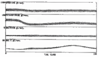

(f)

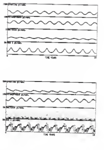

Figure 53. Comparison of simulation runs of the trophic chain salt marsh model with predator harvest to those with push-pull predator harvest. Solar input frequency - 1 cycle per year. Temperature - 1 cycle per year, river - 1 cycle per year, and (a) predation is harvest only and varies 365 cycles per year, (b) predation stimulates production as it takes a harvest and varies 365 cycles per year

the model's behavior Figure 54 shows the filter characteristic for several input frequency variables when the total variant power circulating through the model is taken as the output parameter and the variant power entering the model is the input parameter. Solar input frequency variation shows a low pass filter response as discussed above and variation of the temperature input leads to a band of increased energy circulating due to resonance Predator harvest alone gives the low pass pattern but if predator harvest is combined with positive feedback two strong resonance bands occur from 10^4 to 10^2 cycles per year and 0.1 cycle per year The predator push-pull function brings about the greatest amount of circulating variant power at all but the lowest frequency River DOC frequency variation gives a notched pattern for variant power circulating in the model

Figure 54(a) shows variant power and tells only half the story of power in the chain model The other half is provided by also considering the changes in mean power with frequency variation Figure 54(b) gives the total power circulating through the trophic chain model for the input frequency variables given in 54(a). From Figure 54(b) we can see that the greatest power circulating occurs for solar input frequency about 0.1 cycle per year At input frequency 1 cycle per year the model with predator harvest variation yields the greatest amount of power circulating. For higher frequencies from 100 to 365 cycles per year, resonances set up by the push-pull interactions give the most circulating power The strong rise in circulating variant power seen at lowest frequency in Figure 54(a) and the precipitous fall in total

Figure 54. Filter characteristics of the trophic chain model given in Figure 50 when the total power and the ratio of circulating variant power to input variant power are evaluated for variations in the input frequencies (1) Sun varies, (2) temperature varies, (3) river varies, (4) predator harvest varies, (5) predator harvest with positive feedback varies. (a) The ratio of circulating variant power to input variant power, (b) the total power circulating.

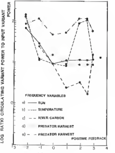
LOG RATIO CIRCULATING VARIANT POWER TO INPUT VARIANT POWER
2
1
0
FREQUENCY VARIABLES
a) —— SUN
b) ----- TEMPERATURE
c) — — RIVER CARBON
d) PREDATOR HARVEST
e) — - PREDATOR HARVEST
POSITIVE FEEDBACK
-3
-2
-1
0
1
2
3
4
LOG FREQUENCY

(a)

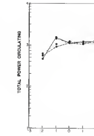
TOTAL POWER CIRCULATING
4
3
-3
-2
-1
0
1
2
3
LOG FREQUENCY

(b)

circulating power in Figure 54(b) reflect the instability of this model at very low frequency when variables tended to go to zero. Further information on the values used to evaluate filter characteristics of the trophic chain model may be found in Tables D-4 and D-5 in Appendix D.

Figure 55 shows the manner in which the trophic chain model handles variable power production and use. Solar input gives a low pass response to frequency variation for both variant power production and use. Temperature shows a strong resonance band at frequencies 100 and 365 cycles per year, while river DOC variation gives a weak resonance band at the same frequencies. When all inputs have an annual cycle predator harvest brings about more variant power use and equal variant power production when compared to the other cases with constant predation. Further information on production and use of power by the trophic chain model may be found in Tables D-6 through D-9 in Appendix D.

The trophic chain model may be examined from the perspective of the total energy captured by the system as seen in Figure 56. The power remaining is the complement of the power captured. Thus, Figure 56(a) shows that the trophic chain captures the most variant power when solar input frequency is 1 cycle per year or less with a peak capture around 0.1 cycle per year corresponding to the minimum of variant power remaining to be used in Figure 56(a). The resonance band at 100-365 cycles per year due to variation in the temperature input is observed to leave the maximum variant power unused. The power remaining shows a similar pattern to that of the variant power remaining [see Figure 56(b)].

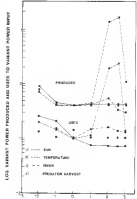

Figure 55 Filter characteristics of the trophic chain marsh model when the ratios evaluated are variant power produced and variant power used to variant power input. (1) Frequency of solar input varies, (2) temperature input frequency varies, (3) river input frequency varies, (4) frequency of predator harvest varies.

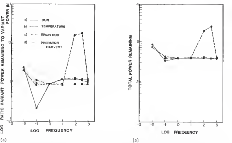

(a) (b)

Figure 56 Filter characteristics of the trophic chain model in Figure 50 when the power remaining and the ratio of variant power remaining to variant power available are evaluated for variations in the input frequencies (1) Solar input frequency, (2) temperature input frequency; (3) river input frequency, (4) predator harvest frequency (a) The ratio of variant power remaining to variant power input, (b) the power remaining.

Figure 57 compares the two versions of the trophic chain model given in Figure 50(a) and (c) to demonstrate how the lack of secondary positive feedbacks alters variant power circulation and capture. The energy captured by the chain is unaffected by variation of the temperature input frequency if there are not secondary positive feedbacks. The model with secondary positive feedbacks is able to capture more energy at its non-resonant frequencies than does its zero feedback counterpart. Resonance markedly reduces the amount of variant power captured. The variant power circulating in the model is slightly greater when there are no secondary positive feedbacks. This condition is reversed when we consider the power circulating through the model [see Figure 57(b)]. Here secondary positive feedbacks cause more power to circulate and account for more power capture except at resonant frequencies.

Figure 58 compares the trophic chain filter characteristics when predator harvest has only negative effects on the prey and when predator harvest has both positive and negative effects. Figure 58(a) gives the frequency response of both versions of the model to variation in the frequency of predator harvest. The variant power remaining is always less for the case when predators are negative feedback only. However, the variant power circulating is greater when predator harvest augments as well as mitigates prey storage. Figure 58(b) shows the power circulating and remaining for the two cases examined. Results seen for total power are similar to those observed for variant power alone. Resonance usually brings about more power circulation but less power capture than does the non-resonance case.

Figure 57. Filter characteristics of the trophic chain model with three secondary positive feedbacks in Figure 50(a) compared to those of the model in 50(c) with no secondary positive feedbacks when temperature input frequency varies. (a) The output-input ratios evaluated are (1) variant power remaining to variant power available and (2) variant power circulating to variant power input. (b) The power remaining (1) and circulating (2) in the two models

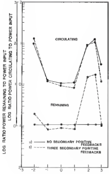
LOG RATIO POWER REMAINING TO POWER INPUT
LOG RATIO POWER CIRCULATING TO POWER INPUT
3
2
1
0
2
1
0
-1
2
CIRCULATING
REMAINING
a) —— NO SECONDARY POSITIVE FEEDBACKS
b) - - - THREE SECONDARY POSITIVE FEEDBACKS
-3
-2
-1
0
1
2
3
LOG FREQUENCY

(a)

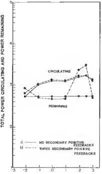
TOTAL POWER CIRCULATING AND POWER REMAINING
5
4
3
2
1
CIRCULATING
REMAINING
a) —— NO SECONDARY POSITIVE FEEDBACKS
b) - - - THREE SECONDARY POSITIVE FEEDBACKS
-3
-2
-1
0
1
2
3
LOG FREQUENCY

(b)

Figure 58 Filter characteristics of the trophic chain model in Figure 50(a) with dotted predator harvest compared to the model given in Figure 50(b) where predators both stimulate and harvest Potamopyrgus. (a) Ratios evaluated are variant power remaining to variant power available and variant power circulating to variant power input Frequency of harvest is variable, other inputs are 1 cycle per year, (b) power circulating and remaining for these two cases

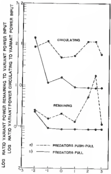
LOG RATIO VARIANT POWER REMAINING TO VARIANT POWER INPUT
LOG RATIO VARIANT POWER CIRCULATING TO VARIANT POWER INPUT
3
2
2
1
1
0
0
-1
2
CIRCULATING
REMAINING
a) PREDATORS PUSH-PULL
b) PREDATORS PULL
-3
-2
-1
0
1
2
3
LOG FREQUENCY

(a)

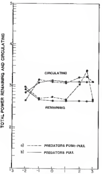
TOTAL POWER REMAINING AND CIRCULATING
5
4
3
2
1
CIRCULATING
REMAINING
a) PREDATORS PUSH-PULL
b) PREDATORS PULL
-3
-2
-1
0
1
2
3
LOG FREQUENCY

(b)

Figure 59 shows how each one of the trophic chain model's components behave when subjected to frequency variations in solar, temperature, or river DOC. Bacteria and *Potamopyrgus* are relatively unaffected by variations in the frequency of solar input. *Spartina* gives a low pass filter pattern with variation of the solar input frequency. Figure 59(b) examines the ratios of variant power of a component to that which enters the component as a function of change in the frequency of temperature input. Here all components are relatively unaffected at the low frequency end of the spectrum of input frequencies. However, at the higher frequencies *Spartina* and *Potamopyrgus* have a notch response whereas DOC gives a band response. Sediment C is unaffected over the range of frequencies tested. Bacteria shows a slow decline at high and low frequency. Variant power into a component can be a variable itself whereas variant power into the system was held constant. Thus, the declining ratio of variant power output to variant power input for bacteria does not necessarily mean that there is less total variant power through the bacteria storage. Figure 59(c) gives the frequency filter response of the five system components to variation in the frequency of river input of DOC. Sediment C and *Spartina* are relatively unaffected at all frequencies. *Potamopyrgus* is a notch filter with minimum power transfer at 100 cycles per year. Bacteria declines to a minimum at 100 cycles per year and then falls precipitously at high frequencies.

Figure 59. Filter behavior of the model components (Figure 50) with respect to the ratios of variant power output to variant power input (a) Solar input frequency varies, (b) temperature input frequency varies, (c) river DOC input frequency varies In all cases input frequencies other than the one tested were set to 1 cycle per year. Predation was held constant. (1) *Spartina*, (2) sediment, (3) DOC, (4) bacteria, (5) *Potamopyrgus*

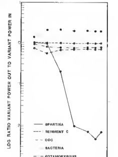
0
-1
-2
-3
LOG RATIO VARIANT POWER OUT TO VARIANT POWER IN
SPARTINA
SEDIMENT C
DOC
BACTERIA
POTAMOPYRGUS
-3
-2
-1
0
1
2
3
LOG SOLAR INPUT FREQUENCY

a)

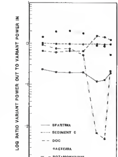
0
-1
-2
-3
LOG RATIO VARIANT POWER OUT TO VARIANT POWER IN
SPARTINA
SEDIMENT C
DOC
BACTERIA
POTAMOPYRGUS
-3
-2
-1
0
1
2
3
LOG TEMPERATURE INPUT FREQUENCY

b)

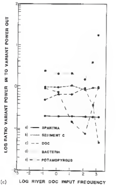
LOG RATIO VARIANT POWER IN TO VARIANT POWER OUT
2
1
0
-1
-2
a) SPARTINA
b) SEDIMENT C
c) DOC
d) BACTERIA
e) POTAMOPYRGUS
-3
-2
-1
0
1
2
3
LOG RIVER DOC INPUT FREQUENCY

(c)

DISCUSSION

The 1,005 simulations of frequency filtration of ecosystem designs for varying inputs given in the results allow several inferences to be made about how ecosystems adapt and process energy. System designs of theoretical minimodels and evaluated salt marsh models were examined and shown to be in part determined by external matching of input frequencies with both system turnovers and resonant frequencies. Matching of a receiving component's turnover with the energy input frequencies available to a system can be responsible for success or failure in a competition for power Aquatic and terrestrial food chains and the paradox of the plankton were used as examples of problems in ecosystem filter design which adaptation to frequency inputs may solve. The self-organization of a new ecosystem around invading *Spartina townsendii sensu lato* at Havelock, New Zealand, was documented and analyzed with frequency response techniques.

Input Frequency Spectra and System Design

Hutchinson (1953) states that because the factors which determine the structure of any isolated part of the universe are not immediately apparent, the predictability or the extraordinariness of a natural phenomenon is difficult to determine If we are able to establish relationships between the structure present at a location or in a time and factors which contribute to producing the structure we have begun to answer Hutchinson's question Odum et al. (1977) suggested that one could predict the structure of an ecosystem by relating its input energies to the observed system structure This study examined the significance of the frequency of input energies in determining the structural characteristics of a system.

There are three aspects of system design examined in this study that determine what system structure will develop in order to satisfy criteria imposed upon non-equilibrium structures by the laws of thermodynamics and the maximum power principle The aspects of system design are (1) the configuration of system components, (2) the interactions and connectance of these components, and (3) the turnover of each component The component turnovers can be directly influenced by the spectrum of forcing frequencies because in order to capture and use more energy in an input variation the turnover of an energy receiving component can be adjusted so that it is fast enough to capture available variant power. This is true because system component storages are low pass filters which have a high frequency cutoff that determines which variations of the input energy are absorbed. One reason that the ecosystem has the capacity to self-design is that living entities can grow, evolve, or substitute species to alter their characteristic turnovers to match changing input spectra

Table 74 shows that turnover arrangements which produce and use the most power usually have an energy receiving unit that matches the fastest input frequency available for use A comparison of input frequencies in column three with the turnover of the receiving units in

Table 74 Input frequency-turnover matching related to maximum power capture and use by storage in several chain models*

Location of Chain Model	Secondary Positive Feedbacks	Input Frequencies		Input Position		Turnover of Receiving Units		Reason for Dominance	
		First	Second	First	Second	Maximum Power In	Maximum Power Out	Power In	Power Out
Figure 23(a)	0	1	---	Q_1	--	10	10	V	V
Figure 23(b)	3	10	---	Q_1	--	10	10	V	V
Figure 23(d)	2	10	---	Q_1	---	1	10	M	V
Figure 23(e)	1	10	---	Q_1	---	10	10	V	V
Figure 29(a)	0	constant	1	Q_1	Q_1	0.1	10	M	V
Figure 29(b)	0	constant	1	Q_1	Q_2	0.1, 10	0.1, 10	V	V
Figure 29(c)	0	constant	1	Q_1	Q_3	0.1, 1	0.1, 1	R	R
Figure 31(a)	3	constant	10	Q_1	Q_1	10	10	V	V
Figure 31(b)	3	constant	1	Q_1	Q_2	---	---	C	C
Figure 31(c)	3	constant	1	Q_1	Q_3	0.1, 1	0.1, 1	M	M
Figure 33(a)	0	1	1	Q_1	Q_1	10	10	V	V
Figure 33(b)	0	10	1	Q_1	Q_2	0.1, 10	0.1, 10	V	V

Table 74—Continued

Location of Chain Model	Secondary Positive Feedbacks	Input Frequencies		First Position		Turnover of Receiving Units		Reason for Dominance	
		First	Second	First	Second	Maximum Power In	Maximum Power Out	Power In	Power Out
Figure 33(b)	0	1	1	Q_1	Q_2	10, 1	10, 1	V	V
Figure 33(c)	0	1	1	Q_1	Q_3	0.1, 1	0.1, 1	R	R
Figure 35(a)	3	10	10	Q_1	Q_1	10	10	V	V
Figure 35(b)	3	10	1	Q_1	Q_2	---	---	C	C
Figure 35(c)	3	1	1	Q_1	Q_3	10, 0.1	10, 0.1	V	V

*V, turnover matches input frequency and variant power capture and use is greatest, M, mean power captured or used is greater for unmatched unit, R, variant power use and capture is greater due to resonance, C, advantages cancel.

columns seven and eight shows that often the receiving unit turnover that produces or uses the most power is matched with the input frequency. Matching occurs when the receiving turnover is equal to the input frequency. Frequency-turnover matching may be overshadowed by resonance when input frequencies match natural frequencies of the system (see Table 74). When more than one energy source is present the turnover arrangement that produces the most power depends on the amount of energy available at each input as well as the matching between input frequencies and receiving component turnovers.

System Boundaries and the Frequency Domain

Frequency response analysis was used to establish some system boundaries in the frequency domain (see Table 75). A useful boundary is one that has included the range of frequencies absorbed by the system, F_b, the high frequency boundary, and F_B, the low frequency boundary, shown in Figure 7 were estimated based on the dynamic properties of the system in the frequency domain. These are the reciprocals of Simon's t_B and t_b boundaries The t_B boundary is an estimate of the length of time between catastrophes which establishes the period of observation and the 1/2 t_b boundary is the time between the pulses at the system's high frequency cutoff which gives a minimum sampling interval of t_b.

The system boundaries can be established in two ways The first method uses variable power used by a system to locate the F_b bound. Another way is to use the manner in which total power is handled by the system. The information gained from observing total power is

Table 75 Boundaries established in the frequency domain for a series of trophic chain models of different component turnover arrangement

Model	Turnover Case	Time Interval for t_b	Time Interval for t_B	Criterion t_b, t_B	Reference
Figure 23(a)	A	1	---	V	Figure 24, Table 33
Figure 23(c)	B, C, D	10	---	V	Figure 24, Table 33
Figure 23(b)	A	0.01	---	M	Table 35
Figure 23(d)	A	0.01	---	M	Table 35
Figure 33(a)	A	1	---	V	Figure 34(a)
Figure 33(a)	B, D	10	---	V	Figure 34(a)
Figure 33(a)	C	50	---	V	Figure 34(a)
Figure 33(b)	A, D	1	---	V	Figure 34(b)
Figure 33(b)	B, C	10	---	V	Figure 34(b)
Figure 33(c)	A	1	1,000	V, M	Figure 34(c), Tables 59 & 60
Figure 33(c)	B, C	10	1,000	V, M	Figure 34(c), Tables 59 & 60
Figure 33(c)	D	0.1	1,000	M, M	Figure 34(c), Tables 59 & 60
Figure 35(a)	A, B	---	---	---	Figure 36, Table 61

Table 75—Continued

Model	Turnover Case	Time Interval for t_b	Time Interval for t_B	Criterion t_b, t_B	Reference
Figure 35(b)	B, C, D	0.1	10	V, M	Table 62, Table 63
Figure 35(c)	B, D	0.1	10	V, M	Table 62, Table 63
Figure 35(c)	A, C	0.1	100	V, M	Table 62, Table 63

*V means the variant power was used to define the boundary, M denotes that mean power was used to define the boundary more general but knowledge of the variant power boundaries is also useful. The two can give contradictory information because as the mean power of a system approaches zero the variation usually increases. Conversely, when variant power use is zero the system may continue to use mean power. Table 75 summarizes the boundaries established in this sutdy from observation of total power or variant power. The F_b boundary for variable power could be established through frequency response analysis by applying faster and faster input signals. However, the F_B boundary was not always found in the systems examined here.

For the case when F_B is not apparent the system may be adapted to incorporate low frequency phenomena. Some F_b boundaries found in the chain model simulations of this study are shown in Figures 24, 30(a), (b), and (c), 34(a), (b), and (c). The F_B boundaries in the sama model series are only found in Figures 30(c) and 34(c) (see Table 58). Allen and Starr (1982) distinguished between low frequency phenomena that are incorporated and those which destroy a system. Systems may tend to evolve to incorporate regular disturbances, e.g., pine forests in the southern United States have included fire. Also, the F_B boundary may not always be apparent because the model has not been structured to include the dynamic process that will establish the F_B bound. Scientists may have a predilection for expressing a problem in terms they are already familiar with and in doing so processes at a larger scale than their image of a system can easily be ignored. If most natural phenomena are ultimately pulsators, the absence of an F_B boundary may indicate that a model needs to be restructured in order to consider the ultimate fate of the system or that lower frequency inputs are required to find F_g.

Transmission and Reception of Signal Frequencies

Figure 50 shows an aquatic ecosystem as analogous to a communication system. The turnovers of system components determine the maximum signal frequency that a unit can send or receive. Figures 42-46 and Figures 51 and 52 demonstrate how signal frequencies are transferred between system components of a salt marsh minimodel (Figure 41) and a salt marsh trophic chain model (Figure 50), respectively. Child and Shugart (1972) demonstrate that in a multiorder cascading linear system the magnitude of signals transmitted and received decreases as they pass up the chain and in the process the phase of these signals is lagged progressively. In terms of Allen and Starr (1982) the higher levels in the chain have slower turnovers and therefore they constrain faster turnover units because they transmit low frequency signals and fail to receive high frequency communications from faster units.

The salt marsh minimodel is unable to receive energy in the semidiurnal tides or daily insolation variations because the turnovers of the receiving components are too slow to capture these frequencies (see Figures 41, 43, 44). Variant energy and signals in fast fortnightly tidal variations in labile N were not received by slow turnover *Spartina* and annual variations transmitted by *Spartina* were not received by slower turnover sediment N. In addition, the initial position of signal reception relative to a secondary receiving unit is important in determining which signals are received and which are not.

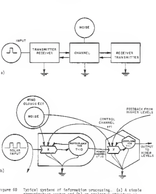

Figure 60 Typical systems of information processing. (a) A simple communication system and (b) an analogous structure in aquatic ecosystems shown in energy circuit language.

Figure 44(d) shows that Spartina receives little variation from a river N signal that is slow enough for it to receive based on its turnover (see Figure 41). However, sediment N of slower turnover is directly connected to the input and thus may receive more of the variation. Figure 45 shows that phase is critical to the transmission and reception of a signal.

Figure 48 shows that the nonlinear salt marsh minimodel has two components with similar properties to Child and Shugart's linear cascade. However, the third component is very different and shows a notch rather than a low pass filter pattern. Under conditions where resonance occurs a fast turnover nonlinear system component can amplify a signal to the point that it can affect slower turnover units in the system [see Figure 52(b) and (c)].

Competition, Turnover, and the Paradox of the Plankton

Given the case when all other things were equal, this study examined the effect of a unit's turnover on the outcome of competition between three units. First, it was noted that if one unit is given a slight advantage or disadvantage by increasing the inflow or outflow it promptly wins the competition in the former case or loses it in the latter. The assumption was made that changing flows is difficult if it is brought about by altering the pathway resistance whereas changing storage capacitance is an easier and biologically feasible method of changing the flow.

Frequency-turnover matching was shown to be important in determining competitive exclusion by the following test. Three units in competition for a constant source with equal flows but unequal turnover do not outcompete each other. Three units in competition for a variable energy source but with equal flows and turnover do not outcompete one another. But if three units of different turnover and equal flow compete for a variable energy source an order of dominance is produced. The unit with the slowest turnover will eventually dominate and exclude units with faster turnover in this competition. The rate at which exclusion occurs is dependent on the frequency and amplitude of the varying energy source. The more closely an input frequency matches the fast turnover unit the more this unit pulses and the faster it is excluded from the system and often the more total power produced by the system (see Table 10). When the signal amplitude input to a matched unit is increased the unit peaks and declines even more rapidly. At frequencies close to the turnover of the fast unit, slower units appear to preempt energy in the variance by capturing more than they can use (see Table 12). However, pulsing by Q_1 probably is the cause of this result. Fast turnover unit storages use variant power more efficiently than do the slow turnover units except when frequency is low when they do equally well.

For single units exploiting a variable energy source, the unit with the fastest turnover draws the most power (see Table 8). For linear competition the unit with faster turnover also draws the most power (see Table 3). Exclusion occurs in the autocatalytic system at the point of energy capture. Thus, there must be two opposing forces governing the adjustment of an autocatalytic time constant in this system. The first is a pressure to be a little bit slower than a competitor in order to survive and the second is to be as fast as possible in order to maximize energy capture.

These observations may be applicable to the paradox of the plankton as stated by Hutchinson (1961). Essentially the problem is how can so many different species of plankton exist together when they must compete for the same essential nutrients, light, etc., in the same space and time.

Hutchinson (1961) proposed that the dilemma could be solved if a nonequilibrium situation held due to the fact that season fluctuation occurred before competitive exclusion. This, of course, would not apply to the plankton of some tropical waters. Kemp and Mitsch (1979) proposed that frequencies of physical turbulence matched to plankton turnovers would allow coexistence of a number of plankton species. While this may be true, a careful reading of their paper shows that the model which they simulated defines a niche separation between the species based on turbulence. Models examined here indicate that there could be niche separation based on a nonequilibrium brought about by alteration of species turnovers. A possible mechanism would have a pressure on phytoplankton to turnover faster and thereby capture more power. This situation turns into a pulse or bloom under competition with other slower turnover units. As the bloom dies back after depleting resources, turnover adjusts to a slower rate as the same or another species is forced into bloom condition by increasing resources and the pressure to keep power high. Thus, the changing turnover of plankton species in response to input frequencies may be sufficient to explain the paradox of the plankton.

Simulation evidence showed that the intensity of competition could be increased by shifting all turnovers to higher values, e.g., bacteria, are under more intense competition than phytoplankton. Matching the unit turnover with input frequency increases competition for closely spaced turnovers. Increasing the spacing between turnovers increases the intensity of competition for a given input frequency (see Table 16)

Trophic Chain
Hierarchy, Turnover, Power, and Stability

The link between hierarchy and the wave filter is the turnover of the system components. Turnover determined by the stocks and flows of an ecosystem establishes a hierarchy immediately. Table 28 shows that frequency effects on power production and use by storage are usually two orders of magnitude less than mean effects and an order of magnitude less than amplitude effects in linear chains. On the other hand, Table 31 shows that frequency effects in an autocatalytic chain can be an order of magnitude less than mean effects, exceeding the effects of amplitude. In autocatalytic systems small changes multiply rapidly and thus small differences due to the frequency-handling properties of a system can determine the model's dynamic behavior.

Four different turnover arrangements shown in Table 76 were examined with respect to their stability and their ability to produce and use power through storages. These turnover arrangements were

Table 78. Four turnover arrangements examined in this study and their power production and power use by storage as compared to their stability. Total number of simulation runs was 532. Each arrangement was simulated 133 times

	1st Level	2nd Level	3rd Level	% Runs with Maximum Power In	% Runs with Maximum Power Out	% of Runs Stable
(1) Case A	Aquatic Grazing Chain			21.8	37.6	82.7
Flow	10.0	1.0	0.10			
Storage	1.0	1.0	1.00			
Turnover	10.0	1.0	0.10			
(2) Case B	Carnivore Chain			23.3	11.2	76.7
Flow	10.0	1.0	0.10			
Storage	10.0	1.0	0.10			
Turnover	1.0	1.0	1.00			
(3) Case C	No Known Example			16.7	15.0	57.1
Flow	10.0	1.0	0.10			
Storage	100.0	1.0	0.01			
Turnover	0.1	1.0	10.00			
(4) Case D	Detritus Chain			25.6	22.6	55.6
Flow	10.0	1.0	0.10			
Storage	100.0	0.1	0.10			
Turnover	0.1	10.0	1.00			

examined for eight combinations of secondary positive feedbacks in a three unit chain model shown in Figure 23. Figures 26 and 28 demonstrate that, in general, the more positive feedbacks the greater the power captured, produced, and used by storages in the chain. On the other hand, more positive feedbacks usually cause the chain to be less stable in the sense that more simulation runs of time 1,000 had all components go to zero before the end of the run. Table 76 gives the percentage of 133 runs that were stable for each turnover arrangement. Table 76 also shows the percentage of runs in which each of the four turnover arrangements generated the most power production and power use by storages.

Stability and power generated by the trophic chain configurations were determined by the connectedness expressed as the number of secondary positive feedbacks as well as the turnover arrangement of the components. Simulation revealed that models (a), (d), and (b) from Figure 23 were the most stable, models (f) and (g) were completely unstable and models (c), (e), and (h) were stable for a small number of runs. Chain (h) had a smaller percentage of power fed back and it produced less power and used more power than other one feedback models (see Figure 25).

Models with positive feedback were able to produce and use more power by storages because they maintained greater efficiency for power transfers up the chain. The pattern of power used by storages is radically shifted when the efficiency of energy transfer up the chain is high so that the majority of power is used by the highest quality unit rather than the lowest quality unit of the chain. Model (b) (Figure 23) with three secondary positive feedbacks captured and produced more power than did model (d) (Figure 23) which used more power in storages because it maintained higher levels of power use by units one and two of the chain but less use at unit three then occurred for model (b). This suggests that there may be an optimum number of secondary positive feedbacks for power use by storages which is not necessarily the same as the number of secondary positive feedbacks that optimize power capture and production. The advantage of model (b) in power production was due primarily to the greater efficiency of mean power transfer up the chain. Whereas the advantages of (b) and (d) in power capture and use by storage, respectively, were largely due to more efficient handling of variant power.

The turnover arrangement of the three chain components was also important in determining the stability and power production and use by storages of the trophic chain models. Of the four different turnover arrangements shown in Table 76 Cases A and B were by far more stable than Cases C and D. All four turnover cases were stable for model (a) (Figure 23) with zero positive feedbacks when there was no excess energy available for capture by the chain. For model (b) (Figure 23) with no excess energy available only chains with Case A and B turnovers had stable runs. Only a few input frequencies were stable but power production and power use by storage was very much greater for those runs. Thus, more energy seems to be required to support systems with secondary positive feedbacks which in turn capture more of the available energy and facilitates its transfer up the chain. When the eight models in Figure 23 were simulated with excess energy available to support increased positive feedback, turnover Cases A and B gave stable runs for models (a), (b), (c), (d), (e), and (h). However, turnover Cases C and D gave stable runs only for models (a) and (h) from Figure 23.

The four turnover cases stable for the zero secondary feedback model gave different characteristics to the pattern of power production and use observed for the model storages. All turnover cases showed resonance peaks at low frequencies but Cases A and B had a single peak at 0.01 cycles/time unit whereas Cases C and D had double peaks at 0.01 and 0.0001 cycles/time and 0.1 and 0.001 cycles/time unit, respectively. Power production and use at high frequencies was dominated by Case A with a fast high frequency cutoff. Power production and use at low frequency was dominated by two resonance peaks of Cases C and D. Dominance in power production and use by Case D was due to the generation of variant power in resonance whereas Case C dominance was mostly due to increased mean power generation at low frequency.

Kozlovsky (1968) compared efficiencies calculated from data representing five ecosystems and this information was used to determine how closely characteristics of the trophic chain minimodels corresponded to real systems. The trophic chain models were constructed so that there would be a 10% transfer of energy between trophic levels. This condition satisfied Lindemann's efficiency between the assimilation at level n-1 as shown by Kozlovsky (1968) to be around 10% for all five of the ecosystems studied. The ecological efficiency was set low (1%) for the first transfer from solar energy to green plants but higher (10%) for trophic levels 2 and 3. These values also correspond to Kozlovsky's calculations for lake ecosystems. In addition, Kozlovsky showed assimilation efficiency or the ratio of assimilation to ingestion to be low for the first level and high (80-100%) for higher trophic levels, and the minimodels also reflected this condition. Kozlovsky demonstrated that the ratio of respiration to assimilation was rather variable (10-80%) for the five systems he studied. In the minimodels this ratio is high (80-90%) which Kozlovsky showed was typical of a marsh ecosystem.

Kozlovsky distinguishes between but does not separate internal respiration needed to support and maintain storage and external respiration in activities of food gathering, etc. Energy circuit language makes it easy to make this separation theoretically although it may be quite difficult to demonstrate empirically. A set of models was simulated with large second law losses due to external respiration. Large losses of energy or material across interactions result in heavily damping the system's dynamic behavior. A drastic drop in the effectiveness of secondary positive feedback to facilitate power production and use occurs and this drop is not accompanied by increased stability (see Figure 29). Chains with these large losses do not capture as much available power as do systems with small losses across the interactions.

Aquatic versus Terrestrial Food Chains

Table 77 gives the flow, storage, and turnover characteristics of two aquatic, one terrestrial, and one interface ecosystem. Three of the turnover arrangements given in Table 76 occur in Table 77 Cases A-D differ only in rates of turnover as defined in Table 76 The first three trophic levels of the aquatic grazing chain are equivalent to Case A Case B is seen as the last three trophic levels of the aquatic grazing and detritus chains Case D is represented by the second, third, and fourth levels of the marsh and rainforest ecosystems. From the information given above on power production and stability it is no surprise that turnover Cases A and B occur in the two aquatic systems. Based on power and stability information it is also not surprising that Case C did not occur However, Case D occurs in both the marsh and terrestrial ecosystems despite the fact that it is the least stable of all the arrangements examined The extra power available when this arrangement of turnovers is in resonance probably is not enough to offset the disadvantage of limited stability in the competition for survival. One possible explanation for the apparent widespread occurrence of Case D with large storages such as detritus is that it has the hierarchical structure of Case A This would be true if there were no positive feedbacks from higher trophic levels back to the detritus which supports their productivity A hierarchical perspective on this problem leads to the observation that in the case examined turnover rates of higher trophic levels are too fast to send a signal powerful enough to bring about changes in the detritis storage

Table 77. Four evaluated trophic chains are given with flows, biomass, and turnover representing aquatic and terrestrial systems. All flows in g dry wt/m^2-day, storages units are g dry wt/m^2, turnover is per day

	Producers	Herbivores	1st Carnivore	2nd Carnivore	3rd Carnivore	
(A) Near Shore Grazing Chain (Kemp, 1977)						
Flow	0.643	0.0459	0.0035	0.0008	0.000014	
Biomass	0.333	0.0300	0.0760	0.0210	0.000530	
Turnover	1.900	0.1500	0.0460	0.0360	0.026000	
	Producers	Detritus	Detrivores	1st Carnivores	2nd Carnivore	3rd Carnivore
(B) Near Shore Detritus Chain (Kemp, 1977)						
Flow	6.704	4.5670	2.2590	0.0320	0.00530	0.0009
Biomass	446.300	695.6000	15.0140	0.6430	0.15200	0.0036
Turnover	0.015	0.0065	0.1500	0.0490	0.03500	0.0250

Table 77—Continued

	Producers	Detritus	Bacteria	Potamopyrgus
(C) New Zealand Salt Marsh (This Study)				
Flow	11.800	11.60000	26.40	3.480
Biomass	1,015.000	9,017.00000	2.24	13.400
Turnover	0.012	0.00210	11.80	0.026

	Leaves	Litter	Soil Microbes	Animals
(D) Tropical Rain Forest (Odum, 1970)				
Flow	9.400	3.77000	1.70	1.100
Biomass	939.000	14,630.00000	0.85	6.800
Turnover	0.010	0.00025	2.00	0.160

Therefore, control may be exerted in these cases by an upper trophic level feedback to the leaves of *Spartina* that replenish the storage of detrital material. Each element of an ecosystem represents many levels of nested hierarchy in addition to that level shown by the turnovers in Table 77. The behavioral action of animals may also be of lower frequency than their inputs and processes so that high quality feedbacks controlling slow turnover components are certainly possible. Such systems also have resonant properties which give additional advantages in energy flow as was demonstrated by the New Zealand salt marsh trophic chain simulations. This arrangement of a fast producer, a large slow storage and a very fast consumer or consumer chain is similar to a pulsing model investigated by Richardson and Odum (1981). It may not be unreasonable to speculate that trophic chains are fundamentally of Case A type with the possibility of developing Case B if there are enough levels. If the chain is built on a large storage rather than a constant flow, pulsing may occur and lead to dramatic increases in power use and production.

Peterson and Curtis (1979) showed that transfer of energy to higher trophic levels was more efficient in high latitude plankton benthic ecosystems and less efficient in the tropical plankton-benthic systems. The minimodel simulations along with this information on efficiency indicate that tropical plankton systems will be more heavily damped than their temperate counterparts which will have more of a tendency to resonate under variable input.

Kozlovsky (1968) showed that the ratio of respiration to assimilation increased with increasing trophic levels in lakes and springs but not in marshes Simulation showed that systems with Case A turnovers (see Table 36) can radically alter the ratio of respiration to assimilation at higher trophic levels whereas this was not true for systems with Case D turnovers One might speculate from this result that lakes, streams, and aquatic ecosystems in general are systems with many secondary positive feedbacks

The Interaction of a Second Energy Source and Maximum Power

One problem of both theoretical and practical interest is to determine the influence of a second energy source which interacts at different levels in a trophic chain. Two constraints were imposed on the model to aid in this evaluation First, total power entering the system was a constant and second the same amount of embodied energy was introduced at each level in the chain. Since embodied energy increased by a factor of approximately 10 at each level in the chain the total power input at level n+1 was about 10% of the energy input at level n

A three unit chain with one constant energy source entering at Q_1 and a second variable energy source entering at Q_1, Q_2, or Q_3 was simulated over a range of input frequencies (see Figures 29 and 31) In addition, a three unit chain model with two variable energy sources was tested in a similar manner (see Figures 33 and 35). The frequency filter properties of those models were largely determined by the position of the second input source A second input at Q_1 or Q_2 was a low pass filter, and a second input at Q_3 was a band pass filter for both constant and variable inputs at the chain base (see Figures 30 and 34). The main difference between these two patterns was that the resonance peaks were stronger and more numerous when both inputs were variable. The turnover configuration of the model determined the size and number of the resonance peaks or bands by establishing different natural frequencies of oscillation in the system.

Two configurations of each chain model were simulated, one with no secondary positive feedbacks and the other with three secondary positive feedbacks. In general, the three feedback model produced and used more power in its storages but was less stable than its zero feedback counterpart. Turnover Case D produced and used the most mean square power in its storages when a second input entered the zero secondary positive feedback model at Q_3. However, when the chain model was configured with three secondary positive feedbacks a second input at Q_1 usually produced and used the most power in storages with Case A turnover.

The power produced and used by storages of the chain with zero secondary positive feedbacks were compared at three input positions for the second energy source. (Compare Table 51 to 58.) The model with a constant energy at the chain base gave more power production and use than the model with two variable sources when the second input interacted at Q_2 or Q_3. However, the model with two variable energy sources generally produced and used more power when the second input interacted at Q_1. The model with one constant and one variable source produced and used the most power because it maintained more mean power in the system. When the model with two variable sources produces and uses the most power, it is usually due to greater production and use of variant power. When the second input enters at Q_1 the interaction of two variable sources produces and uses more power in resonance than does one constant and one variable source which obtains some additional energy from a faster high frequency cutoff. When a second input enters at Q_2 or Q_3 the ratio of variant power used by storages to that input to the system is greatest for the model with one constant energy and one variable energy input. However, the model with two variable energies produces and uses a greater absolute amount of variable power in its storages for these second input positions.

The model configuration with three secondary positive inputs (Figures 31 and 35) usually produced and used more power through its storages when two variable inputs were supplied to the system regardless of the position of interaction. (Compare Table 55 to 61.) The configuration with variable inputs at Q_1 and Case A turnovers produced the most power. Power used by storages was greatest for the zero feedback configuration with one constant and one variable energy entering at Q_3 and Case D turnovers except for its unstable frequencies 0.001 and 0.0001 when the aforementioned configuration dominates power used as well as power produced.

Case A turnover was the most stable arrangement examined. When all simulations of Case A turnover were examined, the single energy source produced and used more power through storages than did either of the two energy source models.

From the above discussion of the position of energy sources and maximum power production and use by trophic chains several observations can be made. Power sources presented to the base of the chain are the most effective in production and use of power for the models with Case A turnovers. Chains with Case A turnovers are more stable than other turnover arrangements and therefore probably are found most often in natural systems. If a chain with no secondary positive feedbacks captures a second energy input over and above that energy available at the cahin's base it is most likely to give maximum power production and use by storages if it enters at Q_3 or the highest unit of the chain. If entry at Q_3 does not give a stable system then Q_2 is the best input location to give maximum power production and use. Brown (1980) and Limburg (1981) identified input at the highest chain level as being most effective in facilitating power use in a five unit chain and three unit web, respectively. A chain with three secondary positive feedbacks would be able to produce and use the most power through storages if the second input entered at Q_1 and its frequency and phase matched the input at the chain base. In general, one could speculate that less connected systems might be better able to handle high quality variable inputs than more connected systems if power use and production are used as the criteria for evaluation.

Maximum Power in Competition

Odum (1982) showed that when three units of linear quadratic and superquadratic dynamics are in competition each unit wins in order as thresholds of increasing energy are crossed. A similar result was found in this study when linear and autocatalytic competition between three units were compared. (Compare Tables 9 and 10.) Linear competition accounted for more power production and use at low energy input, whereas, autocatalytic competition produced and used the most power when energy captured was increased.

Costanza (1978) showed that there is more energy available for use in a constant signal than in a periodic signal and that the periodic signal contains more useful energy than a random signal if system power use is used as the criterion for evaluation. This study demonstrated that the power production and use by a system's storages can be dependent on the frequency matching of turnover and inputs. When matching occurs the power produced and used by a system of storages in competition or in a chain can be greater for a periodic than for constant input (see Tables 10 and 12).

In general, if low pass filters are present, slower input frequencies give greater power production and use by a system. This pattern can be altered if resonance phenomena occur due to the matching of internal natural frequencies with external input frequencies or simply by matching external input frequencies (see Table 18).

Autocatalytic units are able to capture more excess energy available than are linear units over a similar time period (see Table 8). If all storages and flows are equal there is no difference between power captured by linear and autocatalytic systems. However, if these systems are given variable inputs the autocatalytic system captures more power if energy is above a threshold.

Odum (1982) correlates the power on a pathway with the mathematical power of the expression governing the pathway. There may also be a relationship between the number of secondary positive feedbacks which interact to give the pathway expressions and the energy flow on those pathways. This study indicates that more secondary positive feedbacks give greater power production and use but also require higher thresholds of available energy for their support

In competition between three autocatalytic units modulation of matched input signals gives more power production and use than is found when the same two frequencies are superposed (see Table 18) However, when the signals are unmatched that is they have different frequencies, superposition does better than modulation in the production and use of power Unmatched signals lessen the intensity of competition allowing units to survive for longer time periods and thus there is a less intense pulse of the excluded units. If a system of three competing units can only set one turnover to match a modulated signal of two frequencies the most power is produced and used by the system and by the matched unit if the turnover of the unit matches the sum of the input frequencies (see Table 20). If the turnovers of all three units in the system can be adjusted then the most power production and use by the system occurs when units have turnovers equal to the sum of the input frequencies, the difference of the input frequencies and the lowest input frequency.

Stability

Stability is a concept with several meanings to the field of ecology. For example, Lewontin (1969) discusses at least five aspects of stability that are commonly employed for the analysis of ecosystems May (1973) distinguishes between local and global stability by describing a landscape of hills and valleys representing the system's stability surface. The lowest elevation on the surface is stable globally and each valley represents a point of local stability. In this study a simulation run is considered stable if one component of the system is not zero after a run time of 1,000 units. Thus, systems that are unstable have been driven to the zero limit set for each component by limiting storages to positive values. May (1973) observed that several types of system webs of increasing complexity tended to be increasingly unstable. Two main cases considered were a community matrix of logistic growth equations and a matrix of randomly constructed species interactions which could be either positive or negative in effect. May points out that Gardner and Ashby (1970) demonstrated that complex systems which are structured in subgroups with intense interactions are more stable than randomly structured webs.

The stability of trophic chain minimodels from Figure 23 is given in Table 78. Figure 51 shows the connectance matrices for the eight models of Figure 23. Table 78 and Figure 26 show that greater connectance in the chain leads to less stable systems with higher energy flow. When Table 28 is compared with Table 26(A) it is apparent that chains with small second law losses across interactions have a local

Table 78 The stability, connectance, interaction strength, and power for trophic chain models in Figure 23

Model	# Positive Feedback	Connectance* %	Interaction† Strength	% Stable (n=12)	Average Power In	Average Power Out
a	0	55.6	21.96	83.30	102.6	91.00
b	3	88.9	13.97	50.00	281.7	102.10
c	2	77.8	15.96	16.67	130.5	54.34
d	2	77.8	16.71	50.00	278.9	102.40
e	1	66.7	18.33	50.00	133.7	56.55
f	1	66.7	18.60	0.00	0.0	0.00
g	2	77.8	15.94	0.00	0.0	0.00
h	1	66.7	18.30	33.33	102.9	91.13

*Figure 51 defines connectance.

†Interaction strength is taken as the average energy flow at time = 0

a)

	Q_1	Q_2	Q_3
Q_1	1	1	0
Q_2	0	1	1
Q_3	0	0	1

e)

Q_1	Q_2	Q_3
1	1	0
0	1	1
0	1	1

b)

Q_1	1	1	0
Q_2	1	1	1
Q_3	1	1	1

f)

1	1	0
1	1	1
0	0	1

c)

Q_1	1	1	0
Q_2	1	1	1
Q_3	0	1	1

g)

1	1	0
1	1	1
1	0	1

d)

Q_1	1	1	0
Q_2	0	1	1
Q_3	1	1	1

h)

1	1	0
0	1	1
1	0	1

Figure 61 Connectance matrices for the models given in Figure 23. Connectance is defined as the percentage of non-zero values in the matrix.

stability maximum at three secondary positive feedbacks. Table 78 showed that for the series of models given in Figure 23 certain feedback configurations are more stable than others. Perhaps the two factors that in part determine web complexity in the real world are power and stability which have antagonistic effects here but not necessarily in real systems (see May, 1973). However, as Table 78 and Figure 26 show, certain chain structures give high power generation combined with surprising stability. [See models (b) and (c).] This general pattern is one which has controlling positive feedbacks from the high quality unit back to lower quality units in the chain.

Besides connectance the intensity of component interactions also determines the system's stability. Table 76 showed that model (b) with the greatest connectance had the least average energy on an interaction pathway. Conversely, model (a) with the least connectance had the greatest average energy of interaction. May's measure of the interaction strength was s, the average standard deviation of the flow on all pathways. Briand (1983) examined 40 food webs and showed that systems with constant environments were more connected and had less intense interactions than systems in fluctuating environments. According to the web and chain models examined here one would expect more constant environments with more highly connected food webs to produce and use more energy. If the systems are corrected for the thermodynamic intensity or temperature the power generated may also increase for more connected systems in constant environments. May (1973) observed that more connected systems must have more natural frequencies of oscillation and therefore have a greater chance of being unstable Briand's study is interesting because it indicates that systems with higher connectance occur in constant environments where the greater number of natural frequencies will not usually be subjected to perturbations. This study shows that systems which are highly connected and in fluctuating environments may develop energy flows that are maintained at high level across a wide frequency band By keeping the mean level of flow high the ability of resonance to cause variations in the variant power generated is mitigated [see Figure 54(a) and (b)].

Stability analysis was also used in this study to define the boundaries of a system in the frequency domain as shown in Figure 34(c) and discussed above. Stability has also been discussed in relation to the four turnover arrangements shown in Table 75.

Discrete, Nonlinear Competition
and the Iteration Interval

May (1974) discussed the kinds of behavior possible from simple nonlinear equations representing biological populations as the intrinsic rate of increase r is augmented These equations give a rich variety of behavior including stable limit cycles of different frequency and chaotic or random behavior. In this case chaotic behavior was represented by cycles of arbitrary periods May notes that completely deterministic nonlinear equations give behavior that is indistinguishable from chaos when r is above a threshold This observation becomes even more interesting when r is recognized as the energy source for May's population models. From this perspective random or noisy behavior could be an energy based phenomenon

In this study, initial models were switched from analog simulation to digital simulation and in the process questions arose with regard to the significance of the iteration interval. Because of the iteration interval discrete systems can have very different properties from their continuous counterparts. This is highly significant for ecosystems since there are many cases of discrete phenomena observed, e.g., breeding time of certain populations, the outbreak of disease, migration, cycles, etc.

The iteration interval was recognized as a kind of system filter that could determine the survival of components. Increasing the iteration interval effectively acts as an increase of r for May's population models and therefore a sensitive range of bifurcation and stable limit cycles and chaos is passed as dt is increased (see Figures 17 and 18, Tables 6 and 7). Of course, this interesting behavior is merely an artifact if the system under investigation is continuous, but what about the case when it has discrete components? How should such systems be represented in simulation and are simulation results different from those obtained by assuming that the system is continuous? The competition and trophic chain minimodels were given an alternative formulation based on the assumption that these systems were discrete. The component turnovers were used to set iteration intervals with the same ratio of dt to time constant. Fast component DO loops were then nested inside slower component DO loops to simulate discrete behavior. In this formulation a component with discrete long generation time could not exploit fast variations (see Appendix A).

The results of simulation were different in the case of competition between three units. (Compare Tables 21-23 to 12.) The fast turnover unit was able to outcompete slower turnover units when the input frequency matched the fast turnover. Thus, the effect of slow units preempting variant power from the fast unit was negated. Nested simulation of the trophic chain model with Case A turnovers gave results very similar to the simulation with the same dt. (Compare Table 64 to 58.) The use of hierarchically structured programs may be the appropriate method for handling systems with discrete aspects.

Limitations on Frequency Response Analysis

Frequency response analysis was performed by holding the input signal's amplitude and mean constant and varying the input frequency. This approach is useful in identifying possible system boundaries, resonance points, and cutoffs but it does not show what the frequency response would be to the actual signals entering a system. In general, the energy based development of hierarchies imposes an order of increasing amplitude as frequency becomes slower. However, the maximum amount of variance in the system is often found at high frequencies because the second law of thermodynamics requires that energy be concentrated as it is upgraded (Odum, 1983). External forcing frequencies often have their variation heavily concentrated at one or more specific frequencies, e.g., solar inputs are concentrated at daily and annual frequencies. Thus, the frequency response at these frequencies becomes most important. Establishing system boundaries for low frequency inputs by observing whether a signal is incorporated or catastrophic may be one of hte more useful applications of the frequency response techniques.

Self-Organization of Ecosystem Design by Invading *Spartina*

Flora and fauna from all over the world have been transported by man into the long isolated islands of New Zealand. Elton (1958) discussed some of the consequencies of biological invasion. Sometimes an introduced species (such as the red deer in New Zealand) expands rapidly without predators, parasites, competitors and other ecological constraints present in its native ecosystem. Another species may be unable to establish itself, or occupy only a limited area like the white tail deer which lives mainly on Stewart's Island, New Zealand. Whole ecosystems are not introduced into new areas although often predators and parasites may be imported to counter the invasion of an unwanted species.

The introduction of *Spartina townsendii* and its fertile polyploid form *Spartina angilca* into New Zealand was ecologically powerful. *Spartina* forms the basis of an entire salt marsh ecosystem which has the capability of radically altering the landscape and the patterns of water circulation and sediment deposition in suitable tidal areas. *Spartina townsendii sensu lato* (includes both forms) has been remarkably effective invading the Marlborough Sounds region of New Zealand. Erosion rates and the nutrient content of rivers have increased due to clearcutting, conversion to pasture, and fertilization by man. Thus, conditions in New Zealand today are probably more favorable for development of extensive salt marshes than they have been previously. The indigenous salt marsh in the Kaituna River estuary is composed of an association of *Juncus* and *Leptocarpus* which does not usually colonize further seaward than mean high water neap tide. The tidal zone seaward of the natural marsh was ordinarily an extensive mud flat. This area of mud flat is rapidly being taken over by *Spartina* at the mouth of the Kaituna River and elsewhere in the Marlborough Sounds region. Odum et al. (1983) note that the *Spartina townsendii* system is much more productive than the indigenous mud flat it has displaced. Therefore, this change is apparently an example of maximum power selection in which a new self organizing system has replaced the old ecosystem allowing adaptation to utilize more of the available energies of sun, tide, river sediment, and nutrients. Odum et al. (1983) also make the point that the success of the hybrid *Spartina* may illustrate how microevolutionary changes can feed back to effect broad reorganization of ecosystems and landscapes into more productive, potentially useful systems to maximize energy use under different conditions.

This study examined three aspects of *Spartina* self-organization at the Kaituna River estuary with evaluated minimodels. Competition, trophic chain self-organization and a marsh overview minimodel were simulated and the frequency response of the models was analyzed.

Competition between *Spartina* and *Juncus*-*Leptocarpus* Marshes

Since *Juncus*-*Leptocarpus* has less tolerance for inundation than *Spartina* it exists in the marsh on higher ground whereas *Spartina* is found in the low marsh. Competition between these two will usually be along their boundary. Where competition occurs for territory suitable for both species a simulation model showed *Spartina* eliminated *Juncus* and *Leptocarpus* within five and two years, respectively (see Figure 39). *Spartina* has the fastest turnover, then comes *Juncus* and finally *Leptocarpus* turns over the slowest. The order of dominance found by simulating a model evaluated with real data was just the opposite of the results seen in the theoretical case with all flows equal where the slowest unit turnover wins out in the end. The result given for the real case is undoubtedly due to the fact that power production and use by *Spartina* is apparently greater than that for the *Juncus*-*Leptocarpus* association. The superiority of the unit with fastest turnover is due to its greater productivity.

Salt Marsh Filter Relationships

Odum (1982) briefly investigated the consequences of additive and multiplicative interaction between low frequency small amplitude high quality energies and high frequency large amplitude low quality energy. Multiplication gave a pattern of amplitude modulation where the amplitude of the fast signal increased when the slower signal amplitude was high and decreased when it was low. Addition of signals resulted in only small variations of the high frequency amplitude because the amplitude of the low frequency signal was small compared to that of the high frequency.

When the frequency properties of nonlinearity versus those of linearity were compared in the salt marsh minimodel, two distinct patterns were observed. Signals entering a storage were superposed while those entering multipliers were modulated giving the two types of output discussed above (see Figure 42). If nonlinearity is a part of real ecosystems then we should be able to observe the distinct pattern of the modulation of interacting energy or material signals. This would be an excellent experiment for future field study.

Most models with storages have a high frequency cutoff associated with the component based on its turnover. The marsh minimodel simulation showed that the labile N storage was not of fast enough turnover to capture the variation in the semidiurnal tide. The Spartina storage captured annual variations but not those with higher frequency. In addition to the high frequency cutoff the position and manner of the input signal's interaction is important in determining what frequencies are captured (see Tables 43 and 44).

Transmission of frequencies through the model was enhanced if the frequency entered through a multiplier and mitigated if it entered via a storage. The distance (number of storages) through which a signal must travel in a model also caused signal attenuation as shown by Child and Shugart (1972). Solar input was dominant over river and tide input in the frequency response analysis performed on this model. Labile N was sensitive to all inputs, Spartina was sensitive only to solar energy, sediment N was sensitive to both solar input and river input frequencies.

The patterns of power use by the salt marsh minimodel reflect these observed in the analysis of variant power use. Table 73 shows that variant power accounts for less than 10% of the total power yet changes in variant power contribute 10 to 80% of the changes observed for total power when solar input frequency varies. The frequency response with respect to solar energy gives the strongest pattern of the three inputs. Both total and variant power captured, circulating and produced have a minimum at frequency 10 cycles/year and increase as frequency increases or decreases. Variant power exported has a maximum at 10 cycles/year and decreases if frequency changes. The significant factor here may be that the minimum power is processed at a solar input frequency that is unlikely to occur. The *Spartina* high frequency cutoff is set to capture annual variations and lower frequencies. High frequencies are treated as constants by slow storages so power increased for fast input. If the system cannot use the mean square power it is lost as export. In this context there is a local minimum of power lost in export at solar input frequency 1 cycle/year. Maximum power capture and production was also at this frequency when tide and river were varied. So the marsh minimodel has a filter design which is adapted to do well at annual input frequencies that carry much of the variant power available for use.

Longitudinal turbulent exchange in an estuary was modeled as proportional to the concentration gradient of the substance. The frequency response of this formulation is a band pass filter with maximum transmission at 10 cycles/year. Turbulent exchange imposes a notch filter pattern on the labile N storage which one would expect to be a low pass filter like its sister components sediment N and *Spartina*.

Trophic Chain Characteristics and Self-Organization

One point of interest for successfully invading species is how they will alter the ecological and trophic relationships in their new home. The major food chain of the *Spartina* marsh ecosystem at Havelock, New Zealand, consists of *Spartina townsendii sensu lato* which produces detritus and exudes organic matter upon which bacteria flourish. The bacteria in turn are consumed by a deposit and organic film feeding snail *Potamopyrgus antipodium zealandiae*. It is quite likely that this snail is consumed by ducks and bottom feeding fish like the flounder both of which are found on the marsh. *Potamopyrgus* is the key indigenous species organized into a new *Spartina* based food chain. *Potamopyrgus* is found only beneath rocks and driftwood in the native marsh, but it can occur in abundance on brackish tidal platforms near river mouths (Morton and Miller, 1968). *Potamopyrgus*'s surprising abundance (70,000 animals/m^2) on the marsh at Havelock may be based upon the provision of abundant food and shelter by the *Spartina* and a paucity of competitors suitably adapted to exploit the marsh habitat. Similar conditions of abundant food and few competitors occur on mud flats at the river mouth where *Potamopyrgus* is usually quite abundant.

Frequency response analysis of the trophic chain model revealed patterns of high frequency cutoffs and modulation consistant with observations of the marsh minimodel. However, strong resonances were set up by frequency variation of inputs to the trophic chain model that did not appear in the marsh minimodel. The strength of an input frequency interaction depends on how close the affected component is to the input signal as well as the component turnovers. Temperature input was most effective in producing resonance in the bacteria and DOC storages. The kinetics of temperature interaction were modeled as stimulating both production and consumption which favored resonant behavior. This observation was supported by simulation of the model with a similar push-pull formulation for predator harvest which also set up resonance in the bacteria and DOC storages. In addition, resonance only occurred over a temperature input frequency band from 100 to 365 cycles per year interacting with an annual variation of river DOC, and solar input. Perhaps the interaction of annual rhythms with daily rhythms of variation is an important factor in producing pulsing behavior or resonance in ecosystems. This speculation needs testing.

The frequency response analysis of the marsh trophic chain model was carried out with respect to four system parameters: the power circulating, the power produced, the power used by storages and the power remaining. The power circulating is the sum of energy or matter moving on all system pathways and is similar to system ascendency expressed in terms of information by Ulanowicz (1980). The power remaining is the complement of power captured, thus minima of power remaining indicate that power captured by the system is a maximum.

Frequency response analysis of the trophic chain model revealed that there is a tradeoff between the maximum power captured and the maximum power circulating for inputs that give resonance. A resonant input frequency maximizes the power circulating in the model but causes the power captured to be minimal. Predators with push-pull effects brought about the greatest amount of variant power circulation for all inputs at all frequencies. However, the total power circulating was only greatest at high frequencies for this input. In contrast power captured was least for inputs with resonant frequencies. Power produced and used by inputs that give resonance is greater at resonant frequencies but less for nonresonant frequencies than inputs which do not give resonance. Absence of secondary positive feedbacks did not change the resonant properties of the system, thus it was structurally stable with respect to these interactions. Lack of positive feedbacks did uncouple the power captured from the power circulating so that resonance in the system no longer diminished the power captured. This suggests that secondary positive feedbacks from resonant components to the energy capturing component may be avoided in competitive ecosystems. The presence of secondary positive feedbacks causes more energy capture at low frequency than does the case with no secondary positive feedbacks. The total power circulating is greatest for the case with feedbacks even though the variant power circulating is less. This supports the theoretical results that increased power from positive feedbacks is a mean effect.

This tradeoff between power captured and power circulating may be significant when viewed in the context of ecosystem development. System designs that maximize power captured are most important in competition, but a design that maximizes power circulating may be the ultimate goal of a climax system. Lower system connectance may preserve the ability to capture energy while maintaining high resonant levels of power circulation where a compromise is required. Systems with secondary positive feedback capture more power at nonresonant frequencies and generate more circulating power at almost all frequencies, so they should be selected most of the time in both successional and climax ecosystems. When they do not occur it may be due to the existence of resonance driven by one of the system inputs.

Only two of the four inputs to this system produced resonant behavior. A solar input frequency of 0.1/year causes the maximum power capture and circulation in the system. The frequency response of all the system parameters to variations in solar energy is a low pass filter pattern. The maximum power circulating and used by storage at the annual input frequency is given by the model that includes predation. There is no difference in power production and capture between a model with predators and one without.

When predators have a push-pull action on their prey they produce more variant power circulation but they capture much less variant power than does the system with predator harvest only. The power circulating is greater for resonant frequencies and at low frequency but less at intermediate frequencies. Power captured was less for the predator push-pull configuration. These observations may be significant for systems that are harvested such as fisheries. Appropriate feedbacks to stimulate system productivity are important, but exploiters must avoid push-pull effects that can lead to a less competitive or unstable system or component.

Frequency response analysis indicated that the marsh trophic chain model was not adapted to incorporate disturbances with periods of 100 years or greater. The model was most sensitive to harvest by predators and could be stabilized by adjusting this parameter as frequency input was changed. The most unstable cases occurred for inputs that caused resonant behavior. Some of this instability may be contributed by the storage of DOC without a linear drain.

Ecosystem Adaptation and Variable Resources

The simulations of theoretical and evaluated ecosystem models indicate that adaptation of system design by changing component turnovers can facilitate the capture, low pass, and use of available variable resources. Frequency response patterns of both theoretical evaluated ecosystems showed characteristic patterns explicable in terms of concepts from communications engineering. Low and pass and band pass filters, resonant peaks and high frequency cutoffs were found to be characteristics of highly nonlinear ecosystem models. Evidence supports the concepts that hierarchical ecosystem organization is most stable and that increasing positive feedbacks are required to exploit additional power in the system as well as contributing to more power capture. Frequency adaptation by changing turnover may define niche separation in competition. The operation of the second law of thermodynamics was found to damp system oscillations. When resonance did occur in evaluated ecosystems there was a tradeoff between power circulating in the system and power captured in competition with others. Ecosystem organization in part depends on adaptation to the frequency of available resources. Frequency is important to the design of ecosystems.

SUMMARY

The following points summarize results relating to ecological competition and organization.

1. More power was used in competition by linear units for small energy input but autocatalytic competition used more power when energy input was large.
2. In general, constant signals were more easily captured and supplied more power than periodic signals, periodic signals were superior to random inputs. When input signal frequencies matched the natural frequencies of a system resonant power from variable inputs exceeded the power available from constant input.
3. Autocatalytic units exploit excess available energy more efficiently than linear units.
4. Competition is intensified by input frequency-turnover matching, turnover separation and an upward shift in the range of turnover considered.
5. The fastest turnover unit uses the most power for a single linear or autocatalytic unit not in competition. This is also true for linear units in competition.
6. Autocatalytic units in competition give more total power use as input frequency is decreased, and more total power production

for inputs matched to frequency turnover. Power production is high because matching causes the fast turnover unit to pulse, contributing a burst of power before it is excluded.

7. When there are high frequency inputs available for use, the system which matches its high frequency cutoff to receive variant power captures and uses more power than a system which fails to exploit the high frequency energy.

8. Both variability in the input functions and separation of unit turnovers are necessary to bring about an order of dominance in digital models where all flows are initially equal.

9. Modulation (multiplication) of two input frequencies transformed and used more power than superposed (added) inputs when the input frequencies were equal and in phase, but not when they were unequal. Noisy signals gave more power when they were modulated than when they were superposed.

10. Actual data on a salt marsh system in New Zealand showed that pathway flows were not equal and that the fast turnover unit established dominance quickly under conditions where it captured more available energy.

11. In general, trophic chain models with increasing numbers of secondary positive feedbacks in multiplicative interactions transformed more power but were less stable than units with fewer feedbacks.

12. All models of competition, trophic chains, and webs tested displayed increasing power use by storage at lower input frequencies as would be expected for low pass filters.

13. Increased power generated by greater numbers of secondary positive feedbacks in webs and chains was a mean effect

14. Feedback configurations were highly variable in their stability, and configurations existed where high positive feedback was associated with high stability.

15 Hierarchically arranged turnovers ($Q_1 = 10$, $Q_2 = 1.0$, $Q_3 = 0.1$) where the most stable (82.7%) and used the most power in storages (37.6%).

16. The position of a second energy source entering a chain was the most important factor determining the type of wave filter type observed When the second energy entered at a low trophic level, a low pass filter with resonant peaks was found, for a second input in the middle of a trophic chain a low pass filter was observed and for a second input at the end of the trophic chain a band pass filter was shown by frequency analysis

17 Matching turnover properties like resonance and high frequency cutoffs to input frequencies usually determined the pattern of power capture and use.

18. Power transformation was increased by adding a second energy source at the end of the trophic chain in systems with few secondary positive feedbacks The optimum position for a second energy source to increase power transformation in a system with three secondary positive feedbacks was the base of the trophic chain

19. Where the total energy available to the system was constant, the total power transformed by the system was maximized for a single input at the base of the chain
20. Pathways with cooperation between parallel units of different turnover stabilized webs for most input frequencies by preventing competitive exclusion of the fast turnover unit. More power was captured than for webs with competition alone
21. Filter design developing during self-organization of an invading Spartina salt marsh had a minimum energy adsorption at 10 cycles per year and was therefore well adapted to capture solar input variations at higher and lower frequency
22. Input variability not used by the marsh system was exported to the sound ecosystem.
23. Longitudinal turbulence of exchange with the estuary was found to give a notch filter pattern to the fast turnover labile N storage.
24. Variable input accounted for less than 10% of the power input to the model but it usually accounted for 40 to 80% of the total change in power observed
25. Self-organization of a new trophic chain based on invading Spartina included the indigenous snail Potamopyrgus as the major detritivore in abundance on the marsh floor
26. The interaction of diurnal temperature input frequencies with annual frequencies of river and solar input produced resonance in DOC and bacteria system components of a trophic chain model based on data from New Zealand, Florida, and Georgia.

27. Resonance set up in this trophic chain allows the greatest production of power circulating in the model but power captured in competition is a minimum for the resonant case.

28. If secondary positive feedbacks from resonant components to the power receiving unit of the chain are broken, power capture is uncoupled from power circulating

29. The second law of thermodynamics acts to mitigate the effect of resonance within a trophic chain.

30. Stimulating both production and consumption of a component tends to cause resonant behavior.

31. Optimum conditions for power captured in competition were different from the optimum conditions for power transformation in the coupled system network

Some general summarizing points follow:

32. Frequency response analysis revealed wave filter types, high frequency cutoff, resonance, and modulation in basic ecosystem designs and evaluated ecosystem models.

33. Frequency is important in ecosystem design and this importance was demonstrated by combining concepts from ecology and systems engineering.

APPENDICES

APPENDIX A
COMPUTER PROGRAMS

Computer programs used in this study were written in Fortran 4 plus. The programs used in this study are structured so that many different simulation models can be run using the same two basic programs These two programs were adapted from programs written by John Richardson for use with the Digital Equipment Corporation (DEC) PDP11-34 computer. The programs Enter, Alter, and Plotting for the LA120 are exactly as he wrote them. Enter and Alter create and rearrange a data file, respectively, that is then input to the main programs The program Output calculates the mean square power, the mean, the variance, the maximum, the minimum and the standard deviation for ten variables The Stats section of this program was adapted from a similar routine written by Chet Kylstra for his Data acquisition class, GGPLOT gives the time series output of a simulation model for the DEC VTC 100 terminal. Programs for the three New Zealand marsh models are given in this appendix and and following each program is a list of date input The equations and stocks and flows for the theoretical models have been given in the text and computer programs for them can be easily written from this information Programs for hierarchically nested versions of autocatalytic competition and the trophic chain models are contained here as programs Comnest and Chainest.

```
[illegible]
[illegible] E4 E5 E6,E7 E8 E9 E10 E11 E12 E13 E14 E15
[illegible] ********************************************
[illegible] A1 A0 11 A2 B1 C2 C3 B2 E2 R4 R5 R6 R0 HX(1),LX(1)
[illegible] HX(5) HX(6) HX(7) HX(8) HX(9) HX(10) HX([illegible]) HX(2)
[illegible] HX(5) HX(6) HX(7) HX(8) HX(9) HX(10) E[illegible]
DEFI[illegible] E2
[illegible]
[illegible] EFFICIENTS
X2=R[illegible]
K3=R3/(Q2*R0
K4=R4/(Q3*R0)
[illegible]=R5/Q1
[illegible]=R6/Q2
KT=R7/Q3
START OF LOOP ***********************************************
WRITE(7,130)E5,W,DOM,E5,HITON
FORMAT( [illegible] A1,A2,A1,A3)
CALL REFR1
GO TO 35
CALL REFR
IF(F[illegible]-LT XD[illegible])CALL REFR1
D3=K4*Q3*R0
D5=K2*Q3
Q3=Q[illegible]*(D3-D5)
IF (Q3.LT.1.0E-10) Q3=0
DO 330 K=1,10
D2=[illegible]*Q2*R0
D5=K6*D2
Q2=Q2+DT2*(D2-D5)
IF (Q2.L[illegible] 0E-10) Q2=0
DO 320 J=1,10
INPUT SINE WAVES
A[illegible]=A0*SIN(V0*T)
WA=A0*SIN(V0*T)
[illegible]=A1*SIN(V1*T)
[illegible]=A2*RAN(N)-(A2/2)
RATE EXPRESSIONS
R0=(J0+WA+[illegible]+ND)/(1+K2*Q1+K3*Q2+K4*Q3)
[illegible] K2*Q1*R0
[illegible]=K6*Q1
STORAGE A[illegible]MULATIONS
Q1=Q1+DT[illegible]*(D[illegible]-D[illegible])
[illegible] (Q[illegible] 0E-10) Q1=0
[illegible]
[illegible]
```

```
      PROGRAM "HAINES"
C     DEFINE VALUES
      DT=2.E-7/10
      ET=1.E-7/100
      T=0
C     CALCULATE COEFFICIENTS
      K0=R0/(Q1*R1*R0)
      K1=R0/(Q1*R1*R0)
      K2=R2/(Q1*R0*R1)
      K3=R3/(Q2*Q1)
      K4=R4/(Q3*Q2)
      K5=R5/Q1
      K6=R6/Q2
      K7=R7/Q3
C     START OF LOOP ****************************************************
      WRITE(3,10)ESC,ZIBOM,ESC,MITOR
10    FORMAT(' ',A1,A3/1,A3)
      CALL REPR1
      GOTO 5
5     CALL REPR
      IF(ET1(T,CT)-LT.20)CALL REPR1
      D6=K7*Q3
      Q3=Q3+DT*(D3-D6)
      IF (Q3.LT.1.0E-10) Q3=0
      DO 333 N=1,10
      D3=K4*Q3*Q2
      D5=K6*Q2
      Q2=Q2+DT2*(D2-D5-D3)
      IF (Q2.LT.1.0E-10) Q2=0
      DO 300 J=1,10
C     INPUT SINE WAVES
      W0=A0*SIN(V0*T)
      WA=A1*SIN(V1*T)
      WB=A*SIN(J*T)
      R0=A2*RAN(1)-(A2/2)
      R1=A3*RAN(3)-(A3/2)
C     RATE EXPRESSIONS
      R0=(J0+WA+N0)/(1+K0*Q1*R1)
      R1=(J1+WB+N1)/(1+K1*Q1*R0)
      D1=K2*Q1*R0*R1
      D2=K3*Q2*Q1
      [illegible]
      Q1=Q1+DT*(D[illegible]-D1-D2)
      IF (Q1.LT.1.0E-10) Q1=0
      [illegible]
      [illegible]
```

```
                 R
      [illegible] RING(15) [illegible]  X(50)
      [illegible]
      FORMAT('  WHAT IS THE FILE NAME FOR OUTPUT ')
      READ(5,2)(FILE(I),I=1,4)
2     FORMAT(4A4)
      OPEN(UNIT=1,NAME=FILE,TYPE='NEW',FORM='UNFORMATTED')
      WRITE(5,3)
3     FORMAT(' WHAT IS THE DESCRIPTION OF THE FILE 60 CHARS OR LESS ')
      READ(5,4)(STRING(I),I=1,15)
4     FORMAT(15A4)
      WRITE(5,5)
5     FORMAT('  HOW MANY PIECES OF DATA IN THE FILE ? 50 OR LESS ')
      READ(5,6)N
6     FORMAT(I3)
      DO 20 I=1,N
      WRITE(5,7)I
7     FORMAT('  DATA VALUE NUMBER ',I3,2X)
      READ(5,8)X(I)
8     FORMAT(G12.5)
20    CONTINUE
      WRITE(1)(STRING(I),I=1,15),N,(X(I),I=1,N)
      CLOSE(UNIT=1)
      END
      PROGRAM ALTER
      DIMENSION STRING(15),X(8)
      DIMENSION INFILE(8),FILOUT(8)
      WRITE (5,1111)
1111  FORMAT('  WHAT IS THE NAME OF THE INPUT FILE  ')
      READ(5,1112)(INFILE(I),I=1,8)
1112  FORMAT(8A2)
      OPEN(UNIT=1,NAME=INFILE,FORM='UNFORMATTED',TYPE='OLD')
      READ(1)(STRING(I),I=1,15),N,(X(I),I=1,N)
      CLOSE(UNIT=1)
      WRITE(5,17)N,(STRING(I),I=1,15)
17    FORMAT(' ',I3,2X,15A4)
      WRITE(5,3)
3     FORMAT('  WHAT IS THE NEW DESCRIPTION OF THE FILE 60 CHARS OR LESS')
      READ(5,4)(STRING(I),I=1,15)
4     FORMAT(15A4)
12    DO 20 I=1,N
      WRITE(5,7)I,X(I)
7     FORMAT('  VARIABLE NO ',I3,' VALUE IS ',G13.8)
20    CONTINUE
21    CONTINUE
      WRITE(5,30)
30    FORMAT('  NUMBER OF THE VARIABLE TO CHANGE 0=TO END -1 TO
     + REREAD LIST ')
      READ(5,31)I
31    FORMAT(I3)
      IF(I.EQ.0)GOTO40
      IF(I.LT.0)GOTO12
      WRITE(5,32)I,X(I)
32    FORMAT('  ',I3,' VARIABLE VALUE = ',F8.4,' NEW VALUE = ')
      READ(5,33)X(I)
33    FORMAT(G13.8)
      GOTO21
40    CONTINUE
      WRITE(5,1)
1     FORMAT('  WHAT IS THE FILE NAME FOR OUTPUT ')
      READ(5,2)(FILOUT(I),I=1,8)
2     FORMAT(8A2)
      TYPE 123, FILOUT
123   FORMAT(2X,8A4)
      OPEN(UNIT=2,NAME=FILOUT,FORM='UNFORMATTED',TYPE='NEW')
      WRITE(2)(STRING(I),I=1,15),N,(X(I),I=1,N)
      CLOSE(UNIT=2)
      END
      THIS SET OF SUBROUTINES IS FOR PLOTTING ON THE LA120
      SUBROUTINE PLT(Q,ISTR)
      BYTE ISTR,IMAT(100)
      COMMON /AREA/IMAT
      IQ=IFIX(Q)
      IF (IQ.LT.1)IQ=1
      IF (IQ.GT.100)IQ=100
      IMAT(IQ)=ISTR
      RETURN
      END

      BASIC LINE REFRESH SUB

      SUBROUTINE REFR
      BYTE IMAT(100)
      COMMON /AREA/IMAT
      DO 10 I=1,100
10    IMAT(I)=' '
      DO 20 I=1,10
      N=I*10
20    IMAT(N)='.'
      RETURN
      END

      EVERY 10 LINES REFRESH SUB

      SUBROUTINE REFR1
      BYTE IMAT(100)
      COMMON /AREA/IMAT
      DO 10 I=1,100
10    IMAT(I)='-'
      DO 20 I=1,10
      N=I*10
20    IMAT(N)='I'
      RETURN
      END
      PROGRAM OUTPUT
      DIMENSION FELNAM(6) [illegible] VX(10)
      BYTE FILE(16)
      BYTE OUTPUT(100) IST [illegible]
      BYTE AREA
      REAL K0,K1,K2 K3 K4,K5 K6 K7 K8 K9 [illegible] F1 [illegible] J1 J2 [illegible]
     1,INV KRV KRM K0
      REAL MSD(10),NX(10),MX(10) L(10)
      INTEGER NAMES(10)
      COMMON/AREA/OUTPUT
      EQUIVALENCE (IN VX(1)) (E VX(2)) (KR VX(3)) (S1 VX(4 [illegible]
     1,(J2 VX(6)) (Q1 VX(7)) (Q4 VX(8)) (Q6 VX(9)) (Q2 VX( [illegible]
      DATA WIDON/ [3W / WIDOFF/ [1W'/ HITON/ [3E / HITOFF/ [ [illegible]
      DATA L/10*1.0E37/
      DATA FILE/16*0/
      DATA NAMES/'IN  ' 'E  ' 'KR  ' 'S1  ' 'J1  ' 'J2  ','Q1  ' 'Q4  ' 'Q6  ' [illegible]
      DATA N/10*0 /
      FTI(A,B)=ABS(AINT(A/B)-A/B)
      WRITE(5 100)
100   FORMAT('  WHAT IS THE DATA FILE FOR THIS MODEL RUN ?
      READ(5,101)(FILE(I) I=1 16)
101   FORMAT(16A1)
      WRITE(5 99)
99    FORMAT('  HOW LONG TO RUN? ')
      READ(5 98)TIME
98    FORMAT(F6 0)
      OPEN(UNIT=1 NAME=FILE TYPE= OLD  FORM  UNFORMATTED )
      READ(1)E1 E2 E3 E4 E5 E6 E7 E8 E9 E10 E11 E12 E13 E14 E15
C     COEFFICIENTS ********************************************
     1NUM JD S A0 A1 A2 A3 V0 V1 V2 V3 P0 P1 P2 P3
     1D1,D2 D3 K K0 K1 K2 K3 K4 K5 K6 K7 K8 K9,NX(1) NX(2)
     1NX(3) NX(4) NX(5) NX(6) NX(7) NX(8) NX(9),NX(10) MX(1),MX(2)
     1MX(3) MX(4) MX(5) MX(6) MX(7) MX(8) MX(9),MX(10) XN
      CLOSE(UNIT=1)
      ESC=27
      N=XN
C     SET OUTPUT VECTOR AND FLAG **********************************
      WRITE(5,102)
102   FORMAT(' OUTPUT TO TERMINAL (0) OR PRINTER (1) )
      READ(5,103)IOFLAG
103   FORMAT(I1)
      IN=IOFLAG+1
      GOTO (1 2) IN
1     OPEN(UNIT=3 NAME= [illegible] )
      GOTO 3
2     WRITE(5 88)
88    FORMAT('  WHAT IS THE FILE OR DEVICE FOR OUTPUT? [illegible]
      READ(5 89)(FILNAM(I) I=1 6)
89    FORMAT(6A4)
      OPEN UNIT [illegible] NAME=FILNAM)
3     CONTINUE
```

```
      WRITE(3 107)E1 E2 E3 E4 E5 E6 E7 E8 E9,E10 E11 E12 E13 E14 E15
107   FORMAT(   ,15A4 //)
      WRITE(5 108)
108   FORMAT(     WHAT IS THE TIME INTERVAL DT ')
      READ(5 109)DT
109   FORMAT(G8 3)
      TYPE 20
20    FORMAT(     WHAT IS THE PLOTTING INTERVAL? ')
      ACCEPT 25,CP
25    FORMAT(G8 3)
      XDT=DT/CP
      CP=CP*10
C     DEFINE VALUES
C     DIFFERENT FOR EACH MODEL
C     CALCULATE COEFFICIENTS
C     DIFFERENT FOR EACH MODEL
C     START OF LOOP ****************************************************
      WRITE(3 130)ESC WIDON ESC,NITON
130   FORMAT('+  A1 A3,A1 A3)
      CALL REFR1
      GOTO 35
5     T=T+DT
      CALL REFR
      IF(PT1(T CP) LT DT)CALL REFR1
C     INPUT SINE WAVES
C     DIFFERENT FOR EACH MODEL
C     RATE EXPRESSIONS
C     DIFFERENT FOR EACH MODEL
C     STORAGE ACCUMULATIONS
C     DIFFERENT FOR EACH MODEL
C     CALCULATE STATS
      DO 30 I=1 N
      IF (VX(NX(I)) GT H(I)) H(I)=VX(NX(I))
      IF (VX(NX(I)) LT L(I)) L(I)=VX(NX(I))
      A(I)=A(I)+VX(NX(I))
      V(I)=V(I)+VX(NX(I))**2
30    CONTINUE
      IF(PT1(T CP) GE XDT)GOTO 1101
35    DO 40 I=1 N
      IST=I+87
      XC=VX(NX(I))*(100 /MX(I))
      CALL PLT(XC IST)
40    CONTINUE
      WRITE(3,110)(OUTPUT(I) I=1 100)
110   FORMAT(        1  100A1)
1101  IF(T LT TIME)GOTO 5
      WRITE(3 131)ESC WIDOFF ESC NUTOFF
131   FORMAT( +  A1 A3 A1 A3)
C     OUTPUT STATS
      T9=T/DT
      DO 50 I=1 N
      A(I)=A(I)/T9
      V(I)=ABS(V(I)-A(I)**2)
      S(I)=SQRT(V(I))
      MSQ(I)=SQRT(A(I)**2+D(I)**2)
13    CONTINUE
      WRITE(3,111)
111   FORMAT(// 5X,'---VARIABLE---+---MAXIMUM---+---MINIMUM---+---SCALE
     1---+')
      WRITE(3,112) (NAMES(NX(I)),H(I),L(I),MX(I),I=1,8)
112   FORMAT(5X,A10,5X,G10.4,5X,G10.4,5X,G10.4)
      WRITE(3,114)
114   FORMAT(/ 5X,'---VARIABLE---+---AVERAGE---+---VARIANCE---+---STD-DEV-
     1---+---MEANSQ---+')
      WRITE(3,113) (NAMES(NX(I)),A(I),V(I),S(I),MSQ(I),I=1,8)
113   FORMAT(5X,A10,5X,G10.4,5X,G10.4,5X,G10.4,5X,G10.4)
      WRITE(3,119)DT
119   FORMAT('  TIME STEP FOR THIS RUN = ',F6.4)
      WRITE(3,120)(FILE(I),I=1,16)
120   FORMAT('  DATA FILE DESIGNATION FOR THIS RUN ',16A1)
      END
      PROGRAM GPLOT
      BYTE FILE(16)
      REAL K0,K1,K2,K3,K4,K5,K6,K7,K8,K9,K10,K11,J0,J1,J2,KM,KR,N1,N2
     1,INV,KAV,KRM,K12,K13,K14,K15,K16,K17
      BYTE ABSC(80)
      BYTE ORD1(80),ORD2(80),ORD3(80),ORD4(80)
      BYTE MAX1(80),MAX2(80),MAX3(80),MAX4(80)
      BYTE ITIME1(80),ITIME2(80),ITIME3(80),ITIME4(80)
      BYTE ZRAD(80)
      WRITE(5,100)
100   FORMAT('  WHAT IS THE DATA FILE FOR THIS MODEL RUN ? ')
      ACCEPT 101, (FILE(I),I=1,16)
101   FORMAT(16A1)
      WRITE(5,99)
99    FORMAT('    HOW LONG TO RUN? ')
      READ(5,98)TIME
98    FORMAT(G8.3)
      OPEN(UNIT=1,NAME=FILE,TYPE='OLD',FORM='UNFORMATTED')
      READ(1)E1,E2,E3,E4,E5,E6,E7,E8,E9,E10,E11,E12,E13,E14,E15
C     COEFFICIENTS *********************************************
     1NUM,J0,J1,J2,E,KR,S,A0,A1,A2,A3,V0,V1,V2,V3,A0,A1,A2,A3,M1,M2,SA
     1SC,S,DOL,A,R,N0,R1,R2,R3,R4,R5,R6,R7,R8,R9,R10,R11,R12,R13,R14
     1R15,R16,R17,EM,KEN
      CLOSE(UNIT=1)
      WRITE(5,108)
108   FORMAT('    WHAT IS THE TIME INTERVAL DT ')
      READ(5,109)DT
109   FORMAT(G8.3)
      TYPE 20
20    FORMAT('      WHAT IS THE PLOTTING INTERVAL? ')
      ACCEPT 25,CP
25    FORMAT(G8.3)
C     DEFINE INITIAL VALUES
      IDT=0
      ICT=0
      T=0
C     CALCULATE COEFFICIENTS
C     DIFFERENT FOR EACH MODEL
C     GGPLOT DATA FOR MARSH TROPHIC CHAIN
      DATA ABSC/'T',' ','I',' ','M',' ','E',' ',' ','Y',' ','E','A','R','S',70*0/
      DATA ORD1/'D','O','C',[illegible]
     1 [illegible] 67*0/
      DATA ORD2/[illegible]
     1 [illegible] 64*0/
      DATA ORD3/[illegible]
     1 [illegible] 58*0/
      DATA ORD4/[illegible]
     1 [illegible] 64*0/
      DATA ITIME1/[illegible] 79*0/
      DATA ITIME2/[illegible] 79*0/
      DATA ITIMER/'1 [illegible] 5*
      DATA MAX1/ 5 [illegible] 0 ,7*
      DATA MAX2/ 5  7*0
      DATA MAX3/ 1  5  0  7*0/
      DATA MAX4/ 1' 5',0',0',7*0/
      DATA ZERO/ 0',7*0/
      GGPLOT SETUP
      CALL GGO0
      CALL GGINIT
      CALL GGERA
      CALL GGAXIS(0 0 767 479)
      CALL GGBOX(T 50 30 757 479)
      CALL GGBOX(T 50 140 757 250)
      CALL GGBOX(T 50 250 757,390)
      CALL GGTEXT(T 47 27 ZERO 1 0)
      CALL GGTEXT(T 25,140 MAX1 1,0)
      CALL GGTEXT(T 35,250 MAX2 1 0)
      CALL GGTEXT(T 20 390 MAX3 1 0)
      CALL GGTEXT(T 10,470 MAX4 1 0)
      IF (TIME EQ 1 ) GO TO 10
      IF (TIME EQ 10 ) GO TO 11
      IF (TIME EQ 100 ) GO TO 12
      IF (TIME EQ 1000 ) GO TO 13
10    CALL GGTEXT(T,747 27,ITIME1 1 0)
      GO TO 14
11    CALL GGTEXT(T,737 27 ITIME2,1 0)
      GO TO 14
12    CALL GGTEXT(T 732 27 ITIME3 1 0)
      GO TO 14
13    CALL GGTEXT(T 727 27 ITIME4 1 0)
14    CALL GGTEXT(T 350,20 ABSC 1 0)
      CALL GGTEXT(T,51 135 ORD1 1 0)
      CALL GGTEXT(T 51 250 ORD2 1 0)
      CALL GGTEXT(T 51 355 ORD3 1 0)
      CALL GGTEXT(T 51 467 ORD4,1,0)
      CALL GGRLT(T 45 85 0)
      CALL GGVEC(T 50 85)
      CALL GGRLT(T 45 105 0)
      CALL GGVEC(T 50 105)
      CALL GGRLT(T 45 305,0)
      CALL GGVEC(T 50,305)
      CALL GGRLT(T 45 415 0)
      CALL GGVEC(T 50 415)
      CALL GGRLT(T 40 25 0)
      CALL GGVEC(T 403 30)
      START LOOP ****************************************
9     CONTINUE
      INPUT SINE WAVES
      DIFFERENT FOR EACH MODEL
      RATE EXPRESSIONS
      DIFFERENT FOR EACH MODEL
      STORAGE ACCUMULATIONS
```

```
       DIFFERENT FOR EACH MODEL
       IF (ICT.NE.IOT) GO TO 1101
       IT=IT*707.)/ITIME*365.)+50
       OUTPUT VARIABLES FOR MARSH TROPHIC CHAIN MODEL
       CALL GGPLT(3,IT,IBOC,1)
       CALL GGPLT(4,IT,ISP,1)
       CALL GGPLT(5,IT,IB,1)
       CALL GGPLT(6,IT,IR,1)
       T=T+DT
       ICT=0
       IOT=CP/DT
       GOTO 1111
1101   T=T+DT
       ICT=ICT+1
1111   IF(T.LT.(TIME*365.))GOTO 5
       ACCEPT 1000,X
1000   FORMAT(G8.4)
       CALL GDOFF
       END
```

```
PROGRAM NBRCOM
NEW ZEALAND MARSH COMPETITION MODEL
DEFINE VALUES
IDT=0
ICT=0
T=0
CALCULATE COEFFICIENTS
K2=R2/(Q1*R0)
K3=R3/(Q2*R0)
K4=R4/(Q3*R0)
K5=R5/Q1
K6=R6/Q2
K7=R7/Q3
K0=R01/(Q1*R0)
K1=R1/((Q2+Q3)*R0)
OUTPUT DATA
INPUT SINE WAVES
CONTINUE
WC=A0*SIN(V0*T)
WA=A0*SIN(V0*((T+120)/365 ))
WB=A1*SIN(V1*T)
WD=A2*RAN(1)-(A2/2)
RATE EXPRESSIONS
R0=(W0+WA+WB+WD)/(1+K0*Q1+K1*(Q2+Q3))
D1=K2*Q1*R0
D2=K3*Q2*R0
D3=K4*Q3*R0
D4=K5*Q1
D5=K6*Q2
D6=K7*Q3
STORAGE ACCUMULATIONS
Q1=Q1+DT*(D1-D4)
Q2=Q2+DT*(D2-D5)
Q3=Q3+DT*(D3-D6)
IF (Q1 LT 1.0E-10) Q1=0
IF (Q2 LT 1.0E-10) Q2=0
IF (Q3 LT 1.0E-10) Q3=0
ID1=Q1*20.+270
ID2=Q2*20.+270
ID3=Q3*20.+270
ID4=D4*20.+30
ID5=D5*20.+30
ID6=D6*20.+30
IT=(T*TOT )/(TIME*365 )+50
IF (IT NE IT") GO TO 110
```

```
[illegible]
  3     18 PIECES OF DATA
  1950.00
  550.000
0.000000
0.600000
0.000000
0.000000
0.000000
  202.500
  150.000
  175.000
  3013.00
  2822.00
  3.42000
  1.82000
  1.85000
0.970000
0.875000
  1.99000
```

```
PROGRAM NZMARP
NEW ZEALAND MARSH MACROS [illegible] MODEL
DEFINE INITIAL VALUES
ICT=0
ICT=0
T=0.
CALCULATE COEFFICIENTS
K0=R0/(Q1*R)
K1=R1/(Q1*R)
K2=R2/Q2
K3=R3/Q3
K4=R4/((Q1-N3)*(E+KR))
K5=R5/(Q1*R)
K6=R6/(Q3*(E+KR))
K7=R7/Q2
K8=R8/Q2
K9=R9/(S*Q3)
K10=J1/(A1*KR)
K11=J2/(N2*KR)
CGPLOT DATA
CGPLOT SETUP
START LOOP ****************************************
CONTINUE
INPUT SINE WAVES
WC=A0*SIN(V0*T)
INV=A0*SIN(V0*((T+P0)/365.))
EV=A1*SIN(V1*((T+P1)/365.))
KRV=A2*SIN(V2*((T+P2)/365.))
SV=A3*SIN(V3*((T+P3)/365.))
IN=IDO+INV
R=IN/(1+K0*Q1)
E=EM+EV
KR=KRM+KRV
S1=S+SV
RATE EXPRESSIONS
J1=K10*(N1*KR)
J2=K11*(N2*KR)
D1=J1+K3*Q2+K9*S1*Q3
D4=K5*Q1*R
D7=K4*((N3-Q1)*(E+KR))
D2=K1*Q1*R
D5=K2*Q2
D8=K7*Q2
D3=J2+K8*Q2
D6=K9*S1*Q3+K6*Q3*(E+KR)
STORAGE ACCUMULATIONS
Q1=Q1+DT*(D1-D4+D7)
Q2=Q2+DT*(D2-D5-D8)
Q3=Q3+DT*(D3-D6)
IF (Q1 LT 1.0E-10) Q1=0.
IF (Q2 LT 1.0E-10) Q2=0.
```

```
      IF (Q3.LT.1.0E-7C) [illegible]
      IQ1=Q1*.11+30
      IQ2=Q2*.11+140
      IQ3=Q3*.11+250
      IIN=IN*.011+350
      IF (ICT.NE.IDT) GO TO 101
      IT=(T*707.)/(TIME*365.)+50
      CALL GGPLT(3,IT,IIN,1)
      CALL GGPLT(4,IT,IQ1,1)
      CALL GGPLT(5,IT,IQ2,1)
      CALL GGPLT(6,IT,IQ3,1)
      T=T+DT
      ICT=0
      IDT=CP/DT
      GOTO 1111
 101  T=T+DT
      ICT=ICT+1
   1  IF(T.LT.(TIME*365.))GOTO 5
      ACCEPT 1000,K
1000  FORMAT(G6.4)
      CALL GGOFF
      END
```

```
SZMARFN V8-1 21
FOR    77 PIP
 3450 00
0 234000
0 235000
 243000
 346000
 1 00000
 2250 00
 262000
 214000
0 000000
0 28300
 163 350
0 628300
0 28300
 120 000
 273 750
 212 000
0 070000
0 552000
0 551000
0 100000
0 264000
 524 000
 657 000
 563 000
 5067 00
 4 00000
 1 16000
0 211000
0 243000
0 727000
0 250000E-01
 2 11000
0 784000
0 5 5000
 540000
 450000
```

```
PROGRAM NZMARC
NEW ZEALAND MARSH TROPI[illegible]
DEFINE INITIAL VALUES
IBT=0
ICT=0
T=0
CALCULATE COEFFICIENTS
K0=R0/(SP*B*P*B)
K1=R1/(SP*B*P*B)
K2=R2/SP
K3=R3/SP
K4=R4/SC
K5=R5/(SC*P)
K6=R6/(SC*P)
K7=R7/(B*E)
K8=R8/P
K9=R9/(DOC*B*P*E)
K10=R10/(B*P*DOC*E)
K11=R11/(DOC*P*B*E)
K12=R12/(B*P)
K13=R13/(B*P)
K14=R14/SP
K15=R15/KR
K16=R16/(P*S)
K17=R17/SC
COPLOT DATA
START LOOP ******************************************************
CONTINUE
INPUT SINE WAVES
WC=A0*SIN(V0*T)
INV=A0*SIN(V0*((T+P0)/365 ))
EV=A1*SIN(V1*((T+P1)/365 ))
KRV=A2*SIN(V2*((T+P2)/365 ))
SV=A3*SIN(V3*((T+P3)/365 ))
IN=J0+INV
M=IR/(1+K8*SP*B*P)
E=EM+EV
KR=KRM+KRV
S1=S+SV
RATE EXPRESSIONS
D1=K1*SP*B*P*R
D2=K2*SP+K3*SP+K14*SP
D3=K3*SP+K5*SC*P
D4=K4*SC+K5*SC*P+K17*SC
D5=K1*MM+K4*SC+K10*B*P*DOC*E+K15*KR
D6=K9*DOC*B*P*E
D7=K11*DOC*B*P*E
D8=K7*B*E+K12*B*P
D9=K13*B*P
D10=K8*P+K16*P*S1
STORAGE ACCUMULATIONS
```

```
SP=SP+DT*(B1-B2)
 SC=SC+DT*(B3-B4)
DOC=DOC+DT*(B5-B6)
B=B+DT*(B7-B8)
P=P+DT*(B9-B10)
IF (SP.LT.1.0E-10) SP=0
IF (SC.LT.1.0E-10) SC=0
IF (DOC.LT.1.0E-10) DOC=0
IF (B.LT.1.0E-10) B=0.0
IF (P.LT.1.0E-10) P=0
IDOC=DOC*2.2+30
IB=B*22.+140
ISC=SC*.733+250
ISP=SP*.0733+360
```

```
NARUHU
 OB     KB PIE  2  P KATA
  3450 00
0 028000
0 000020
 29 1000
 348000
 1 4000
 2250 00
 10 0030
 214000
0 080000
 6 28300
 2293 30
 6 28300
 2293 30
 120 000
 105 000
 212 000
 105 000
0 070000
0 050000
 589 000
 5230 00
 1 30000
  8 5000
 27 7000
 577 000
 5192 00
 6 84600
 1 93000
 1 40000
 8 57000
 523 000
 532 900
 3 37000
 1 70000
 55 1000
 30 7700
 15 2700
 11 8000
 2 02000
  5500
 5 10000
0 056000
   7000
  0 3000
 4 7000
```

APPENDIX B
DEVELOPMENT OF A SALT MARSH COMPETITION MODEL

A competition model was developed for invading Spartina townsendii and the Juncus-Leptocarpus association which occupies the native marsh at the Kaituna River saltmarsh, Havelock, N Z. Figure B-1 shows that Spartina and the Juncus-Leptocarpus association are not intermixed throughout the marsh. Rather, there is a distinct boundary separating the flora. Any competition between Spartina and Juncus-Leptocarpus must be visualized as occurring along this boundary or as taking place in an unoccupied area which is open to colonization by both. For this model a hypothetical meter square is taken along the floral boundary. This area is considered to be occupied by an average biomass of the grasses based on the samples taken nearest to the actual boundary at Havelock, N Z.

Figure 38 shows a simple model for competition between Spartina and the Juncus-Leptocarpus association. The pathway and storage symbols given there may be used to write the following equations:

For a single energy source (without dotted lines on Figure 38)

(1) $Q_1 = k_2 Q_1 R_0 - k_3 Q_1$

(2) $Q_2 = k_4 Q_2 R_0 - k_5 Q_2$

Figure B-1 A map drawn from an aerial photograph of the *Spartina* and *Juncus-Leptocarpus* marsh at Havelock, N.Z., February 26, 1979. The floral boundary and the watershed areas of (A), Causeway Creek, (B) Marsh Creek, and (C), Fish Creek are as shown. Scale 122.7 m = 1 cm.

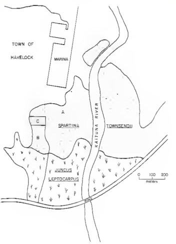
TOWN OF
HAVELOCK
MARINA
A
C
B
SPARTINA
TOWNSENDII
KAITUNA RIVER
JUNCUS
LEPTOCARPUS
ROAD
0 100 200
meters

(3) $Q_3 = k_6 Q_3 R_0 - k_7 Q_3$

(4) $R_0 = \frac{I}{(1 + k_0 Q_1 + k_1 (Q_2 + Q_3))}$

For a second energy source (dotted lines on Figure 38)

(1) $Q_1 = k_2 Q_1 R_0 R_1 - k_3 Q_1$

(2) $Q_2 = k_4 Q_2 R_0 R_1 - k_5 Q_2$

(3) $Q_3 = k_6 Q_3 R_0 R_1 - k_7 Q_3$

(4) $R_0 = \frac{1}{k_0 Q_1 R_1 + k_1 (Q_2 + Q_3) R_1}$

(5) $R_1 = \frac{I}{k_{00} Q_1 R_0 + k_{01} (Q_2 + Q_3) R_0}$

An estimate of the sunlight incident on the marsh in January 1982 was obtained from the average of 10 years of solar insolation data taken by the New Zealand Meteorological Service for Wellington and Nelson (see Table B-1) Weather at Havelock is usually similar to conditions at Nelson or Wellington and therefore the average of these two weather stations is used to estimate solar insolation for Havelock, I_0 for t_0 = January 19, 1982, is then assumed to be equal to the 10-year average of the January values in Table B-1 or 5,769 Cal/m^2-day

Biomass values for the three grasses were measured by harvest, January through April 1982, and these values are given in Table B-2

Table B-1. Solar insolation data for Havelock estimated as the average of Nelson and Wellington

	Langleys/Day											
Year	Jan	Feb	Mar	Apr	May	Jun.	Jul	Aug	Sep	Oct.	Nov	Dec
1979	596	461	301	237	139	124	137	181	283	400	493	597
1978	588	535	363	191	148	113	132	208	276	441	550	561
1977	504	492	374	261	165	111	122	169	283	419	526	548
1976	482	469	358	270	176	124	140	195	304	381	515	474
1975	576	455	344	275	169	135	153	179	337	432	510	561
1974	635	441	410	201	172	140	121	214	275	421	592	650
1973	594	547	353	244	161	126	148	196	325	454	498	624
1972	621	531	396	275	173	153	155	226	334	443	465	569
1971	564	494	419	282	162	127	157	208	340	419	544	588
1970	611	550	334	277	164	123	161	184	302	401	560	580
10-year mean	577	497	361	251	165	127	141	196	306	421	525	576

Table 8-2 Mean values with standard errors for live and dead biomass in vegetation of the Kaituna River marsh, Havelock, N.Z.

Location	Type	Jan 19 g/m^2 Mean ± S.E.	Feb 19 g/m^2 Mean ± S.E.	Mar 16 g/m^2 Mean ± S.E.
Spartina creekside	Live	1,090.0 ± 73.4	1,131.2 ± 70.8	1,147.6 ± 124.2
	Dead	420.4 ± 77.4	319.8 ± 57.4	347.6 ± 16.5
Spartina flats	Live	716.3 ± 40.3	953.3 ± 112.6	354.5 ± 120.0
	Dead	299.5 ± 24.1	197.0 ± 33.6	297.6 ± 42.7
Juncus	Live *Juncus*	517.9 ± 75.2	609.0 ± 25.3	409.5 ± 14.9
	Live *Leptocarpus*	613.6 ± 222.9	469.0 ± 106.2	544.1 ± 233.8
	Dead	446.2 ± 29.3	542.0 ± 57.3	540.1 ± 233.8
	Total live	1,131.5 ± 67.9	1,077.9 ± 96.0	953.6 ± 217.3
Leptocarpus	Live *Leptocarpus*	1,284.2 ± 76.3	1,189.2 ± 142.1	1,177.0 ± 107.0
	Live *Juncus*	86.7 ± 22.5	25.1 ± 25.1	43.6 ± 17.0
	Dead	776.1 ± 76.2	727.8 ± 149.3	819.1 ± 106.0
	Total live	1,370.9 ± 81.2	1,214.4 ± 127.1	1,220.6 ± 100.3

January values for Spartina from the flats and the Juncus and Leptocarpus from the Juncus area were used in order to bast approximate values for the vegetation at the floral boundary. Dry weight is converted to g C by multiplying by 0.58 g C/g dry wt. These values are then divided by 2 to put them on the basis of a half meter square. Spartina biomass, Q_1, is then 207.5 g C/m^2, Juncus biomass, Q_2, is 150 g C/m^2, and Leptocarpus biomass, Q_3, is 178 g C/m^2.

Graphs of vertical light penetration were used to estimate the albedo for each of the three grasses (see Figure B-2). Differences between the measured radiation above the grass and that measured 10 cm into the grass were assumed to be mainly due to the scattering and reflection of radiation since the amount of biomass present for absorption was small. Based on these readings Spartina has an albedo of about 10%, Juncus around 20%, and Leptocarpus about 15%. If these values are weighted by the biomass present in our hypothetical meter square the average albedo is 14.46% which gives a value of 834 Cal/m^2-day for R_0 in Figure 38. If we now assume that the incident sunlight used is partitioned between the grasses according to the amount of biomass present, Spartina receives about 2,013 Cal/m^2-day on pathway k_0 and Juncus-Leptocarpus takes 2,522 Cal/m^2-day on pathway k_1.

Grass primary production in the Kaituna River salt marsh was estimated from harvest measurement estimates of net primary production made in New Zealand and gas metabolism estimates of net primary production and respiration for Spartina and Juncus species in Florida. Studies on the photosynthetic metabolism of Spartina anglica in Great Britain indicate

Figure B-2 Light penetration graphs in salt marsh corrected for sun angle to the vertical, February 18, 1982 (a) *Spartina*, (b) *Spartina*, (c) *Leptocarpus*, (d) *Juncus*, (e) *Juncus*

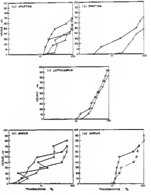
(a) SPARTINA
(b) SPARTINA
(c) LEPTOCARPUS
(d) JUNCUS
(e) JUNCUS
HEIGHT cm
TRANSMISSION %
0
10
20
30
40
50
60
70
80
90
100
10
100

that its photosynthetic metabolism is probably as great as C4 plants from more tropical climates (Smith et al., 1982). Thus, combining production data from Florida and New Zealand salt marshes may not be unreasonable. Respiration data from three years in Florida studies were used when July and August temperature readings were comparable to those measured in January in New Zealand (see Table 8-3). From harvest estimates net primary production for *Spartina* on the flats was 4.91 g C/m^2-day from January 19 to February 16, 1982 (see Table 8-2). The air temperature in New Zealand for January sample days was about 28°C. The average *Spartina* respiration for three summers in Table 8-3 was 1.93 g C/m^2-day at temperature 28.4°C. The estimated GPP for *Spartina* is 6.84 g C/m^2-day (GPP = NPP + R). Similarly, *Juncus* net primary production estimated by harvest was 1.89 g C/m^2-day. Average respiration for *Juncus* for the three Florida summers was 2.74 g C/m^2-day at an average temperature of 30.1°C. If we assume that *Juncus* and *Leptocarpus* have similar respirations and that *Juncus* metabolism in Florida is similar to its metabolism in New Zealand then 46% of the respiration is prorated to *Juncus* based on biomass estimates giving 1.25 g C/m^2-day in *Juncus* respiration and a GPP for *Juncus* of 3.14 g C/m^2-day. The complement of *Juncus* respiration is then *Leptocarpus* respiration or 1.49 g C/m^2-day. If *Leptocarpus* at the Havelock marsh is close to steady state at the time of January measurements then respiration and loss to dead must balance Gross Primary Production. The loss to dead from the *Juncus*-*Leptocarpus* complex was 1.99 g C/m^2-day from January to February 1983 (Table 8-2) and most of this loss was

Table 8-3. Gas metabolism data and concomitant conditions for Spartina and Juncus species of marshes at Crystal River, Florida

Date	# Samples	Air Temp °C	Insolation kcal/m^2-day	NPP g C/m^2-day	Respiration g C/m^2-day	GPP g C/m^2-day	Live Biomass g/m^2
8/03/73	2	28.3	3,500	6.30 ± 1.15	1.22 ± 0.31	7.52 ± 1.37	530 ± 35
7/16/77	2	26.1	2,038	2.50 ± 1.5	1.69 ± 0.20	4.19 ± 1.7	510 ± 32
7/01/78	4	30.8	2,407	2.82 ± 0.40	2.90 ± 0.11	5.72 ± 0.44	453 ± 47
Spartina average		28.4	2,648	3.87 ± 1.01	1.93 ± 0.21	5.81 ± 1.17	497 ± 38
7/28/73	2	28.3	3,500	4.52 ± 0.75	3.22 ± 0.46	7.74 ± 0.84	---
7/20/77	4	31.2	4,593	5.06 ± 0.44	1.73 ± 0.02	6.78 ± 0.46	941 ± 108
7/01/78	4	30.8	2,407	3.66 ± 0.52	3.28 ± 0.38	6.93 ± 0.89	1,230 ± 135
Juncus average		30.1	3,500	4.41 ± 0.57	2.74 ± 0.86	7.15 ± 0.73	1,086 ± 122

Source: Data from Young (1974), Odum and Caldwell (1978), and Caldwell and Odum (1978) contributed by *Leptocarpus*. If 75% of the standing dead is assumed to be *Leptocarpus*, then 1.49 g C/m^2-day was lost to dead by *Leptocarpus* giving 2.98 g C/m^2-day GPP for *Leptocarpus* (GPP = Respiration + Loss to dead). The remaining 0.50 g C/m^2-day is lost to dead by *Juncus* which is then given a GPP value of 3.64 g C/m^2-day. The Gross Primary Production for the *Juncus*-*Leptocarpus* association is then 5.62 g C/m^2-day which compares favorably with *Juncus* GPP measured in Florida of 7.15 g C/m^2-day at slightly higher temperature. One-half of the values given for pathway flows must be taken to get the numbers on Figure 38.

Values on the dotted pathways in Figure 38 were calculated based on a C:N requirement of 5.5:1 for marsh grass. Nitrogen was assumed to be the limiting growth factor for marsh grasses and therefore almost all of the available supply was utilized.

APPENDIX C
DEVELOPMENT OF A MINIMODEL FOR THE KAITUNA RIVER SALT MARSH

The Kaituna salt marsh minimodel consists of an invading *Spartina townsendii* storage, a labile nitrogen storage, and a sediment nitrogen storage. Solar energy and available nitrogen are assumed to be the major factors determining growth of *Spartina*. The model is driven by three forcing functions—sun, tide, and river flow. The evaluated model is shown in Figure 41 with the symbols for storages, sources, and pathway coefficients that are needed to write the following equations.

(1) $$Q_1 = k_{11}N_1K - k_5Q_1R + k_3Q_2 + k_9Q_3 + k_4(N_3 - Q_1)(E + K)$$

(2) $$Q_2 = k_1Q_1R - k_7Q_2 - k_2Q_2$$

(3) $$Q_3 = k_{12}N_2K + k_8Q_2 - k_9Q_3 - k_6Q_3(E + K)$$

(4) $$R = \frac{I}{(1 + k_0Q_1)}$$

(5) $$I = 3{,}450 + 2{,}250 \sin(2\pi\ f((T + 120)/365))$$

(6) $$E = 5.4\mathrm{x}10^5 + 2.02\mathrm{x}10^5 \sin(2\pi\ f((T + 10.5)/14))$$

(7) $$K = 4.5\mathrm{x}10^5 + 2.14\mathrm{x}10^5 \sin(2\pi\ f((T + 212)/365))$$

When the recycle aid is active in Figure 41, the k_9Q_3 terms in Equations (1) and (3) became k_9Q_3S. Some values in Figure 41 were estimated from measurements made on the marsh at Havelock, N.Z., during the summer of 1982. Other information came from New Zealand meteorological and hydrological reports and unpublished watershed studies of the Waitemata Harbour near Auckland, N.Z. Where data from New Zealand was unavailable an estimate for the unknown parameter was made based upon either the literature or our knowledge of marsh ecosystems. The following notes describe how the approximate values of flows shown in Figure 41 were determined. Solar input is the 10 yr mean of Nelson and Wellington stations measured by Epply pyrohelíometer taken as an estimate of Havelock insolation. The mean was 3,450 Cal/m^2-day and amplitude was 2,250 Cal/m^2-day. Kaituna River flow is estimated from the mean of a 5 yr flow record at station 59003 in the Kaituna River. Storm events > 10,000 cu ft/sec were removed and the flow is entered as a sine wave of wet and dry seasons. The mean flow was 4.5×10^5 m^3/day and the amplitude of seasonal pulse was 2.14×10^5 m^3/day. Tidal input is taken from the Nelson tide heights adjusted to Havelock and input as a fortnightly sine wave of exchange volume. The mean exchange was 5.4×10^5 m^3/day and fortnightly amplitude was 2.02×10^5 m^3/day.

Estimation of the C and N in sediment of the Kaituna estuary was performed under the following assumption. Kaituna River mud flats are assumed to be similar to mud flats of the Waitemata Harbour with regard to the content of ROC, readily oxidizable carbon. If the clay content of bare mud and Spartina mud at Havelock is similar then the difference in organic matter content on ignition is all organic matter and not bound water. The organic matter content of Spartina mud is then the average ROC value for Waitemata Harbour mud plus the percentage difference between Spartina and bare mud at Havelock. A C:N ratio of 5.5:1 for detritus and 10:1 for sediment organic matter was used. Average ROC from upper Waitemata Harbour data was 1.83% with an average TKN of 1,818 mg/kg. The C:N ratio for these sediments is ~10:1. These were intertidal samples taken away from the channel with clay contents of >50%.

There was 1.35% more organic matter in Spartina mud at Havelock than in bare mud as measured by loss on ignition. This material was assumed to have a C:N ratio of 5.5:1, 1.35% organic matter x 0.58 g C/g organic matter = 0.783% C ÷ 5.5 g C/g N = 0.142% N + 0.183% N = 0.325% N in Spartina sediment at Havelock and 2.61% C in the same sediment. Sediment N content for a m^2 by 0.1 m deep volume with density about 2.0 g/cc is then $2.0 x 10^5$ g sediment x 0.00325% N or about 650 g sediment N m^{-2}.

The organic nitrogen exported from the marsh in sediment and detritus was estimated from sediment exchange data taken at Havelock. Figure C-1 shows the diurnal record of particulate matter and ash content for Causeway Creek sediment station on March 16, 1983. Table C-1 gives the mean concentrations of suspended matter for ebb and flood tide. Ebb tide was observed to run for 7.33 hrs and flood tide for 5.67 hrs.

Assuming that ebb and flood tide have about the same mean velocity, more water leaves the marsh surface than is brought in by the

Figure C-1. Diurnal record of the particulate matter and ashed content of the particulate matter on inflowing and outflowing tide, March 16, 1982.

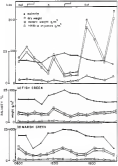
tide
out
in
out
salinity
dry weight
mineral weight g/m³
volatile organics g/m³
200
25
100
0
(a) FISH CREEK
SALINITY ‰
weight g/m³
(b) MARSH CREEK
0600
1200
1800
(c) CAUSEWAY CREEK
TIME, hrs

Table C-1 Mean tidal concentrations of suspended matter in three creeks of the Kaituna River marsh over a 15 hr sampling, March 16, 1982, neaptide

Creek Area and Location	Mean Flood g/m³ n = 5			Mean ebb g/m³ n = 5			Net g/m²* Total Transport		
	Seston	Mineral	Volatile	Seston	Mineral	Volatile	Seston	Mineral	Volatile
Causeway 777 350 m²	29.2±4.3	23.50±4.3	5.5±0.44	30.8±3.7	25.4±3.2	5.35±0.55	18.53 in 22.40 out	13.38 in 18.55 out	3.34 in 3.90 out
Marsh 68 821 m²	33.1±3.7	28.14±3.5	4.8±0.27	29.7±2.4	25.3±2.3	3.80±2.0	18.73 in 21.26 out	15.98 in 18.45 out	2.77 in 2.77 out
Fish 2 535 m²	61.3±11.0	52.80±11.0	10.0±1.20	122.8±34.0	105.9±31.8	18.20±2.80	34.60 in 89.00 out	29.40 in 77.90 out	5.70 in 11.83 out

*Assumed 25% more ebb water than flood if ebb is 7.33 hrs and flood is 5.57 hrs; mean values are ± one standard error tide, the additional water enters from the river flow. The average height of the tidal prism on March 16 was measured to be 0 566 meters The area of Causeway Creek is 277,350 m^2. Flood water volume into the marsh is approximately 277,350 m^2 x 0 566 m = 156,980 m^3 water input. Ebb tide carries 29% more water than flood tide so 202,504 m^3 water leave the marsh On flood tide, 23 5 g/m^3 x 156,980 m^3 - 3,689,030 277,350 m^2 = 13 30 g/m^2 On ebb tide, 25 4 g/m^3 x 202,504 m^3 = 5,143,601 g 277,350 m^2 = 18.56 g/m^2, 18.55 g/m^2 out - 13 30 g/m^2 in = 5.25 g/m^2 mineral matter exported. A similar calculation gives a net export of 0.57 g/m^2 organic matter. These results are given in Table C-2.

If sediment N is exported in proportion to mineral matter then 5.25 g/m^2 exported x 0.00325% N in sediment = 0 017 g N/m^2 exported. If 0 57 g/m^2 x 0.58 g C/g = 0 331 g C exported. If C N ratio is 10 1 then 0.17 g C/m^2 of this organic matter is from the sediment Then 0 161 g C exported has the Spartina C N ratio of 5 6 1 or 0 028 g N/m^2 + 0.017 g N/m^2 = 0 046 g N/m^2 exported on March 16, 1982, from the Havelock marsh These figures are per tide so ~0 092 g N/m^2 is exported per day On January 19 there was only 60% of March 16's water on the marsh, so N loss was lower. Flow J_6 in Figure 41 is tidal and should be at least doubled to account for daily loss A loss of 0 104 g N/m^2-day would balance the sediment N tank and not be unreasonable Flow J_6 as simulated is somewhat too low.

Inorganic nitrogen exchange through mixing was evaluated as follows Nitrogen concentration in the river and estuary were assumed

Table C-2. Estimate of net suspended matter, erosion, and sedimentation at Kaituna River marsh, March 16, 1982

		Erosion (-) or Sedimentation (+) g/m^2 per tide		
Location	Area	Seston	Mineral	Volatile
Causeway	277,360	-5.96	-5.25	-0.57
Marsh	66,871	-2.52	-2.54	0.00
Fish*	2,535	-54.40	-47.90	-6.13

*Estimate of average height of tide prism taken from 76 measures over this area at high tide for March 16, 1982 = 0.566 meters to be similar to average values recorded in the Lucas Creek and Lucas estuary of the Waitamata Harbour. The watersheds of both areas have a similar land use pattern, that is about 20% bush and 80% pasture. The average river content of N was 0.552 g N/m^3 and 0.100 g N/m^3 was the average estuarine content of N. Average Kaituna River discharge = 4.6x10^5 m^3/day. Marsh area is 817,068 m^2. On January 19 river discharge was 3.459x10^5 m^3 and tidal exchange was 3.38x10^5 m^3. Total ebb flow was 6.838x10^5 m^3. 0.552 g N/m^3 x 0.50 river water = 0.276 g N/m^3 entered from the river; 0.100 g N/m^3 x 0.50 tide water - 0.050 g N/m^3 entered from the sound; 0.326 g N/m^3 is the concentration N on the marsh.

Storage Q_1 was estimated at high water or 1.0 m on January 19 to be equal; 0.276 g N/m^2 present on the marsh minus 0.0414 g N/m^2 returning from estuary = 0.236 g N/m^2-day exported. Flow J_4 in Figure 41 is 0.233 g N/m^2-day. On January 19 river input was 0.552 g N/m^3 x 3.459 x 10^5 m^3 = 1.909x10^5 g N ÷ 817,068 m^2 = 0.234 g N/m^2-day import from river is flow J_{11} in Figure 41. Similarly, flow J_{12} is 0.235 g N/m^2-day which is the inflow or organic nitrogen assumed to go to the sediments.

The standing stock of live Spartina is seen from Table 8-2 to be 903 g dry wt/m^2 for January 19, 1983, 903 g/m^2 x 0.58 g C/g = 524 g C/m^2 is the storage Q_2 of Spartina in Figure 41. The net production of Spartina on the marsh from January-February 1982 was 2.88 g C/m^2-day. See Table 8-2. On the average respiration was 40% of net production at the Crystal River control site for the summer of 1980

(Odum and Caldwell, 1980). An estimate of *Spartina* respiration of 1.16 g C/m^2-day may be reasonable for flow J_2. J_3 = 0.211 g N/m^2-day follows directly if C:N = 5.5:1 for *Spartina*. A minimum estimate for GPP, J_1 is then 4.0 g N/m^2-day (NP + RESP). The input from live to dead *Spartina*, flow J_7 was 2.11 g C/m^2-day from January-February 1982 (Table 8-2) and so flow J_8 follows as 0.384 g N/m^2-day. A better estimate of net production would include the loss to dead in net production, 4.99 g C/m^2-day + respiration 2.0 g C/m^2-day = gross primary production, 7.0 g C/m^2-day. Both these numbers are within the range of values measured for *Spartina* in the summer over 5 years of sampling at Crystal River, Florida.

The uptake of inorganic N by *Spartina* is then 4.0 g C/m^2-day 5.5 g N/g C = 0.727 g N/m^2-day for flow J_5 in Figure 41. Solar insolation for January 19 was 5,630 Cal/m^2-day from 10 yr average already given. The albedo for *Spartina* has been measured at about 10%. Thus, the value of R is 563 Cal/m^2-day. Hopkinson and Day (1977) estimated the remineralization of nitrogen by microbes and macrofauna to be about 0.289 g N/m^2-day. This value was used as a first approximation to flow J_9. The actual value used for J_9 was 0.515 g N/m^2-day which was set to balance the N requirements of *Spartina* and export on labile N supplies. The nature of the recycle aid is unspecified and is simply entered as a sine wave of mean 1.0 and amplitude 0.5.

Several ratios of output to input parameters were used to evaluate the frequency response of the salt marsh minimodel at the system level as well as at the component level. One parameter used to show the amount of power captured by the system is given as J_{10} in Figure 41, R is the energy remaining which can be used and it is the complement of J_{10}. A second parameter of interest is the total power circulating on all the pathways within the system. This parameter is abbreviated J_{circ} and equals the sum of pathway flows J_1, J_2, J_7, J_5, and J_5 expressed in equivalent units. The power produced by this model is simply the flow J_1 and power used is J_2. The power input to the model or J_{in} is the sum of the powers on J_7, J_{11}, and J_{12} in equivalent units. The power exported is J_{ex} and is calculated as the sum of J_4 and J_6 in Figure 41.

Output to input ratios for the individual components are simply taken as the sum of the power in outflows of the storage to the sum of the inflows to the storage. For example the outflows from the labile nitrogen tank are J_5 and J_4, the inflows to this tank are J_{11}, J_9, and J_3 so the output-input ratio evaluated is $(J_5 + J_4)/(J_{11} + J_9 + J_3) = Q_{out}/Q_{in}$.

Table C-3 Total power, mean power, and variant power for all pathways in the salt marsh minimodel in Figure 41 when the solar input frequency is variable The input frequency of tide is 26 cycles per year, river input is 1 cycle per year

Input Frequency Solar	E	J_{10}	J_{11}	J_{12}	J_1	J_2	J_3	J_4	J_5	J_6	J_7	J_8	J_9	I
							Total Power on Pathways							
10,000.00	321.2	3.490	0.323	0.324	2.762	0.003	0.1310	0.534	0.502	0.0580	1.869	0.3090	0.5490	3.818
1,000.00	313.6	3.487	0.321	0.322	2.752	0.899	0.1300	0.523	0.800	0.0500	1.635	0.2980	0.8410	3.789
100.00	307.5	3.424	0.321	0.322	2.703	0.880	0.1200	0.550	0.491	0.0590	1.619	0.2940	0.5800	3.799
10.00	412.0	3.395	0.321	0.322	2.880	0.003	0.1290	0.500	0.487	0.0800	1.607	0.2880	0.5370	3.798
1.00	413.2	3.402	0.321	0.322	2.800	0.800	0.1290	0.562	0.480	0.0500	1.618	0.2940	0.5380	3.791
0.10	384.0	3.440	0.321	0.322	2.719	0.873	0.1410	0.571	0.484	0.0570	1.770	0.3220	0.5630	3.790
0.01	320.0	3.478	0.321	0.323	2.713	0.974	0.1410	0.540	0.497	0.0520	1.773	0.3230	0.5620	3.802
							Mean Power on Pathways							
10,000.00	292.0	3.183	0.307	0.309	2.520	0.001	0.1310	-0.527	0.456	0.0480	1.657	0.3020	0.5480	3.484
1,000.00	288.8	3.163	0.306	0.306	2.497	0.100	0.1360	0.521	0.454	0.0480	1.833	0.2970	0.5400	3.449
100.00	325.2	3.124	0.374	0.308	2.468	0.007	0.1290	-0.523	0.448	0.0490	1.614	0.2840	0.5280	3.449
10.00	342.9	3.100	0.304	0.306	2.452	0.002	0.1280	-0.624	0.448	0.0490	1.609	0.2920	0.5370	3.448
1.00	337.9	3.111	0.304	0.305	2.456	0.878	0.1270	-0.522	0.446	0.0480	1.587	0.2910	0.5380	3.448
0.10	312.0	3.130	0.304	0.306	2.477	0.893	0.8300	0.546	0.459	0.0510	1.824	0.2950	0.5800	3.450
0.01	293.0	3.180	0.305	0.308	2.494	0.880	0.1290	-0.529	0.453	0.0500	1.612	0.2830	0.5490	3.453
							Variant Power on Pathways							
10,000.00	29.1	365	0.015	0.015	0.242	0.003	0.0007	0.007	0.046	0.0000	0.012	0.0030	0.0030	335
1,000.00	27.6	324	0.017	0.017	0.255	0.001	0.0002	0.032	0.047	0.0000	0.002	0.0003	0.0002	350
100.00	57.3	300	0.017	0.017	0.227	0.001	0.0002	0.038	0.043	0.0011	0.002	0.0004	0.0001	350
10.00	63.8	288	0.017	0.017	0.228	0.001	0.0001	0.048	0.042	0.0011	0.002	0.0004	0.0002	348
1.00	55.3	281	0.017	0.017	0.230	0.011	0.0020	0.040	0.042	0.0011	0.019	0.0040	0.0001	348
0.10	52.8	302	0.017	0.017	0.229	0.080	0.0116	0.070	0.043	0.0012	0.148	0.0270	0.0030	349
0.01	75.0	318	0.017	0.017	0.249	0.088	0.0130	0.517	0.045	0.0020	0.181	0.0290	0.0130	349

Table C-4. Total power, mean power, and variant power for all pathways in the salt marsh minimodel in Figure 41 when the tidal input frequency is variable. The input frequency of both river and sun are 1 cycle per year

Input Frequency Tide	S	J_{10}	J_{11}	J_{12}	J_1	J_2	J_3	J_4	J_5	J_6	J_7	J_8	J_9	I
						Total Power on Pathways								
1 000.00	404.9	3.400	0.371	0.322	2.684	0.080	0.126	0.565	0.480	0.050	1.615	0.364	0.530	3.350
100.00	403.0	3.407	0.321	0.322	2.685	0.080	0.129	0.564	0.480	0.051	1.616	0.294	0.536	3.380
10.00	403.2	3.402	0.321	0.332	2.686	0.080	0.129	0.561	0.480	0.050	1.616	0.294	0.536	3.390
1.00	381.6	3.421	0.331	0.322	2.700	0.093	0.126	0.563	0.491	0.050	1.633	0.295	0.533	3.390
0.10	404.1	3.403	0.331	0.322	2.685	0.080	0.129	0.561	0.480	0.049	1.616	0.294	0.535	3.350
0.01	400.0	3.408	0.321	0.232	3.680	0.083	0.128	0.580	0.489	0.080	1.003	0.292	0.545	3.081
						Mean Power on Pathways								
1 000.00	340.1	3.100	0.304	0.306	2.454	0.087	0.123	0.522	0.440	0.049	1.595	0.290	0.536	3.449
100.00	330.5	3.110	0.304	0.306	2.455	0.070	0.123	0.532	0.445	0.049	1.566	0.291	0.530	3.449
10.00	337.9	3.110	0.304	0.305	2.456	0.073	0.123	0.522	0.445	0.049	1.593	0.291	0.536	3.446
1.00	326.0	3.133	0.304	0.305	2.465	0.081	0.123	0.531	0.440	0.048	1.603	0.293	0.533	3.449
0.10	336.4	3.110	0.304	0.306	2.455	0.070	0.127	-0.521	0.445	0.048	1.567	0.291	0.535	3.449
0.01	335.3	3.110	0.305	0.298	2.461	0.074	0.123	-0.529	0.447	0.049	1.500	0.206	0.545	3.453
						Variant Power on Pathways								
1 000.00	84.0	291	0.017	0.013	0.230	0.011	0.002	0.043	0.043	0.001	0.019	0.004	0.000	349
100.00	65.1	291	0.013	0.013	0.230	0.011	0.003	0.047	0.043	0.001	0.030	0.004	0.000	349
10.00	65.3	291	0.013	0.042	0.230	0.011	0.002	0.048	0.042	0.001	0.019	0.004	0.000	348
1.00	55.6	298	0.013	0.012	0.235	0.011	0.002	0.041	0.042	0.002	0.020	0.004	0.000	349
0.10	65.3	292	0.013	0.012	0.230	0.011	0.002	0.040	0.042	0.001	0.016	0.008	0.000	349
0.01	84.9	290	0.013	0.012	0.226	0.010	0.001	0.039	0.042	0.001	0.018	0.003	0.000	340

Table C-5. Total power, mean power, and variant power for all pathways in the salt marsh minimodel in Figure 41 when the river input frequency is variable. The input frequency of sun is 1 cycle per year, input frequency of tide is 26 per year

Input Frequency River	R	J_{10}	J_{11}	J_{12}	J_1	J_2	J_3	J_4	J_5	J_6	J_7	J_8	J_9	T
						Total Power on Pathways								
1 000.00	402.5	3.403	0.321	0.322	2.608	0.088	0.129	0.565	0.488	0.050	1.610	0.294	0.530	3.790
100.00	408.5	3.398	0.321	0.322	2.603	0.088	0.129	0.567	0.488	0.050	1.615	0.294	0.530	3.789
10.00	415.6	3.397	0.321	0.322	2.601	0.087	0.129	0.582	0.487	0.053	1.614	0.294	0.530	3.790
1.00	483.2	3.402	0.321	0.322	2.608	0.088	0.129	0.582	0.488	0.050	1.616	0.294	0.530	3.790
0.10	410.3	3.399	0.321	0.322	2.603	0.088	0.129	0.583	0.488	0.052	1.616	0.294	0.551	3.780
0.01	402.8	3.380	0.321	0.322	2.598	0.087	0.127	0.592	0.488	0.053	1.605	0.291	0.550	3.801
						Mean Power on Pathways								
1 000.00	337.4	3.112	0.304	0.306	2.456	0.078	0.127	0.523	0.447	0.049	1.597	0.291	0.530	3.449
100.00	340.5	3.108	0.304	0.306	2.454	0.077	0.127	0.523	0.445	0.049	1.595	0.290	0.530	3.449
10.00	301.7	3.107	0.304	0.306	2.453	0.077	0.127	0.523	0.449	0.049	1.595	0.29	0.531	3.449
1.00	337.9	3.111	0.304	0.306	2.456	0.078	0.127	0.522	0.448	0.049	1.597	0.291	0.530	3.449
0.10	330.9	3.103	0.304	0.306	2.454	0.078	0.127	0.535	0.446	0.050	1.596	0.291	0.550	3.449
0.01	358.3	3.055	0.305	0.306	2.443	0.067	0.126	0.529	0.444	0.050	1.579	0.287	0.542	3.453
						Variant Power on Pathways								
1 000.00	95.4	.291	0.017	0.017	0.230	0.011	0.002	0.042	0.042	0.001	0.019	0.004	0.000	.349
100.00	88.0	.288	0.017	0.017	0.229	0.011	0.000	0.043	0.042	0.001	0.019	0.004	0.000	.349
10.00	69.5	.288	0.017	0.017	0.228	0.011	0.002	0.044	0.042	0.001	0.019	0.004	0.006	.349
1.00	85.3	.291	0.017	0.012	0.230	0.011	0.002	0.040	0.042	0.001	0.019	0.000	0.000	.349
0.10	70.5	.290	0.017	0.012	0.229	0.011	0.000	0.040	0.042	0.002	0.020	0.004	0.002	.349
0.01	84.3	.285	0.017	0.017	0.225	0.010	0.001	0.063	0.041	0.003	0.017	0.003	0.008	.349

APPENDIX D
THE DEVELOPMENT OF A SALT MARSH TROPHIC CHAIN MODEL

A model of a salt marsh trophic chain was developed based on observation of the Kaituna River salt marsh at Havelock, New Zealand Supplementary information from salt marsh studies at Sapelo Island (Pomeroy and Wiegert, 1981) and from the United Kingdom (Newell, R C , 1985) were incorporated in the model The evaluated model given in Figure 50(a) shows a chain beginning with Spartina townsendii which contributes both dissolved organic carbon and detritus to storages in the system Bacteria exploit the reservoir of DOC and in turn they are fed upon by the snail Potamopyrgus which turns over large quantities of sediment in order to strip it of bacteria The model is driven by four forcing functions—sun, temperature, river DOC, and predator harvest of Potamopyrgus Each pathway storage and source in Figure 50(a) is given a symbol so that the following equations for the model may be written directly

(1) $SP = k_1*SP*P*B*R - k_2*SP - k_3*SP - k_{14}*SP$

(2) $SC = k_3*SP - k_4*SC - k_5*SC*P + k_6*SC*P - k_{17}*SC$

(3) $DOC = k_{14}*SP + k_{15}*R + k_4*SC - k_9*DOC*B*P*E + k_{10}*DOC*B*P*E$

(4) $B = k_{11}*DOC*B*P*E - k_7*B - k_{12}*B*P$

(5) $P = k_{13}*B*P - k_8*P - k_{18}*S*P$

(6) $R = I/(1 + k_0*SP*B*P)$

For the model given in Figure 50(b) the first term in Equation (5) becomes $k_{13}*B*P*S$, the third term in Equation (4) is $k_{12}*B*P*S$, the third and fourth terms in Equation (2) become $k_5*SC*P*S + k_6*SC*P*S$ For the model version in Figure 50(c) all secondary feedbacks are removed and the equations which are altered become

(1) $SP = k_1*SP - k_2*SP - k_3*SP - k_{14}*SP$

(2) $SC = k_3*SP - k_4*SC - k_5*SC + k_6SC - k_{17}*SC$

(3) $DOC = k_{14}*SP + k_{15}*K + k_4*SC - k_9*DOC*B*E + k_{10}*DOC*B*E$

(4) $B = k_{11}*DOC*B*E - k_7*B - k_{12}*B*P$

(6) $R = I/(1 + k_0*SP)$

Evaluation of the Trophic Chain Model

The sunlight incident upon the marsh was estimated as previously described in Appendix B and C. The albedo of Spartina was estimated by the method stated in B and found to be about 10% Therefore, of the 5,769 Cal/m^2-day, I, incident on the marsh about 5,192 Cal/m^2-day, R_0, were captured by the Spartina leaving 577 Cal/m^2-day, R, remaining For the subsequent pathway evaluation all the k_i values in Figure 50(a) are given as J_i values, indicating that flows are given instead of coefficients of transfer.

The gross primary production and respiration of the Spartina marsh were estimated in Appendix 9 and these values are used here as well. The GPP of Spartina flow J_1 is taken as 6.84 g C/m^2-day. The Spartina respiration J_2 as in Appendix B is 1.93 g C/m^2-day leaving 4.91 g C/m^2-day net production. Field measurements for January-February 1982 gave a figure of 2.12 g C/m^2-day loss from standing dead. Some of this loss is to DOC and some is to sediment carbon. Gallagher and Pfeiffer (1977) found that dead Spartina exuded about 200 μg C/g dry weight · hours submerged and that live Spartina exuded about half this amount. Therefore,

200 μg C/g dry wt · hr submerged x 299 g dry wt/m^2

x 12 hrs submerged per day = 0.718 g C/m^2-day

100 μg C/g dry wt · hr submerged x 716 g dry wt/m^2

x 12 hrs submerged per day = 0.859 g C/m^2-day

0.718 g C/m^2-day exuded by dead + 0.859 g C/m^2-day exuded

by live = 1.58 g C/m^2-day DOC exuded by Spartina

is flow J_{14} in Figure 50(a)

2.12 g C/m^2-day loss from dead - 0.718 g C/m^2-day exuded DOC

= 1.4 g C/m^2-day carbon input to the sediment, flow J_3

The biomass of *Spartina*, storage SP, includes both live and standing dead measured in January 1982 as 589 g C/m^2 on the flats. Sediment carbon, storage SC, was estimated as in Appendix C and was taken to be 5,230 g C/m^2 for the top 10 cm of sediment. Information for the salt marsh aerobic bacteria was taken from work done at Sapelo Island, Georgia. The bacteria biomass, B, in the upper 1 cm of a tall *Spartina* marsh was about 1.3 g C/m^2 in February 1974 (Christian et al., 1981). The DOC available as a substrate for such bacteria in the Duplin River, Georgia, for July 1972 was about 7 mg C/l = 7 g/m^3 x 1.5 m water at high tide = 10.5 g/m^2 is taken as the value for DOC in Figure 50.

Christian and Hall (1978) have investigated the organic carbon uptake rates for Sapelo Island marsh bacteria. If all the DOC is potentially bacterial substrate then 5.47 hr, the mean turnover time with respect to substrate, can be used to estimate and uptake of 1.28 mg C/l • hr. For the whole water column of 1.5 m this gives 1.92 g C/m^2-hr and uptake for 24 hrs is 46.1 g C/m^2, flow J_9 in Figure 50(a). If we assume that bacterial assimilation is 33% then 15.33 g C/m^2-day are assimilated, flow J_{11}, of which 22% is remineralized according to Christian and Hall (1978) giving 3.37 g C/m^2-day bacterial respiration, flow J_7. Assuming that most of the net production is transferred to the next trophic level, 11.5 g C/m^2-day are taken by *Potamopyrgus* as flow J_{12}. The remainder of DOC not used is returned to the DOC pool, a flow of 30.77 g C/m^2-day as J_{10}.

The biomass of *Potamopyrgus* was measured in January 1982 in Havelock, N.Z., to be 77.7 g C/m^2, storage P (see Table D-1). The respiration of *Littorina* from the Sapelo marshes of Georgia was

Table D-1. Biomass of _Potamopyrgus_ in _Spartina_ marsh

Number per m^2	Ash Free Dry Weight g/m^2
41,320	155.5
71,910	249.9
25,060	51.2
56,890	132.3
55,550	180.0
22,261	35.4

calculated by Mishina and Odum (1963) from data on Zn^{65} excretion for several sizes of snails and from Smalley's (1968) data on respiration of large (15-20 mm) *Littorina*. Smalley gives 0.55 ml O_2/g for large snails. The respiration rate for small snails was estimated to be 0.77 ml O_2/g times 1.429 mg O_2/ml = 1.107 mg O_2/g + 0.58 g C/g dry wt x 0.5 mg C/mg O_2 = 0.955 mg C/g C·hr x 77.7 g C/m^2 = 74.2 mg C/hr x 24 hrs ÷ 1,000 mg/g = 1.789 g C/m^2-day respiration of *Potamopyrgus* or flow J_8. *Potamopyrgus* was assigned an assimilation efficiency of 15% which gave 2.02 g C/m^2-day for flow J_{13}. The snail population is assumed to be in steady state so 0.24 g C/m^2-day or more may be lost through predation flow J_{16}. Turnover of sediment carbon by *Potamopyrgus* is assumed to be 100% of the upper centimeter per day or 5.23 g C/m^2-day. Assuming 12 g C/m^3 is the concentration of DOC in the Kaituna River, 5.18 g C/m^2-day enter the marsh as flow J_{15}.

The DOC tank requires a value of 8.57 g C/m^2-day input from sediment carbon in order to balance. This leaves a net increase of 2.73 g C/m^2-day which is assumed to be lost or buried in deeper layers.

The nutritional relationship assumed to exist between the small snail *Potamopyrgus* and bacteria in the marsh sediment was based on the work done by R. C. Newell (1965) on a similar small snail *Hydrobia ulvae* on the muddy shores of the Thames estuary. Both sediment and bacteria are assumed to be taken by the deposit feeding snail and then returned to the sediment in the form of pseudofeces, as Newell observed for *Hydrobia*. This model had a tendency to be somewhat unstable in the long run but it could be balanced by increasing the predation pressure on Potamopyrgus. In nature this pressure is probably supplied by such birds as ducks and such fish as flounder which consume the similar species Hydrobia in Europe (Fish and Fish, 1974, and Anderson, 1971). Tables D-2 and D-3 show that both these animals are a part of the marsh ecosystem.

Input and Output Parameters Used for Analysis of the Trophic Chain Model

The system output-input parameters used to evaluate the frequency response of the salt marsh trophic chain model are given using the J_i's for the k_i's in Figure 50(a).

(1) $$J_{circ} = J_1 + J_{14} + J_3 + J_4 + J_5 + J_6 + J_9 + J_{10} + J_{11} + J_{12} + J_{13}$$

(2) $$J_{produced} = J_1 + J_{11} + J_{13}$$

(3) $$J_{used} = J_2 + J_7 + J_8$$

(4) $$J_{in} = J_1 + J_{15} + E_c$$

(5) $$J_{out} = J_{16} + J_{17} + J_2 + J_7 + J_8$$

In addition, I is the power available to the model and R is the power remaining for use by the system. In determining the output-input ratios for variable power the variation input by temperature, E_c in Equation (4) was figured into the total variation entering the model. This was

Table B-2 Fish collected from a blocked tidal creek in Havelock, N.Z. Drainage area = 2535 m^2 (see Figure B-1), February 17, 1982

Fish Species	# Collected	Total Wet Wt. gms	Gms of Species per m^2
Retropinna retropinna (smelt)	70	329.0	0.1300
Rhombosolea retiaria (black flounder)	4	2.8	0.0011
Galaxias maculatus (Inanga, whitebait)	14	65.6	0.0260
Aldrichetta forsteri (yellow eyed mullet)	3	141.0	0.0560
Gobiomorphus gobiodes (giant bully)	8	59.2	0.0230
All fish	99	597.6	0.2360

Table D-3 Exploratory bird counts in Kaituna River marsh and mudflat, 11-12 a.m., February 19, 1982

Area	Area ha	Species	Birds per ha
Spartina east of river	24.5	Gallinules	0.290
		Ducks	0.650
		Herons	0.045
		Harrier	0.021
		Gulls and terns	0.004
			1.000
Spartina west of river	5.7	Gallinules	0.880
		Ducks	0.170
		Gulls and terns	0.140
			1.190
Mud area north of marsh		Ducks	0.910
		Herons	0.048
		Gulls and terns	0.190
			1.580

Note: Based on fraction of time over area divided by area done by calculating the variability introduced at the temperature interaction in equivalent units as if there was a direct proportion between the amplitude of temperature variation and the amplitude of the carbon signal generated at the interaction. Since this is not a real flow of material it was not added into the total mean square power input to the system which comes only from the sun and river forcing functions.

The push-pull type of interaction employed to simulate temperature action was first used by Eyring and Eyring (1963) and adapted for use in energy language models by Kemp (1977). The interaction includes both a positive and negative effect of temperature on a storage which represents an increase in anabolic as well as catabolic processes brought about by temperature.

Table 0-4 The total power on pathways and sums of pathways in the trophic chain models in Figure 50(a), (b), and (c)

Input Frequencies Sun, Temperature, River	J_{in}	J_{circ}	R	Harvest J_{19}	Net Sediment C Circulating In $J_3+(J_5+J_5)$	OOC in $J_{15}+J_{14}+J_4$	Sediment Loss J_{17}	Sediment C Circulating in J_5	OOC Uptake J_9
(A) Sun Varies									
1,000, 1.0, 1.0	11.590	1,257.0	398.4	0.557	11.670	17.08	2.757	556.3	50.73
365, 1.0, 1.0	11.590	1,258.0	398.3	0.557	12.170	17.68	2.758	556.3	50.73
100, 1.0, 1.0	11.590	1,259.0	398.1	0.558	11.670	17.09	2.760	557.2	50.75
10, 1.0, 1.0	11.590	1,231.0	399.2	0.556	11.670	17.06	2.749	554.0	50.64
1.0, 1.0, 1.0	11.590	1,150.0	396.9	0.537	10.780	16.61	2.602	514.9	49.13
0.1, 1.0, 1.0	11.710	1,627.0	333.9	0.718	14.220	18.76	2.239	693.4	55.16
0.01, 1.0, 1.0	11.380	467.3	857.5	0.381	4.727	12.09	1.153	187.7	33.72
(B) Temperature Varies									
1.0, 1,000, 1.0	11.580	1,119.0	412.8	0.528	10.390	16.44	2.550	487.6	51.51
1.0, 365, 1.0	9.728	1,426.0	2,671.0	0.309	11.210	16.29	2.707	561.7	121.70
1.0, 100, 1.0	10.360	1,394.0	1,937.0	0.398	11.400	16.60	2.736	563.4	105.10
1.0, 10, 1.0	11.690	1,095.0	337.1	0.524	10.180	16.35	2.521	479.0	48.43
1.0, 1.0, 1.0	11.580	1,150.0	396.9	0.537	10.780	16.61	2.606	514.9	49.13
1.0, 0.1, 1.0	11.660	906.3	427.4	0.430	8.570	15.25	2.174	390.4	44.92
1.0, 0.01, 1.0	11.170	546.1	718.7	0.314	5.372	12.19	1.245	226.8	33.87

Table D-4--Continued

Input Frequencies Sun, Temperature, River	J_{1n}	J_{circ}	R	Harvest J_{16}	Net Sediment C Circulating In $J_3 + (J_6 + J_5)$	ODC In $J_{15} + J_{14} + J_4$	Sediment Loss J_{17}	Sediment C Circulating in J_5	ODC Uptake J_9
(C) River Varies									
1.0, 1.0, 1,000	11.590	1,202.0	399.1	0.551	11.280	16.96	2.713	530.1	49.80
1.0, 1.0, 365	11.580	1,199.0	404.4	0.550	11.180	16.94	2.708	528.6	49.93
1.0, 1.0, 100	11.570	1,180.0	419.3	0.548	11.080	16.88	2.691	523.4	50.55
1.0, 1.0, 10	11.590	1,206.0	408.7	0.551	11.180	16.97	2.718	531.9	50.31
1.0, 1.0, 1.0	11.580	1,150.0	396.9	0.537	10.780	16.61	2.602	514.9	49.13
1.0, 1.0, 0.1	11.600	1,462.0	376.2	0.793	13.490	18.71	3.267	652.0	55.11
1.0, 1.0, 0.01	---	---	---	---	---	---	---	---	---
(D) Predators Vary [Figure 50(a), dotted lines]									
3,650	11.560	1,060.0	413.6	0.559	9.876	16.16	2.461	462.9	47.74
1,000	11.590	1,150.0	396.9	0.570	10.680	16.61	2.602	505.3	49.13
365	11.580	1,149.0	397.0	0.570	10.780	16.45	2.601	505.0	49.12
100	11.580	1,150.0	397.0	0.570	10.680	16.61	2.602	505.2	49.13
10	11.580	1,141.0	398.4	0.567	10.580	16.56	2.588	501.2	49.00
1.0	11.580	1,218.0	391.6	0.567	11.380	16.88	2.690	537.8	49.98
0.1	11.560	1,058.0	415.3	0.457	9.974	16.92	2.386	463.2	47.06
0.01	11.10	609.0	735.6	0.365	5,970	12.61	1.389	256.3	34.98

Table D-4—Continued

Input Frequencies Sun, Temperature, River	J_{in}	J_{circ}	R	Harvest J_{16}	Net Sediment C Circulating In $J_3 + (J_6 + J_5)$	DOC In $J_{15} + J_{14} + J_4$	Sediment Loss J_{17}	Sediment C Circulating In J_5	DOC Uptake J_9
(E) Predator Push-Pull Varies, Figure 50(b)									
1,000	13.550	1,193.0	434.7	0.577	11.170	16.51	2.576	627.4	49.93
365	10.340	1,518.0	2,144.0	0.446	12.860	16.80	2.816	635.9	94.30
100	11.300	1,491.0	998.4	0.448	11.700	17.07	2.802	618.6	97.95
10	11.570	1,092.0	429.2	0.510	10.280	16.05	2.427	478.8	47.49
1.0	11.470	1,126.0	489.0	0.521	10.560	16.20	2.480	496.2	47.77
0.1	11.550	1,256.0	443.5	0.824	11.580	17.34	2.836	556.0	50.60
0.01	11.010	396.9	834.7	0.414	3.934	11.17	0.931	166.8	31.54
(F) Chain in Figure 50(c), Sun Varies									
1,000	11.520	1,079.0	451.7	0.520	10.060	16.22	2.485	469.0	50.78
365	11.520	1,449.0	451.7	0.472	11.860	17.19	2.794	569.4	123.50
100	11.520	1,322.0	451.7	0.496	11.260	16.86	2.690	533.0	100.0
10	11.520	1,049.0	451.7	0.514	9.864	16.08	2.445	457.4	47.61
1.0	11.520	1,096.0	451.7	0.526	10.260	16.32	2.518	480.1	48.25
0.1	11.520	896.4	451.7	0.428	8.464	15.19	2.157	385.8	44.72
0.01	11.490	456.3	450.2	0.304	4.660	11.74	1.067	183.3	33.00

Table D-5. Ratios of output to input variant power used to evaluate the chain models in Figure 58(a), (b), and (c)

Input Frequencies: Sun, Temperature, River	$\frac{J_{circ}}{J_{in}}$	$\frac{J_{out}}{J_{in}}$	$\frac{R}{I}$	Spartina $\frac{J_2+J_3+J_{14}}{J_1}$	Sediment C $\frac{J_4+J_5+J_{17}}{J_3+J_6}$	DOC $\frac{J_{19}}{J_{15}+J_{14}+J_4+J_{10}}$	Bacteria $\frac{J_7+J_{12}}{J_{11}}$	Potamopyrgus $\frac{J_8+J_{16}}{J_{17}}$
(A) Sun Varies								
1,000, 1.0, 1.0	11.140	0.085	0.119	0.0072	0.987	0.708	1.912	0.795
365, 1.0, 1.0	11.190	0.085	0.119	0.0048	0.975	0.704	1.912	0.750
100, 1.0, 1.0	11.280	0.085	0.119	0.0072	0.988	0.718	1.971	0.775
10, 1.0, 1.0	11.070	0.086	0.119	0.0096	0.975	0.695	1.912	0.750
1.0, 1.0, 1.0	9.263	0.114	0.089	0.2000	0.997	0.667	2.057	0.758
0.1, 1.0, 1.0	28.650	0.314	0.022	0.9680	0.976	0.545	2.041	0.790
0.01, 1.0, 1.0	67.200	0.413	0.226	0.3890	0.998	0.723	1.364	0.914
(B) Temperature Varies								
1.0, 1,000, 1.0	11.680	0.145	0.102	0.2000	0.998	1.266	0.550	0.224
1.0, 365, 1.0	104.100	2.376	1.706	0.1340	0.994	1.485	0.870	0.005
1.0, 100, 1.0	88.670	1.905	1.510	0.1240	0.996	1.535	0.915	0.007
1.0, 10, 1.0	6.228	0.124	0.084	0.2030	0.980	0.565	1.789	0.629
1.0, 1.0, 1.0	9.269	0.114	0.089	0.2000	0.997	0.567	2.057	0.758
1.0, 0.1, 1.0	12.000	0.563	0.083	0.2020	0.983	0.609	1.963	0.760
1.0, 0.01, 1.0	126.20	0.448	0.194	0.2340	0.996	0.647	1.438	0.924

Table D-5—Continued

Input Frequencies Sun, Temperature, River	$\frac{J_{circ}}{J_{in}}$	$\frac{J_{out}}{J_{in}}$	$\frac{R}{I}$	Spartina $\frac{J_2+J_3+J_{14}}{J_1}$	Sediment C $\frac{J_4+J_5+J_{17}}{J_3+J_6}$	DOC $\frac{J_{19}}{J_{15}+J_{14}+J_4+J_{10}}$	Bacteria $\frac{J_7+J_{12}}{J_{11}}$	Potamopyrgus $\frac{J_8+J_{16}}{J_{13}}$
(C) River Varies								
1.0, 1.0, 1,000	15.500	0.134	0.107	0.195	0.989	0.048	17.300	1.000
1.0, 1.0, 365	1,775	0.141	0.113	0.199	0.976	0.376	3.917	0.364
1.0, 1.0, 100	3.304	0.166	0.125	0.200	0.885	0.931	1.539	0.077
1.0, 1.0, 10	2.470	0.151	0.117	0.201	1.087	0.669	2.112	0.148
1.0, 1.0, 1.0	9.269	0.114	0.089	0.200	0.977	0.667	2.057	0.758
1.0, 1.0, 0.1	24.850	0.765	0.111	0.201	0.990	0.496	2.486	0.933
1.0, 1.0, 0.01	---	---	---	---	---	---	---	---
(D) Predator Harvest Varies [Figure 50(a) dotted lines]								
3,650	13.050	0.090	0.095	0.202	0.990	0.622	1.919	1.650
1,000	8.869	0.132	0.089	0.200	0.997	0.607	2.128	1.676
365	8.874	0.133	0.089	0.200	0.963	0.599	2.129	1.758
100	8.892	0.132	0.089	0.200	0.997	0.612	2,129	1.727
10	9.147	0.133	0.089	0.200	0.988	0.620	2.300	1.727
1.0	15.310	0.169	0.058	0.200	0.979	0.630	2.564	1.816
0.1	11.640	0.131	0.083	0.200	0.975	0.639	1.925	1.361
0.01	140.300	0.422	0.235	0.237	0.996	0.658	1.345	1.023

Table D-5—Continued

Input Frequencies Sun, Temperature, River	$\frac{J_{circ}}{J_{in}}$	$\frac{J_{out}}{J_{in}}$	$\frac{R}{I}$	Spartina $\frac{J_2+J_3+J_{14}}{J_1}$	Sediment C $\frac{J_4+J_5+J_{17}}{J_3+J_6}$	DOC $\frac{J_{19}}{J_{15}+J_{14}+J_4+J_{10}}$	Bacteria $\frac{J_7+J_{12}}{J_{11}}$	Potamopyrgus $\frac{J_8+J_{16}}{J_{13}}$
(E) Predator Push-Pull, Figure 50(b)								
1,000	56.31	0.169	0.119	0.201	0.981	1.064	3.616	0.205
365	115.30	1.495	1.763	0.097	0.980	1.478	1.049	0.024
100	114.60	1.045	0.529	0.189	0.982	1.478	0.887	0.024
10	52.53	0.233	0.135	0.195	0.982	0.698	2.794	1.217
1.0	47.71	0.066	0.211	0.199	0.979	0.612	1.200	2.261
0.1	116.30	0.366	0.169	0.208	0.989	0.691	2.129	1.170
0.01	85.98	0.377	0.252	0.231	0.998	0.654	2.110	1.016
(F) Chain Model in Figure 50(c), Sun Varies								
1,000	30.32	0.150	0.108	0.200	0.969	1.260	0.538	0.240
365	124.10	2.779	0.108	0.200	0.999	1.485	0.876	0.005
100	86.08	2.010	0.108	0.200	0.968	1.479	0.922	0.008
10	11.06	0.129	0.108	0.200	0.989	0.665	1.900	0.659
1.0	10.65	0.114	0.108	0.200	0.986	0.594	1.987	0.759
0.1	12.66	0.166	0.108	0.200	0.997	0.591	1.956	0.752
0.01	36.31	0.366	0.108	0.227	0.995	0.622	1.602	0.912

Table 0-6. The mean square power, mean power, and variant power produced and used by the chain model in Figure 50(a) when the solar input frequency varies

Input Frequency	Spartina	Bacteria	Potamo-pyrgus	Spartina	Bacteria	Potamo-pyrgus	Produced	Out
	MSQ Power Produced			MSQ Power Out			Total MSQ Power	
1,000, 1.0, 1.0	4.487	16.87	2.439	1.612	2.658	1.872	23.80	6.142
365, 1.0, 1.0	4.487	16.87	2.440	1.612	2.658	1.872	23.80	6.142
100, 1.0, 1.0	4.487	16.88	2.441	1.612	2.658	1.873	23.81	6.143
10, 1.0, 1.0	4.486	16.84	2.435	1.612	2.658	1.868	23.76	6.138
1.0, 1.0, 1.0	4.481	16.34	2.348	1.628	2.664	1.804	23.17	6.096
0.1, 1.0, 1.0	4.608	18.34	2.663	1.815	2.824	1.935	25.61	6.574
0.01, 1.0, 1.0	4.304	11.21	1.507	1.691	2.605	1.113	17.02	6.409
	Mean Power Produced			Mean Power Out			Total Mean Power	
1,000, 1.0, 1.0	4.072	16.70	2.400	1.611	2.563	1.848	23.17	6.022
365, 1.0, 1.0	4.072	16.70	7.400	1.611	2.563	1.849	23.17	6.023
100, 1.0, 1.0	4.072	16.71	2.401	1.611	2.563	1.849	23.18	6.023
10, 1.0, 1.0	4.071	16.67	2.395	1.610	2.563	1.845	23.14	6.018
1.0, 1.0, 1.0	4.060	16.20	2.315	1.595	2.566	1.785	22.58	5.946
0.1, 1.0, 1.0	4.113	18.17	2.623	1.527	2.717	1.912	24.91	6.256
0.01, 1.0, 1.0	3.505	10.46	1.344	1.382	2.539	1.002	15.31	4.923

Table C-6—Continued

Input Frequency	Spartina	Bacteria	Potamopyrgus	Spartina	Bacteria	Potamopyrgus	Produced	Out
	Variant Power Produced			Variant Power Out			Total Variant Power	
1,000, 1.0, 1.0	0.416	0.170	0.039	0.001	0.096	0.024	0.624	0.120
365, 1.0, 1.0	0.415	0.170	0.040	0.001	0.095	0.023	0.625	0.119
100, 1.0, 1.0	0.415	0.170	0.040	0.001	0.096	0.024	0.625	0.120
10, 1.0, 1.0	0.415	0.170	0.040	0.002	0.096	0.023	0.625	0.123
1.0, 1.0, 1.0	0.421	0.140	0.033	0.033	0.098	0.013	0.594	0.160
0.3, 1.0, 1.0	0.496	0.170	0.040	0.188	0.107	0.023	0.705	0.318
0.01, 1.0, 1.0	0.799	0.750	0.163	0.309	0.066	0.111	1.712	0.486

Table D-7 The mean square power, mean power, and variant power produced and used by the trophic chain model in Figure 50(a) when the frequency of temperature input varies

Input Frequency	*Spartina*	Bacteria	*Potamo-pyrgus*	*Spartina*	Bacteria	*Potamo-pyrgus*	Produced	Out
	MSQ Power Produced			MSQ Power Out			Total MSQ Power	
1.0, 1,000, 1.0	4.474	17.13	2.360	1.623	2.727	1.774	23.96	6.124
1.0, 365, 1.0	2.623	40.48	5.182	0.835	6.759	1.927	48.29	9.521
1.0, 100, 1.0	3.255	34.95	4.703	1.109	5.645	1.912	42.91	8.666
1.0, 10, 1.0	4.487	16.11	2.300	1.628	2.706	1.761	22.90	6.095
1.0, 1.0, 1.0	4.481	16.34	2.348	1.628	2.664	1.804	23.17	6.096
1.0, 0.1, 1.0	4.443	14.94	2.069	1.613	2.726	1.665	21.48	6.004
1.0, 0.01, 1.0	4.089	11.27	1.485	1.478	2.767	1.164	16.84	5.409
	Mean Power Produced			Mean Power Out			Total Mean Power	
1.0, 1,000, 1.0	4.045	16.03	2.284	1.589	2.571	1.761	22.36	5.921
1.0, 365, 1.0	1.941	15.88	2.223	0.799	2.780	1.915	20.04	5.494
1.0, 100, 1.0	2.689	16.20	2.296	1.081	2.678	1.899	21.19	5.658
1.0, 10, 1.0	4.058	15.83	2.266	1.594	2.584	1.747	22.26	5.925
1.0, 1.0, 1.0	4.060	16.20	2.315	1.595	2.566	1.785	22.58	5.946
1.0, 0.1, 1.0	4.067	14.78	2.074	1.579	2.562	1.650	20.92	5.791
1.0, 0.01, 1.0	3.657	10.70	1.379	1.438	2.578	1.087	15.74	5.103

Table 0-7—Continued

Input Frequency	*Spartina*	Bacteria	*Potamopyrgus*	*Spartina*	Bacteria	*Potamopyrgus*	Produced	Out
	Variant Power Produced			Variant Power Out			Total Variant Power	
1.0, 1,000, 1.0	0.429	1.100	0.076	0.034	0.156	0.013	1.605	0.203
1.0, 365, 1.0	0.682	24.600	2.959	0.036	3.979	0.012	28.240	4.027
1.0, 100, 1.0	0.566	18.750	2.407	0.028	2.967	0.013	21.720	3.006
1.0, 10, 1.0	0.429	0.180	0.034	0.034	0.122	0.014	0.643	0.170
1.0, 1.0, 1.0	0.421	0.140	0.033	0.033	0.098	0.013	0.594	0.150
1.0, 0.1, 1.0	0.426	0.160	0.025	0.034	0.164	0.015	0.611	0.213
1.0, 0.01, 1.0	0.432	0.570	0.106	0.040	0.189	0.077	1.108	0.306

Table 0-8. The mean square power, mean power, and variant power produced and used by the chain model in Figure 50(a) when the frequency of river input varies

Input Frequency	Spartina	Bacteria	Potamo-pyrgus	Spartina	Bacteria	Potamo-pyrgus	Produced	Out
	MSQ Power Produced			MSQ Power Out			Total MSQ Power	
1.0, 1.0, 1,000	4.484	16.56	2.365	1.630	2.798	1.815	23.41	6.243
1.0, 1.0, 365	4.479	16.60	2.359	1.626	2.810	1.813	23.45	6.251
1.0, 1.0, 100	4.466	16.81	2.400	1.623	2.842	1.806	23.68	6.271
1.0, 1.0, 10	4.476	16.73	2.390	1.627	2.823	1.817	23.60	5.690
1.0, 1.0, 1.0	4.481	16.34	2.348	1.626	2.664	1.804	23.17	6.096
1.0, 1.0, 0.1	4.521	18.33	2.625	1.644	3.073	1.834	25.48	6.551
1.0, 1.0, 0.01	---	---	---	---	---	---	---	---
	Mean Power Produced			Mean Power Out			Total Mean Power	
1.0, 1.0, 1,000	4.065	16.55	2.361	1.597	2.645	1.812	22.98	6.054
1.0, 1.0, 365	4.061	16.54	2.358	1.596	2.645	1.810	22.96	6.051
1.0, 1.0, 100	4.047	16.48	2.349	1.590	2.644	1.803	22.88	6.037
1.0, 1.0, 10	4.059	16.67	2.363	1.594	2.645	1.814	22.99	6.053
1.0, 1.0, 1.0	4.060	16.20	2.315	1.595	2.566	1.785	22.58	5.946
1.0, 1.0, 0.1	4.099	18.19	2.595	1.611	2.905	1.814	24.68	6.330
1.0, 1.0, 0.01	---	---	---	---	---	---	---	---

Table 0-8—Continued

Input Frequency	Spartina	Bacteria	Potamopyrgus	Spartina	Bacteria	Potamopyrgus	Produced	Out
	Variant Power Produced			Variant Power Out			Total Variant Power	
1.0, 1.0, 1,000	0.419	0.010	0.004	0.033	0.153	0.003	0.433	0.189
1.0, 1.0, 365	0.418	0.060	0.011	0.032	0.165	0.003	0.489	0.200
1.0, 1.0, 1000	0.419	0.330	0.052	0.033	0.198	0.003	0.801	0.234
1.0, 1.0, 10	0.418	0.160	0.027	0.033	0.178	0.003	0.605	0.214
1.0, 1.0, 1.0	0.421	0.140	0.033	0.033	0.098	0.019	0.594	0.150
1.0, 1.0, 0.1	0.422	0.140	0.030	0.033	0.168	0.020	0.595	0.221
1.0, 1.0, 0.01	---	---	---	---	---	---	---	---

Table D-9 The mean square power, mean power, and variant power produced and used by the model in Figure 50(a) when the frequency of predator harvest varies [dotted portion of Figure 50(a)]

Input Frequency	Spartina	Bacteria	Potamo-pyrgus	Spartina	Bacteria	Potamo-pyrgus	Produced	Out
	MSQ Power Produced			MSQ Power Out			Total MSQ Power	
1.0, 1.0, 1.0, 3,650	4.459	15.88	2.269	1.621	2.667	1.737	22.61	6.025
1.0, 1.0, 1.0, 1,000	4.481	16.34	2.348	1.628	2.668	1.804	23.17	6.100
1.0, 1.0, 1.0, 365	4.481	16.34	2.347	1.628	2.664	1.804	23.17	6.096
1.0, 1.0, 1.0, 100	4.481	16.34	2.347	1.626	2.664	1.804	23.17	6.096
1.0, 1.0, 1.0, 10	4.479	16.29	2.340	1.627	2.664	1.798	23.11	6.089
1.0, 1.0, 1.0, 1	4.468	15.62	2.391	1.630	2.754	1.858	23.49	6.242
1.0, 1.0, 1.0, 0.1	4.456	15.65	2.248	1.618	2.561	1.805	22.35	5.984
1.0, 1.0, 1.0, 0.01	4.063	11.63	1.585	1.474	2.519	1.222	17.28	5.215
	Mean Power Produced			Mean Power Out			Total Mean Power	
1.0, 1.0, 1.0, 3,650	4.039	15.72	2.233	1.587	2.570	1.716	21.99	5.873
1.0, 1.0, 1.0, 1,000	4.060	16.20	2.314	1.595	2.566	1.785	22.57	5.946
1.0, 1.0, 1.0, 365	4.060	16.20	2.314	1.595	2.566	1.784	22.57	5.945
1.0, 1.0, 1.0, 100	4.060	16.20	2.314	1.595	2.566	1.785	22.57	9.946
1.0, 1.0, 1.0, 10	4.058	16.16	2.307	1.594	2.565	1.779	22.53	5.938
1.0, 1.0, 1.0, 1	4.067	16.48	2.353	1.597	2.615	1.823	22.90	6.035
1.0, 1.0, 1.0, 0.1	4.037	15.49	2.212	1.585	2.463	1.781	21.74	5.829
1.0, 1.0, 1.0, 0.01	3.663	10.99	1.453	1.436	2.438	1.139	16.10	5.013

Table D-9--Continued

Input Frequency	Spartina	Bacteria	Potamo-pyrgus	Spartina	Bacteria	Potamo-pyrgus	Produced	Out
	Variant Power Produced			Variant Power Out			Total Variant Power	
1.0, 1.0, 1.0, 3,650	0.420	0.160	0.036	0.034	0.097	0.021	0.616	0.152
1.0, 1.0, 1.0, 1,000	0.421	0.140	0.034	0.033	0.098	0.019	0.595	0.150
1.0, 1.0, 1.0, 365	0.421	0.140	0.033	0.033	0.098	0.020	0.594	0.151
1.0, 1.0, 1.0, 100	0.420	0.140	0.033	0.033	0.098	0.019	0.594	0.150
1.0, 1.0, 1.0, 10	0.421	0.130	0.033	0.033	0.099	0.019	0.594	0.151
1.0, 1.0, 1.0, 1	0.421	0.140	0.038	0.033	0.139	0.035	0.599	0.207
1.0, 1.0, 1.0, 0.1	0.419	0.160	0.036	0.033	0.098	0.024	0.615	0.155
1.0, 1.0, 1.0, 0.01	0.410	0.640	0.132	0.038	0.081	0.083	1.182	0.202

Table D-10 The mean square power, mean power, and variant power produced and used by the model in Figure 50(b) when the frequency of a push-pull predator harvest varies

Input Frequency	Spartina	Bacteria	Potamopyrgus	Spartina	Bacteria	Potamopyrgus	Produced	Out
	MSQ Power Produced			MSQ Power Out			Total MSQ Power	
1.0, 1.0, 1.0, 1,000	4.442	16.60	2.592	1.614	2.644	1.793	23.63	6.051
1.0, 1.0, 1.0, 365	3.230	31.36	4.611	1.045	4.945	1.967	39.20	7.957
1.0, 1.0, 1.0, 100	4.194	32.57	4.435	1.421	4.642	1.927	41.20	7.990
1.0, 1.0, 1.0, 10	4.460	15.79	2.217	1.620	3.051	1.722	22.47	5.393
1.0, 1.0, 1.0, 1	4.367	15.88	2.258	1.601	2.610	1.770	22.51	5.961
1.0, 1.0, 1.0, 0.1	4.450	16.83	2.343	1.622	3.454	1.548	23.62	6.624
1.0, 1.0, 1.0, 0.01	3.930	10.49	1.338	1.425	3.084	0.924	15.76	5.433
	Mean Power Produced			Mean Power Out			Total Mean Power	
1.0, 1.0, 1.0, 1,000	4.024	16.10	2.309	1.581	2.496	1.774	22.43	5.651
1.0, 1.0, 1.0, 365	2.530	16.39	2.364	1.019	2.465	1.945	21.28	5.429
1.0, 1.0, 1.0, 100	3.470	16.64	2.326	1.367	2.935	1.905	22.44	6.207
1.0, 1.0, 1.0, 10	4.039	16.61	2.171	1.588	2.818	1.700	21.82	6.106
1.0, 1.0, 1.0, 1	3.995	15.77	2.235	1.572	2.608	1.750	22.00	5.930
1.0, 1.0, 1.0, 0.1	4.031	16.45	2.243	1.588	3.235	1.497	22.72	6.320
1.0, 1.0, 1.0, 0.01	3.532	10.05	1.212	1.389	2.916	0.857	14.60	5.162

Table 0-10—Continued

Input Frequency	Spartina	Bacteria	Potamopyrgus	Spartina	Bacteria	Potamopyrgus	Produced	Out
	Variant Power Produced			Variant Power Used			Total Variant Power	
1.0, 1.0, 1.0, 1,000	0.418	0.500	0.283	0.033	0.148	0.019	1.201	0.200
1.0, 1.0, 1.0, 365	0.700	14.970	2.247	0.026	2.480	0.022	17.920	2.528
1.0, 1.0, 1.0, 100	0.724	15.930	2.110	0.054	1.707	0.022	18.760	1.763
1.0, 1.0, 1.0, 10	0.421	0.160	0.046	0.032	0.233	0.022	0.647	0.287
1.0, 1.0, 1.0, 1	0.372	0.110	0.023	0.029	0.002	0.020	0.505	0.051
1.0, 1.0, 1.0, 0.1	0.419	0.380	0.100	0.034	0.219	0.051	0.899	0.304
1.0, 1.0, 1.0, 0.01	0.399	0.430	0.126	0.036	0.168	0.067	0.954	0.271

Table D-11 The mean square power, mean power, and variant power produced and used by the chain model in Figure 50(c) without secondary positive feedbacks when the frequency of temperature input varies

Input Frequency	Spartina	Bacteria	Potamo-pyrgus	Spartina	Bacteria	Potamo-pyrgus	Produced	Out
	MSQ Power Produced			MSQ Power Out			Total MSQ Power	
1.0, 1,000, 1.0	4.418	16.89	2.320	1.604	2.727	1.746	23.63	6.077
1.0, 365, 1.0	4.418	41.08	5.294	1.604	6.891	1.887	50.97	10.380
1.0, 100, 1.0	4.418	33.27	4.468	1.604	5.605	1.841	42.16	9.050
1.0, 10, 1.0	4,418	15.83	2.254	1.604	2.796	1.727	22.50	6.037
1.0, 1.0, 1.0	4.418	16.05	2.229	1.604	2.661	1.767	22.77	6.032
1.0, 0.1, 1.0	4.418	14.87	2.088	1.604	2.725	1.657	21.38	5.988
1.0, 0.01, 1.0	4.404	10.98	1.439	1.598	2.767	1.128	16.82	5.493
	Mean Power Produced			Mean Power Out			Total Mean Power	
1.0, 1,000, 1.0	3.997	15.80	2.245	1.571	2.571	1.732	22.04	5.874
1.0, 365, 1.0	3.997	16.77	2.346	1.571	2.954	1.874	23.11	6,399
1.0, 100, 1.0	3.997	16.46	2.322	1.571	2.776	1.828	22.78	5.175
1.0, 10, 1.0	3.997	15.66	2.220	1.571	2.583	1.712	21.88	5.855
1.0, 1.0, 1.0	3.997	15.90	2.265	1.571	2.563	1.747	22.16	5.881
1.0, 0.1, 1.0	3.997	14.71	2.063	1.571	2.562	1.642	20.77	5.775
1.0, 0.01, 1.0	3.972	10.56	1.354	1.560	2.578	1.067	15.88	5.205

Table 0-11—Continued

Input Frequency	Spartina	Bacteria	Potamopyrgus	Spartina	Bacteria	Potamopyrgus	Produced	Out
	Variant Power Produced			Variant Power Out			Total Variant Power	
1.0, 1,000, 1.0	0.421	1.090	0.075	0.033	0.156	0.014	1.586	0.203
1.0, 365, 1.0	0.421	24.310	2.948	0.033	3.937	0.013	27.680	3.983
1.0, 100, 1.0	0.421	16.780	2.146	0.033	2.829	0.013	19.350	2.875
1.0, 10.0, 1.0	0.421	0.170	0.034	0.033	0.123	0.015	0.625	0.171
1.0, 1.0, 1.0	0.421	0.150	0.020	0.033	0.098	0.020	0.591	0.151
1.0, 0.1, 1.0	0.421	0.160	0.025	0.033	0.163	0.015	0.606	0.211
1.0, 0.01, 1.0	0.432	0.430	0.085	0.038	0.169	0.061	0.947	0.268

Table D-12 Ratios of output to input used to evaluate the power produced and used for the trophic chain models in Figure 50(a), (b), and (c)

Frequency	Sun	Temperature	River	Predator	Predator Push-Pull	Temperature NF
			Power Produced Output to Input Ratio			
1,000.00	0.436	1,112	0.302	0.414	0.838	1.106
365.00	0.437	16,640	0.341	0.414	10.450	19.280
100.00	0.437	13.740	0.559	0.414	10.790	13.480
10.00	0.437	0.445	0.422	0.407	0.451	0.435
1.00	0.414	0.414	0.414	0.417	0.364	0.412
0.10	0.467	0.424	0.414	0.429	0.627	0.422
0.01	0.917	0.739	---	0.800	0.651	0.632
			Power Used Output to Input Ratios			
1,000.00	0.084	0.141	0.132	0.104	0.140	0.141
365.00	0.083	2.373	0.140	0.105	1.474	2.774
100.00	0.084	1.903	0.163	0.104	1.025	2.003
10.00	0.086	0.118	0.149	0.105	0.200	0.119
1.00	0.101	0.104	0.104	0.144	0.037	0.105
0.10	0.211	0.148	0.163	0.108	0.212	0.147
0.01	0.260	0.204	---	0.136	0.186	0.192

REFERENCES

Allen, T. F. H., and T. Starr. 1982. Hierarchy Perspectives for Ecological Complexity. University of Chicago Press, Chicago.

Anderson, A. 1971. Intertidal activity, breeding and floating habit of *Hydrobia ulvae* in the Ythan Estuary. Jour. Mar. Biol. Assoc. of the U.K. 51:423-37.

Briand, F. 1983. Environmental control of food web structure. Ecology 64(2):253-263.

Brillouin, L. 1962. Science and Information Theory. Academic Press, Inc., New York.

Brogan, W. L. 1974. Modern Control Theory. Quantum Publishers, New York.

Brown, M. T. 1980. Energy Basis for Hierarchies in Urban and Regional Landscapes. Ph.D. dissertation. University of Florida, Gainesville.

Caldwell, J. W., and H. T. Odum. 1979. Annual record of metabolism of estuarine ecosystems at Crystal River, Florida. Annual Report to the Florida Power Corporation. Contract #QEA-00014.

Campbell, G. A. 1922. Physical theory of the electric wave-filter. Bell System Technical Journal 1(2):1-32.

Child, G. I., and H. H. Shugart, Jr. 1972. Frequency response analysis of magnesium cycling in a tropical forest ecosystem. *In* B. C. Patten (ed.), Systems Analysis and Simulation in Ecology, Vol. II. Academic Press, New York, pp. 103-135.

Christian, R. R., and J. R. Hall. 1978. Experimental trends in sediment microbial heterotrophy, radioisotopic techniques and analysis. *In* B. C. Coull (ed.), Ecology of Marine Benthos. Univ. South Carolina Press, Columbia, S.C., pp. 67-88.

Christian, R. R., R. B. Hanson, J. R. Hall, and W. J. Wiebe. 1981. Aerobic microbes and meiofauna. *In* C. R. Pomeroy and R. G. Wiegert (eds.), The Ecology of a Salt Marsh. Springer-Verlag, New York, pp. 113-116.

Costanza, R. C. 1978. Unpublished paper. University of Florida, Gainesville.

Cruz, J. B., Jr., and M. E. Van Valkenburg. 1967. Introductory Signals and Circuits. Ginn and Company, Waltham, Mass.

DiStefano, J. J., III, A. R. Stubberud, and I. J. Williams. 1967. Feedback and Control Systems. Schaum Publishing Co., New York.

Elton, C. S. 1958. The Ecology of Invasions by Animals and Plants. Methuen, London.

Eyring, H., and E. M. Eyring. 1963. Modern Chemical Kinetics. Van Nostrand Reinhold Co., New York.

Fish, J. D., and S. Fish. 1974. The breeding cycle and growth of Hydrobia ulvae in the Dovey Estuary. Jour. Mar. Biol. Assoc. of the U.K. 54:685-697.

Forrester, J. W. 1961. Industrial Dynamics. MIT Press, Cambridge, Mass.

Gallager, J. L., and W. J. Pfeiffer. 1977. Aquatic metabolism of the standing dead plant communities in salt and brackish water marshes. Limnol. and Oceanogr. 22:562-564.

Gardner, J. R., and W. R. Ashby. 1970. Connectance of large dynamical (cybernetic) systems: critical values for stability. Nature 228:784.

Grodins, F. S. 1963. Control Theory and Biological Systems. Columbia University Press, New York.

Halliday, D., and R. Resnick. 1974. Fundamentals of Physics. John Wiley and Sons, Inc., New York.

Hopkinson, C. S., and J. W. Day. 1977. A Model of the Barataria Bay salt marsh ecosystem. In C. A. S. Hall and J. W. Day (eds.), Ecosystem Modeling in Theory and Practice. Wiley Interscience, New York, pp. 235-266.

Hutchinson, G. E. 1953. The concept of pattern in ecology. Proceedings of the Academy of Natural Sciences 105:1-12.

Hutchinson, G. E. 1961. The paradox of the plankton. American Naturalist 95:137-146.

Kaituna River Watershed Study unpublished flow records, New Zealand.

Kemp, W. M. 1977. Energy Analysis and Ecological Evaluation of a Coastal Power Plant. Ph.D. dissertation. University of Florida, Gainesville.

Kemp, W. M., and W. J. Mitsch. 1979. Turbulence and phytoplankton diversity: A general model of the "paradox of plankton." Ecological Modelling 7:201-222.

Koestler, A. 1967. The Ghost in the Machine. Macmillan, New York.

Koslovsky, D. G. 1968. A critical evaluation of the trophic level concept. 1, ecological efficiencies. Ecology 49(1):48-60.

Lam, H. Y. F. 1979. Analog and Digital Filters: Design and Realization. Prentice-Hall, Inc., Englewood Cliffs, N.J.

Lee, Y. W. 1960. Statistical Theory of Communication. John Wiley and Sons, Inc., New York.

Lewontin, R. C. 1969. The meaning of stability. In Diversity and Stability in Ecological Systems. Brookhaven Symposium in Biology No. 22. National Bureau of Standards, U.S. Department of Commerce, Springfield, Va., pp. 13-24.

Limburg, K. E. 1981. Energy Sources and Design of Marine Ecosystems. M.S. thesis. University of Florida, Gainesville.

Lotka, A. J. 1922. Contribution to the energetics of evolution. Proc. Nat. Acad. Sci. 8:147-151.

Luce, G. G. 1971. Biological Rhythms in Human and Animal Physiology. Dover Publications, New York.

MacFarlane, A. G. J. (ed.). 1979. Frequency-Response Methods in Control Systems. IEEE Press, New York.

May, R. M. 1973. Stability and Complexity in Model Ecosystems. Princeton University Press, Princeton, N.J.

May, R. M. 1974. Biological populations with nonoverlapping generations: Stable points, stable cycles, and chaos. Science 186:645-647.

Milhorn, H. T. 1966. The Application of Control Theory to Physiological Systems. W. B. Saunders, Philadelphia.

Milsum, J. H. 1966. Biological Control System Analysis. McGraw-Hill, New York.

Mishima, J., and E. P. Odum. 1963. Excretion rate of Zn^{65} by *Littorina irrorata* in relation to body size and temperature. Limnol. and Oceanogr. 8:34-44.

Montague, C. L. 1980. The net influence of the mud fiddler crab, *Uca pugnax*, on carbon flow through a Georgia salt marsh: The importance of work by macroorganisms to the ecosystem. Ph.D. dissertation, University of Georgia, Athens.

Morton, J., and M. Miller. 1968. The New Zealand Sea Shore. Collins, London-Auckland.

Newell, R. C. 1965. The role of detritus in the nutrition of two marine deposit feeders, the Prosobranch *Hydrobia ulvae* and the bivalve *Macoma balthica*. Proceedings of the Zoological Society of London 144:25-45.

New Zealand Meteorological Service. Tables of solar insolation for Wellington and Nelson. New Zealand Meteorological Service, Wellington, New Zealand.

Nyquist, H. 1932. Regeneration theory. Bell System Technical Journal 11:126-146.

Odum, H. T. 1960. Ecological potential and analogue circuits for the ecosystem. Am. Sci. 48:1-8.

Odum, H. T. 1967. Biological circuits and the marine systems of Texas. *In* T. A. Olson and F. J. Burgess (eds.), Pollution and Marine Ecology. Interscience, New York.

Odum, H. T. 1970. Summary: An emerging view of the ecologycal system at El Verde. *In* H. T. Odum and R. F. Pigeon (eds.), A Tropical Rain Forest, Book 3. Office of Information Services, U.S. Atomic Energy Commission, Washington, D.C.

Odum, H. T. 1971. Environment, Power, and Society. Wiley-Interscience, New York.

Odum, H. T. 1972. An energy circuit language for ecological and social systems: Its physical basis. *In* B. C. Patten (ed.), Systems Analysis and Simulation in Ecology, Vol. II. Academic Press, New York, pp. 140-210.

Odum, H. T. 1978. Energy quality control of ecosystem design. *In* P. F. Dame (ed.), Marsh-Estuarine Systems Simulation, Belle W. Baruch Library in Marine Science, No. 8. University of South Carolina, Columbia, South Carolina, pp. 221-235.

Odum, H. T. 1982. Pulsing, power, and hierarchy. In W. J. Mitsch, R. K. Ragade, R. W. Bosserman, and J. A. Dillon, Jr. (eds.), Energy and Systems. Ann Arbor Science, Ann Arbor, MI., pp. 33-59.

Odum, H. T. 1983. Systems Ecology. John Wiley and Sons, New York.

Odum, H. T., and J. W. Caldwell. 1978. Annual record of metabolism of the estuarine ecosystems at Crystal River, Florida. Annual Report to the Florida Power Corporation, Supplement No. 1. Contract #QEA-00002.

Odum, H. T., and Caldwell, J. W. 1980. Annual record of metabolism of estuarine ecosystems at Crystal River, Florida. Annual Report to the Florida Power Corporation. Contract #QEA-00002.

Odum, H. T., W. Kemp, M. Sell, W. Boynton, and M. Lehman. 1977. Energy analysis and the coupling of man and estuaries. Environmental Management 1(4):297-315.

Odum, H. T., G. A. Knox, and D. E. Campbell. 1983. Organization of a new ecosystem, exotic *Spartina* salt marsh in New Zealand. Center for Wetlands, University of Florida, Gainesville.

Odum, H. T., and E. C. Odum. 1976, 1981. Energy Basis for Man and Nature. McGraw-Hill, New York.

Onsager, L. 1931. Reciprocal relations in irreversible processes, I. Physical Review 37:405-425.

Otnes, R. K., and L. Enochson. 1978. Applied Time Series Analysis, Vol. 1, Basic Techniques. John Wiley and Sons, New York.

Palmer, J. D. 1974. Biological Clocks in Marine Organisms: The Control of Physiological and Behavioral Tidal Rhythms. John Wiley and Sons, New York.

Palmer, J. D. 1976. An Introduction to Biological Rhythms. Academic Press, New York.

Petersen, G. H., and M. A. Curtis. 1979. Differences in energy flow through major components of subarctic, temperate, and tropical marine shelf ecosystems. *In* Fourth National Oceanographic Symposium, Johannesburg and Capetown, South Africa.

Pomeroy, L. R., and R. G. Wiegert (eds.). 1981. The Ecology of a Salt Marsh. Springer-Verlag, New York.

Prigogine, Ilya. 1982. Order out of chaos. *In* W. J. Mitsch, R. K. Ragade, R. W. Bosserman, and J. A. Dillon, Jr. (eds.), Energetics and Systems. Ann Arbor Science, Ann Arbor, Mich.

Richardson, J. R., and H. T. Odum. 1981. Power and a pulsing production model. *In* W. J. Mitsch, R. W. Bosserman, and J. M. Klopatek (eds.), Energy and Ecological Modeling. Elsevier, Amsterdam, pp. 641-648.

Sandberg, I. W. 1964. Bell System Technical Journal 43 1601-1608.

Shugart, H. H., Jr., D. E. Reichle, N. T. Edwards, and J. R. Kercher. 1976. Ecology 57 99.

Simon, H. A. 1973. The organization of complex systems. *In* H. H. Pattee (ed.), Hierarchy Theory. George Braziller, New York, pp. 1-29.

Smalley, A. E. 1958. The Role of Two Invertebrate Populations, *Littorina irrorata* and *Orchelinum fidicinum* in the Energy Flow of a Salt Marsh. Ph.D. thesis, University of Georgia, Athens.

Smith, Alison M., H. W. Woolhouse, and D. A. Jones. 1982. Photosynthetic carbon metabolism of the cool temperate C_4 grass *Spartina anglica*. Hubb. Planta 156 441-448.

Ulanowicz, R. E. 1980. An hypothesis on the development of natural communities. Journal of Theoretical Biology 85 223-245.

Van Nostrand's Scientific Encyclopedia. Fifth Edition. 1976. Van Nostrand Reinhold, New York.

Waide, J. B., J. E. Krebs, S. P. Clarkson, and E. M. Setzler. 1974. *In* R. Rosen and F. M. Snell (eds.), Progress in Theoretical Biology, Vol. III, Academic Press, New York, pp. 261-345.

Waide, J. B., and J. R. Webster. 1976. Engineering systems analysis: Applicability to ecosystems. *In* B. C. Patten (ed.), Systems Analysis and Simulation in Ecology, Vol. IV. Academic Press, New York, pp. 329-371.

Waitemata Harbour Study unpublished data. New Zealand.

Young, D. 1974. Studies of Florida gulf coast salt marshes receiving thermal discharge. *In* J. W. Gibbons and R. R. Shartiz (eds.), Thermal Ecology, Conf-730505. U.S. Atomic Energy Commission Technical Information Center, Washington, D.C., pp. 533-550.

BIOGRAPHICAL SKETCH

Daniel E. Campbell was born December 26, 1947, in Richmond, Virginia, the son of Ray Smith Campbell and Thelma Pauline Elam. He was educated in the public school system and graduated from Caroline High School in 1966. He attended the Virginia Military Institute and graduated with a B.S. in 1970 with honors in biology. He attended the University of Virginia Medical School for one year and then dropped out. After a short time in the army and travel in Europe he again entered graduate school at Old Dominion University in Norfolk, Virginia. He graduated with an M.S. in oceanography in 1977. In 1976, he came to the University of Florida to study for a Ph.D. under Dr. H. T. Odum. In 1982 he participated in a joint New Zealand-United States exchange with Dr. Odum and Dr. Knox. In 1982 he was married to Kathleen Ann Trimmer and that year also saw the birth of their son, Elliott. In 1983, he accepted a job with the Department of Natural Resources in Maine.

I certify that I have read this study and that in my opinion it conforms to acceptable standards of scholarly presentation and is fully adequate, in scope and quality, as a dissertation for the degree of Doctor of Philosophy

H T Odum

Howard T Odum, Chairman
Graduate Research Professor
of Environmental Engineering
Sciences

I certify that I have read this study and that in my opinion it conforms to acceptable standards of scholarly presentation and is fully adequate, in scope and quality, as a dissertation for the degree of Doctor of Philosophy

Wayne C. Huber
Professor of Environmental
Engineering Sciences

I certify that I have read this study and that in my opinion it conforms to acceptable standards of scholarly presentation and is fully adequate, in scope and quality, as a dissertation for the degree of Doctor of Philosophy

Barney L Capehart

Barney L Capehart
Professor of Industrial and
Systems Engineering

I certify that I have read this study and that in my opinion it conforms to acceptable standards of scholarly presentation and is fully adequate, in scope and quality, as a dissertation for the degree of Doctor of Philosophy

Edward S Deevey, Jr
Graduate Research Professor
of Zoology

I certify that I have read this study and that in my opinion it conforms to acceptable standards of scholarly presentation and is fully adequate, in scope and quality, as a dissertation for the degree of Doctor of Philosophy

Frank G Nordlie
Frank G. Nordlie
Professor of Zoology

This dissertation was submitted to the Graduate Faculty of the College of Engineering and to the Graduate Council, and was accepted as partial fulfillment of the requirements for the degree of Doctor of Philosophy

April 1984

Hubert A. Bevis
Dean, College of Engineering

Dean for Graduate Studies
and Research